VOLUME 159 • 2007

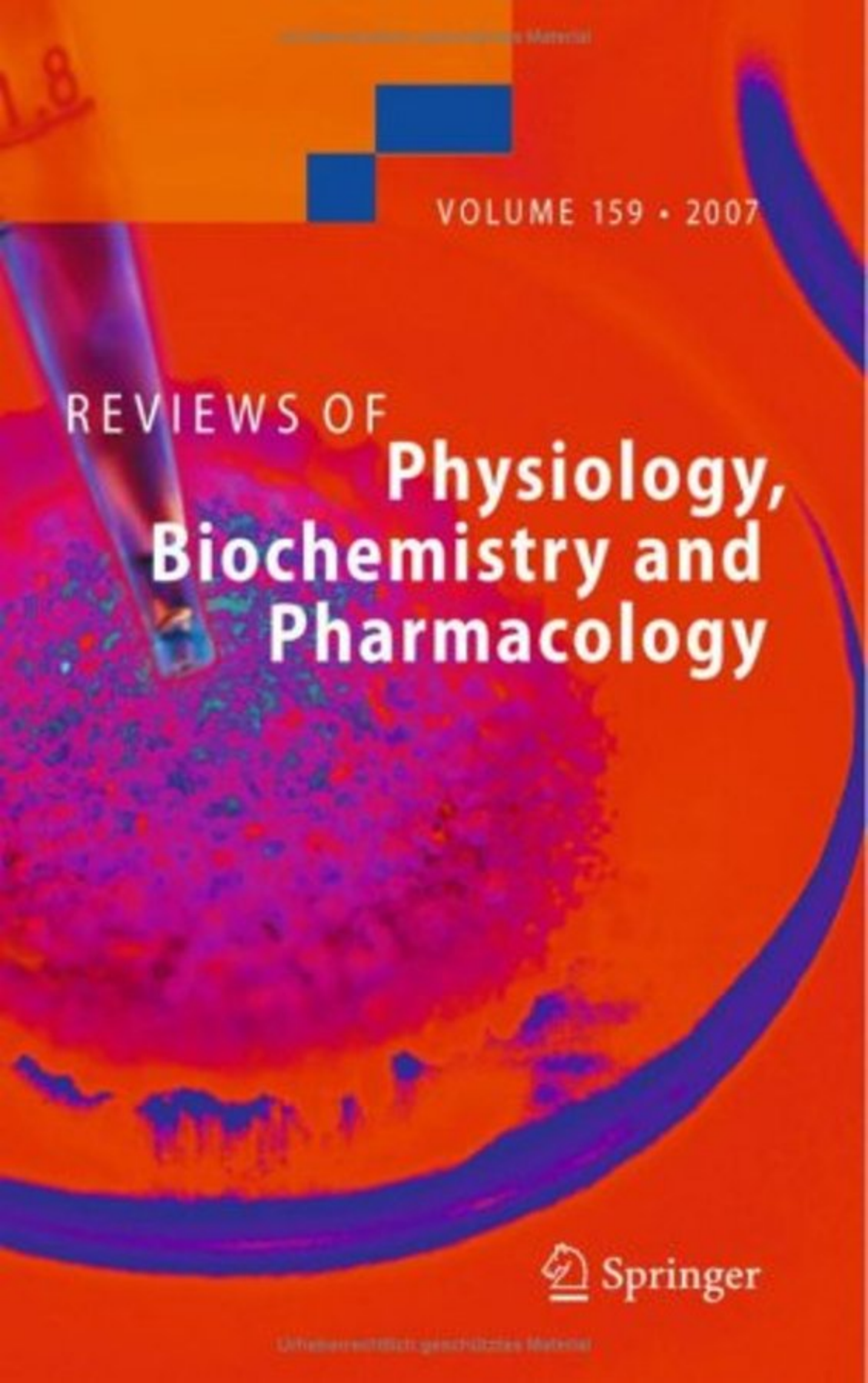

REVIEWS OF Physiology, Biochemistry and Pharmacology

Springer

Reviews of

159 Physiology Biochemistry and Pharmacology

Springer

Library of Congress-Catalog-Card Number 74-3674

ISSN 0303-4240
ISBN 978-3-540-73799-5 Springer Berlin Heidelberg New York

Springer is a part of Springer Science+Business Media

springer.com

Editor: Simon Rallison, London
Desk Editor: Anne Clauss, Heidelberg
Typesetting and Production: LE-TEX Jelonek, Schmidt & Vöckler GbR, Leipzig
Cover: WMXDesign GmbH, Heidelberg

Printed on acid-free paper 14/3100YL – 5 4 3 2 1 0 – SPIN 12073825

Rev Physiol Biochem Pharmacol (2007) 159:1 –77
DOI 10.1007/112_2007_0701

R. S. Harrison · P. C. Sharpe · Y. Singh · D. P. Fairlie

Amyloid peptides and proteins in review

Published online: 24 April 2007

Abstract Amyloids are filamentous protein deposits ranging in size from nanometres to microns and composed of aggregated peptide β-sheets formed from parallel or anti-parallel alignments of peptide β-strands. Amyloid-forming proteins have attracted a great deal of recent attention because of their association with over 30 diseases, notably neurodegenerative conditions like Alzheimer's, Huntington's, Parkinson's, Creutzfeldt-Jacob and prion disorders, but also systemic diseases such as amyotrophic lateral sclerosis (Lou Gehrig's disease) and type II diabetes. These diseases are all thought to involve important conformational changes in proteins, sometimes termed misfolding, that usually produce β-sheet structures with a strong tendency to aggregate into water-insoluble fibrous polymers. Reasons for such conformational changes *in vivo* are still unclear. Intermediate aggregated state(s), rather than precipitated insoluble polymeric aggregates, have recently been implicated in cellular toxicity and may be the source of aberrant pathology in amyloid diseases. Numerous *in vitro* studies of short and medium length peptides that form amyloids have provided some clues to amyloid formation, with an α-helix to β-sheet folding transition sometimes implicated as an intermediary step leading to amyloid formation. More recently, quite a few non-pathological amyloidogenic proteins have also been identified and physiological properties have been ascribed, challenging previous implications that amyloids were always disease causing. This article summarises a great deal of current knowledge on the occurrence, structure, folding pathways, chemistry and biology associated with amyloidogenic peptides and proteins and highlights some key factors that have been found to influence amyloidogenesis.

Peptide amyloids, strands and sheets

Over the last two decades a number of diseases have been linked to "defective" protein folding (Gregersen et al. 2005). Following ribosomal synthesis of linear polypeptide chains of

R. S. Harrison · P. C. Sharpe · Y. Singh · D. P. Fairlie (✉)
Institute for Molecular Bioscience, Centre for Drug Design and Development,
University of Queensland, QLD 4072 Brisbane, Australia
e-mail: d.fairlie@imb.uq.edu.au · Fax: +61-7-3346-2990

amino acids, normal folding in the endoplasmic reticulum (ER) produces proteins in specific conformations that confer very specific biological functions. A substantial amount of cellular energy is dedicated to the task of protein folding, entropically facilitated by agents such as molecular chaperones, peptidyl-prolyl isomerases, and protein disulphide isomerases (Dobson 2003; Zhang and Kaufman 2006). The ER also has a very sophisticated quality control system to guarantee the structural fidelity of proteins, involving glycosylation and deglycosylation to ensure that only correctly folded proteins are secreted and that misfolded proteins are degraded through the ubiquitin proteasome system (UPS) (Dobson 2003). Incorrectly folded proteins trigger complex biological responses within the cell, such as the heat shock response and the unfolded protein response (UPR) that initiate transcription and translation of specific genes to assist in protein folding or apoptosis. These responses increase the degradation of misfolded proteins and enhance the protein-folding capacity of the ER (Zhang and Kaufman 2006). Overloading or failure of these systems results in accumulation and often aggregation of non-functional proteins within the cell (Zhang and Kaufman 2006), such aggregated proteins being called "amyloids".

Amyloid strictly refers to "extracellular deposits of protein fibrils with a characteristic appearance in the electron microscope (Fig. 1i–iii), a typical X-ray diffraction pattern (Fig. 1iv) and affinity for Congo red with concomitant green birefringence" (not shown; Westermark et al. 2005). However, much of the scientific literature has used a substantially expanded definition of amyloid to include any amorphous aggregates of native and recombinant proteins and peptides, as well as synthetic unnatural peptides, that possess some but not necessarily all of the above characteristics (Westermark 2005). The formation of amyloid (amyloidogenesis) has been historically associated with a heterogeneous group of diseases in which normal soluble proteins aggregate to form insoluble amyloid fibres (Lachmann and Hawkins 2006; Merlini and Westermark 2004). Amyloids are unusual in being kinetically stable structures (Dobson 2003; Selkoe 2003) that can persist for long periods and accumulate within tissues to form visible plaques (Dobson 2003). Amyloid proteins were first recognised in 1959 to have similar microscopic structural characteristics (Cohen and Calkins 1959) independent of their diverse origins. In 1968, the first amyloid cross-β structure was determined (Geddes et al. 1968) and implicated aggregated peptide β-strands as the key structural feature of amyloids.

β-strands are extended saw-toothed sequences of amino acids with amide bonds being almost coplanar with side chains that alternate above and below the plane of the peptide backbone. The idealised peptide β-strand has torsional angles (ϕ, ψ, τ) of –139°, 135° and –177° respectively (Fig. 2i; Gillespie et al. 1997). Isolated β-strands are uncommon in proteins, normally existing in hydrogen bonded pairs that constitute β-sheet structures (Fig. 2ii). Historically the β-strand has been considered a random structure rather than a discrete element of protein secondary structure; however, it is now recognised as a fundamental element of peptide structure that is recognised by a very wide range of bimolecular receptors, including proteolytic enzymes (Fairlie et al. 2000; Tyndall and Fairlie 1999; Tyndall et al. 2005), major histocompatibility complex (MHC) proteins (Brown et al. 1993) and farnesyl transferases (Qian et al. 1994).

β-sheets are parallel or anti-parallel alignments of two or more β-stranded peptides that are held together by inter-strand hydrogen bonds (Fig. 2ii). Of itself, the β-sheet is not an unusual structure since it accounts for more than 30% of the secondary structure of all proteins. β-Sheets consisting of strands aligned in parallel feature twelve-membered hydrogen-bonded rings, while those with strands in anti-parallel arrays are characterised by alternating 10- and 14-membered H-bonded rings. Dihedral angles commonly found in parallel ($\phi = -119°$, $\psi = 113°$) and anti-parallel ($\phi = -139°$, $\psi = 135°$) β-sheets are closer to those

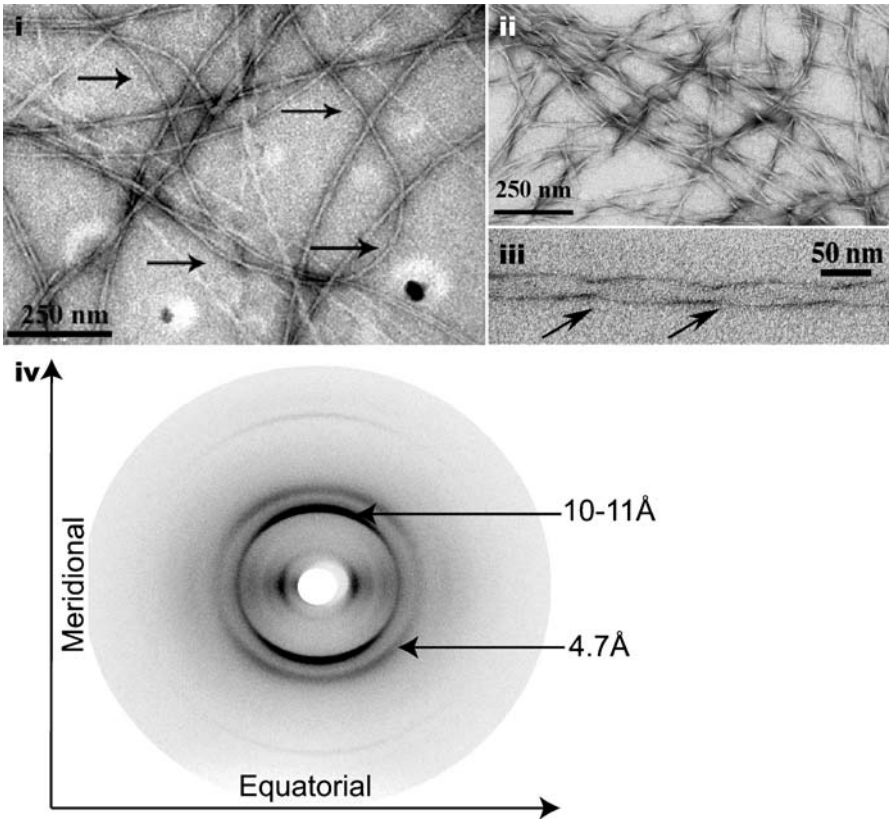

Fig. 1i–iv Methods of identifying amyloid formation. **i–iii** Typical electron micrographs of amyloid fibrils showing their linear, unbranched and flexible nature (**i**) and repeating twists of fibrils at regular intervals (**ii** and **iii**). **iv** Classic X-ray diffraction pattern. The 4.8-Å meridional arc is due to spacing between β-strands, with the peptide chains running 90° to the direction of the fibril axis. The equatorial spacing (10–11 Å) is due to the spacing between β-sheets, and varies with side chain composition

of the fully extended single-strand conformation ($\phi = \psi = \pm 180°$) than β-turns or α-helices. The β-sheet usually acts as a scaffold to stabilise protein architecture, but it is also an important recognition motif in some protein–protein and protein–DNA interactions that mediate biological processes and some notable diseases. For example, the arc and met repressors proteins (Raumann et al. 1994; Somers and Phillips 1992) and TATA box-binding proteins (Kim et al. 1993a, b; Nikolov et al. 1995) bind DNA via a β-sheet. β-Sheets also mediate clustering of membrane ion channel proteins (Doyle et al. 1996), and interactions between lymphocyte function-associated antigen-1 (LFA-1) and intercellular adhesion molecule-1 (ICAM-1) (Michne and Schroeder 1996). β-Sheet-containing proteins are able to fold rather than aggregate despite the observation that the edges of regular β-sheets appear pre-disposed to further H-bonding with other β-strands. Proteins normally avoid aggregation by positioning their charged side chains, β-bulges or proline residues, or by covering strands with protein loops (Richardson and Richardson 2002). The importance of these protection devices is highlighted by the difficulty of *de novo* design of β-proteins, known for their general insolubility and aggregation. Thus what sets amyloid peptides and proteins apart from most proteins is their greater tendency to aggregate. Historically, aggregates were defined by tinc-

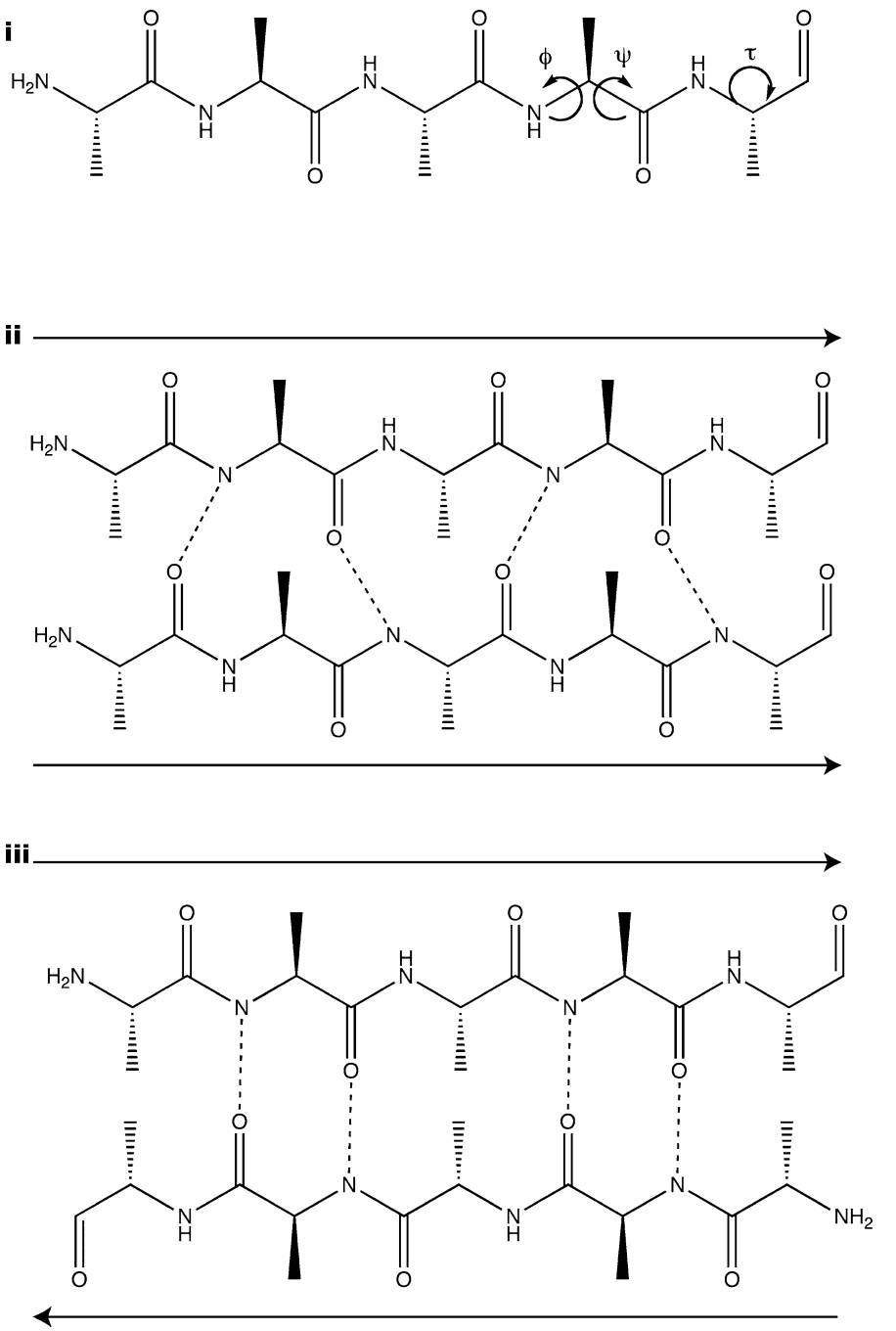

Fig. 2 i β-Strand schematic showing ϕ, ψ and τ angles where ϕ is the angle about the N-Cα bond, ψ is the angle about the Cα-C bond and τ is the angle about the N-Cα-C (peptide) bond. **ii** and **iii** β-Sheet schematics showing the H-bond network (*dashed lines*) between NH and C=O backbone residues of adjacent parallel and anti-parallel strands (direction shown by *arrows*)

torial properties, staining with dyes such as Congo red (Klunk et al. 1999) and thioflavin T (LeVine 1999) and they are notably more resistant to proteolysis than other proteins (Knauer et al. 1992; Koscielska-Kasprzak and Otlewski 2003) no doubt because of the need for individual β-strands, rather than the paired β-strands of β-sheets, to be recognised by proteases (Fairlie et al. 2000; Loughlin et al. 2004; Tyndall et al. 2005).

The structures of amyloid fibres have been investigated for the past 40 years using a wide range of techniques. Aggregates are typically fibrillar in electron microscopy images (Fig. 1i–iii), generally with a linear, unbranched structure of variable length and 60–120 Å in diameter (Makin and Serpell 2002). The generally accepted model of amyloid structure is depicted by a unique X-ray diffraction pattern (Fig. 1iv) characteristic of a cross-β structure, the peptide strand being almost perpendicular to the fibril axis (Fig. 3i; Serpell et al. 1999). The first amyloid protein X-ray crystal structure was the egg stalk of the lacewing *Chrysopa* solved in 1968 (Geddes et al. 1968). Geddes identified a cross-β structure where the protein consists of extended polypeptide chains, that folds back on itself to form a β-sheet perpendicular to the length of the fibril and β-ribbons associated face-to-face to form the width of the fibril (Fig. 3ii, iii and iv). A strong meridional reflection at 4.7 Å is indicative of the spacing between β-strands, a weaker equatorial reflection at 9.8 Å is due to inter-sheet spacing perpendicular to the fibril axis. This characteristic X-ray pattern is now routinely associated with the aligned amyloid fibrils (Serpell et al. 1999) and cross-β structure (Baxa et al. 2005; Blake and Serpell 1996; Makin and Serpell 2005; Malinchik et al. 1998; Nelson et al. 2005; Petkova et al. 2004; Siemer et al. 2005; Sikorski et al. 2003; Wang et al. 2005). The β-sheet nature of aggregates has also been established through numerous studies using circular dichroism, solid state nuclear magnetic resonance (NMR), and infrared spectroscopies.

The 3D structure of Alzheimer's Aβ18–32 (Fig. 3ii and iii), was shown to form a β-hairpin with an intermolecular salt bridge that is the basic unit for fibril growth (Luhrs et al. 2005). The crystal structure of *Saccharomyces cerevisiae* Sup35 was determined to 1.3 Å and shown to form sheets with distinctly different "wet" and "dry" interfaces (Fig. 3iv; Nelson et al. 2005). In this structure, the role of steric fit of the opposing sidechains—forming a "steric zipper"—was identified as a fundamental feature of these particular fibrils, and the authors proposed that it could also play a role in other amyloid fibrils. Very recently, the structures of CA150 and β2-microglobulin were determined by solid-state NMR spectroscopy (Ferguson et al. 2006; Iwata et al. 2006), both forming extended β-hairpin structures with tightly packed sidechains at the interface of the β-strands. α-Synuclein has a predominantly β-sheet core with a static N-terminal region and comparatively "dynamic" C-terminal tail (Heise et al. 2005). In addition to the 4.7 Å reflection, synchrotron radiation has revealed additional weaker, higher-angle reflections including a second reflection at approximately 4.7 Å for the transthyretin molecule. The additional reflections (2.39–2.41 Å and 3.2 Å, 2.8–2.9 Å, 2.22–2.27 Å and 2.00–2.02 Å) occur frequently and their absence from some images may be because they are too weak in intensity to be distinguished from noise. The similar diffraction patterns can only occur if the fibrils have well-defined and ordered molecular structures, and thus an interpretation of these results was that these amyloid fibrils have a β-sheet that is twisted to form a helix (Blake and Serpell 1996).

It has been suggested that the amphiphilicity of the peptide plays a significant role in determining whether peptide strands within the fibril are parallel or anti-parallel (Gordon et al. 2004). Parallel β-sheets in proteins usually adjoin α-helices, suggesting that they are inherently less stable on their own than are anti-parallel β-sheets. The Alzheimer's Aβ1–40 and Aβ10–35 peptides both have hydrophobic C-termini, and their reported assembly into parallel β-sheets (Petkova et al. 2002) allows the juxtaposition of the hydrophobic portions of the peptides, shielding them from aqueous solution. An anti-parallel disposition would

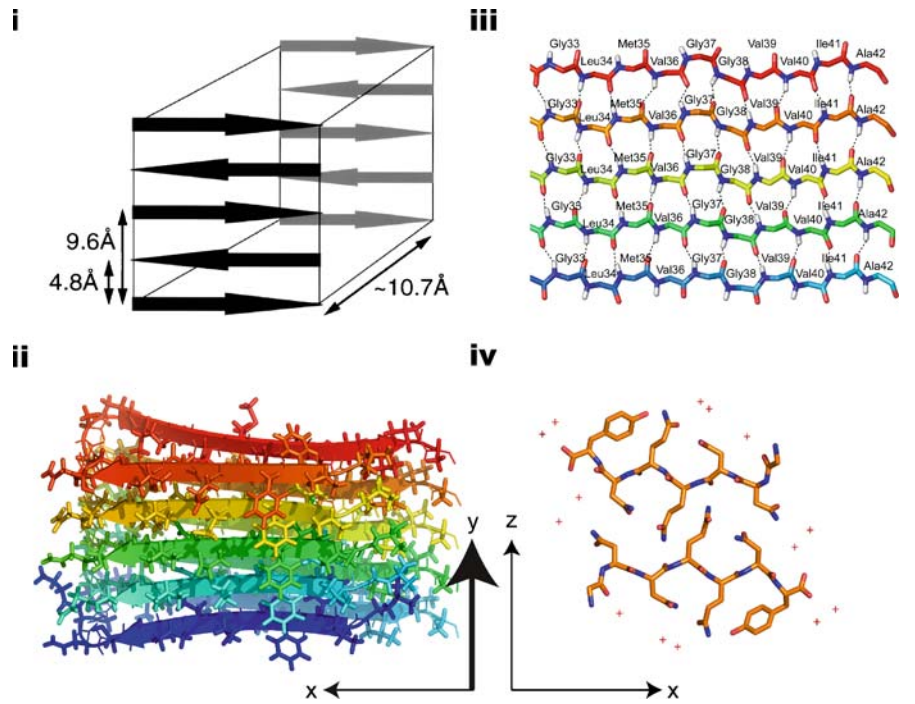

Fig. 3i–iv Cross-β structure of amyloid. **i** Idealised cross-β structure relating distances observed in the X-ray diffraction pattern to the structure. The 4.8-Å meridional arc is due to the spacing between β-strands, with the peptide chains roughly 90° to the direction of the fibril axis. The equatorial spacing 10–11 Å is due to the spacing between β-sheets, and varies with side chain composition. Figure taken from Serpell (2000) **ii** The solid-state NMR structure of Aβ18–42 showing cross-β structure (pdb code 2BEG) (Luhrs et al. 2005). **iii** Enlargement of Aβ34–42 showing parallel β-sheet and hydrogen bond network (*dashed lines*) between adjacent strands. **iv** Crystal structure of Sup35 (pdb 1YJP) (Nelson et al. 2005) showing alignment of GNNQQNY monomers and highlights the role of steric interactions between the sidechains in these fibrils. Figures generated by MacPyMOL (for MacOS X, DeLano Scientific, South San Francisco)

be costly energetically because of the forced association of hydrophobic and hydrophilic regions. Aβ16–22 and Aβ34–42 both have a centrally located hydrophobic segment and thus no advantage of sequestration of hydrophobic regions provided by either a parallel or anti-parallel arrangement. The anti-parallel β-sheet arrangements found for these two peptides may then be the result of favourable charge interactions between side chains or termini, or improved H-bonding. The role of amphiphilicity was investigated for the Aβ16–22 peptide and an *N*-acylated octanoic derivative, which had increased amphiphilicity because of the long alkyl tail (Gordon et al. 2004). Oct-Aβ16–22 formed fibrils that appeared identical under the microscope to those of Ac-Aβ16–22, but solid-state NMR spectra for isotopically labelled samples showed a parallel β-sheet arrangement in contrast to that found for the acetylated derivative (Gordon et al. 2004).

In 2002, Perutz et al. (2002a) proposed an alternative structure for amyloid protofibrils, a water-filled nanotube formed by a polyglutamine protein. This model is a parallel β-helix consisting of an extended polypeptide chain wrapping around a cylindrical template, where adjacent strands of the helix are connected through H-bonds (Fig. 4) and is based on two key features of the polyglutamine diffraction data; the absence of a 10-Å reflection and the presence of a weak, low-angle reflection of 31 Å.

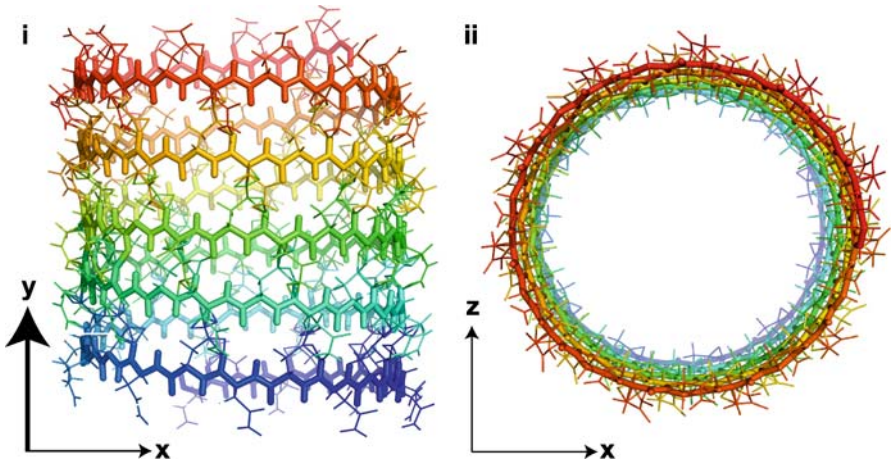

Fig. 4i, ii Alternative β-helix structural model proposed for amyloid proposed by Perutz et al. (2002a) showing parallel β-strand alignment (**i**) and the helical "nanotube" viewed from the top (**ii**). The fibril length is shown in the *y* plane (*bolded*). Model generated in InsightII (v.2000, Accelrys) using a poly-Asn peptide with a repeating pair of ϕ and ψ values ($\phi_1 = 160°$; $\psi_1 = -170°$ and $\phi_2 = -161°$; $\psi_2 = 168°$), backbone and sidechains shown as *sticks*, illustrated in MacPyMOL (for MacOS X, DeLano Scientific, South San Francisco). (Adapted from Perutz et al. 2002a)

In support of this model, Kishimoto et al. (2004) have studied the structure of fibres formed by three fragments of the yeast prion protein Sup35. Dried, oriented samples used gave a meridional arc at 4.7 Å due to β-strands perpendicular to the fibre axis. In addition, a broader equatorial arc observed around 9 Å was absent from fibrils prepared in a hydrated state, although a 4.7 Å reflection was present. This suggested that the β-sheet stacking observed in the dried fibrils was an artefact of sample preparation. The diffraction data for the hydrated state are consistent with a β-helix or nanotube arrangement proposed by Perutz et al. (2002a) with 20 amino acid residues in the turn of the helix. A β-helical nanotube would have a water-filled interior, and collapse of the tube upon dehydration would result in the formation of stacked β-sheets and hence the 9 Å equatorial reflection in the X-ray diffraction pattern with similar diffraction data for α-synuclein (Serpell et al. 2000) and Aβ (Inouye et al. 1993). However, the Perutz model has been highly controversial and the preponderance of evidence appears now to be in conflict with this model.

At a macromolecular level, aggregates are typically fibrillar in electron microscopy images (Fig. 1i–iii) generally with linear, unbranched fibrils of variable length. Each fibril is thought to consist of several protofilaments, the number being specific to the particular amyloid protein. Improved imaging of protofilaments has revealed that certain fibrils are clearly helical, with the protofilaments slowly twisting around each other (Fig. 5). For Aβ34–42 fibrils, the twisted fibril "unwinds" under denaturing conditions (Halverson et al. 1990) and for Aβ1–40 at high pH (Fraser et al. 1992), suggesting that these protofilaments are associated through both electrostatic and hydrophobic interactions. However, it has also become very clear that there are several amyloid fibril forms, even from the same protein sample (Ferguson et al. 2006; Heise et al. 2005; Iwata et al. 2006).

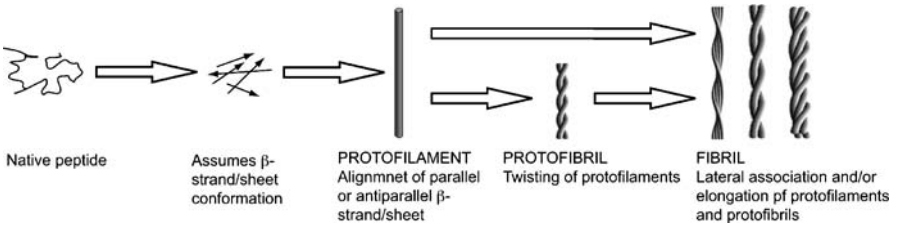

Fig. 5 Hierarchy of amyloid fibril formation. Native protein or peptide unfolds and acquires a β-strand secondary structure. These β-strands align (either in a parallel or anti-parallel arrangement) to form sheets and protofibrils with the direction of the β-strand perpendicular to the fibril axis. (Adapted from Kad et al. 2003)

Amyloid occurrence

Many amyloid proteins are now known (Tables 1, 2 and 3) and although they vary in primary sequence, origin and significance in normal versus aberrant physiology, they all share the property of forming water-insoluble stable aggregates with β-sheet structures. In recent years, amyloid proteins have been found throughout the human body, in a variety of different species (Kelly and Balch 2003), and to play a key functional role in some cases (e.g. human melanosomes; Berson et al. 2003; Fowler et al. 2006). These discoveries have challenged the previous implication that amyloids occur through defective protein folding and cause disease, suggesting instead that amyloids may comprise evolutionally conserved folds that perhaps have important, as yet unidentified, roles in normal cellular physiology.

Amyloids in disease

Over 30 human diseases (Dobson 2004; Hirschfield 2004; Merlini and Westermark 2004; Stefani and Dobson 2003) are now associated with amyloidogenesis (Table 1), the formation of aggregated β-sheet structures that appear as water-insoluble deposits of "amyloid" fibrils. Amyloidosis can be classified very broadly into either localised or systemic amyloidosis, depending on the location of the amyloid fibres and the genetic (hereditary) or acquired nature of the precursor protein. Among examples listed (Table 1) of localised amyloidosis in the brain are Alzheimer's disease caused by aggregated β-amyloid protein and tau protein; spongiform encephalopathies such as Creutzfeldt-Jakob disease (humans), scrapie (sheep), bovine spongiform encephalopathy (mad cow disease) due to cellular prion PrP^c proteins; familial polyneuropathy due to aggregated transthyretin; Huntington's disease (HD) due to aggregated huntingtin protein and Parkinson's disease due to aggregated α-synuclein. Among systemic amyloidoses are amyotrophic lateral sclerosis (ALS) due to aggregated superoxide dismutase; type II diabetes due to aggregated amylin or islet amyloid peptide and medullary thyroid carcinoma due to aggregated calcitonin (see Table 1).

The first evidence for involvement of protein misfolding and aggregation in these diseases came at post-mortem from sufferers of neurodegenerative disorders (Alzheimer et al. 1995). The most researched, localised form of amyloidosis is Alzheimer's disease, characterised by the deposition of neuritic amyloid plaques and neurofibrillary tangles. Extracellular plaques, consisting mainly of 42-residue amyloid-β proteins (Aβ), form around cerebral vessel walls and in the brain parenchyma. As a result, Alzheimer's patients lose their memory, cognitive abilities and their personality can change dramatically (Mattson 2004). Other molecules found in Alzheimer's amyloid plaques include proteoglycans, α_1-

Table 1 Pathological amyloid proteins and their precursors, associated diseases and amyloidogenic sequences

Amyloid type	Sequence or mutated wild-type sequences	Disease or involved tissues
As described and approved by the Nomenclature Committee of the International Society of Amyloidosis		
β2-Microglobulin (Aβ2M)	Res 20–41 (SNFLNCYVSGFHPSDIEVDLLK) (Hasegawa et al. 2003) Res 21–31 (NFLNCYVSGFH) (Hasegawa et al. 2003) Res 72–99 (PTEKDEYACRVNHVTLSQPKIVKWDRDM) (Ivanova et al. 2003) [for review, see also Jones et al. (2003)]	Peri-articular and occasionally associated with long term dialysis, Haemodialysis-related amyloidosis
(Pro)calcitonin (ACal)	Res 14–18 (DFNKF) (Reches et al. 2002)	Medullary carcinoma of the thyroid
α-S2C casein (ACas)	Res 81–112 (ALNEINQFYQKFPQYLQYLYQGPIVLNPWDQV) (Niewold et al. 1999) Res 81–113 (ALNEINQFYQKFPQYLQYLYQGPIVLNPWDQVK) (Niewold et al. 1999) Res 81–125 (ALNEINQFYQKFPQYLQYLYQGPIVLNPWDQVKRNAVPITPTLNR) (Niewold et al. 1999)	Mammary gland corpora amylacea (from *B. taurus*)
Aβ-Protein precursor (Aβ)	Res 11–25 (EVHHQKLVFFAEDVG) (Tjernberg et al. 1999) Res 14–23 (HQKLVFFAED) (Tjernberg et al. 1999) Res 16–23 (AcKLVFFAG-NH_2) (Balbach et al. 2000) Res 34–42 (LMVGGVVIA) (Lansbury et al. 1995) Res 25–35 (GSNKGAIIGLM) (Pike et al. 1995) Res 19–20 (FF) (Reches and Gazit 2003)	Alzheimer's disease
ABri	RTVKKNIIEEN (mutation in the terminal codon leading to an 11-residue terminal extension) (Gibson et al. 2005)	Familial British dementia
ADan	LFLNSQEKHY (mutation in the terminal codon leading to a 10-residue extension) (Gibson et al. 2005)	Familial Danish dementia
APin	Res 1–46 of hypothesised FLJ3 gene (MPYVFSFKMPQEQGQMFQYYPVYMVLPWEQPQQTVRRSPQQTRQQQ) (Solomon et al. 2003)	Calcifying epithelial odontogenic tumours (Pindborg tumours)
Apolipoprotein AI (AapoAI)	Residues 1–93 of ApoAI (Andreola et al. 2003)	Familial amyloid polyneuropathy III
Apolipoprotein AII (AapoAII)	(GSVQTIVFQPQLASRTPTGQS) Stop78G or Stop78S mutations resulting in a 21-residue extension shown at the C-terminal of the protein (Benson et al. 2001)	Hereditary renal amyloidosis
Apolipoprotein AIV (AapoAIV)	*wt* protein (Bergstrom et al. 2001, 2004)	Systemic amyloidosis
Atrial natriuretic factor (AANF)	*wt* protein (Johansson et al. 1987)	Atrial amyloidosis

Table 1 (continued)

Amyloid type	Sequence or mutated wild-type sequences	Disease or involved tissues
Cystatin C (ACys)	L68Q mutation (Ghiso et al. 1986)	Hereditary renal amyloidosis, hereditary cerebral amyloid angiopathy
Fibrinogen α-chain (AFib)	R554L (Benson et al. 1993), E526V (Uemichi et al. 1994), 4904delG (Uemichi et al. 1996)	Hereditary renal amyloidosis
Gelsolin (AGel)	Res 183–210 (FNNGDCFILDLGNNIHQWCGSNSNRYER) (Fadika and Baumann 2002; Maury et al. 1994); D187 mutant often involved (D187 N, D187Y) (Benson et al. 2001) Res 182–192 (SFNNGDCFILD) (Maury et al. 2003) Res 183–191 (FNNGNCFIL) (Maury et al. 2003) Res 184–190 (NNGNCFI) (Maury et al. 2003)	Hereditary renal amyloidosis
Genetically variant transthyretin (ATTR)	Over 100 point mutations; for a recent review, see Ando et al. (2005)	Familial amyloid polyneuropathy
Insulin (AIns)	*wt* protein (Storkel et al. 1983)	Iatrogenic amyloidosis
Islet amyloid polyprotein, (Amylin) (AIAPP)	Res 20–29 SNNFGAILSS (Tenidis et al. 2000) Res 30–37 TNVGSNTY (Nilsson and Raleigh 1999) Res 22–29 NFGAILSS (Azriel and Gazit 2001) Res 24–29 GAILSS (Nilsson and Raleigh 1999) Res 22–27 NFGAIL (Tenidis et al. 2000) Res 23–27 FGAIL (Tenidis et al. 2000)	Type II diabetes
Kerato-epithelin (AKer)	R124C (Schmitt-Bernard et al. 2000), P501T (Kawasaki et al. 1999), V505D (Tian et al. 2005), L518P (Hirano et al. 2000), L527R (Funayama et al. 2006), N544S (Nakagawa Asahina et al. 2004) mutations of the betaig-h3 (TGFBI) gene, A546D and P551Q missense changes (Aldave et al. 2004)	Lattice corneal amyloid dystrophy
Lactoferrin (ALac)	Res 539–546 (NAGDVAFV) (Nilsson and Dobson 2003)	Amyloidosis in seminal vesicles, cornea and brain
Lysozyme (ALys)	Compound heterozygosity in exon 2 (Thr70Asn) and exon 4 (Trp112Arg) (Rocken et al. 2006)	Hereditary renal amyloidosis, hereditary non-neuropathic systemic amyloidosis
Medin (AMed)	Res 147–154 (NFGSVQFV) (Haggqvist et al. 1999)	Aortic medial amyloidosis
Monoclonal immunoglobulin heavy chain (AH)	Deletion of domains (first CH1, hinge and second CH2 heavy-chain constant regions) compare to *wt* protein (Eulitz et al. 1990)	Immunoglobulin heavy chain amyloidosis

Table 1 (continued)

Amyloid type	Sequence or mutated wild-type sequences	Disease or involved tissues
Monoclonal immunoglobulin light chain (AL) or fragments	No common amyloidogenic consensus sequence (Bellotti et al. 2000); λ light chain more prominent in depositions than κ chains (Isobe and Osserman 1974); most often involves λ VI light chains (Solomon et al. 1982); mutations in the framework regions of VL region are most effective at disrupting native folding (Bellotti et al. 2000)	Immunoglobulin light-chain, amyloidosis, myeloma-associated amyloidosis, monoclonal plasma cell dyscrasias
Normal plasma transthyretin (ATTR)	*wt* protein (Gustavsson et al. 1991)	Senile systemic amyloidosis, cardiac involvement
Prion protein (APrP)	Res 106–126 (KTNMKHMAGAAAAGAVVGGLG) (Florio et al. 2003; Forloni et al. 1993) Res 178–191 (DCVNITIKQHTVTT) (Gasset et al. 1992); Res 202–218 (DIKIMERVVEQMCTTQY) (Gasset et al. 1992) Res 113–127 (AGAAAAGAVVGGLGG) (Gasset et al. 1992) Res 113–120 (AGAAAAGA) (Gasset et al. 1992)	Spongiform encephalopathies
Prolactin (APro)	Res 7–21 (GAARCQVTLRDLFDR) (Westermark et al. 1997) Res 20–34 (DRAVVLSHYIHNLSS) (Westermark et al. 1997) Res 43–57 (RYTHGRGFITKAINS) (Westermark et al. 1997)	Amyloidosis in the pituitary gland, prolactinomas
Semenogelin I (ASgI)	Res 1–142 of *wt* semenogelin I (Linke et al. 2005)	Senile seminal vesicle amyloidosis
Serum amyloid A protein (AA) or fragments	Res 2–12 (SFFSFLGEAFD) (Westermark et al. 1992)	Chronic inflammatory diseases, secondary systemic amyloidosis
As reported in the literature, with all or some of the amyloid characteristics		
α_{1A} voltage-dependent calcium channel subunit	Mutations leading to increase in polyglutamine stretches (Q6–17 normal; Q21–30 pathological) (Mantuano et al. 2003)	Spinocerebellar ataxia type 6 (SCA6)
α-Synuclein (Lewy bodies)	Res 8–18 (GAVVTGVTAVA) (el-Agnaf and Irvine 2002) Res 8–16 (GAVVTGVTA) (Bodles et al. 2001) Res 6–14 (VGGAVVTGV) (Du et al. 2003; H.Y. Hu, personal communication)	Parkinson's disease (neurons)
Androgen receptor protein	Mutations leading to increase in polyglutamine stretches (Q11–35 normal, Q40–62 pathological) (Katsuno et al. 2004)	Spinal and bulbar muscular atrophy (Kennedy's disease)
Ataxin 1, 2 or 3	Mutations leading to increase in polyglutamine stretches Type I: Q4–39 normal; Q40–83 pathological (Limprasert et al. 1997) Type II: Q15–24 normal; Q36–52 pathological (Figueroa and Pulst 2003) Type III: Q14–41 normal. Q55–82 pathological (Shehi et al. 2003) Type VII: Q4–18 normal; Q38–130 pathological (Lebre and Brice 2003)	Spinocerebellar ataxia type 1 (SCA1), Spinocerebellar ataxia type 2 (SCA2), Spinocerebellar ataxia type 3 (SCA3) (Machado Joseph Disease) Spinocerebellar ataxia type 7 (SCA7)

Table 1 (continued)

Amyloid type	Sequence or mutated wild-type sequences	Disease or involved tissues
Atrophin-1	Mutations leading to increase in polyglutamine stretches (Q7–23 normal; Q49–75 pathological) (Kanazawa 1998; Oyanagi 2000; Tsuji 1999)	Dentatorubral-pallidoluysian atrophy (DRPLA)
Huntingtin bodies (Huntingtin protein)	Mutations leading to increase in polyglutamine stretches (Q10–35 normal; Q36–120 pathological) (Kagan et al. 2001; Ross 2002)	Huntington's disease (neurons)
Lung surfactant protein C	Res 9–22 (VVVVVVVLVVVVIV) (deMello and Lin 2001; Hosia et al. 2002; Schmitt-Bernard et al. 2000; Seymour and Presneill 2002; Trapnell et al. 2003)	Pulmonary alveolar proteinosis
Polyadenine-binding protein 2	Mutations to increase number of Ala residues in Ala-stretch Res 2–11 (AAAAAAAAAA) (Brais 2003; Fan and Rouleau 2003; Giri et al. 2003)	Oculopharyngeal muscular dystrophy
Superoxide dismutase 1	G37R, L38 V, G41S, G41D, H43R, G85R, G93C, G93A, E100G, L106 V, I114T (Rosen et al. 1993)	Amyotrophic lateral sclerosis
TATA-box binding protein	Mutations leading to increase in polyglutamine stretches (Q25–42 normal; Q43–66 pathological) (Nakamura et al. 2001; Tsuji 2004)	Spinocerebellar ataxia 17
Tau (neurofibrillary tangles)	Res 306–311 (VQIVYK) (Goux et al. 2004) Res 307–311 (QIVYK) (Goux et al. 2004) Res 308–311 (IVYK) (Goux et al. 2004) Res 309–311 (VYK) (Goux et al. 2004)	Fronto-temporal dementias, Alzheimer's disease (neurons)

antichymotrypsin and apolipoprotein E (Atwood et al. 2002). In normal physiology, amyloid precursor protein (APP) is proteolytically cleaved by β- and γ-secretases to form a range of β-peptides known as Aβ39–43. It has been proposed that Aβ is secreted in response to neuronal activity and that it acts to downregulate excitatory synaptic transmission, providing a homeostatic mechanism for regulation of levels of neuronal activity (Esteban 2004; Kamenetz et al. 2003). Tangles in Alzheimer's disease consist of aggregates of hyperphosphorylated tau protein and are present in the cytoplasm of degenerating neurons. The structure of Tau protein is still uncertain, although recently suggested to be α-helical (Sadqi et al. 2002). Patients with Parkinson's disease exhibit aggregates of Lewy bodies within the cytoplasm of neurons from the substantia nigra, the major constituent being a fragment of α-synuclein protein (el-Agnaf and Irvine 2002). Prion diseases (Aguzzi and Haass 2003) are characterised by formation of protease-resistant aggregates rich in β-sheeted prion peptides (Baskakov et al. 2002; Forloni et al. 1993; Petchanikow et al. 2001; Prusiner and DeArmond 1994). Patients with Huntingtin's disease exhibit intranuclear deposition of huntingtin protein, containing a long polyglutamine repeat (Walling et al. 1998), and such repeats have also been found in other disease-causing proteins (La Spada and Taylor 2003).

We now know that amyloid deposits can form in virtually every organ, tissue and region of the human body. They can lead to life-threatening diseases due to catastrophic toxic effects on one or more vital organs, but the identities of all of these amyloids have not yet been properly characterised. Amyloid proteins, either wild-type or mutant forms, are synthesised at multiple sites, secreted into the plasma, transported by the circulatory system, and deposited in tissues. In ALS, aggregates of superoxide dismutase (SOD1) build up within cell bodies and axons of motor neurons (Rowland and Shneider 2001). Human calcitonin, a 32-residue peptide that normally inhibits osteoclasts and protects against excessive bone resorption (Breslau 2000), also assembles into amyloid fibrils that are linked to medullar carcinoma of the thyroid (Kamihira et al. 2000). Amyloid deposits found in patients with type II diabetes originate from accumulation in the pancreas of the proteins known as amylin or islet amyloid peptide (Nilsson and Raleigh 1999).

Human gelsolin is an 80-kDa intracellular or 83-kDa extracellular protein that is generated from alternate transcription initiation sites and messenger RNA (mRNA) splicing (Kwiatkowski et al. 1986). A single point mutation, either D187N or D187Y, results in systemic familial amyloidosis of Finnish type (FAF) causing an onset of ophthalmologic, dermatologic and neurologic symptoms in the third to fourth decade of life (Table 1; Kiuru 1998; Maury 1991). Wild-type gelsolin is transcribed, then stabilised by binding calcium ions, after which it is secreted from the cell as a full-length soluble protein (Yin 1987). However, this single mutation prevents calcium binding (Chen et al. 2001a), destabilising the mutant which is then cleaved by furin in the trans-Golgi network, and then by one or more β-gelsolinases after secretion, producing full-length gelsolin or fragments which can self-assemble into amyloid fibrils (Chen et al. 2001a). Ultimately, the point mutation results in altered proteolytic processing of mutant gelsolin to produce amyloid fibrils, which are later released into the cytoplasm and deposited in tissues around the body.

There is still considerable debate about the role and importance of amyloid formation in each of the various diseases described in Table 1 (Chromy et al. 2003; Kayed et al. 2003; Volles and Lansbury 2003; Walsh et al. 2002). Except for polyglutamine-containing proteins, the listed disease-causing amyloidogenic proteins appear to have little in common. They vary in length, hydrophobicity and native secondary structure. Moreover, proteins that are stable *in vivo* are still able to undergo transitions under destabilising conditions, such as pH extremes or addition of organic solvents, that lead to amyloid formation (Fändrich et al. 2001, 2003; Pertinhez et al. 2001). These observations, together with the finding of

amyloids in many different species, have led to the suggestion that all proteins may have an inherent capacity to form amyloid under suitable denaturing conditions (Table 2; Chiti et al. 1999; Dobson 1999). Indeed it appears that there are specific regions within proteins that are responsible for the formation of these protein aggregates, and that perhaps folding mechanisms, chaperones and other environmental conditions within the cell regulate protein aggregation. Key differences have been observed in the formation of pathological (Table 1) and non-pathological (Table 3) amyloids. For example, in gelsolin amyloid disease, proteolysis of gelsolin by furin is a slow unregulated process, whereas Mα (component of Pmel17 in humans, Table 3) is also initiated by furin but forms very quickly in membrane-defined compartments (Fowler et al. 2006). Fowler et al. have suggested that key differences in packaging and assembly between physiologically important and pathological amyloids may determine the usefulness of the protein by managing reactive toxic species and reducing damage to the cell.

Non-pathological amyloids

The list of amyloid proteins with no known pathological role in disease has grown dramatically in recent years (Table 2 and 3), and it now seems more likely than not that amyloids have important roles in normal physiology. A number of proteins, including a variety of human proteins, which are not known to form amyloids *in vivo*, have been shown to form amyloids *in vitro* under certain destabilising conditions. However, human coagulation factor XIII forms amyloid fibrils under physiological conditions suggesting that amyloid fibrils may actually form *in vivo* as well. Similarly, fibronectin type III-9 module from *Mus musculus* and triacylglycerol lipase from *Candida antarctica* are not known to form amyloid fibrils *in vivo* but form amyloid *in vitro* under physiological conditions (Table 2).

In humans, perhaps the best-known example of an aggregated β-sheet containing fibrous protein is β-keratin, an aggregated β-sheet-containing protein. β-Keratin is the major constituent of human nail, bird feather calamus and rachis, and reptile scales and claws. This differs from amyloids by having a β-structure in which the peptide chains are parallel, rather than perpendicular, to the direction of the fibril axis.

Insects and arachnoids produce well-known amyloids. Silk and spider webs, like β-keratin, also differ from amyloids in being fibrous β-sheet proteins composed of peptide strands that are parallel, rather than perpendicular, to the direction of the fibril axis. For the process of silk formation by spiders, it has been proposed that fibrils in the silk gland have an initial cross-β structure (Kenney et al. 2002; Table 3) that, when stretched, assume parallel β-structures. However, X-ray diffraction for a peptide derived from the central domain of the A class of chorion proteins, derived from *Antheraea polyphemus* eggshells, displayed β-sheets perpendicular to the fibril axis, the same cross-β structure that occurs in amyloid proteins (Iconomidou et al. 2000; Table 3). The stability and strength of the amyloid fibres provides mechanical and biological protection for the oocyte and developing embryo from a variety of environmental and predatory hazards.

Bacteria also form amyloids that appear to be used in normal physiology (Gebbink et al. 2005). *Escherichia* and *Salmonella* species use highly aggregated fibres, called curli, to assist in the colonisation of inert surfaces and to form biofilms (Chapman et al. 2002; Loferer et al. 1997). Chapman and co-workers (2002) described a protein called CsgA, isolated from the cell surface of *Escherichia coli*, that has the characteristic features of amyloid fibrils. Isolated fibres were 6–12 nm in width and of varying lengths (Table 3). Circular dichroism (CD) spectra indicated a secondary structure rich in β-sheet, and the fibres bound the

Table 2 Non-amyloidogenic proteins or peptides that form amyloid fibrils *in vivo*

Protein	Species	Conditions (reference)
α-, β-, γ-Crystallins	*B. taurus*	10 mg/mL peptide, 0.1 M phosphate buffer, pH 7.4, 60°C, 24 h (Meehan et al. 2004) 10 mg/mL peptide, 10% TFE, pH 2.0, 60°C, 4 h (Meehan et al. 2004)
α1 Anti-trypsin C-terminal peptides	*H. sapiens*	15 mM Tris, pH 7.4, 0.15 M NaCl (Bironaite et al. 2001; Janciauskiene et al. 1995)
κ-Casein	*B. taurus*	Reduction and carboxymethylation, 37°C, pH 6.75, 25 mM PIPES, 80 mM KCl (Farrell et al. 2003)
β-Lactoglobulin	*B. taurus*	pH 7.0, 37°C, 3–5M urea, 10–30 days (Hamada and Dobson 2002)
α-Spectrin SH3 domain	*Gallus spp.*	N47A: pH 3.0, 37°C, 30 mg/mL, several days (Morel et al. 2006)
Acetylcholinesterase fragment (residues 586–599)	*H. sapiens*	200 μM peptide concentration, 10 mM phosphate buffer, pH 7.0 (Cottingham et al. 2002; Greenfield and Vaux 2002)
Acidic fibroblast growth factor	*N. viridescens*	65°C (Srisailam et al. 2003) 8–50% TFE (Srisailam et al. 2002)
Acylphosphatase	*Equine spp.*	15–25% TFE (Plakoutsi et al. 2004) 25% TFE (Monti et al. 2004) 25% TFE, 50 mM acetate buffer, pH 5.5 (Chiti et al. 2002a) 19–35% TFE, 50 mM acetate buffer, pH 5.5 (Calamai et al. 2003; Chiti et al. 2000, 1999)
Albebetin (ABB) and derived peptides	Synthetic	20 mg/mL of peptide in 20 mM Tris buffer (pH 7.3), 0.2% NaN, 57°C (Lavrikova et al. 2006)
Albumin	*B. taurus*	Glycation: 37°C, 140 mM NaCl, 2.7 mM KCl, 10 mM Na_2HPO_4, 1.8 mM KH_2PO_4, 1 M D-glucose-6-phosphate disodium salt hydrate, 0.05% NaN_3, pH 7.3 (Bouma et al. 2003)
Alcohol dehydrogenase	*S. cerevisiae*	> 7.3 M ethanol, 25°C, 10 min (Shimizu et al. 2004)
Amphoterin peptide 12–27	*H. sapiens*	PBS, pH 7.2, 4 days, 37°C (Kallijärvi et al. 2001)
Anti-freeze protein type 1 (AFP)	*Platichthys spp.* (flounder)	Multiple freeze–thaw cycles, pH 4 or 7 (Graether et al. 2003)
Apo-cytochrome C_{552}	*H. thermophilus*	C11A C14A double mutant, 20 mM phosphate buffer, pH 7.3 (Pertinhez et al. 2001)
Apomyoglobin	*Equine spp.*	pH 9.0, 55–75°C (Fändrich et al. 2003) W7FW14F mutant, pH 7 (Sirangelo et al. 2004)
Betabellin 15D and 16D	Synthetic	50% CH_3CN (Inouye et al. 2002) 5 mM MOPS, 250 mM NaCl, pH 7 (Lim et al. 2000)
CA150 (second WW domain)	*H. sapiens*	10 mM sodium phosphate, pH 7.0, 0.02% sodium azide (Ferguson et al. 2006)
Caspase-activate DNase (CAD domain)	Not specified	50 uM protein, 20 mM Gly-HCl, pH3.4, 35°C, 20 h (Uegaki et al. 2005)
Coagulation factor XIII	*H. sapiens*	pH 7.4, PBS, 37°C, 3 days (Kallberg et al. 2001)
Cold shock protein A	*E. coli*	pH 2 (Alexandrescu 2001; Alexandrescu and Rathgeb-Szabo 1999)

Table 2 (continued)

Protein	Species	Conditions (reference)
Cold shock protein B	*B. subtilis*	10 or 90% CH_3CN, formate buffer, pH 4.0 (Gross et al. 1999; Wilkins et al. 2000)
Copper metallochaperone CCH C-domain	*A. thaliana*	Tris-HCl 25 mM, pH 7.2 (Mira et al. 2004)
Cytochrome c	*B. taurus* *H. thermophilus*	50 mM Tris-HCl, pH 9.0, 75°C, 12 h (de Groot and Ventura 2005) C11A and C14A (Pertinhez et al. 2001)
Endostatin	*H. sapiens*	8 M urea, 10 mM imidazole, 10 mM β-mercaptoethanol (Kranenburg et al. 2003) 1-Stearoyl-2-oleoyl-sn-glycero-3-phosphocholine—phosphatidylserine (8:2 molar ratio), 20 mM HEPES, 0.1 mM EDTA, pH 7.4 (Zhao et al. 2005)
FBF 28 WW domain	*M. musculus*	10 mM NaPi, pH 7, 150 mM NaCl, 37°C (Ferguson et al. 2003)
Fibronectin type III-9 module	*M. musculus*	pH 7.4, 37°C (Briknarova et al. 2003; Litvinovich et al. 1998)
GAGA factor	*Drosophila spp.*	300 mM KCl, pH 7.6–8.5 (Agianian et al. 1999)
Glycophorin A (residues 70–86)	*H. sapiens*	Hexafluoro-2-propanol, 25°C, 30 min, 6–14 days, shaking 200 rpm (Liu et al. 2005)
Glycoprotein B	Herpes simplex virus 1	20 mM MOPS, pH 7.4 (Cribbs et al. 2000)
Hydrogenase maturation factor Hyp-F (N-terminal)	*E. coli*	25% TFE, 50 mM acetate, pH 5.5 (Calamai et al. 2003)
Insulin	*B. taurus*	68°C, pH 2.6 (Bouchard et al. 2000; Burke and Rougvie 1972; Waugh 1957)
Methionine aminopeptidase	*P. furiosus*	3.65 M Gu·HCl, pH 2.9 (Yutani et al. 2000)
Monellin and monellin B chain	*D. cumminsii*	40–60°C, pH 2.5 (Konno 2001)
p53	*H. sapiens*	*wt* and R37H: 0.25–3.2 mg/mL in 20 mM phosphate, pH4.0, 50 mM NaCl, increasing temperature to 95°C and then cooling to 25°C (Lee et al. 2003) R37H: 10 mM phosphate, 50 mM NaCl adjusted to pH 4.0 (Galea et al. 2005)
p85 phosphatidyl inositol-3-kinase (SH3 domain)	*B. taurus*	pH 2.0 (Polverino de Laureto et al. 2003)
Phosphatidylinositol 3-kinase (P13-SH3 domain)	*B. taurus*	10 mg/mL at 20 mM NaH_2PO_4, pH 2.0 at room temperature or 4°C (Guijarro et al. 1998)
Phosphoglycerate kinase	*S. cerevisiae*	10 mM HCl (pH 2), 150 mM NaCl (Damaschun et al. 2000; Damaschun et al. 1999; Modler et al. 2003)
Presenilin 1 and presenilin 2 peptides	*H. sapiens*	(Synthetic) 5 mg/mL at room temperature overnight (Maury et al. 1997)
Procarboxypeptidase A2 activation domain	*H. sapiens*	pH 3.0, 95°C, 30 min (Villanueva et al. 2003; Villegas et al. 2000)

Table 2 (continued)

Protein	Species	Conditions (reference)
Protein G (β1 domain) (*wt* and mutants)	*Staphylococcus spp.*	50 mM $NaCH_3COOH$, pH 5.2, 61–65°C, 300 rpm, 24–36 h (Ramirez-Alvarado et al. 2000; Wang et al. 2005) Seeding with preformed crystals (Ramirez-Alvarado et al. 2000)
Prothymosin α	Mammalian	100 mM Gly·HCl, pH 2.5–3.5, 37°C (Pavlov et al. 2002)
R61 D-alanyl-D-alanine transpeptidase	*Streptomyces R61*	pH 7.4, PBS, 37°C, 3 days (Kallberg et al. 2001)
RNase Sa	*S. aureofaciens*	35% TFE, pH 3.5, 6 h (Schmittschmitt and Scholtz 2003)
Stefin A (cystatin A)	*H. sapiens*	86°C, 2 h, pH 2.5, 0.15 M NaCl, Gly·HCl (Jenko et al. 2004)
Stefin B (cystatin B)	*H. sapiens*	15 mM acetate, 150 mM NaCl, pH 4.77 (Zerovnik 2002; Zerovnik et al. 2002)
Thermostable direct haemolysin TDH	*V. parahaemolyticus*	10 mM phosphate, heating between 60°C and 80°C, pH 7.4 (Fukui et al. 2005)
Triacylglycerol lipase	*C. antarctica*	pH 7.4, PBS, 37°C, 3 days (Kallberg et al. 2001)
Triacylglycerol lipase	*C. antarctica*	PBS, pH 7.4, 37°C, 3 days (Kallberg et al. 2001)
Urease	*C. ensiformis*	Guanidium hydrochloride (McDuff et al. 2004)

Table 3 Non-pathological amyloid proteins with function

Protein	Species	Function	Tissue	Reference(s)
CPEB	*Aplysia spp.*	Memory storage	Neuronal	Darnell 2003; Si et al. 2003
CgsA subunit	*E. coli*	Surface adhesion and biofilm formation	Curli	Chapman et al. 2002; Gebbink et al. 2005
AgfA	*Salmonella spp.*	Surface adhesion and cell-cell interactions	Tafi	Collinson et al. 1991
Pmel17 (Mα)	*H. sapiens*	UV protection	Melanosome	Berson et al. 2003
Sup 35p	*S. cerevisiae*	Hereditable transmission	Prion	Diaz-Avalos et al. 2003; Kishimoto et al. 2004
Ure2	*S. cerevisiae*	Hereditable transmission	Prion	Bousset et al. 2003
Rnq1	*S. cerevisiae*	Hereditable transmission chemical protection	Prion	Derkatch et al. 2004
Chorion	Silkmoth species	Physical and	Oocyte	Hamodrakas et al. 2004; Iconomidou et al. 2000
Het-S	*S. cerevisiae*	Hereditable transmission	Prion	Coustou-Linares et al. 2001; Dos Reis et al. 2002
Hydrophobins	Most fungi	Adhesion to hydrophobic surfaces	Hyphae	Gebbink et al. 2005; Mackay et al. 2001
Chaplin	*S. coelicolor*	Adhesion to hydrophobic surfaces	Hyphae	Elliot et al. 2003

dye Congo red, with the characteristic shift in the absorbance maximum and extinction coefficient. Recombinant CsgA formed fibres after standing for 4–12 h. Amyloid formation by CsgA is apparently tightly controlled, as there are a number of proteins which interact in the assembly process and which are controlled by two operons. CsgB is thought to aid in the nucleation of the fibrils, and both proteins are stabilised by the lipoprotein CsgG (Loferer et al. 1997). Interactions between bacterial curli and human proteins (fibronectin, β-2-microglobulin, MHC-1, immunoglobulin G) are known, raising the possibility that bacterial infection may mediate amyloid diseases (Olsen et al. 1989, 1998). NMR spectroscopy (Schwarz-Linek et al. 2003) was used to study interactions between a triple-stranded β-sheet of fibronectin and an unfolded region of a binding protein from *Staphylococcus aureus*, binding being accompanied by a conformational change in the bacterial peptide to a fourth anti-parallel strand. It seems likely that this type of interaction occurs between curli amyloid and fibronectin. The fibronectin type III module has been found to assemble into amyloid fibres independently (Litvinovich et al. 1998).

Three yeast prions in *S. cerevisiae* (Sup35, Ure2 and Rnq1 proteins) and one in the filamentous fungus *Podospora anserina* (Het-s) (Uptain and Lindquist 2002) are used for transmission of hereditable characteristics. These cellular proteins participate in diverse cellular functions. Yeast prions enable the intergenerational transmission of phenotype independently of DNA/RNA transmission. Prion proteins can undergo a conformational change, which alters the function of the protein and consequently the phenotype of the cell. Hydrophobins found in most fungi (Gebbink et al. 2005) have also been shown to have amyloid-like characteristics by binding to Congo red with characteristic green birefringence (Mackay et al. 2001). These proteins are used for adhesion purposes to hydrophobic surfaces and have a β-sheet core, although they could not be shown to have a distinct cross-β structure like amyloids. Similarly, the filamentous bacteria *Streptomyces coelicolor* produces chaplins that are used to attach to hydrophobic surfaces in a similar manner to hydrophobins in fungi

(Elliot et al. 2003). Previously shown to produce fibrils, chaplin from *S. coelicolor* can bind thioflavin T (Claessen et al. 2003), suggesting they too possess amyloid structure.

Viral peptides also form amyloids (Table 2). For example, a peptide derived from herpes simplex virus (HSV) glycoprotein B (gB) forms fibrils *in vitro* and nucleates assembly of Aβ fibrils (Cribbs et al. 2000). The peptide corresponding to residues 22–42 of HSV1 gB formed long, uniform fibrils at pH 7.4. The region investigated had significant similarity to the C-terminal region of Aβ and, like Aβ peptide, exhibited neuronal toxicity. This raises the possibility of a connection between viral infection and sporadic cases of Alzheimer's disease.

Perhaps the most significant recent development in amyloid research is the discovery of physiologically relevant amyloid proteins in human tissue (Fowler et al. 2006), especially in mature melanosomes. Melanosomes are highly abundant organelles generated in specialised cells within the skin and eyes (Hearing 2000; Marks and Seabra 2001) and contain glycoprotein Pmel17, known to play a role in pigmentation (Raposo and Marks 2002). Recent research has shown that Pmel17 is processed intralumenally by furin to produce an amyloid peptide fragment (Mα) (Table 3; Fowler et al. 2006). Mα has the ability to nucleate fibril formation to generate pre-melanosome fibrils (Berson et al. 2003; Fowler et al. 2006). Fowler et al. (2006) have also shown that Mα amyloid appears to play a role in sequestering highly reactive species and thus reducing the toxicity associated with melanin formation.

It now seems likely that more proteins will be discovered that naturally form amyloid with physiological roles, and this is suggested by the finding of amyloid receptors such as RAGE (receptors for advanced glycation end products) (Bamberger et al. 2003; Deane et al. 2003; Matsunaga et al. 2002; Schmidt et al. 2000) and also by the capacity of proteases such as cathepsins to cleave proteins in amyloid deposits (Bohne et al. 2004). These protective mechanisms within the cell suggest that amyloid proteins are physiologically relevant and that the cell has developed mechanisms to protect itself from its deleterious effects. Similarly, if amyloids were only present as the end point of slow, degenerative diseases, and not present in normal healthy physiology, it is logical to assume that there would be minimal evolutionary selection for these clearance mechanisms due to the often late-onset and mortality of these diseases.

Conformational changes leading to amyloid

Amyloidogenesis is thought to involve both (1) aggregation of short peptides and unstructured native proteins into more highly structured oligomers that ultimately form protofibrils and fibrils, and (2) conformational changes in natively structured proteins that produce, or expose otherwise buried, regions of appropriately structured/unstructured peptide sequences capable of initiating aggregation. It is now widely accepted that conformational changes from the native state of a protein precede aggregation of amyloidogenic proteins in a self-propagating and ordered manner to produce fibrils with a cross-β structure, their β-pleated sheets being arranged at approximately 90° to the direction of the long axis of the fibrils. The nature and causes of conformational changes between various polypeptide structural components and their aggregated β-sheets associated with amyloid remain poorly understood. Experimental detection and study of the properties of intermediates in amyloid formation, difficult though it might be due to their transient nature and subsequent water-insolubility of products, can provide valuable insights to structural transitions involved, aggregation states

and mechanisms, and processes of amyloid fibril assembly. Some of the most important studies on conformational transitions are now described.

Helix-sheet folding

There is tantalising evidence for a mechanistic role in amyloidogenesis of helical-containing intermediates, and several of the observations that support this are discussed below (Kirkitadze et al. 2001; Walsh et al. 1999). A helix-sheet conformational transition has often been associated with the onset of amyloidogenic diseases, and the precise mechanism by which an α-helix unwinds to form a β-sheet has been the subject of a great deal of theoretical and experimental work. It is well known that peptides with α-helical propensity can be induced to adopt even greater α-helical content by alignment in parallel on an appropriately sized template (Fairlie et al. 1998; Mutter and Vuilleumier 1989; Wong et al. 1998). Thus while bringing α-helices together encourages intermolecular (inter-peptide) interactions, this appears to lead to thermodynamically more stable α-helices.

An analysis of the chain-length dependence of the α-helix to β-sheet transition in polylysine by Dzwolak et al. (2004) revealed a role for non-ideal helices in the aggregation process. The polylysine model is a simpler system in many ways than an aggregating protein, with a single type of inter-residue interaction and no defined tertiary structure. There was a minimum chain length below which the transition to β-sheet aggregates was not observed. Above this minimum chain length, the transition temperature decreased as the chain length increased. It was found that chain length had an effect on the secondary structure of the polypeptide chain. For the shortest, 3-kDa polymer, a single amide-I peak was observed in the infrared (IR) spectrum, consistent with α-helical structure. This corresponded to an α-helix approximately six turns long, which is of a typical length for helices found in proteins. The 3-kDa polymer did not form β-sheet-containing aggregates. As the molecular weight of the polymer increased, peak shifts were observed and a new band appeared at 1620 cm^{-1}. It was suggested that this was due to the presence of two sub-populations of helices. Dipole-moment-induced coupling of helices would lead to the partial displacement of water from the inter-helical space and the hydrophobic environment thus created could be responsible for the observed shift from 1638 cm^{-1}, assigned to an α-helical conformation, to 1641 cm^{-1}. The conclusion reached by Dzwolak et al. (2004) was that distorted helices with turns were a prerequisite for folding to β-sheets. There are other reports of a transient increase in helical content of proteins immediately prior to formation of amyloid fibrils (Kirkitadze et al. 2001; Walsh et al. 1999). Kirkitadze et al found that helix formation is a key step in Aβ fibril assembly (Kirkitadze et al. 2001), the oligomeric intermediates displaying significant helicity. Deconvolution of CD spectra revealed a steady increase in helical content with time, which then fell away as the β-strand concentration increased. The several alloforms of Aβ studied all shared a correlation between the kinetics of formation of the helical containing intermediates and that of fibril formation.

Apolipoprotein A-1 is made up of repeating amphiphilic helices, and a heptad repeat pattern similar to that seen for coiled-coil proteins. However, in aqueous buffer at neutral pH the protein has a random coil structure. At pH 3, there is a gain in structure, as the internal fluorescence shows the three Trp residues are in a hydrophobic pocket (Andreola et al. 2003). CD studies show an acquisition of helical structure at lower pH. The protein is not, however, stable at pH 4, forming insoluble material after around 5 min, the process being one of intermolecular association and then precipitation. Andreola et al. (2003) have hypothesised that the formation of these amyloid aggregates requires the peptide to pass from

a random to a helical conformation to the final stable β-sheet conformation. A lag-phase is observed between the adoption of β-sheet structure and the formation of fibrils (ca. 72 h). The conformational switch to fibrils with β-structure thus occurs after aggregation.

Helical intermediates have also been observed for fibril growth on surfaces. The effect of hydrophobic surfaces on amyloid growth has been investigated for the interaction of Aβ1–40 on a hydrophobic teflon surface (Giacomelli and Norde 2003). Adsorption at pH 10 results in the promotion of α-helical conformation, with increases in β-sheet structure as the surface of the particles becomes more crowded. At pH 7, there is a mixture of α- and β-structure present, even at the lowest protein concentrations investigated. As the surface coverage increased, the lateral interactions between adsorbed peptides began to compete with the peptide-adsorbent surface interactions and the initial helical content gave way to β-sheeted structure.

Hua and Weiss (2004) examined the mechanism of insulin fibril formation after thermal denaturation in acidic solution using ultra-rapid ^{1}H-^{15}N NMR spectroscopy. It had previously been found that the intermediates at 70°C were substantially helical. Acquisition of β-sheet structure occurred simultaneously with the appearance of well-defined fibrils. The structure of the intermediates was also investigated prior to aggregation, utilising low insulin concentration and ionic strength to delay the onset of aggregation. CD spectra demonstrated substantial retention of α-helicity. Secondary structure alterations in monomers could be assigned to particular regions of the protein by the use of NMR spectroscopy. The process involved represented segmental rather than global unfolding, with some helical elements and long-range interactions maintained.

The hypothesis that distorted helices play an essential role in amyloid formation can explain the seemingly paradoxical effects observed when the structure-stabilising solvent 2,2,2-trifluoroethanol (TFE) was added to aqueous solutions of proteins (Chiti et al. 1999, 2000, 2001; Dong et al. 1998; Plakoutsi et al. 2004; Srisailam et al. 2003; Zerovnik et al. 2002). At intermediate concentrations, TFE is able to induce or accelerate amyloid formation for several proteins, but at higher concentrations it suppresses fibril formation by stabilising the formation of non-native α-helical structure. Solvent conditions which lower the energy barrier to helix formation will facilitate fibril formation if, at the same time, the energy barrier for conversion of helical-containing intermediates to fibrils is not substantially increased. At intermediate TFE concentrations, shorter stretches of helical structure should be preferred. In a study of the dependence of aggregation and folding on residue sequence identity (Chiti et al. 2000), human muscle acylphosphatase (AcP) mutants with conservative single amino acid mutations introduced throughout the entire sequence, were studied in 25% aqueous TFE which was sufficient to unfold all the mutant proteins, allowing effects of substitution on aggregation to be separated from effects on protein folding stability. It was found that the regions of AcP responsible for initiating aggregation also had a high degree of hydrophobicity and a propensity to form β-sheets, but were outside the regions responsible for forming folding nuclei. This study may suggest that an α-helical structure is not necessarily required for amyloidogenesis since that peptide had no detectable structure in solution. However, many amyloidogenic proteins either have some observable α-helical structure or could conceivably adopt a transient helical structure. An α-helix to β-strand transition, therefore, may still be a key event in amyloid formation and in our opinion cannot be ruled out, even considering the AcP mutant study, as an essential intermediate.

Propensity of α-helical sequences to form β-sheets

Kallberg et al. proposed that there are comparatively small regions of proteins that are responsible for fibril formation, particularly α-helices with amino acid sequences that are strongly predicted to form a β-structure and able to initiate amyloid formation (Kallberg et al. 2001). In a sample of 1,324 non-redundant proteins from the Protein Data Bank (PDB), differences were examined between experimentally determined secondary structures and those predicted by a secondary structure prediction algorithm. They found that 37 of the proteins (2.8%) contained a 7-residue or greater stretch that was predicted to be β-strand but was found to be helical (α, 3_{10} or π); 17 of these proteins contained stretches of 9 or more residues. These came from a wide range of proteins, including single helical peptides and large globular proteins, that varied in their cellular location being nuclear, cytosolic, integral and peripheral membrane proteins and extracellular. No consensus pattern could be detected, although our own analysis using the pattern rule suggested by Lopez de la Paz and Serrano (2004) suggests that three of these stretches (from Aβ, human prion protein (PrP^c), bacteriorhodopsin) may be amyloid-forming.

The same group (Päiviö et al. 2004) has examined the environment of the discordant helices for the 30 or so examples identified. The interactions in these regions were assessed by examining the solvent-accessible surface area of each residue in the discordant helix as determined by the neighbouring residues and comparing the values calculated for a Gly-X-Gly tripeptide. The helices fell into three categories. One group had helices that were almost completely buried. A second group had a periodic variation every three to four residues; 50% of the residues were buried, corresponding to helices located at the protein surface. There were six helices in the third group that were exposed along their entire length. Three of those are known to be lipid-associated in their native environment. In two of the cases the discordant helices are used in the formation of oligomers, which would help to stabilise those regions. The remaining example, for which no stabilising interactions are apparent, was Aβ. This lack of stabilising interactions likely contributes to the aggregation tendency of this peptide, whereas all the other examples identified would be stabilised by interaction with either protein or lipid environments. Päiviö et al. stress that inherent secondary structure propensities are not sufficient to be used for prediction of conformation of an amino acid sequence, but that factors such as the local environment are also important and need to be considered. The drawback of the α/β mismatch approach for the identification of novel amyloid-forming proteins is its reliance upon protein structure information. Also, not all amyloidogenic proteins or peptides contain α-helices, for example β2-microglobulin contains seven β-strands, which show no correlation between secondary structure propensity and fibrillisation (Jones et al. 2003).

Johansson's method identified sequences from well-known amyloidogenic proteins, such as Aβ16–23, PrP179–191 (helix 2), and SP-C (lung surfactant associated protein C). Several proteins, not previously identified as fibril-forming, were also detected such as coagulation factor XIII, a triacylglycerol lipase, and a transpeptidase. Subsequent investigations of coagulation factor XIII, the specific triacylglycerol lipase and transpeptidase in physiological-like solutions, did in fact show the formation of fibrils (Kallberg et al. 2001; Table 2), thus supporting a correlation between β-strand-favouring α-helical sequences in proteins and amyloid fibril formation. The explanation proposed for this link (an α/β mismatch) is that as the helix unfolds, an intermediate is formed. The high β-strand propensity of these segments means that they are less likely to return to their original α-helical conformation compared to sequences where the α-helix is strongly stabilised. Once a surface-exposed β-strand is formed, without the protective features that prevent

aggregation in normal β-sheet rich proteins, then oligomerisation can occur. Independent support for this hypothesis can be drawn from results involving helix stabilisation in other peptides and the effect on amyloid formation. For example, a set of four peptides of the form Ac-EACARXZAACEAAARQ-NH_2, where X=A or V and Z=A or Aib, was synthesised (Kumita et al. 2003). Aib is known to act as a strong helix-stabiliser (Kaul and Balaram 1999; O'Neil and DeGrado 1990; Toniolo et al. 1993). The peptide (X=V, Z=Ala) was found to be extremely insoluble in water, water/acetonitrile mixtures and methanol. The peptide (X=V, Z=Aib) was, however, soluble even in high concentrations in water. The addition of a single methyl group was sufficient to cause this change.

In vitro studies on Aβ peptide mutations found that removing the discordant nature of the 16–23 region by selective substitutions (K16A/L17A/F20A and V18A) that increased helical propensity was sufficient to avoid fibril formation (Soto et al. 1995; Tjernberg et al. 1996). Similarly, Tjernberg et al. (2002) used synthetic tetrapeptides to confirm that a propensity for β-sheet is required to produce amyloid fibrils. Mutation studies which change the propensity of the primary sequence from β-sheet to α-helical prevent amyloid formation (Kallberg et al. 2001; Nilsson et al. 1998; Soto et al. 1995; Tjernberg et al. 1996), further supporting the significance of secondary structure propensity. Finally, an interesting NMR solution structure (Coles et al. 1998) of Aβ1–40 in sodium dodecyl sulphate (SDS)-water (simulating to some extent a water-membrane environment) showed that this peptide has two distinct structural domains, an unstructured region (1–14) and a helical region (helix 15–24, kink 25–27, helix 28–36). When Aβ is a component of the membrane-spanning amyloid precursor protein APP, the C-terminal region of Aβ is likely to be α-helical within the lipophilic cell membrane. However, when APP is spliced by β- and γ-secretase it cannot be α-helical, since the β-strand conformation is required for recognition and cleavage by these proteases (Fairlie et al. 2000; Tyndall and Fairlie 1999; Tyndall et al. 2005). Once Aβ is released into the extracellular circulation, it has no well-defined structure in water. A key observation (Coles et al. 1998) was the presence of multiple Gly residues, along one face of the α-helical region of Aβ that we predicted to be helix-destabilising. This in-built sequence propensity for helix destabilisation may be a factor in facilitating both exit of Aβ from the membrane and its conformational transition to an aggregating β-strand.

Unstable 3_{10}-helical intermediates

Short peptide helices are conformationally flexible, rapidly interconverting between α-helical and 3_{10}-helical structures. Dehner has found that a fast equilibrium exists between the two helical forms, with the helices being flexible on a nanosecond to picosecond time scale and undergoing transitions from 3_{10}- to α-helical conformations (Dehner et al. 2001). It seems possible to us that 3_{10}-helical regions might be important, unstable, intermediates in the unwinding of an α-helix to a β-strand and may play a fundamental role in the transformation of α-helical regions of proteins and peptides into amyloid fibrils. We discuss some evidence for this proposition below.

The equilibrium between the two helical forms is clearly affected by the polarity of the solvent, with low polarity solvents favouring 3_{10}-helicity (Pengo et al. 2003). In the presence of high concentrations of TFE, short stretches of 3_{10}-helicity can merge to form longer and more stable α-helical stretches, and indeed folding of peptides and proteins from random coil to α-helix has been associated with an unstable intermediate 3_{10}-helix. In favouring a stable α-helix, TFE deepens the energy well of the helical state, thereby disfavouring subsequent

conversion to fibrils. A 3_{10}-helix is more elongated, narrower and less stable than the more compressed α-helix (Fig. 6) because of several close van der Waals contacts and suboptimal hydrogen bond geometry. However, an α-helix can be gradually transformed into a 3_{10}-helix whilst maintaining a near-helical conformation, since the conformational space for the two conformations overlap (Toniolo and Benedetti 1991).

For β-lactoglobulin and α-chymotrypsin, a transient α-helical intermediate was identified by CD spectra (minima at 208 and 222 nm) and IR spectra (an amide-I band at 1,654 cm^{-1} in H_2O) *en route* to intermolecular β-sheets (Dong et al. 1998). Tcherkasskaya et al. (2003) proposed a possible role for 3_{10}-helical intermediates along the pathway to β-sheet aggregation. The adoption of a 3_{10}-helical structure in aqueous solution implies a loss of short-range interaction in the peptide chains and a destabilisation of the more stable α-helical structure. Theoretical studies have indicated that an aqueous environment stabilises α-helical structure, whereas hydrophobic environments are more favourable to β-folded structures. A 3_{10}-helix to β-strand/sheet transition would require even less energy and thus be more favoured and could be driven in an auto-catalytic manner by the increase in hydrophobicity of the protein oligomer.

A mutant Arc repressor protein illustrates the possibility of a finely balanced interconversion of 3_{10}-helix and β-sheet. Cordes et al. (2003) made a double mutant of the Arc repressor protein by swapping the 11th and 12th residues (N11L and L12N). These changes in the N-terminal region caused a significant change in the secondary structure of the protein. The two strands of the anti-parallel β-ribbon of the native protein were each replaced by irregular 3_{10}-helices, spanning residues 9 to 13. Importantly, the new structure retains the same number of hydrogen bonds as the native structure. The side-chain packing is less efficient though in the helices compared to the two-stranded β-sheet, as shown by the increase in the solvent-accessible surface area by around 968 $Å^2$. The single N11L mutant was able to adopt either structure.

There are also several reports of intermolecular interactions between otherwise α-helical peptides favouring 3_{10} structure (Dehner et al. 2001; Yoder et al. 1997). Identifying transient 3_{10} structure in intermediates is technically difficult because of several similarities in spectral characteristics with those of α-helices, but this is a hypothesis that would benefit from more careful and more detailed investigation. For example, the CD deconvolution algorithms used by Kirkitadze et al in his study of Aβ aggregation were unable to estimate the separate contributions from α-helical and 3_{10}-helical conformations (Kirkitadze et al. 2001). Many CD spectra reported for amyloidogenic peptides appear to show molar ellipticity minima at approximately 205 nm with a shoulder at approximately 220 nm, and the ratio of $\theta_{222}/\theta_{205}$ is usually 0.4–0.6 (as expected for 3_{10}-helicity) rather than 0.7–1.1 (expected for α-helicity).

Recently, we investigated (Y. Singh, P.C. Sharpe, A.W. McDowall, D.P. Fairlie, submitted) whether amyloid formation could be induced for a water-soluble, amphipathic, 15-residue α-helical peptide H-[AEQLLQEAEQLLQEL]-NH_2 (Lieberman and Sasaki 1991; Sasaki and Kaiser 1989; Tahmassebi and Sasaki 1998) not known to aggregate or form fibrils. At pH 4 this peptide is indefinitely stable (at least 8 months without change at pH 4) as an unaggregated α-helix, but when multiple copies were constrained in parallel alignment on a template as a 4α-helix bundle, helix→sheet conformational changes occurred in minutes to days (Figs. 7 and 8), depending upon concentration and pH, and resulted in deposition of amyloid fibrils.

The process was mediated by an α-helix to 3_{10}-helix transition, as clearly evidenced by CD spectra (Fig. 7i), IR spectra (not shown), and especially 2D-NMR spectra (Fig. 8iii), *en route* to β-strand, then β-sheet and amyloid fibrils (analysed by TEM). The compelling Nuclear Overhauser Enhancement Spectroscopy (NOESY) data (Fig. 8iii) contrast dramat-

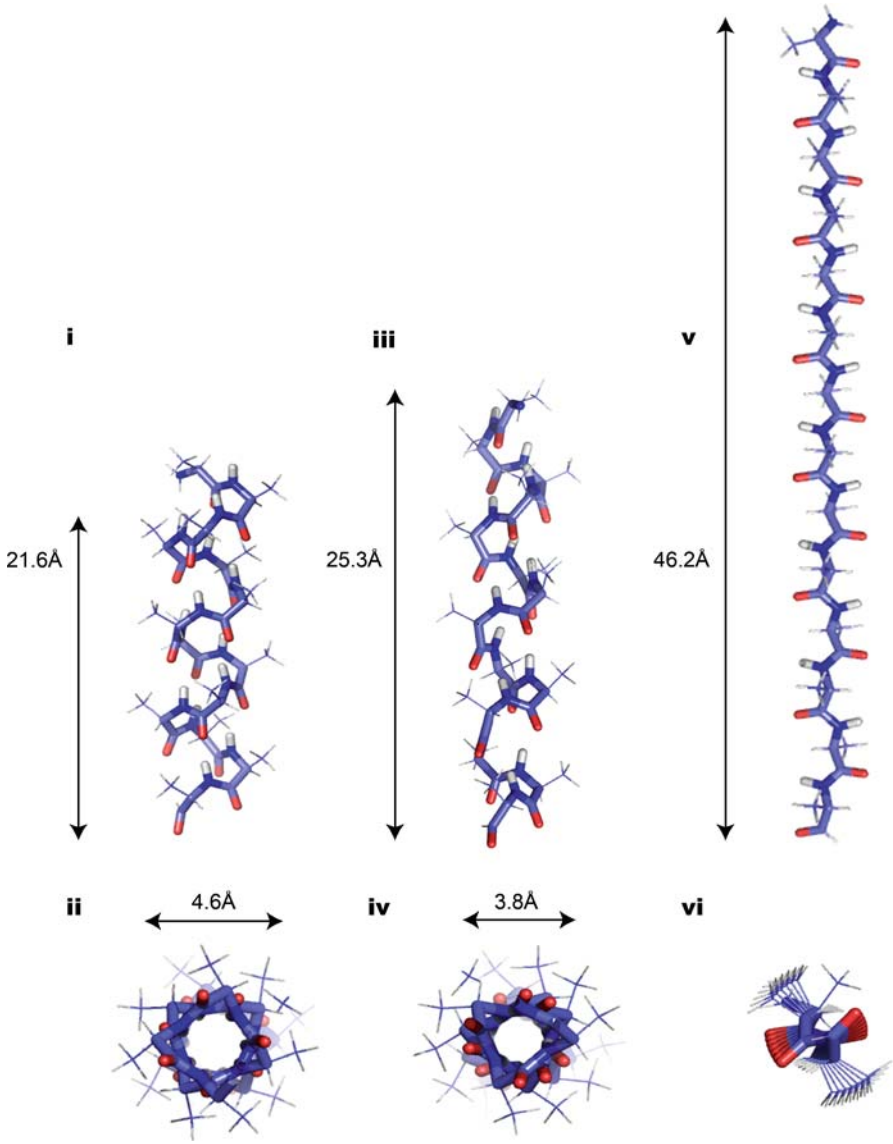

Fig. 6i–vi Dimensions of peptide backbone secondary structure intermediates proposed to be in the pathways to amyloid formation. Side views showing the comparative lengths of each structure; α-helix (**i**), 3_{10}-helix (**iii**) and β-strand (**v**) due to differences in H-bonding (not shown). Top views showing the comparative diameters of α-helix (**ii**), 3_{10}-helix (**iv**) and β-strand (**vi**). Backbone residues (*sticks*), sidechains (*lines*), carbon (*light blue*), nitrogen (*dark blue*), hydrogens (*white*) and oxygen (*red*). Figures generated using InsightII (v. 2000, Accelrys) and MacPyMOL (for MacOS X, DeLano Scientific, South San Francisco)

ically with corresponding spectra (not shown) for the initial free peptide and 4α-helix bundle, where prominent αN i→ (i+3) and especially i→ (i+4) NOE correlations typical of α-helicity were observed. As far as we are aware, this is the first three-dimensional structural validation of a 3_{10}-helical intermediate during α-helix to β-sheet folding for a fibril-forming peptide (Y. Singh, P.C. Sharpe, A.W. McDowall, D.P. Fairlie, submitted). The unusual stabil-

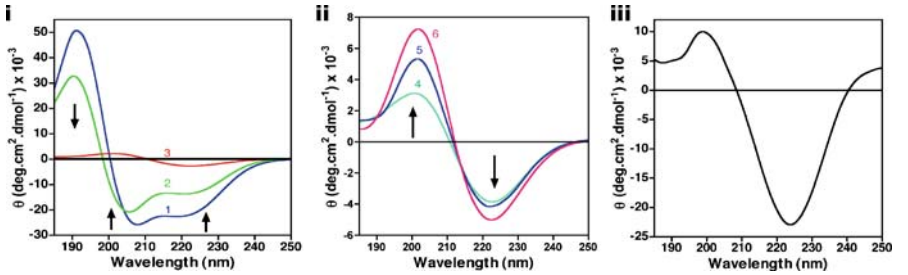

Fig. 7i–iii Helix-sheet-nanofibre transitions of a 4-helix bundle (pH 4) from an α-helix (**i** *1*) to 3_{10}-helix (**i** *2*) to β-strand (**i** *3*) to β-sheet (**ii** *4–6*) and finally to mature fibrils (**iii**), for four equivalents of H-[AEQLLQEAEQLLQEL]-NH_2 covalently tethered to a cyclic peptide template. *Arrows* show the direction of change over time. Images taken from Singh et al. (Y. Singh, P.C. Sharpe, A.W. McDowall, D.P. Fairlie, submitted), some spectra were removed for easy interpretation. Figures illustrated and modified with Prism4 (version 4.0b, GraphPad)

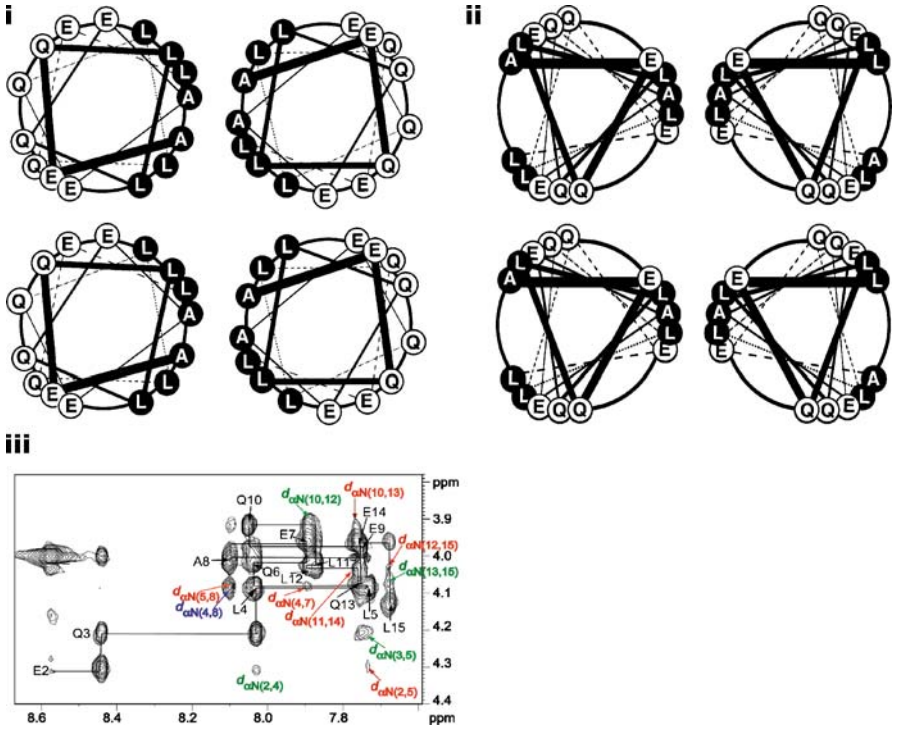

Fig. 8i–iii The 4-helix bundle as shown for the α-helix (**i**) and the 3_{10}-helix (**ii**). **iii** Nuclear Overhauser Enhancement Spectroscopy (NOESY) spectrum of 4-helix bundle (αN Region) at pH 4 in 25% MeCN/phosphate buffer corresponding to Fig. 7i (*line 2*) showing αN(*i*→ *i*+2; *green*) and αN(*i*→ *i*+3; *red*) NOE correlations typical of 3_{10}-helicity

ity of these 3_{10}-helix and β-strand intermediates was attributed to their parallel arraying that enabled intra-bundle H-bonds between Glu/Gln side chains. Glu residues near a helix–helix interface destabilise α-helices through H-bonding (Fezoui et al. 2000). A 3_{10}-helix is longer and narrower than an α-helix, representing a stretched intermediate along the pathway to the even longer and narrower β-strand, which pairs to form β-sheets. Forcing α- to 3_{10}-

helicity would unfavourably solvent-expose hydrophobic residues that need to redistribute from the inner surface of a 4α-helix bundle (Fig. 8i) to the outer surface of a 3_{10}-helix bundle (Fig. 8ii). Thus, in this case, the intra-bundle inter-chain hydrogen bonding of polar Glu/Gln side chains promotes inter-bundle hydrophobic interactions, aggregation and nanofibre/fibril formation.

Interestingly, amyloidosis of Aβ, β2-microglobulin, α-synuclein, lysozyme, apolipoproteins, prothymosin and other proteins is similarly enhanced in acidic media (Andreola et al. 2003; Hoyer et al. 2002; Jones et al. 2003) where Glu/Asp side chains protonate to uncharged H-bond donors. Also mutation to a hydrogen-bonding glutamine in Aβ (E22Q) (Gerhartz et al. 1998), cystatin C (L68Q) (Yazaki et al. 2002) and transthyretin (L55Q) (Huang et al. 1998) promotes amyloidosis *in vitro*/vivo, glutamine-containing yeast prions aggregate to fibrils, huntingtin protein has a polyglutamine sequence, and polyglutamine proteins are recruited into fibrils. Thus polar amide/acid side chains may assist the aggregation of these peptides as well. Whether these aggregations also involve α→3_{10}→strand→sheet folding transitions remains uncertain.

Helices, turns, strands, sheets and aggregation

Conformational transition from an α-helix to a β-sheet in the example above involves a 3_{10}-helical intermediate. It is important to realise that while α-helices involve back-to-back α-turns (13-membered hydrogen-bonded rings), 3_{10}-helices involve back-to-back β-turns (10-membered hydrogen bonded rings; Fig. 9i). This ring contraction has the effect of elongating and narrowing the helix, the 3_{10}-helix being also notoriously less stable than an α-helix in part because back-to-back β-turns are conformationally unstable and partly because this structural reorganisation redistributes side chains leaving hydrophobic residues exposed to water (Fig. 8). This may be a factor in promoting aggregation. It seems likely that unwinding of a 3_{10}-helix involves stepwise cleavage of β-turns *en route* to the even more elongated β-strand that has no intramolecular hydrogen bonds (Fig. 9ii), and examples may be discovered in the future where an isolated β-turn or two can be detected during helix-sheet refolding.

The thermodynamic driving force for amyloid formation is unquestionably the formation of aggregated β-strands that define complex β-sheet assemblies, involving two intermolecular H-bonds per peptide residue plus additional side chain–side chain interactions that help stabilise and propagate strand aggregation. However, it seems likely that the folding pathway to amyloid could potentially be accessed by any protein structural motif as

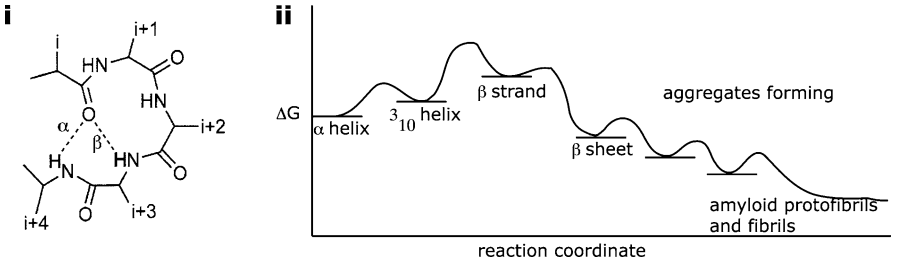

Fig. 9 i α-Turn versus β-turn showing the differences in H-bond connectivity. An α-turn is an i→i+4 H-bond whereas a β-turn (as seen in 3_{10}-helices) is an i→i+3 H-bond. **ii** Schematic showing hypothetical energy diagram for conformational change from α-helix (α-turns), to 3_{10}-helix (β-turns), to β-strand, to β-sheet, which finally aligns to form aggregates and fibrils, representing the lowest energy states

long as formation of a β-sheet is feasible and ultimately favoured. It may be that amyloid formation is kinetically very unfavourable for many sequences because of an inherently low sequence-related propensity to form strands/sheets, or alternative formation of stable structures (e.g. helix bundles, native folds that bury potentially amyloidogenic sequences, etc.), or propensity for competing proteolytic degradation of unaggregated β-strands now known to be selectively cleaved by proteases (whereas β-sheets and α-helices are not; Fairlie et al. 2000; Tyndall et al. 2005).

Although formation of aggregated β-sheets is thermodynamically more stable, the entropic advantage provided by aggregation of α-helices or 3_{10}-helices might also be helpful in speeding up the folding transition(s). Clearly parallel alignment of the Gln/Glu-rich amphipathic helical peptide discussed in the previous section was a key factor in being able to observe α→β refolding and amyloid formation. In that case both bringing the peptides together and the capacity of α-helical Glu/Gln residues to form inter-peptide hydrogen bonds was sufficient to form a stable peptide aggregate that was predisposed to conformational switching. It remains to be seen if artificially encouraged alignments of other peptides also convert to aggregated strands/sheets; we think that this is very likely if they also have strand/sheet propensity.

Importance of protein unfolding

Since the formation of amyloid fibrils involves changes in secondary structure, an obvious question is whether this occurs through partially folded intermediates or randomly structured segments. Clues to the structure of partially folded intermediates have been provided by spectroscopic studies, by the effects of single residue mutations, and by varying conditions under which intermediates form.

To resolve this issue, Fändrich et al. investigated the thermal denaturation of apomyoglobin (Fändrich et al. 2003), a globular protein at room temperature that undergoes a two-state thermal denaturation, with the midpoint of the transition (T_m) at 61°C. Many proteins form non-fibrillar aggregates upon heating, but apomyoglobin readily forms fibrils in the temperature range 55–75°C. Above 75°C there was a pronounced reduction in fibril formation. Pre-formed fibrils were unstable at the higher temperatures. They showed that although a partially folded intermediate state was indicated, this had the same secondary structure composition as the native apomyoglobin, and the authors concluded that, at least in this instance, the precursors of amyloid structure were unfolded chain segments. They reserved the possibility that partial folding may be a step in amyloid formation for some proteins, such as some β-sheet proteins. In support of their argument, they noted that very short peptides and several polyamino acids have the capacity to form amyloid fibrils. Such short peptides lacked the capacity to fold into stable folded species; a minimum of 20 residues has been suggested as being required to form a stable α-helix in aqueous solution (Scholtz and Baldwin 1992). Solid-state NMR investigations of fibrils formed by Aβ1–40 (Petkova et al. 2002) and a transthyretin peptide fragment (Jaroniec et al. 2002) have shown the existence of only intermolecular hydrogen bonding along the peptide main chain. Although not conclusive, this supports unfolded precursors being involved in amyloid formation, at least for these two examples. There are also indications that the so-called unfolded conformation may be a misnomer, in that there may actually be discernible structure present, biased towards extended main chain conformations, which would be able to undergo alignment into amyloid fibrils.

In hereditary amyloidoses, the mutant protein cannot form the native folded state and is destabilised relative to the wild-type protein, thus making the mutant more susceptible to misfolding and/or unfolding. Mutations also affect the formation of intramolecular bonds in the protein as shown by the p53 R337H mutant associated with adrenocortical carcinoma in children. This mutation disrupts the intermonomer salt bridge and, at least for a portion of the mutant proteins, results in partial destabilisation (Galea et al. 2005). This principle was also shown by non-amyloidogenic endostatin, which was able to form amyloid fibrils by removing disulphide bond-forming cysteines (He et al. 2006). The cause of protein destabilisation and unfolding resulting in acquired amyloidosis is less clear. It is generally accepted that an increase in sporadic mutations can cause proteins to misfold and form amyloid fibrils, but is also proposed that an increase in local protein concentration may result in amyloid formation as a result of molecular crowding.

External factors such as pH or the presence of denaturing conditions can initiate destabilisation, and such stimuli within the cell might similarly cause destabilisation. Eakin et al. showed that increased Cu^{2+} concentrations caused a *cis–trans* isomerisation of Pro32 of β-2-microglobulin, initiating amyloid fibril formation (Eakin et al. 2006). Interestingly, structural analysis of this mutant showed a native-like folding intermediate, where the destabilised intermediate was very similar to the wild-type protein except for the perturbation of the edge of the strands (Jahn et al. 2006), resulting in self-assembly of the mutant proteins without the requirement of complete unfolding. By unfolding, hydrophobic regions may become solvent-exposed, aromatic residues brought to the surface, and secondary structures, previously stabilised by tight packing and intramolecular interactions, could then be destabilised.

Amyloid formation

The formation of amyloid can be considered to involve (1) conformational changes (away from the native state) in key regions of a protein or peptide, (2) intermolecular interactions that result in aggregated intermediates and (3) further aggregation in three dimensions to produce growing fibrils.

Initial aggregation

The detection of monomeric or early aggregation states has been difficult experimentally due to their transitory nature, their presence at only low concentrations and usually in an ensemble of conformations, and the speed with which insoluble aggregates are formed especially when seeded. In recent years, however, some progress has been made in identifying these early aggregates, providing some information on the oligomerisation process.

Using scanning tunnelling microscopy, Aβ1–40 has been identified as a predominately monomeric and dimeric species that associate via end-to-end interactions to form larger oligomers with the characteristic cross-β structure (Losic et al. 2006). Similar observations have been made using photo-induced cross-linking of unmodified proteins where monomers, dimers, trimers and tetramers of Aβ1–40 have been identified (Bitan et al. 2003a, 2001, 2003b; Huang et al. 1997) and shown to exist in a rapid equilibrium with each other. Interestingly, Aβ1–42 has been shown to oligermerise through a different pathway to Aβ1–40, showing the presence of pentameric/hexameric paranuclei (Bitan et al. 2003a, b) which self-associate to form larger oligomers. Most recently, atomic force microscopy

and Western blot analysis have been used to identify both small oligomers (monomers to penta/hexamers) as well as larger oligomers (up to 24-mers) of Aβ1–42 (Arimon et al. 2005). Wang and Colon (2005) have investigated a non-amyloidogenic form of *M. musculus* serum amyloid A, which comprises monomers and hexamers below 25°C but upon heating (>37°C) disaggregates to form unfolded monomers and then protofibrils.

Similar studies have also been done on other known amyloidogenic proteins. Insulin has been shown to exist as stable dimers, tetramers and hexamers in the gas phase using nanoflow electrospray mass spectroscopy and at higher concentrations up to 12-mers (Nettleton et al. 2000). High-resolution atomic force microscopy at low pH has provided images of monomer and dimeric insulin (Jansen et al. 2005), and the images suggest that monomers and dimers may adhere directly to the protofilaments via lateral association (Jansen et al. 2005). α-Synuclein has been shown to comprise monomers, dimers and trimers through photo-induced cross-linking of unmodified proteins, and it is thought that the dimers and trimers may initiate further aggregation (Nettleton et al. 2000).

Strategies to prevent or diminish the damage caused by amyloid disease could concentrate on increasing the energy barrier to formation of the structurally perturbed intermediate, whether by increasing the stability of the native state or by decreasing the stability of the intermediates on the pathway to aggregation. The formation of the structurally perturbed intermediate will have an obvious relationship to the thermodynamics of unfolding of the protein. Carpenter's study of the unfolding and fibril formation of a recombinant light chain variable domain SMA used pressure, temperature and the presence of a co-solute to characterise the energetics of the aggregation system (Kim et al. 2002). Apparent activation energies of pre-nucleation assembly, nucleation and growth were determined from Arrhenius plots. It was found that increases in protein concentration, pressure and temperature all increased the rates of pre-nucleation assembly and led to exponential growth rates and decreased the nucleation lag time. There were indications that the critical nucleus size was independent of pressure, protein concentration and temperature over the ranges investigated. The first order dependence of pre-nucleation assembly, nucleation and growth on the protein concentration suggested that the rate-limiting step for the reaction is the conformational change in the protein. An Arrhenius dependence on temperature was shown for pre-nucleation assembly, nucleation and growth. ΔG^*, similar in value for all three processes, was dominated by solvent effects. The activation energy E_a and ΔH^* were similar in value for nucleation and growth (around 159±18 kJ/mol and 96±22 kJ/mol, respectively). The values observed for assembly of the pre-nucleation intermediate were smaller (119±31 kJ/mol E_a and 116±25 kJ/mol ΔH^*). The ΔV^* values associated with pre-nucleation, nucleation and growth corresponded to 13%, 11% and 26% of $\Delta V_{\text{dissocation}}$. This suggests that the transition states have only partially unfolded structures, only slightly different from the native state.

Kelly and co-workers studied the energetics of transthyretin amyloid formation (Hammarström et al. 2002). Kinetic versus thermodynamic stability of aggregates was distinguished using single mutant *transthyretin* (*TTR*) variants assessed by urea titration, with concentration of the tetramer determined by binding of fluorescent resveratrol. The tetramers associated with disease mutants had lower denaturation midpoints for dissociation, indicating that they were less stable than the wild-type protein. The L55P and V30M variants were destabilised to a similar degree, but the associated disease states are quite different, including age of onset. The V30M disease phenotype was milder and Kelly et al. connected this to the observed *in vitro* differences in rates of dissociation, with the V30M mutant dissociating slower than the native protein. Their conclusion was that although the thermodynamic stability of a protein will dictate whether it will form amyloid under suitable conditions, the rate of fibril formation is also likely to be important in determining the severity of disease.

Their work showed that mutations which influence the amyloid-forming ability of a protein are possible without concomitant changes in the rate of partial denaturation. The most severe forms of transthyretin-induced disease appear to be those where there is a reduction in both thermodynamic and kinetic stability.

Fibril growth: nucleation and elongation

The generally accepted model for growth of amyloid fibrils is the nucleation-elongation model, where the rate-limiting step is the formation of a nucleus through the self-association of monomers, followed by the rapid growth through addition of monomers to the nucleus leading to fibrils, and finally a steady state when the aggregate and monomers appear to be in equilibrium (Harper and Lansbury 1997; Inouye and Kirschner 2000; Jarrett et al. 1993; Murphy 2002; Pallitto and Murphy 2001).

Three mechanistic stages may be discerned for fibril formation. The first is assembly of oligomeric intermediates from a protein or peptide that may be in the native state or in a partially unfolded aggregate to form a nucleus. This is a thermodynamically unfavourable process and represents the rate-limiting step for fibril formation. In the second stage, which is reached after a critical nucleus size is formed, fibril formation commences. This is favoured by the greater thermodynamic stability of the fibril form compared to the destabilised native protein. The third stage involves the addition of monomeric protein to the growing ends of a fibril, which is a template-induced change from a deposited monomer via reorganisation to regenerate the growing fibril tip.

One of the critical questions for amyloid formation is the size of the oligomers formed. Their size can be derived by a kinetic investigation of the elongation of fibrils. Fay and co-workers (2003) used Oosawa's plot of dependence of rate of fibril growth J(c) on the monomer concentration for polymers, $J(c) = \mathrm{d}c/\mathrm{d}t = k_+[P] - k_-[P]$ for a reversible polymerisation where c and P are the concentrations of monomer and polymer elongation sites respectively and k_+ and k_- are the rate constants for monomer association and dissociation from ends of the polymer. If polymerisation is irreversible, the equation becomes $J(c) = k_+[P]c$. The rate constant k_+ is given by the slope of the line. The critical concentration is given by interpolation to $J = 0$. For Ure2p fibrils, the critical concentration was found to be 40 nM. Although physiological assembly of Ure2p fibrils results in assemblies of α-helical structure (Bousset et al. 2003), the kinetic analysis used is still applicable to amyloid formation. The size of the nuclei can be determined in a separate experiment by graphing log of the reciprocal lag time versus log protein concentration. The slope of the line gives a value m, where the size of the nucleus is given by $(2m - 1)$.

During Aβ aggregation *in vitro*, several stages have been observed. Protofibrils are seen as a transient stage prior to the formation of full-length fibrils. The rate of monomer deposition onto fibrils is dependent on both fibril and monomer concentration. A first-order rate dependence of monomer concentration was also observed for protofibrils. The observation of protofibrils as a transient stage suggests that lateral association to produce fibrils can also occur. Nichols et al. showed through atomic force microscopy (AFM) that the addition of monomer to protofibrils occurs at the ends of protofibrils (Nichols et al. 2002). Protofibril association in the presence of NaCl led to wider strands observed by electron microscopy (EM) (Nichols et al. 2002). Interestingly, it has also been shown that prefibrillar aggregates can be solubilised at near physiological conditions (Calamai et al. 2005), while hydrogen/deuterium exchange in SH_3 domains has shown that amyloid plaques are

dynamic, with monomers dissociating and re-associating through a process of molecular recycling (Carulla et al. 2005).

Templated assembly has also been observed in the formation of amyloid fibrils whereby monomers, exposed to the aggregated form or "seed", convert to an aggregate-prone state and enhance aggregation (Krebs et al. 2000), suggesting that aggregation is induced rather than spontaneous (Murphy 2002). Kinetically, templated assembly has a greatly reduced lag time when compared to the nucleated-assembly process because aggregation nuclei are provided by the template material. This method of inducing amyloid formation has been shown to dramatically increase the rate of amyloid formation of normally non-aggregating peptides (Y. Singh, P.C. Sharpe, A.W. McDowall, D.P. Fairlie, submitted) and has also been linked to the conversion of *wt* prion protein (PrP^{c}) to its pathological isoform (PrP^{Sc}) in Creutzfeldt-Jakob disease and other infectious prion-related diseases (Cohen and Prusiner 1998). Most likely, both mechanisms are active in the formation of amyloid fibrils, with the relative importance of each mechanism depending of the existence of pre-aggregated material (Murphy 2002).

Fibril growth from nuclei remains still only poorly understood. After the nucleus is formed, monomers "attach" to the nucleus and the fibril extends. The most popular mechanism for fibril elongation is the "dock and lock mechanism", where a peptide monomer binds loosely to the end of a fibril, followed by reorganisation on the fibril surface to regenerate a surface capable of further aggregation and has been followed directly by the use of time-lapse AFM. Measuring amyloid formation has been difficult because of the experimental problems in quantifying fibrils and comparing fibril formation under different conditions (Harper and Lansbury 1997). However, it is known that a critical concentration is required, unique to each protein, in order to initiate nucleation and below which monomers remain as predominant species. Massi and Straub (2001) analysed rates for elongation of pre-formed fibrils observed by Esler and co-workers (2000) using radio-labelled peptides to add to pre-existing fibrils. Based on kinetic rates of absorption and desorption onto pre-formed fibrils, deposits, and the rates of re-organisation and de-organisation of peptides at reactive fibril interfaces, a two-step mechanistic model was proposed involving association between the soluble protein and pre-formed fibres to form an intermediate, followed by conformational changes to amyloid by irreversible binding (Cannon et al. 2004; Collins et al. 2004; Esler et al. 2000; Gobbi et al. 2006; Massi and Straub 2001; Scheibel et al. 2004).

An alternative to using radio-labelled peptides, Cannon and co-workers (2004) measured fibril elongation rates for Aβ by immobilising fibrils on a surface and examining by surface plasmon resonance (SPR). This enabled data collection over short periods to monitor rapid reversible interactions as well as slower polymerisation steps. They observed a dynamic equilibrium between immobilised fibrils with peptides in solution, and slow decay in fibril surface in the absence of peptide in solution, consistent with the studies of radio-labelled peptides which found that fibril growth is readily reversible. Reversibility is likely to be essential for the highly ordered nature of aggregates, as one of the principles of supramolecular non-covalent design is that reactions should be readily reversible to allow formation of the lowest-energy product or, in the case of fibrils, the peptide register with the most favourable arrangement. O'Nuallain et al. (2004) have recently showed that the Aβ seeded fibril elongation progresses rapidly to a reproducible endpoint of a 0.7–1.0 μM unpolymerised monomeric peptide and produced a fibril dissociation constants (K_d). Kim et al. (2002) characterised the energetics of the aggregation system of recombinant light chain variable domain SMA and determined the apparent activation energies of pre-nucleation assembly, nucleation and growth increased according to protein concentration, pressure and temperature. The addition of denaturant at low concentrations is predicted to increase the

rate of protein folding by reducing the amount of time spent in misfolded intermediate states. The protein monomers will favour a partially structured collapsed coil state by decreasing the diffusion constant and also lowering the barrier to reorganisation. If this is the dominant effect, then there will be an increase in the rate of fibril elongation. At high concentrations of denaturant, monomers will be predominantly unstructured, causing a decrease in the diffusion constant and hence a decrease in the rate of adsorption.

A degree of sequence specificity has been observed for the incorporation of proteins into amyloid fibrils formed by other proteins. For example, Krebs and co-workers investigated the potential to seed amyloid formation in five proteins by the addition of hen lysozyme fibrils (Krebs et al. 2000). The proteins studied had varying degrees of sequence identity with hen lysozyme, ranging from 99.2% in a single mutant to human α-lactalbumin (36% identity) and bovine insulin, with no sequence identity at all. The reverse situation, seeding protein fibrils into hen lysozyme solutions, was also examined. The results showed that as sequence identity increased, the efficiency of the seeding reaction also increased, as monitored by thioflavin-T fluorescence. Similarity of protein structure, as distinct from sequence, did not result in efficient seeding of hen lysozyme by human α-lactalbumin, which has a very similar native-fold. This emphasises the important role played by side-chain residues in the development of long-range order within the fibrils. Several authors (Hong and Fink 2005; Krebs et al. 2000; Wright et al. 2005) have confirmed these findings for other proteins. Although monomers do not need to be identical to each other, it has been found that the greater the similarity between sequences, the greater the efficiency of aggregation, and that a minimum of 30–40% sequence identity is required in order to interact (Wright et al. 2005). This is not surprising given that amyloid fibrils formed *in vivo* consist largely of one predominant protein.

Other proteins and molecules in the extracellular environment that associate with amyloid plaques and are thought to contribute to plaque stability include serum amyloid P (SAP), glycosaminoglycans (GAGs), collagens, metals, apoprotein E and constituents of basement membranes (for a recent review, see Alexandrescu 2005). Generally speaking, many of these molecules are involved in the formation of supramolecular assemblies (Alexandrescu 2005). SAP is thought to be the most researched of these "accomplices" and is found in all amyloid deposits found *in situ* where it lowers their susceptibility to proteolytic degradation (Pepys et al. 1994). GAGS are also found in most amyloid plaques and are implicated in the nucleation of fibrils (Alexandrescu 2005) as well as stabilising mature fibrils from dissociation (Yamaguchi et al. 2003) and proteolytic degradation (Gupta-Bansal et al. 1995). Furthermore, heparin is known to be a major accomplice protein (Ancsin 2003) by binding to a number of amyloid precursors (Ohashi et al. 2002) as well as the fibrillar forms of amyloid; specifically, heparin has been shown to accelerate amyloidosis of gelsolin by enabling intermolecular β-sheet formation (Suk et al. 2006).

Other mechanisms for fibril growth have been proposed such as linear colloidal aggregation as a mechanism for growth of amyloidogenic proteins Aβ (Carrotta et al. 2005) and *Saccharomyces* Sup35 (Xu et al. 2001), whereby nucleation units form and then join others to form the fibril length. Domain swapping has been associated with general protein aggregation but has also been proposed as a mechanism for amyloid fibril formation (Sinha et al. 2001; Yang et al. 2005; Zerovnik 2002) specifically of cystatin (Janowski et al. 2005; Nilsson et al. 2004) and oxidised β2M (Chen and Dokholyan 2005). Both mechanisms, while possibly applicable to these proteins, are not accepted for amyloid formation.

Energetics of fibril formation

The folding from nascent strings of amino acids to amyloid fibrils has been described by an "amyloid funnel" (Otzen et al. 2000), progress through the funnel being associated with a narrowing of a large number of initial oligomeric states and a decrease in the overall energy of the protein with the presence of various intermediate species shown through experimental work (Ahmad et al. 2005; Fezoui and Teplow 2002; Kirkitadze et al. 2001; Podesta et al. 2006). Bond reorganisation as the protein moves through the funnel may be hindered by the presence of large energy barriers, resulting in the presence and accumulation of these intermediate species. In fact, there may be several, independent folding pathways to the final conformation, apparently influenced by changes in the environment or primary sequence (Bieri et al. 1999; Kiefhaber 1995). Furthermore, the intermediates may be either productive (on-pathway) and assist formation of the native state, or limit folding by forming trapped intermediates which require substantial reorganisation (off-pathway) to reach the final folded conformation (Bollen et al. 2004).

The mechanism of amyloid formation appears to have much in common with the process of nucleation-dependent crystallisation, where a series of thermodynamically unfavourable steps leads to the formation of a nucleus with a critical size. Further addition of monomers is a thermodynamically favourable process. The well-ordered nature of amyloid fibrils is evidence of the involvement of specific molecular interactions, rather than non-specific aggregation by promiscuous hydrophobic contacts. In terms of energetics of the process of fibril formation, three stages may be discerned (Fig. 10). The first is assembly of oligomeric intermediates from native protein or peptide. This is a thermodynamically unfavourable process and represents the rate-limiting step for fibril formation. In the second stage, which is reached after a critical nucleus size is reached, fibril formation commences. This is favoured by the greater thermodynamic stability of the fibril form compared to the native protein. The third stage involves the addition of monomeric protein to the growing ends of a fibril, which is a template-induced change to deposited monomer on the end of a fibril and a reorganisation to regenerate the growing fibril.

Within the oligomeric aggregates, there is a process of molecular shuffling, reducing the number of contact registers by favouring those that result in increased stability (Fig. 10). There may be energy barriers to this reorganisation, which may explain the observation of several fibril forms within samples of the same peptide or protein (Kad et al. 2003). Buxbaum has described this as a process with "multiple starting points, temporal asynchrony or parallel pathways" (Buxbaum 2003). It is conceivable that high local energy barriers exist during the folding (or misfolding) process associated with the entropic cost of association. Eventually, assuming the energy barriers to reorganisation can be overcome, the aggregates will be dominated by the one or two registers that give the best packing and hence the lowest energy structures. This scheme is consistent with the observation of lag phases in amyloid assembly, with a "nucleated assembly" process where, once stable aggregates are formed, they are able to exert a template effect by the recruitment of monomeric species to the surface of the aggregate and in addition to the rapidly growing fibril. Further assembly of early stage oligomers could then be expected to lead to the various later stages that have been detected such as protofibrils and fibrils (Lashuel et al. 2000). Protofibrils apparently associate laterally, resulting in fibrils or ribbon-type filaments, or other non-covalent polymeric assemblies. For unfolded peptide and protein species, the contact sequences will be constantly exposed in the monomer and available for intermolecular association. Aggregation will be determined solely by the side-chain properties and concentration. For natively structured proteins there is a requirement for assembly to be preceded by partial unfolding and

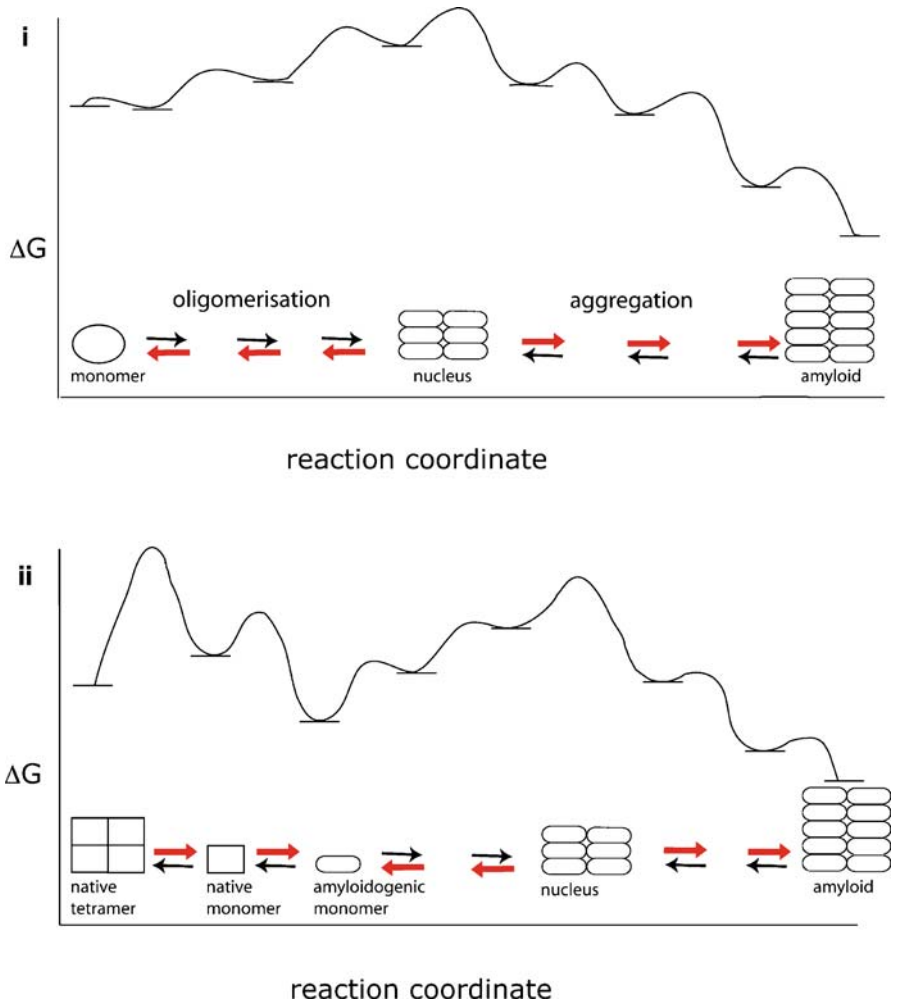

Fig. 10i, ii Energetics of fibril formation. **i** Free energy diagram for assembly of Aβ fibrils according to a nucleation-dependent polymerisation model. The highest energy species along the pathway is the thermodynamic nucleus, which is formed by a series of thermodynamically unfavourable steps. Addition of monomer to the thermodynamic nucleus is thermodynamically favoured. **ii** Free energy diagram for assembly of TTR fibrils. The model has been modified to take into account the requirement for initial disassembly of tetrameric TTR to a monomer, which under denaturing conditions can go on to form amyloid fibrils. (Adapted from Hurshman et al. 2004)

exposure of a particular sequence region. Amyloid formation will then be determined by the particular qualities of the solvent-exposed "sticky sequence".

By comparison to amyloidogenic proteins, it is proposed that natively folded proteins fold much more quickly, limiting the formation of semi-stable intermediates. Clark (2004) suggested that proteins normally have a comparatively smooth funnel, producing "metastable" native proteins. As discussed earlier, chaperones and quality control mechanisms within the cellular environment play a role in "smoothing" the folding pathway, entropically lowering the energy barrier to conformational changes. Additionally, it appears that native proteins have developed protective mechanisms, such as Pro (Wigley et al. 2002) and Gly

(Parrini et al. 2005) residues in helices, or around the edges of native sheets (Richardson and Richardson 2002) to protect against misfolding and aggregation. Furthermore, Otzen et al. described the existence of "structural gatekeepers", which are amino acids not directly involved in protein folding or stability but have been shown, through mutagenesis studies, to influence folding by preventing a misfolded state, although the mechanism is unknown (Otzen et al. 2000; Otzen and Oliveberg 1999). This notion of "structural gatekeepers" has been supported by similar work on acylphosphatase, and it appears that these residues have a role in "smoothing" the protein-folding funnel for native proteins(Chiti et al. 2002b). It is thus plausible that errors or alterations in these mechanisms via sequence mutation or environmental influences can result in previously natively folded proteins forming potentially a variety of non-native intermediates with large kinetic barriers and entering the "jagged" amyloid funnel.

Aggregates and toxicity

One reason for intense interest in the early stages of amyloid formation is evidence that small soluble oligomeric peptides are more toxic to the cell than fibrils themselves. Amyloid fibrils may in fact be protective, removing toxic oligomeric intermediates from circulation. There is now a great deal of evidence to support the toxic oligomer hypothesis, including the fact that there is a poor correlation between disease severity/symptoms and amyloid load measured at post-mortem for patients who died from amyloid-associated diseases. A great deal of research has concentrated on the role of Aβ oligomers in Alzheimer's disease, a subject reviewed recently by Klein et al. (2004). In transgenic mice expressing human APP and Aβ, deficits in neurological function were observed prior to amyloid formation (Oddo et al. 2003). Small Aβ-derived diffusible ligands (ADDLs), small oligomers of Aβ, were found to inhibit long-term potentiation in hippocampal slices within 45 min at doses as low as 100 nM. Interestingly, treatment of transgenic mouse models with Aβ antibodies reversed memory failure within 24 h after a single injection, without eliminating plaques (Dodart et al. 2002; Kotilinek et al. 2002). ADDL concentrations were up to 70-fold greater in AD patients compared to normal controls, with average excesses of 12-fold. The dominant species of ADDL derived from *in vitro* sources is made up of dodecamer with a pI of 5.6. $A\beta_{1-42}$ monomer has been found to rapidly assemble in solution into pentamer/hexamer units, termed a "paranucleus" which can then continue self-association to give larger assemblies.

Other amyloid species have given similar results (Schaffar et al. 2004). Over-expression of α-synuclein in COS-7 cells showed formation of non-fibrillar inclusion prior to detection of fibrillar assemblies. These inclusions were associated with Golgi fragmentation and a reduction in cell survival. No correlation has been observed between Parkinson's disease causing mutation and acceleration of fibril formation, suggesting that fibrils are not the agent causing the neurological damage in this disease. The A30P α-synuclein mutant forms more protofibrils than the wild-type protein and has more rapid formation, but is slower to progress to form fibrils, meaning that the A30P protofibrils may have a longer lifetime (and thus cause more cumulative damage) than the wild-type protein. Protofibrils formed from α-synuclein have been found to cause leakage from synthetic vesicles, whereas the monomer protein and fibrils do not have this property. In HD, neuronal disruption can be detected prior to the appearance of aggregates of the huntingtin protein. The apparent targets for the toxic effect are a number of transcription factors, including the TATA-box binding protein, a component of the general transcription initiation complex, and the transcriptional coactiva-

tor cAMP-response element binding protein (CREB)-binding protein. Schaffar et al. (2004) have shown that monomers and small oligomers of polyglutamine expanded huntingtin, Htt-53Q, inactivate these transcription factors. TATA binding protein (TBP) binding to DNA was completely inhibited by incubation with soluble oligomeric species of Htt-53Q. Pre-formed aggregates did not, however, sequester the transcription factors. It would thus appear that small more soluble aggregates could represent the putative toxic agents.

Oligomeric assemblies of proteins that are not associated with amyloid diseases have also been found to be toxic. Bucciantini and co-workers investigated the effects of oligomers of PI3-SH_3 and HypF-N on cell survival (Bucciantini et al. 2002), both proteins forming amyloid fibrils *in vivo* under denaturing conditions but do not appear to be linked with any disease. The cytotoxicity of pre-fibrillar intermediates was assessed using the MTT reduction inhibition assay [MTT, 3-(4,5-dimethylthiazol-2-yl)-2,5-diphenyltetrazolium bromide]. Granular aggregates of PI3-SH_3 reduced cell viability at concentrations greater than 1 μM. When administered as fibrils, there was no reduction in cell viability for either of the two cell lines used. Control experiments using the soluble form of the protein also had no effect. HypF-N aggregates showed time-dependent toxicity behaviour, reaching a maximum after 48 h of incubation. Cell death was also detected, with 40% cell death at 2.5 μM protein concentration, using the trypan blue internalisation test. The decline in toxicity after 48 h was connected with the increasing concentration of fibrils, with a decline in other aggregate forms. The mature form of the fibrils appeared innocuous. A subsequent paper showed that HypF-N aggregates induced permeabilisation of artificial liposomes to Ca^{2+} (Relini et al. 2004). Interactions were observed for vesicles made from negatively charged phospholipids (phosphatidylserine), but not neutral phosphatidylcholine. The maximum effect was observed after 50 h of incubation, which corresponds to the time observed for maximum toxicity in the MTT assay. The lowest Ca^{2+} permeabilisation activity was observed with mature fibrils. The permeabilisation also appeared to be size-selective, being higher for free Ca^{2+} than for calcium. These observations about permeabilisation are relevant to the proposed mechanism for general amyloid toxicity with respect to the formation of non-specific ion channels in the membranes of cells. This connection held up when pre-fibrillar aggregates of HypF-N were added to cells (Bucciantini et al. 2004). The effects on Ca^{2+} levels in the cytosol were measured using fluorescent probes. Intracellular Ca^{2+} levels rose by a factor of 2 after 3 h exposure to a 20 μM solution of protein aggregates, compared to the control. A significant increase in levels of reactive oxygen species was also observed, which could be alleviated by prior administration of reducing agents such as vitamin E. An accumulation of the pre-fibrillar aggregates occurred in the vicinity of the plasma membrane.

Factors affecting amyloid formation

A diverse range of factors has been shown to influence, often profoundly, the aggregation of amyloidogenic proteins and peptides. These include amino acid composition and sequence; peptide length, concentration, pI and solubility; and environmental conditions such as pH, temperature, solvent, metal-binding, macromolecular packing, membrane interactions and post-transitional modifications. Some of these effects are outlined below.

Peptide composition

Amino acid sequence

There is overwhelming support for the idea that the primary amino acid sequence, or changes within it, are responsible for initiating aggregation (Kammerer et al. 2004; Williams et al. 2006). From various mutagenesis studies, it has become clear that key residues are important in driving aggregation. This work has been taken further, identifying specific regions within a protein or peptide or peptide that are responsible for aggregation, allowing for the prediction of amyloidogenic proteins from their primary sequence (Lopez de la Paz and Serrano 2004; Pawar et al. 2005). Pawar et al. (2005) described these "sensitive" regions as either "aggregation-prone", which forms part of the sheet core in resulting fibrils, or "aggregation-susceptible", which could possibly initiate aggregation as a result of mutations. These regions were identified based on the intrinsic aggregation propensities of the amino acids, calculated according to sequence hydrophobicity, secondary structure propensity and charge (Pawar et al. 2005); alternatively, Sanchez de Groot et al. (2005) used Aβ experimental mutational data.

Chiti and co-workers carefully analysed the dependence of both aggregation and folding on residue sequence identity (Chiti et al. 2000). Human muscle acylphosphatase (AcP) mutants were constructed with conservative single amino acid mutations introduced throughout the whole sequence. The studies were carried out in 25% aqueous TFE solution, where all the mutant proteins were unfolded, allowing effects of substitution on aggregation to be separated from effects on protein folding stability. It was found that the regions of AcP responsible for initiating aggregation were those possessing a high degree of hydrophobicity and propensity to form β-sheets, but which are outside the regions responsible for forming folding nuclei. Using experimental data, they developed an equation to explain the effects of mutations on the aggregation rate with experimentally derived coefficients (Chiti et al. 2003).

$$\ln\left(v_{\mathrm{mut}}/v_{\mathrm{wt}}\right) = A\Delta\ \text{Hydrophobicity} + B\left(\Delta\Delta G_{\text{coil-}\alpha} + \Delta\Delta G_{\beta\text{-coil}}\right) + C\Delta\ \text{Charge}$$

where v_{mut} is the rate of aggregation of the mutant protein; v_{wt} is the rate of aggregation of the wild-type protein; A, B and C are the experimentally determined factors for the dependence of $\ln(v_{\mathrm{mut}}/v_{\mathrm{wt}})$ on each parameter (0.633, 0.198, and –0.491 respectively); ΔHydrophobicity is the change in the hydrophobicity of the polypeptide chain; $(\Delta\Delta G_{\text{coil-}\alpha} + \Delta\Delta G_{\beta\text{-coil}})$ is the propensity to convert from α-helical to β-sheet structure, and ΔCharge is the change in the overall charge of the protein.

The calculated rates were in good agreement with those determined experimentally, for conditions under which the polypeptide chain was unstructured. For the 27 mutations for which suitable data were available, the correlation was 0.85 (with $P < 0.0001$), with a slope value of 0.94. For mutations in the single protein, AcP, the correlation also held ($r = 0.756$, $P < 0.0001$, slope = 0.96). They also noted that very short peptides and several polyamino acids both have the capacity to form amyloid fibrils. These short peptides, however, lack the capacity to fold into stable folded species [a minimum length of ca. 15 residues has been suggested as being required for the formation of stable α-helix structure in aqueous solution (Scholtz and Baldwin 1992)]. Solid-state NMR investigations of fibrils formed by Aβ1–40 (Petkova et al. 2002) and a transthyretin peptide fragment (Jaroniec et al. 2002) have shown the existence of only intermolecular hydrogen bonding along the peptide main chain. Although not conclusive, this is supportive of unfolded precursors being involved in amyloid formation, at least for these two examples. There are also indications that the so-

called unfolded conformation may be a misnomer in that there may actually be discernible structure present, biased towards extended main chain conformations, which would be able to undergo alignment into amyloid fibrils.

Pawar et al. were able to show that the generic factors affecting amyloidosis are hydrophobicity, secondary structure propensity and charge and used these to create intrinsic *Z*-scores for aggregation of any polypeptide, enabling calculation and comparisons between different polypeptide sequences (Pawar et al. 2005).

$$P_{\mathrm{agg}} = \alpha_{\mathrm{hydro}} I^{\mathrm{hydro}} + \alpha_{\alpha} I^{\alpha} + \alpha_{\beta} I^{\beta} + \alpha_{\mathrm{pat}} I^{\mathrm{pat}} + \alpha_{\mathrm{ch}} I^{\mathrm{ch}}$$

where P_{agg} is the propensity of the given peptide to aggregate, I^{hydro} is the hydrophobicity of the sequence, I^{α} is the α-helical propensity, I^{β} is the β-sheet propensity, I^{pat} is the hydrophobic patterning and I^{ch} represents the absolute value of the net charge of the sequence. α is determined experimentally and weights the individual factors (pH must be stipulated and hydrophobicity and secondary structure propensities normalised for the length of the chain).

$$Z_{\mathrm{agg}} = \left(P_{\mathrm{agg}} - \mu_{\mathrm{agg}}\right)/\sigma_{\mathrm{agg}}$$

where Z_{agg} is the intrinsic *Z*-score for aggregation, μ_{agg} is the average value for P_{agg} over a set of random polypeptides having the same length as the sequence of interest and σ_{agg} is the corresponding standard deviation of the average.

Chiti et al. (2002b) have recently presented data showing that, at least for AcP, the regions of protein sequence responsible for protein aggregation are distinct from those which determine the rate of protein folding. These results suggest "kinetic partitioning" of the aggregating and folding processes, although both involve nucleation around which the nascent chain assembles and folds via bond formation and rearrangement.

Polyglutamines

The first peptide motif definitely identified as amyloidogenic was that of long polyglutamine stretches. Huntington's disease (HD) is the best known of nine similar disorders which involve the expansion of polyglutamine repeats within proteins caused by increases in the number of CAG trinucleotide repeats [Table 1; the other known diseases are spinal and bulbar muscular atrophy (SBMA), spinocerebellar ataxia types 1, 2, 3, 6, 7 and 17 (SCA) and dentatorubral-pallidoluysian atrophy (DRPLA)]. HD is an inherited neurodegenerative disorder caused by a gene defect on chromosome 4 that causes selective loss of neurons, particularly in the striatum with a prevalence of approximately 1 in 10,000 in Caucasian populations, with lower frequencies reported in non-Caucasian populations. All individuals with HD appear to share a CAG trinucleotide repeat expansion mutation, which results in a variable length polyglutamine stretch within the N-terminal of the huntingtin protein. The CAG repeat encodes a run of consecutive glutamine residues 17 amino acids downstream from the initiator methionine. The polyglutamine tract is succeeded by a proline-rich segment of 29 prolines followed by the remainder of huntingtin, which extends to more than 3,100 amino acids. The HD mutation alters a CAG trinucleotide repeat that is polymorphic on normal chromosomes, comprising 10–35 units. On HD chromosomes, the repeat is expanded to more than 35 CAGs and can range as high as 150 or more, although most HD alleles have 40–50 CAG units.

The length of the CAG repeat accounts for about 60% of the variance in age at onset. Poly(Gln) stretches of 38 or more carry the risk of disease. Repeat lengths of 38 to 39 are associated with the late onset form of the disease (60- to 80-year age range) with slow,

progressive disease. Repeat lengths greater than 70 residues lead to an aggressive form of HD, with patients having onset of symptoms between the ages of 5 and 15 years. Interestingly, the threshold of tolerance for glutamine expansions varies between different poly-Q proteins, suggesting that the stability of these proteins also depends on their individual sequences, where the polyglutamine region is located in the protein, and perhaps the nature of the regions that surround the glutamine repeat (Chow et al. 2004).

This dependence on the length of the polyglutamine repeat has led researchers to investigate artificial peptides with varying numbers of glutamines in order to better understand this correlation between the number of repeats and the severity of disease. *In vitro* studies of polyglutamine peptides were hampered by their insolubility in water. This was overcome by using peptides with charged residues at the termini (Perutz et al. 1994). Perutz used the peptide $E_2Q_{15}K_2$ to overcome this problem, with the charged residues providing additional solubility. At pH 7, precipitation was observed to produce particles with a thickness of 70–120 Å and of varying length. Perutz et al. have proposed that the huntingtin protein may have a β-helix structure once assembled in the amyloid fibril, giving a narrow tube with a central water-filled cavity (Perutz et al. 2002a). Such a cylindrical structure would require a length of at least 40 residues, to complete two turns of a β-helix. A review collating evidence for this proposal, including for other proteins, has appeared (Wetzel 2002).

Wetzel has investigated in detail the kinetics of aggregation for peptides of the type $K_2Q_nK_2$ (Chen et al. 2002). Polyglutamine peptides regardless of repeat length were found to adopt a random coil state in solution. Aggregates of the same polyglutamine peptides had a CD spectrum dominated by β-sheet structure. They found no evidence for adoption of a β-sheet structure in the peptides before aggregation. This was also reflected in the sharp isodichroic point at 219 nm in the CD spectrum, indicating a transition between two structural states with no significant population of intermediates. This transition was studied for $n = 28$, 36 and 47.

The kinetic behaviour observed for the polyglutamine peptides displayed a kinetic lag phase, which could be shortened or abolished by seeding the solution, consistent with a nucleated growth mechanism. Their kinetic analysis was used to determine the "critical nucleus", i.e. the number of monomers that associate together to form the nucleus. All three peptides had values for the critical nucleus close to 1. The aggregation kinetics of polyglutamine peptides are known to be strongly dependent on the number of polyglutamine repeats. It had been found previously that the elongation rates for polyglutamine peptides above about $n = 36$ changed very little. This means that differences in aggregation rate must be due to differences in the equilibrium constant between disordered monomer and the folded nucleus. Subject to several assumptions, a value of 0.5 kcal/mol is suggested as the difference in free energy of folding between Q35 and Q38. The kinetic model used has an energetically unfavourable transition from a natively folded molecule. Chen and co-workers were able to use the kinetic parameters collected to estimate the role that nucleation kinetics might play in age-of-onset of HD. For the Q_{47} peptide at a concentration of 0.1 nM, a lag-phase estimate of 31 years was found, which is within the range expected for HD patients with this repeat length (30–40 years). The corresponding periods for the Q_{36} and Q_{28} peptides were 141 years and 1,273 years, respectively. Although disease is not known in individuals with $n \leq 36$, individuals with a repeat length of 38 tend to develop HD around age 70. This shows that these *in vitro* studies do have applicability to the processes that occur in these diseases. Chen and co-workers have noted that although peptides containing glutamine repeats up to 42 still formed fibrils, they did not show birefringence when bound to Congo red (Chen et al. 2002). This suggests a greater degree of order in the longer peptides. There is also evidence

that the huntingtin protein is able to recruit other polyglutamine proteins into the amyloid, even though they are unable on their own to form amyloid (Chen et al. 2001b).

Proteins associated with neurodegenerative diseases are not the only ones found to be glutamine- or asparagine-rich. Yeast prions for example are known to contain a larger percentage of Gln residues than proteins in general (Perutz et al. 2002b). Michelitsch and Weissman (2000) carried out a survey of 31 complete and several partial proteomes. They searched for Q/N-rich domains within proteins, defined as the occurrence of 30 or more glutamine or asparagine residues within a window of 80 consecutive residues. This conservative definition was chosen to only select the proteins most likely to be capable of forming amyloids or prions.

The biological functions associated with Q/N-rich proteins were varied, including transcription and translation factors, nucleoporins, DNA- and RNA-binding proteins and vesicular trafficking proteins. Q/N-rich regions were nearly absent from the proteomes of the thermophilic organisms examined. Levels of glutamine in thermophiles and mesophiles display the largest difference of any of the amino acids (1.85% vs 4.31%). Asparagine is also on average less abundant. This may be due to evolutionary pressure to avoid chemical instability associated with deamidation of these residues, which would be more significant at higher temperatures. The lower Q/N content could also be to avoid problems with protein aggregation.

Other polyamino acids

The dependence of amyloidogenicity on amino acid sequence can be addressed by the use of polyamino acids. Polymers of a single amino acid type enable the study of polypeptides without the competing complications of stable tertiary structure. Fändrich and Dobson (2002) looked at the structure of polymers of poly-L-lysine, poly-L-glutamic acid and poly-L-threonine. Poly-L-lysine is known to adopt several secondary structures depending on solution conditions. At pH 7, the polypeptide adopts a random coil conformation. Increasing the pH to 11.1 causes the adoption of an α-helical conformation. This is lost upon heating, to give an irreversible change to a β-sheet form. The random coil state can be regenerated by lowering the pH to neutrality.

Electron microscopy of the heated pH 11.1 solutions found the presence of fibrils of up to 11 nm wide and of variable length. Ribbon type structures were also observed, with helical twists of around 100 nm. Heating of poly-L-glutamic acid at pH 4 also produced fibrils. Poly-L-threonine was also found to form aggregates and, furthermore, did not require heating to do so. The necessity for a certain degree of solubility to enable amyloid formation was shown by the polymers of alanine, valine, leucine, isoleucine, phenylalanine and tyrosine. These polymers precipitated rapidly from aqueous solution and were thus unable to form ordered aggregates. There are several important conclusions that can be drawn from this study. The first is that the nature of the side chain may not be as important as the main-chain contributions to stability of the amyloid aggregate. Different polyamino acids still remained capable of forming amyloid [see also Koga et al. (2003) for an example of amyloid formation by a polyamino acid with a modified side chain]. The resultant cross-β structure is not dependent on an initial folded conformation, as this is not accessible by the poly-amino acids. Although side-chain interactions may influence the stability of the amyloid state and may affect the kinetics of the process, they do not appear to control the structure adopted by the amyloid. Some polyamides or nylons are known to adopt a chain arrangement similar to the aggregated polypeptides, despite lacking side chains (Bunn and Garner 1947). It appears then that amyloid formation is the consequence of reduction in

stability of secondary structure that allows the amyloid form to compete. It is also possible for specific side-chain arrangements (such as charge) to destabilise the aggregated state and thus to disfavour amyloid formation.

The study of polyamino acid aggregation is relevant to the number of amyloid diseases known to be due to long repeats of specific amino acids within proteins. The best-known example is, of course, polyglutamine stretches in the huntingtin protein as mentioned above, but there have been also reports connecting the formation of fibrils in muscular dystrophy with poly-L-alanine stretches (Calado et al. 2000) and Holmes et al. have reported a protein with poly-L-leucine repeats that is associated with disease (Holmes et al. 2001). In oculopharyngeal muscular dystrophy, an expansion of the N-terminal poly-alanine stretch in the polyadenine-binding protein 2 (PABP-2) from 10 to 12–17 Ala residues causes nuclear filamentous inclusions (Calado et al. 2000). Short poly-alanine repeats are found in nature. Their only known function is in spider fibre protein, where the poly-alanine segments endow crystalline properties to the fibres. Perutz et al. found that a model peptide containing a poly-alanine stretch $D_2A_{10}K_2$ did not aggregate, remaining strongly α-helical over the pH range investigated (pH 3.5 to 8.3; Perutz et al. 2002b). Giri et al. (2003) found that the peptide Ac-KMA_7GY also adopted exclusively an α-helical structure. However, the related peptide, with a stretch of 11 Ala residues, formed β-sheet. Electron micrographs showed the formation of amorphous clumps, with no fibrils being observed, even after ageing of the solution. There was also a statistically significant difference observed in the ability of the peptides to inhibit cell growth of Chinese hamster V79 cells. The Ala_7 peptide inhibited cell growth 18%, whereas the longer peptide inhibited cell growth by 55%. The longer peptide also induced apoptosis in treated cells. When green fluorescent protein (GFP) was fused to 19–37 alanines, the cells had high levels of intracellular aggregates and nuclear fragmentation (Rankin et al. 2000). Ma and Nussinov (2002) have undertaken a molecular dynamics simulation of alanine-rich sequences AGAAAAGA and AAAAAAAA. They simulated the stabilities of pre-formed β-sheet oligomers in aqueous solution and found that the oligomers were stable when 6 or 8 peptides were associated together.

Hydrophobic residues

Not surprisingly, hydrophobicity plays a major role in aggregation and amyloid formation because the exposure of hydrophobic residues to water is entropically unfavourable and forces protein association, protecting these regions from the polar environment. Appropriately then, globular proteins have tended to evolve without long strands of hydrophobic residues in most of their primary sequence (Schwartz et al. 2001). Where long stretches of hydrophobic residues are found they often perform membrane-associated or membrane-penetrating functions. These hydrophobic sequences can be accommodated within the globular structure, preventing exposure to the environment, or at the surface of the protein for specific interactions. Importantly, some, but not necessarily all, known amyloidogenic proteins contain a hydrophobic core (Aβ residues 17–21 and 32–42, α-synuclein residues 71–82, islet amyloid polypeptide residues 22–27 and AcP 16–31). It is thus conceivable that denaturation and partial unfolding of globular proteins can lead to the exposure of hydrophobic residues, promoting aggregation to overcome the unfavourable interactions. Similarly, sequence mutations from hydrophilic to hydrophobic residues in certain "aggregation-prone" or "aggregation-sensitive" regions can lead to the formation of "sticky regions" which associate to initiate aggregation. However, not all amyloidogenic proteins are globular or contain hydrophobic regions. Other factors therefore must influence aggregation.

Gazit (2002) has pointed out the importance of aromatic π-stacking in the peptide self-assembly process. The three aromatic amino acids are among the six with the lowest frequency of occurrence in proteins. Tyrosine and phenylalanine have occurrences of 3.2% and 3.9% respectively, whereas tryptophan has an even lower occurrence of only 1.3%. This low frequency could be the result of selection pressures favouring peptide sequences that are not prone to aggregation. Amyloid proteins often have a short stretch of the protein that is essential for amyloid formation. These minimal fragments have an over-representation of aromatic residues (see Table 1). When peptides containing these fragments are synthesised, then they too have been found to undergo amyloid assembly.

Attractive non-bonded interactions are possible between aromatic rings. π-Stacking would provide two processes essential to the formation of amyloid fibrils:

1. An energetic contribution from the π-stacking, which can help to contribute to the thermodynamic forces driving the assembly process
2. Directionality and order to the alignment of the peptides

The π–π stacking restricts the geometries allowed by the nature of the interaction between the two aromatic moieties, which is consistent with a process of amyloid formation being directed by a short stretch within the peptide. There are four basic geometries allowing for stacking interactions. The parallel-displaced geometry is that most commonly found in structures of proteins (Burley and Petsko 1985). There may also be an entropic contribution provided by π–π stacking in that the release of ordered water molecules on the formation of the intermolecular interactions would be entropically favourable. Azriel and Gazit (2001) undertook an alanine scan of the islet amyloid polypeptide (IAPP)-derived peptide NFGAILSS. The ability to form fibrils was completely abolished by the replacement of Phe with Ala. No other residue replacement had such a dramatic effect. Recently Tracz et al. (2004) reported that substitution of Phe-15 with Ala in a peptide corresponding to residues 10–19 of human amylin significantly reduced amyloid formation.

Studies are beginning to appear using solid-state NMR to investigate the organisation of the peptide chains within amyloid fibrils. Such information has been hard to collect previously because of the insolubility of the fibrils and their lack of crystallinity. One such study of the labelled DFNKF peptide and related peptides from calcitonin (Naito et al. 2004) found that the conformational change from random coil to β-sheet occurred at the vicinity of the F2 residue in pentapeptide DFNKF. In the fibril structure formed by the full-length calcitonin, there was a head-to-tail anti-parallel β-sheet arrangement of the peptide chains. This arrangement had the phenyl rings of two strands (Phe-16) facing each other on the same side of the β-sheet, located in such a manner that they could stack in parallel and make π–π interactions, thus helping to stabilise the fibril structure.

Hydrophobic-hydrophilic patterns

One of the very early patterns identified as amyloidogenic was an alternating pattern of hydrophobic and hydrophilic residues. It is easy to see why this should be. The alternating, zigzag nature of the β-strand can lead to a hydrophobic face and a hydrophilic face. A β-strand can thus form hydrogen bonds to neighbouring strands on either side and in addition make hydrophobic contacts with a third strand above or below it. Amyloid formation then is possible where the aggregation process is sufficiently held in check to allow an ordered assembly within the β-sheet oligomer. This may be by the presence of solubilising groups or charge differences.

Xiong and co-workers (1995) carried out an elegant experiment to assess the significance of the intrinsic secondary-structure propensity of the amino acid residues relative to periodicity in the peptide sequence; the experiment was designed to favour another secondary structure. Four peptides were prepared with their periodicity favouring either an α-helical or β-strand secondary structure. Their constituent amino acids were chosen to either reinforce or work against this periodicity.

The sequences of the peptides were designed so that the repeating pattern of either polar or non-polar residues would match the structural periodicity of an α-helix (3.6 residues per structural unit) or a β-strand (2 residues per structural unit). If the peptides took up their expected secondary structure then they would have an amphiphilic structure. This would then favour oligomerisation to remove the hydrophobic surfaces from contact with bulk solvent. It was found in all cases that, instead of the intrinsic secondary structure favoured by the constituent amino acid residues, the generated secondary structure followed the periodicity.

This study was subsequently extended by the generation of a combinatorial library of synthetic genes expressed in *E. coli* (West et al. 1999). The library was designed to contain 6 β-strand stretches of 7 residues, with the β-strand stretches separated by 4-residue turn regions. The β-strand regions were designed with an alternating pattern of 4 polar and 3 non-polar residues per stretch. The polar residues were allowed to be His, Lys, Asn, Asp, Gln or Glu. The non-polar residues were constrained to be Leu, Ile, Val or Phe. At a protein concentration of 500 μM, the proteins selected for study all had an apparent molecular mass of more than 1,000 kDa. For a 63-residue protein, this would correspond to ca. 140 monomers per oligomer. When these proteins were diluted to 5 μM, the larger oligomers dissociated to give apparent molecular masses of around 29 kDa, which is approximately four times the mass expected for a monomer, suggesting the formation of tetrameric species at lower concentrations. These species reassembled into the larger oligomeric form upon re-concentration. This reversible assembly suggests that these structure are under thermodynamic control.

These repeating hydrophobic–hydrophilic patterns are avoided in proteins. For a 7-residue peptide stretch, comprising 4 hydrophilic and 3 hydrophobic residues, there are 35 ways of arranging the residues. An analysis of 250,514 sequences found that in 7-residue stretches comprising these numbers of hydrophilic and hydrophobic residues, the alternating arrangement was the least common arrangement (Broome and Hecht 2000). It was found that the ability of the designed peptides to form amyloid could be removed by the replacement of one of the non-polar residues in the first, or last, or both β-strand regions by a lysine (Wang and Hecht 2002). This had the effect of adding a charged residue into the strand, a strategy also observed in nature, where natural β-sheet proteins avoid aggregation by the incorporation of negative design elements. This would favour monomers by forcing the altered β-sheet region to be solvent-exposed.

Electrostatic interactions

Although less effective than hydrophobic interactions, charge effects in proteins have been shown experimentally to be important in initiating aggregation (Calamai et al. 2003; Lavrikova et al. 2006; Lopez de la Paz et al. 2005; Takahashi et al. 2002; Tjernberg et al. 2002). Mutations which lead to a decrease in absolute net charge appear to increase the tendency for aggregation and can be rationalised by the electrostatic repulsion of like-charged monomers inhibiting close association and aggregation. It is by the same mechanism that influences of pH and ionic solutions can affect aggregation by influencing the charge of side-chain electrostatic properties and protein monomers. Research on the electrostatic

effects on the aggregation of short peptides showed very different results: neutral or high effective charge prevented amyloid formation whereas a net-positive or net-negative charge favoured regular organisation through maximising the distances between charged peptides (Lopez de la Paz et al. 2002). The differences in the results can be attributed to the fact that proteins are large macromolecules with inherently more complex electrostatics that can influence aggregation.

Other patterns

The search for less readily apparent sequence motifs that specify amyloid formation has been difficult. There has been little absolute sequence identity observed in the amyloid-forming proteins. If, as seems increasingly clear, amyloid formation is driven by short fragments of these proteins, then small peptides should be able to be used to assess the contributions from these short sections and how they affect aggregation. Lopez de la Paz and Serrano (2004) undertook a systematic investigation of the effect of single amino acid changes on the amyloid-forming ability of the hexapeptide STVIIE. Each position was systematically altered with all of the amino acids except for cysteine. This full positional scan was undertaken to determine precisely the interaction between residue and position within the peptide. The β-sheet percentage for each peptide variant was estimated using circular dichroism. Solutions were analysed using EM and the presence and abundance of fibrils was noted. It was found that there was a strong positional dependence. The end positions 1, 2 and 6 were very accepting of changes. All non-positively charged substitutions were tolerated well at position 6 except for Leu and Glu (at neutral pH), which led to the formation of less amyloid material. Positively charges substitutions (R, H, K) in position 6 blocked amyloid formation completely. The middle positions, 3, 4 and 5, were more restricted in the residues that could be replaced and still have fibril formation. For position 5, only three amino acids (the original Ile, Tyr and Phe) were permissible. These all have high β-sheet propensity. This is not merely a question of hydrophobicity, since the β-branched amino acid Val was not suitable. Phenylalanine could be substituted at any position and the resulting hexapeptide would still form amyloid. Differences were observed in tolerances for charged residues. Negatively charged side chains (Asp, Glu, Tyr) could be successfully incorporated at positions 1, 2 and 6. Positively charged residues (Lys, Arg) could only be placed at the first position.

The connection between speed of aggregation and extent of aggregation was examined. The mutations that led to the largest amount of fibrils after a 1 month incubation period were those that only had a very low β-sheet ratio initially. There thus seems to be a connection between slow polymerisation and an enhancement in the extent of fibril formation. However, the pentapeptide STVII is known to be amyloidogenic, and mutations in the sixth position that accelerated amyloid formation also caused formation of large amounts of amyloid material.

Two assumptions were proposed by the authors that would enable their results to be extended to give a pattern rule. They assumed that the relative importance of the sequence positions found for the STVIIE mutants would hold in general for most six-residue amyloidogenic fragments and that most combinations of the allowed residues at a specified position will suffice to specify aggregation. The conclusion that can be drawn from this work is that the degree of amyloidogenicity, at least for shorter peptides, is mainly determined by the amino acids that make up the core (positions 3–5 here) and that the outside residues merely modulate the formation of fibrils.

Although the formulation of this pattern is interesting, the real test is how well it can enable prediction of amyloid sequences. Lopez de la Paz and Serrano scanned the sequences

of several proteins known to form amyloid fibrils either *in vivo* or under denaturing conditions *in vitro*. For many of these proteins, the regions responsible for amyloid behaviour are known, and so these experimentally determined sequences can be compared to those predicted by this pattern. For example, Chiti et al. has shown aggregation of the human muscle AcP protein to be affected strongly by mutations in the region 87 to 98 (experimental conditions pH 5.5, 25% TFE; Chiti et al. 2000). The pattern selected the sequence ^{90}EYSNFS^{95}, within the region determined independently to be intimately connected with the amyloid formation process. The α-spectrin SH_3 domain is not known to aggregate under any conditions, and no matching pattern was detected in the sequence. The related SH_3 domain of phosphatidylinositol-3′-kinase, which shares a high degree of homology and sequence identity, does aggregate under acidic conditions (pH 2.0). Two peptide stretches were found in the P-3′-K SH_3 domain that matched the predicted pattern (^{72}TYVEYI^{77} and ^{73}YVEYIG^{78}) for acidic solutions. Agreement with the pattern was also detected for the *in vivo* amyloid proteins, PrP^c human, human IAPP, Aβ1–42, ApoA and β2m.

As the authors note, the sequence space explored here is small, which means that there are amyloidogenic motifs that escape detection by these pattern rules. For example, the pattern detected in human IAPP was ^{19}SSNNFG^{24}, and a peptide with the sequence ^{19}SSNNFGAIL^{27} has been shown to be amyloidogenic (Tenidis et al. 2000). However, the partially overlapping sequence ^{22}NFGAILSS^{29} has also been shown to form fibrils in solution (Porat et al. 2003), but does not match the described pattern (but it does match the pattern if L, S and S are taken as the first three residues in the pattern and N, F, G as the last three, perhaps indicating some degree of flexibility in the register between peptide strands. A similar argument applies to the amyloid-forming hexapeptide NFGAIL (Tenidis et al. 2000), with counting beginning at Ala. There is thus a need for similar experiments on unrelated sequences to enable the identification of new proteins prone to forming disease aggregates and also to aid the design of *de novo* peptide sequences for new applications.

Peptide length

Reches and Gazit (2003) have recently announced the discovery of nanotubes formed by the phenylalanine dipeptide. After dilution of a 1,1,1,3,3,3 hexafluoro-2-propanol solution of the dipeptide into water, tubular structures were formed within minutes. The persistence length of the nanotubes extended into the micrometre range. IR spectral analysis of the tubes found a sharp peak at 1630 cm^{-1}, consistent with a β-sheet conformation of the amide bond. Upon staining with Congo red, green-gold birefringence was observed, as is commonly observed for amyloid fibrils. The Phe–Trp dipeptide was also found to form tubular structures, but much less efficiently than the dipeptide containing only Phe, with substantial amounts of amorphous aggregates also observed. The diphenylalanine motif is found within the Aβ peptide at a position found to be strongly implicated in amyloid formation.

Intriguingly, investigations by other authors have failed to find evidence for amyloid formation by unmodified tripeptides. Although amyloid formation is claimed for an Ile_3 peptide on the basis of CD and IR spectra, the peptides had oxyethylene side chains attached to either the N-terminus or both termini (Ganesh et al. 2003). Tjernberg et al. investigated the tripeptides KFE, VVV and FFF (Tjernberg et al. 2002). None of these peptides formed fibrils, despite having features that seemed favourable for amyloid formation in related tetrapeptides, such as a complementary arrangement of charges with the peptides or the presence of hydrophobic groups. This is particularly interesting in light of the ability of the phenylalanine dipeptide to form hollow tubules. Amyloid formation appears to become

easier once peptides of four residues in length are reached. Fibrils formed by the tetrapeptides KFFE and KVVE were stained by the dye Congo red and displayed the characteristic green birefringence observed for the naturally occurring amyloids (Tjernberg et al. 2002). The fibrils formed were 1.2 to 1.6 nm in width, which corresponds to the length of the 4-residue extended peptide chain. Interestingly, the two peptides KLLE and KAAAE failed to form amyloid under the same conditions. It was also found that the extent of fibril formation was less when the terminal charges were removed by acetylation and amidation. Low salt concentrations also favoured amyloid formation; i.e. ionic interactions are important in the formation of amyloid species.

One may also in this context point to the difference in aggregation behaviour between $A\beta_{1–40}$ and $A\beta_{1–42}$, where the longer peptide has a faster rate of aggregation *in vitro* and has been connected to earlier onset and a more severe form of disease in Alzheimer's sufferers. Peptide fragments from the islet amyloid polypeptide also differ in their amyloid propensities on the basis of length. NFGAILSS (residues 22–29) is reported to have a faster rate of aggregation than the corresponding peptide formed by residues 22–27 (Azriel and Gazit 2001). It will always be difficult in this context to separate out effects due solely to lengthening the potentially amyloidogenic peptide and those due to the particular contributions from the nature of the added residues.

Solubility, pI and pH

The solubility of globular proteins is determined by the amino acid sequence, the pK_a values of the ionisable residues and other factors such as temperature, pH, ionic strength and the presence of co-solvents. It is well known that most proteins are least soluble in the pH region around their isoelectric point or pI, i.e. the solution pH at which the protein bears no net charge. Schmittschmitt and Scholtz investigated the effects of changes in the pI of RNase Sa and two variants on amyloid fibril formation. The variants were designed to have three or five charge reversals (acidic residues replaced by Lys), resulting in three closely related proteins, with pI values of 3.5, 6.4 and 10.2 (Schmittschmitt and Scholtz 2003). The native sequence forms amyloid fibrils when placed into 30% aqueous TFE solution. The authors assessed protein stability as a function of pH and found that all three variants had their maximum stability around pH 5 (roughly 6–8 kJ/mol). The solubility of the proteins with pH was also investigated and found to be closely connected to the pI values, where each protein was least soluble. The extent of fibril formation as a function of pH was also measured using a thioflavin T fluorescence assay over the pH range 2–9.6. Fibril formation was maximised at pH values where solubility was at a minimum. Conformational stability and the pH dependence of extent of fibril formation showed little correlation. A different survey of 11 other amyloid-forming proteins has revealed a high degree of correlation ($r = 0.98$) between the pH of maximal amyloid formation and pI (Fig. 11; Schmittschmitt and Scholtz 2003).

Lopez de la Paz and co-workers have investigated the effect of peptide charge on amyloid formation in a systematic way by investigating a series of related peptides (Lopez de la Paz et al. 2002), namely KTVIIE, STVIIE, KTVIIT, STVIIT, KTVLIE, KTVIVE, KTVIYE and STVIYE. The peptides were made with either the N-terminal acetylated, the C-terminal amidated, both termini modified or both termini unmodified. In this way, the same peptide sequence could bear a range of possible charges (0, ±1 and ±2) but retain the same sequence. Peptide conformation was monitored using far-UV CD spectroscopy and amyloid formation was detected by EM on carbon-coated EM grids. Some peptide solutions that showed β-

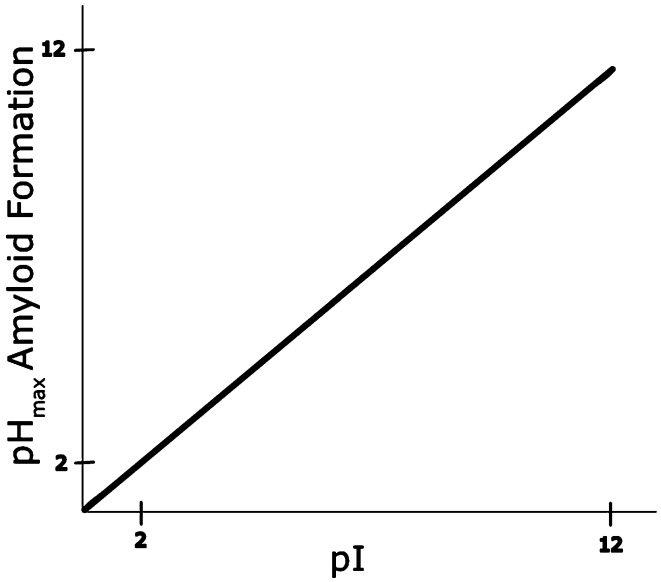

Fig. 11 The relationship between pH of maximal amyloid formation and pI of the amyloid-forming proteins. (Adapted from Schmittschmitt and Scholtz 2003)

sheet formation failed, however, to form fibrils. For peptides that were charged, amyloid fibrils were only observed when the peptides carried a net charge of ±1. Peptides that were neutral overall tended to remain soluble in solution, or only gave amorphous aggregates. The importance of charge was also shown by the effect of increasing ionic strength. Up to a NaCl concentration of 0.1 M, the rate of fibril growth increased with ionic strength, consistent with a reduction in charge-repulsion effects. When the ionic strength was increased further, however, only very short filaments or amorphous aggregates were observable. Amyloid fibrils were formed by STVIIT, when both termini were capped. This peptide carried no charged residues, but the residues were capable of hydrogen bonding and thus increased solubility. If the termini were uncapped, then the molecule still had a net neutral charge, but only amorphous aggregates were formed. Differences were observed in the rate of fibril formation for those peptides that bore a univalent positive charge and those bearing a negative charge. The peptides with a –1 charge were slower to form fibrils, but the fibrils that formed had lower morphological variability. This suggests that where polymerisation is slow, fibril formation comes under thermodynamic control; that is, the most stable fibril structure is formed.

If it is assumed that non-specific aggregation and fibril formation are competing processes, then it can be understood why non-ordered aggregation was observed for the neutral molecules. Where the net charge is zero, there are no uncompensated charges at the β-sheet level, allowing the β-sheets to pack indiscriminately. Multiply charged peptides were apparently unable to form amyloid, probably because of the charge repulsion within the fibril, destabilising it. A single net-positive or -negative charge apparently allows a compromise to be reached. The charge would direct molecular packing by favouring a maximum distance being placed between charged groups on different peptide strands, favouring ordered aggregation. Where no charged groups are present, the self-assembly process will be dictated by the backbone–backbone hydrogen bonds and interactions between side chains.

Protein/peptide concentration

Concentration affects the self-assembly of biomolecules. For surfactants, the existence of a critical micelle concentration is well known; that is, micelles only form when the concentration of the surfactant is above a certain threshold value. Amyloid-forming proteins and peptides may also similarly have a critical aggregation concentration. Fung et al. (2003) investigated the dependence of the assembly process on concentration for the amphiphilic peptide AEAEAKAKAEAEAKAK (named EAK16-II). The assembly process was monitored using surface tension measurements, dynamic light scattering and atomic force microscopy. At the lowest peptide concentrations (0.005 and 0.01 mg/ml) there was no change in the surface tension of solutions with time. At concentrations greater than 0.1 mg/ml there was an exponential decrease in the surface tension. The rate of decrease was most rapid in the first 200 seconds; it then slowly came to equilibrium. For intermediate concentrations there was a lag phase before the exponential decrease in surface tension was observed. The length of this induction period decreased as peptide concentration increased. The observation of complete suppression of the lag-phase once a concentration of 0.1 mg/ml is reached suggests that this is the critical aggregation concentration for this peptide. The induction period exists because a certain number of molecules are needed to adsorb at the surface, before surface tension is affected. The size and amphiphilicity of the particles also affects this.

Interpretation of the AFM images was complicated by the increase in concentration during sample preparation, as the samples were air-dried, causing concentration increases due to evaporation. However, isolated filaments only were found in a 0.05 mg/ml solution, whilst fibrils were found in the solutions with concentrations in the 0.1–0.5 mg/ml range. The fibril width and height were found to increase approximately two-fold and nine-fold respectively, as the concentration was increased tenfold. There was also a sharp increase in the observed density of the fibrils around the 0.1 mg/ml concentration.

The assembly process was also monitored using light scattering. The extent of light scattering is proportional to the particle size. It was found that above the critical aggregation concentration there was a sharp increase in the light scattering with time, whereas below this concentration the intensity was fairly steady, at least over the earliest stages. The critical concentration found using this method was 0.08 mg/ml, which compares well to the 0.1 mg/ml concentration found by the surface tension measurements. The 0.1 mg/ml measurement corresponds to a concentration of 6.04 mM. The critical aggregation constant for Aβ has been reported as about 2.5 mM (Soreghan et al. 1994) though this may be pH-dependent, as a value of 0.1 mM has been reported for a 0.1 M HCl solution (Lomakin et al. 1996).

A similar study of the Aβ1–40 peptide by Lomakin et al. (1996) proposed that particles with a hydrodynamic radius of 7 nm detected prior to significant fibril growth corresponded to micelles. They ascribe the concentration independence observed above the critical aggregation concentration as being the result of a micelle–monomer equilibrium. As free monomers are incorporated into fibrils, the micelle pool is drawn upon, maintaining a monomer concentration slightly above that of the critical aggregation concentration until the micelles are completely depleted. At this stage, the monomer concentration will rapidly fall and hence the growth rate of the fibrils will also rapidly decrease.

The value of the critical concentration for amyloid assembly is dependent on the solvent environment. Fezoui and Teplow have found that fibril formation of Aβ can occur at nanomolar concentrations in aqueous TFE solutions, well below that observed in purely aqueous solutions (Fezoui and Teplow 2002). Yong et al. (2002) found in a small angle neutron scattering experiment that there was no concentration dependence to the size or shape

of Aβ micelles, above the critical micelle concentration. Assemblies of approximately 30 Aβ peptides were found. The effect of increases in peptide or protein concentration is not always to increase the rate of fibril growth. Souillac et al. investigated the kinetics of amyloid formation by the variable domain of an antibody light chain, LEN (Souillac et al. 2003). The lag-phase increased significantly as the protein concentration was increased from 0.01 to 3 mg/ml. The fibril growth rates also decreased with the increase in protein concentration. This indicates that there can be competition with amyloid formation by off-pathway reactions.

Metal binding

There has been a role proposed for metal ions in connection with amyloid diseases, particularly Alzheimer's disease (Bush 2003). The Aβ peptide contains several potential metal-binding residues (His-6, His-13, His-14, Tyr-10), amyloid plaques have been found to contain high levels of copper and iron—and copper has a high affinity for Aβ (Atwood et al. 2000) and strongly potentiates the neurotoxicity of Aβ (Huang et al. 1999)—and chelating agents have been shown to dissolve Aβ amyloid deposits (Cherny et al. 1999). Sequence fragments of Aβ have concentrated upon residues 17–20 and 30–35 as being likely to be responsible for amyloid formation, as these peptide fragments are amyloidogenic on their own. The N-terminus of Aβ is hydrophilic and thus would not be expected to form fibrils under normal circumstances. However, Miura and co-workers found that aggregation could be induced in Aβ3–9 (EFRHDSG) by the addition of Cu(II). With this shorter peptide example, it appears that the hydrophobic interactions that are generally invoked as important to amyloid assembly are replaced by metal-ligand interactions (Miura et al. 2004). Truncations are known to occur *in vivo* to the Aβ peptide, with Aβ species beginning with Glu3 being the dominant species within amyloid deposits in the brains of Alzheimer's disease patients. Studies with full-length Aβ have suggested the formation of cross-links through metal–His bonds in the N-terminal region.

β-2-microglobulin is a 12-kDa polypeptide which is necessary for cell surface expression of the class I MHC. In patients with renal failure, serum levels can rise 5- to 50-fold over the normal level of 0.1 μM. Interestingly, solutions at pH 7 of that protein up to 1 mM remain stable for several months, suggesting the involvement of other factors that cause the deposition of the protein in dialysis-related amyloidosis. The amyloid deposits are formed principally in the joints. Morgan et al. (2001) have recently reported a relationship between exposure to Cu^{2+} and amyloidosis {$[Cu(NH_3)_4(OH)_2]$ is used in the preparation of some cellulose membranes for dialysis and can be released upon exposure to serum}. β2m is able in its native state to bind Cu^{2+}. This was elucidated by ^1H-^1H NOESY spectra, with Cu binding causing paramagnetic broadening of resonances assigned to His31. This residue was conserved across 87 sequence variants. The same group undertook a study of the comparative stability of four mutants and wild-type β2m in the presence of Cu^{2+} and urea (Eakin et al. 2002). For example, *wt*-β2m (2.5 μM) was destabilised 21.0 kJ/mol by the addition of 90 μM Cu^{2+}. The differences in stability observed enabled the conclusion that the changes in stability due to copper were the result of copper binding to the unfolded state. This is most likely to be mediated by co-ordination to His13, His51 and His84. The contribution of Cu^{2+} binding to the stability of the unfolded state is calculated as 17.1 kJ/mol at 20 μM Cu^{2+}. Similarly, Cu^{2+} ions have been shown to accelerate α-synuclein aggregation at physiologically relevant concentrations for a $t_{1/2}$ of 47±5 h (0 μM Cu^{2+}) to 11±3 h (200 μM Cu^{2+})

without altering the resultant fibrillar structures (Rasia et al. 2005). This study showes that Cu^{2+} binds primary at the N-terminus and involves His50 as the anchoring residue.

The effects of metal co-ordination need not be deleterious. Metals are sometimes involved in stabilising proteins otherwise prone to aggregation. SOD1 mutant proteins with impaired metal binding ability are more prone to aggregation (Elam et al. 2003). Apomyoglobin undergoes a thermally promoted denaturation to form fibrils, whereas the metal containing myoglobin is stable to much higher temperatures (Fändrich et al. 2001). There are also indications that the presence of metals can alter the structure of the protofibrils or fibrils formed. Equine lysozyme contains a calcium-binding site and is destabilised when the site is vacant. Fibrils could be formed *in vitro* in the presence of $CaCl_2$ by lowering the pH to 4.5 and increasing the temperature of the solution to 55–57°C (Malisauskas et al. 2003). The fibrils formed were composed of short sections of both bent and straight aggregates between 30 and 100 nm long and around 2 nm high. In the presence of ethylenediaminetetraacetate (EDTA) (to chelate Ca^{2+}), annular structures were the dominant species, with a diameter of 2.0 (±0.5) nm.

Post-translational modifications

There are a number of post-translational modifications that are known to destabilise proteins with respect to aggregation. The likely effect of these modifications is to populate partially unfolded structures that are able to initiate the aggregation process.

Deamidation

Asparagine deamidation is one of the most commonly encountered nano-enzymatic modifications to proteins. Deamidation can result in the formation of several possible products including L- or D-aspartic acid, or formation of the two stereoisomers of isoaspartic acid. In a study of the aggregation of the peptide SNNFPAILSS-NH_2, a variant of the IAPP sequence 20–29, an important role for deamidated impurities was found (Nilsson et al. 2002). Deamidation occurred either in solution or from storage as lyophilised solids. Careful purification of the peptide to remove the deamidation impurities gave solutions that did not aggregate for at least 8 days. However, samples containing less than 5% deamidation products did form amyloid, in a pH-dependent process. At a pH of 5.31 (pD = 5.71) aggregates were formed, some of which resembled classical amyloid fibrils and others formed flat lamellar structures. This study does cause some concern in that amyloid formation studies often involve prolonged incubation either in phosphate buffer solution or at extremes of pH (phosphate is known to be effective at promoting deamidation). Although the effect was most pronounced for the SNNFPAILSS-NH_2 peptide, several other related peptides investigated also showed the same effect. However, the nature of the effect (enhancing, neutral or reducing amyloid formation) will depend on the nature of the sequence.

Isoaspartate formation

Elevated levels of isoaspartate residues have been noted within aged proteins. Aβ extracted from parenchyma contains predominantly isoaspartate residues at positions 1 and 7. The aspartic acid residue at position 23 seems largely unaffected, perhaps because of steric protection by the neighbouring valine. It was found that synthetic Aβ with these substitutions resulted in more stable β-sheets. These two alterations are found near the beginning and

end of what is proposed to be an N-terminal short α-helical section. These changes interfere with the adoption of the native secondary structure, as these residues are unable to be incorporated into α-helices because they have extra CH_2 groups. This may then allow partially folded intermediates to form.

Racemisation

Proteins undergo spontaneous racemisation, with altered proteins increasing with age. Aβ proteins extracted from amyloid plaques have been found to undergo isomerisation or racemisation predominantly at the Asp residues. Tomiyama et al. (1994) investigated the differences between Aβ1–35 and the related peptides containing one or two D-Asp residues. It was found that the extent of aggregation was almost the same for all the peptides studied, as monitored by increases in turbidity of solutions. However, large differences were observed in the rate of aggregation. The Aβ peptide containing a D-Asp at position 23 formed fibrils after 14 days. [D-Asp^{7},D-Asp^{23}]Aβ1–35 and normal Aβ1–35 did not give fibrils until day 21. It took until day 51 for fibrils to be observed in the solution of [D-Asp^{7}]Aβ1–35. Racemisation at position 23 rapidly accelerated peptide aggregation. This position lies after the FF motif found to be independently capable of forming nanotubes (Reches and Gazit 2003). Racemisation at position 7 slowed the rate of aggregation considerably, emphasising that the position of racemisation is critical, not the fact of racemisation per se. Kaneko et al. (2001; Kubo et al. 2002) have found biological implications for the racemisation of Ser-26 in Aβ. Racemisation at that position results in a peptide that *in vitro* failed to give fibrils and was found not to inhibit MTT reduction in HeLa cells or rat hippocampal cultured neurons (whereas toxic Aβ peptides are known to inhibit reduction). However, it was found that treatment with chymotrypsin and aminopeptidase resulted predominantly in fragments [D-Ser26]Aβ25–35. This fragment was found to be highly toxic to rat hippocampal tissue when co-injected with a small amount of ibotenic acid. It also showed significant fibril formation activity, as monitored by a thioflavin T assay. There appears to be little work on the effects of racemisation on other peptides or proteins, but it would appear likely that this process may be of importance in other diseases also.

Glycation

Glycation has also been used to induce aggregation of otherwise stable proteins. The glycation reaction involves the covalent attachment of reducing carbohydrates to the amino groups of proteins, such as lysine or arginine residues or N-termini. These adducts can react further, and a process of oxidation, dehydration and rearrangement gives rise to advanced glycation end-product (AGE) (Maillard reaction; Singh et al. 2001). The formation of these products is associated with a number of diseases, such as renal failure, atherosclerosis and diabetes. Glycation of monomers of Aβ and IAPP results in a speeding up of amyloid formation. Bouma et al. (2003) were able to show that glycation of albumin *in vitro* by incubation with glucose-6-phosphate was sufficient to render it amyloidogenic. After 2 weeks incubation, bundles of aggregates were formed, with lengths ranging from 100 to 150 nm. Lengthening the incubation period to 23 weeks resulted in the formation of fibrous sheets, between 100 and 300 nm long and 5 to 10 nm in diameter. The amyloid nature of these aggregates was shown by the use of X-ray fibre diffraction, CD and thioflavin T fluorescence. It was proposed that glycation may induce aggregation in two ways. The first is that binding of sugars to amino groups in Lys or Arg residues may alter the local environment around those residues and induce partial unfolding. The cross-links formed by AGE may exert mechan-

ical stresses on the protein that induce localised or global unfolding. Exposure of hitherto buried residues to solvent could lead to the formation of intermolecular contacts. Glycation-modified β2m has been found to be the principal component of amyloid fibrils formed in primary localised cutaneous nodular amyloidosis (Fujimoto et al. 2002).

Cysteine modification

An instructive example of the effect of cysteine modification on amyloid formation is provided by the TTR protein. This plasma protein is a tetramer in solution, with four identical 127 amino acid sub-units and is responsible for transport of thyroxine and the retinol-binding protein–vitamin A complex (Hamilton and Benson 2001). Deposition of *wt*TTR occurs in senile systemic amyloidosis (SSA) (Table 1). This is a non-hereditary disorder that affects roughly 25% of individuals over the age of 80. The amyloid fibrils formed consist mainly of *wt*TTR and its fragments, and they build up in the heart.

In contrast, the two other amyloid diseases associated with TTR, familial amyloidotic polyneuropathy-1 (FAP-1) and familial amyloidotic cardiomyopathy (FAC), are both autosomal dominant disorders (Table 1). The deposits of amyloid fibrils in these disorders form in tissues and organs and are made up of variant TTR, *wt* protein and TTR fragments. More than 80 TTR variants have been reported, with the majority of these being associated with disease (Hamilton and Benson 2001). These are single amino acid substitutions, with the exception of a Val122 deletion mutation. It appears that certain amino acid substitutions decrease the stability of the tetramer and favour the formation of amyloidogenic intermediates that can then self-associate to form fibrils. FAP is usually fatal within 7 to 15 years after the appearance of symptoms.

TTR contains one Cys residue, at position 10. *In vivo*, plasma TTR can undergo post-translational modification at this residue. Around 5–15% of the total TTR is unmodified, with the other 85–95% being either *S*-sulphonated or *S*-thiolated (Terazaki et al. 1998). The mixed disulphides formed are predominantly those of cysteine, cysteine glycine and glutathione (Kishikawa et al. 2002), although a homocysteine derivative has also been detected *in vivo* and *in vitro* (Lim et al. 2003b). The *S*-sulphonated product is formed by the attack of sulphite on a *S*-thiolated product. Kelly has looked at the effects of these post-translational modifications on amyloid formation by TTR (Zhang and Kelly 2003). Amyloid formation by TTR involves dissociation of the tetramer, followed by partial unfolding of the monomer to produce amyloid intermediates that self-associate to form the characteristic amyloid fibrils. The highest yields for amyloid formation, as measured by turbidity at 400 nm, occurred over the pH range 4.2 to 4.8. Over this range, the extent of amyloid formation was similar for *S*-Cys TTR, *S*-CysGly TTR, *S*-GSH TTR and the wild-type protein. *S*-Sulphonated TTR showed a decreased tendency to aggregate, and an analysis of the rate of aggregation showed a rate twofold slower than that of the *wt*TTR and the other analogues. Raising the pH to 4.8–5.0 resulted in significant changes. In this pH range, amyloidogenicity for *wt*TTR is low, but the *S*-thiolated proteins studied all had high aggregation tendencies. This may be physiologically relevant, as this pH is accessible in some cellular compartments, such as lysozymes. *S*-Sulphonated TTR was still less prone to amyloid formation than *wt*TTR. This is contrary to the results reported by Kishikawa and co-workers, who found that the *S*-sulphonated TTR had high amyloidogenicity when compared to the *wt* protein, over the pH range 3.5–4.5, as measured by optical density and a Congo red binding assay (Kishikawa et al. 1998).

Altland and Winter have also investigated the stability of *S*-sulphonated TTR mutants (Altland and Winter 1999; Altland et al. 2004), and their results are in agreement with those

of Kishikawa et al. They analysed the stability of sulphonated TTR by isoelectric focussing in a urea gradient. As the concentration of urea increases, there is dissociation of the original tetramer to monomer. The shift of the curves generated to higher urea concentrations corresponds to a higher conformational stability (resistance to unfolding) of the monomer. Sulphite binding to Cys10 was found to have a stabilising effect on TTR tetramers and to increase the tetramer/monomer ratio under equilibrium conditions. They have proposed a structural explanation for this effect, postulating the formation of an extra hydrogen bond between a sulphite oxygen and the main chain nitrogen of Gly75 (Altland and Winter 1999). On the basis of their stability studies, they have proposed a prophylactic role for sulphite and base in delaying the onset of familial amyloidotic polyneuropathy (Altland et al. 2004).

Amyloid formation by TTR involves dissociation of the tetramer species to give a monomer. The same pathway is followed upon denaturation by urea, so the stability of the four proteins was studied by urea denaturation. Resveratrol, a fluorescent molecule, binds to the tetramer and can be used to monitor its concentration. These were measured at a different pH to the amyloid formation (pH 7), and at that pH the dissociation rates were similar to the *wt* rate for each Cys10 variant.

S-Sulphonation may exert a secondary biological effect. TTR has a plasma residence time of only 1–2 days, but *S*-sulphonation is known to extend the half-life of proteins. This may lead to increase plasma concentrations of TTR from the normal levels of 200–400 mg l^{-1}. Reverse-phase HPLC has also shown the *S*-sulphonated TTR to be more hydrophobic than the *S*-cysteinylated TTR, having a longer retention time. There is also likely to be an interaction between Cys10 modification and mutated positions. *In vitro* studies of the *S*-cysteinylated Val30Met TTR mutant have shown that it has a greater propensity to form amyloid fibrils than the unmodified Val30Met TTR, unmodified *wt*TTR or *S*-cysteinylated *wt*TTR, at pH 5.5. Costello has recently reported a disease-causing Phe33Cys TTR mutant (Lim et al. 2003a). The protein isolated from a patient was found to have undergone modification at both Cys33 and Cys10. The effects of double modifications on amyloid propensity have not yet been reported. *In vivo*, the tetramers of TTR will exist as mixtures of Cys10 modified and unmodified monomers. This has been shown to result in changes to the quaternary structure and the ability to bind thyroxine (Pettersson et al. 1989). In human serum, the predominant modification is formation of the *S*-Cys TTR adduct. Cysteine–glycine adducts are also encountered, with the *S*-GSH and *S*-sulphonated being only present in minor amounts. We know of no other reports of cysteine modification upon amyloid-forming potential in other proteins or peptides.

Dityrosine

The formation of covalent linkages between tyrosine residues has been found in Aβ fibrils as well as other structural proteins, such as yeast cell wall proteins. This could arise through oxidative stress. Investigations have shown that dityrosine formation is generally more facile when the fibrils are pre-assembled rather than before (Yoburn et al. 2003), and this suggests that although dityrosine may have a role in strengthening fibrils and rendering them resistant to proteolysis, it does not contribute directly to the formation of the fibrils. Supporting this suggestion, a dityrosine-containing peptide had no greater tendency to polymerise than the natural non-covalently linked peptide (Yoburn et al. 2003).

Methionine oxidation

Alzheimer's disease has been proposed to be the result of oxidative stress (Markesbery 1997) associated with inflammation in the brain, generating noxious free radicals and reactive oxygen species that cause cellular damage (Kay 1997 and references therein). The chief constituent of amyloid neuritic plaques used to diagnose Alzheimer's disease (John et al. 1997) is Aβ, which can produce free radicals and hydrogen peroxide (Behl et al. 1994; Butterfield et al. 1996; Harris et al. 1995; Hensley et al. 1994, 1995; Kay 1997; Kelly et al. 1996). Met-35 of Aβ is susceptible to oxidation *in vitro*, undergoing preferential oxidation to the methionine sulphoxide, which is also likely *in vivo* under conditions of oxidative stress. CD experiments *in vitro* have shown that whereas Aβ1–40 and its Met35 oxidised form both adopt random coil structures in water (pH 4) at low micromolar concentrations, the former aggregates within several days while the latter is stable for at least 7 days under these conditions (Watson et al. 1998). NMR studies revealed that oxidation of Met35 caused significant structural changes in the C-terminal region of Aβ (Watson et al. 1998), and this may be an important clue to the chemistry and biology of Aβ. Methionine in glycine-rich regions of Aβ peptide and prion peptides may be important to their neurotoxicities. A free radical mechanism involving methionine, and requiring peptide β-sheets and a nearby glycine, has been proposed for generating and propagating oxidative damage (Rauk et al. 2000).

Solvent effects

The addition of organic solvents to aqueous peptide solutions can have significant effects on peptide conformation. For example, poly-L-Lys can be induced to change from an initially α-helical state to β-sheet by the addition of low concentrations of short-chain alcohols. The transformation can be reversed by the addition of higher concentrations (Shibata et al. 1992).

TFE is widely known to favour α-helical conformation in peptides when added to aqueous solution (Myers et al. 1998). There are a number of studies that have now shown that the presence of TFE can actually increase the rate of fibril growth of amyloid-forming peptides, until a certain concentration of TFE is reached and reaction rates fall. The dielectric constant for TFE is only about a third of that of water, and TFE-water mixtures have dielectric constants that are a linear function of the mole fraction of TFE. It has been suggested that TFE acts to stabilise the secondary structure of peptides by reducing the hydrogen bonds formed between amides and surrounding water molecules, thus favouring intramolecular hydrogen bonding. α-Helices are both compact (minimising solvent exposure) and maximise hydrogen-bonding and are thus favoured by TFE. Intermolecular β-sheets would also seem to offer similar opportunities for stability. When β-lactoglobulin and α-chymotrypsin were dissolved in 50% aqueous TFE solution, there was an initial rise in α-helical structure within the proteins. However, over time (approx. 90 min) spectral changes were seen in the CD spectrum consistent with adoption of a β-sheet structure. The rate of change increased as protein concentration was increased.

Membrane and surface interactions

The detergent SDS is known to stabilise the α-helical form of peptides when it is present in concentrations above its critical micellular concentration. Below this concentration, it is known to favour the formation of β-strands. SDS may also offer a model for some of

the properties of lipid membranes and offer insights into the interaction between amyloid proteins and membrane environments. Pertinhez et al. (2002) looked at the effect of SDS concentration on a 17-residue fragment derived from the short consensus repeat 3 domain (SRC3) from the human complement receptor CR1. The region selected is thought to be responsible for binding within the protein to two active complement proteins. The peptide adopted a predominantly random coil conformation when dissolved in aqueous solution at pH 4. After 2 days, well-defined fibrils had formed. The CD spectrum recorded in the presence of SDS suggests a large degree of helical structure (minima at 203 and 216 nm, with a maximum at 190 nm). Already after 30 min, changes had occurred in the spectrum. Over 2 days, further changes occurred to give a spectrum typical of β-sheet structure. When the SDS concentration was increased to 20 mM, above the critical concentration for formation of SDS micelles, the peptide spectrum observed was characteristic of an α-helical spectrum and the spectrum was stable for over 2 days. It is possible that the alkyl chains of SDS favour aggregation by interaction with the peptide. Suggestions have been made that interactions with membranes are significant in influencing aggregation and amyloid formation. An investigation of the SDS-PAGE behaviour of Aβ has found that the chromatographical behaviour of peptide fragments is affected by their ability to bind SDS (Kawooya et al. 2003). Recently Knight et al. reported that fibre formation by human islet amyloid polypeptide (hIAPP) is markedly accelerated by lipid bilayers despite adopting an α-helical state on the membrane (Knight et al. 2006).

The *in vitro* interaction of Aβ1–42 with cholesterol and related molecules has been studied. It was found that the presence of these lipophilic molecules increased the extent of formation of long fibrils (Harris 2002). In the presence of anionic phospholipids increased fibrillisation of Aβ has also been observed (Chauhan et al. 2000). Further support for the involvement of other molecules in the amyloid formation process is drawn from studies involving the growth of fibrils on surfaces. The surfaces most intensively studied have been mica and highly oriented pyrolytic graphic. Both of these surfaces offer atomically flat planes, but they differ in their surface chemical properties. Mica is hydrophilic and possesses a negative charge in neutral solution. The surface of highly oriented pyrolytic graphite (HOPG), on the other hand, is highly hydrophobic. Mica surfaces can be chemically modified to change the surface characteristics either by attaching charged groups or converting the mica surface into a more hydrophobic surface.

Zhu et al. investigated the protein SMA (Zhu et al. 2002), a 114-residue fragment from the κIV family of immunoglobulin light chains (LC). Immunoglobulin LCs are involved in several diseases of protein deposition, including AL amyloidosis (also known as primary systemic amyloidosis; Table 1). Interestingly, the LC protein deposits in these diseases are often found associated with basement membranes, and an association between SMA and cell membranes has been reported. Aggregation of SMA occurs via partially folded intermediates. In the experiments carried out by Zhu et al., aggregates were observed to form on mica despite there being no evidence of aggregation in the surrounding solution. The critical concentration for fibril formation in solution was found to be 0.3 mg/ml, but fibrils grew on mica at concentrations down to 50 μg/ml. Two types of aggregation were observed, indicating the existence of multiple pathways to fibril formation. It was possible to observe fibrils growing out of spherical amorphous deposits, which was the predominant growth mechanism under the experimental conditions used. Fibrils also formed from oligomers. Their results indicate significant differences between the processes occurring in solution and those reaction pathways that are available on surfaces. It is possible for surface adsorption to lead to an increase in the concentration of protein in local regions. Two-dimensional lateral diffusion of fibrils on the surface is also possible. There are also indications that adsorption on the

surface could lead to conformational changes in proteins or peptides, which may favour the formation of partially folded intermediates, rendering certain residues more accessible for inter-molecular aggregation.

Kowalewski and Holtzman (1999) have found, in an investigation of the growth of Aβ1–42 fibrils, that fibrils grown on graphite were found to align themselves along three directions at 120° to each other, reflecting an interaction between the fibrils and the atomic arrangement in the graphite layer. This also points to the importance of intermolecular interactions in the formation of β-sheet aggregates. The existence of an ordered first layer may result in a template for subsequent fibril growth, by aiding in the alignment of hydrophobic domains on the substrate surface.

Macromolecular crowding

Most of the investigations of the amyloid-forming potential of peptides have looked at solutions in buffer solution. These are usually dilute salt solutions. Most biological fluids, however, contain macromolecules, such as proteins, nucleic acids and carbohydrates at sufficient concentrations to occupy a significant fraction of the fluid volume. For example, 40% of the volume of neuronal cytoplasm is estimated to be occupied by macromolecules. This may affect the rates and equilibria of macromolecular associations. In this crowded environment, the volume accessible to any given protein is decreased, thus lower volume species will be favoured. These excluded volume interactions are due to the mutual impenetrability of the solutes and a consequent steric repulsion. Substantial volume occupancy can reduce the diffusional mobility of macromolecules, thus increasing the rate of reactions that are not diffusion rate limited. For proteins, this would mean a favouring of pathways that lead to more compact products. Both protofibril and fibril formation involve the formation of more compact structure and should therefore be favoured by molecular crowding. Rates of reactions for which the activation volumes are negative would also be increased, so there are both kinetic and thermodynamic effects. A review of the thermodynamic and kinetic implications of macromolecular crowding for proteins in general has recently appeared (Hall and Minton 2003).

The prediction has been made that increases in the fractional volume occupancy of macromolecules in a physiological fluid should non-specifically accelerate the formation of amyloid by any amyloidogenic protein. Hatters et al. (2002) have looked at the effect of dextran T10 solutions on amyloid formation by human apolipoprotein C-II. The dextran was shown by analytical sedimentation equilibria studies not to form heterocomplexes with the apoC-II and nor was it incorporated into any of the amyloid fibrils studied.

α-Synuclein, the 140-amino acid linked to Parkinson's disease, forms stable solutions *in vitro* of up to 300 μM, where no significant fibrillisation is seen for several months. The cytoplasmic concentration of α-synuclein is estimated at less than 30–60 μM. Shtilerman et al. looked at the effects of the addition of several non-interacting polymers (PEG 400, PEG 3350, PEG 6K, PEG 20K, dextran T-70 and Ficoll-70; Shtilerman et al. 2002). Several polymers were chosen so that effects from the chemical structure of the polymer could be ruled out. In the presence of PEG 2000, at a concentration of 10%, roughly comparable to the crowding in cell cytosol, the lag time for fibril formation was reduced from 80–90 days to around 8–10 days. The acceleration was greater for higher concentrations of the polymers. The results would be consistent with a 100% increase in the rate of fibril formation *in vivo* due to macromolecular crowding. As well as various saccharide polymers, the same effect has also been shown for amyloid formation by α-synuclein in the presence of bovine

serum albumin (BSA) (Uversky et al. 2002). It should also be noticed in this context that amyloid-associated diseases occur most frequently in the aged and also that cellular and tissue hydration decreases substantially with age. For example, a decrease of 7% in the neuronal volume has been observed in aged rats. It has been predicted that a one order of magnitude difference in the effective concentration would result from an increase in the crowding from only 30% to 33%.

As well as age-related reductions in cell volume, there may also be contributions to macromolecular crowding from age-related decline in proteasomal activity. Decreases in protein degradation would result in increases in the concentration of all cytoplasmic proteins. It has been found that inhibition of proteasomal activity leads to the formation of α-synuclein inclusions without, however, significantly increasing the concentration of α-synuclein. Reduced protease activity has been measured in Parkinson's disease brains. Also protease activity in PC12 cells is known to be reduced by over-expression of α-synuclein.

Conclusions and comments

What is now very clear is that amyloidosis is not that unusual in living systems. Amyloids might be reversible stores of protein or be responsible for specific physiological functions that are not well characterised to date. Amyloids are formed through uncontrolled protein aggregation. Protein aggregation itself is now known to be a very common phenomenon, although most proteins are unlike amyloidogenic sequences in that they rarely form oligomers of more than 2–8 units, whereas amyloid polymers can involve the aggregation of many hundreds of monomeric units. β-Sheets appear to be more predisposed to forming higher oligomers because they present multiple interacting surfaces that can seed the deposition and growth through intermolecular hydrogen bonds and side-chain interactions. Interestingly, the unpaired peptide β-strand is the most elongated (linear) unit of protein structure and maximally exposes both backbone hydrogen bonding amide groups as well as side chains for potential intermolecular interactions. Normally this structural unit would be highly solvated by water and is highly prone to degradation by proteolytic enzymes that are now known to uniquely recognise the β-strand (Fairlie et al. 2000; Tyndall et al. 2005). Neither α-helices nor turns, nor β-sheet substrates are recognised or processed by proteases as far as we know to date. The alternatives for a β-strand are to become buried within a protein and thus protected from proteolytic degradation, or to exist in an ensemble of random structures that could ultimately also disappear through proteolytic decomposition of the tiny equilibrium concentration of strand, or to pair with one another to form a stable β-sheet aggregate that affords protection from proteolytic cleavage. Thus, amyloids might simply be reversible stores of proteins that are protected from degradation and elimination from a particular body compartment, or they might be responsible for specific physiological functions that have not yet been identified or well characterised.

Proteins are not static structures but rather dynamic ensembles of multiple interconverting folded and partially folded conformations. The free energy of unfolding for proteins by thermal denaturation is positive but relatively small (20–80 kJ mol^{-1} at room temperature) at less than 0.5 kJ/mole per residue (Doig and Williams 1992), and there seems to have been evolutionary pressure to maintain protein stability at this remarkably low level. Yet even the seemingly subtle mutation of isoleucine to valine, involving the loss of one methylene group, has been shown to decrease the stability of one protein by 7 kJ mol^{-1}, representing a significant fraction of overall protein stability (Shortle et al. 1990). Several reasons for

the relatively low energetic stability have been suggested, but the most likely are to make proteolysis, protein degradation, and protein turnover feasible within the lifetime of a cell, and to make partially unfolded states accessible to facilitate transport and assembly. While these small energetic differences allow protein folding to be sufficiently fast and facile to avoid trapping the protein in misfolded states, they also explain why single mutations can be sufficient to give rise to amyloidogenic intermediates. The equilibrium between helices, turns, strands and sheets is heavily influenced by amino acid sequence, but can also be driven by many environmental factors, and the possible relationships between some of these features and amyloid formation and properties has been outlined above. The molecular processes that underpin protein conformational changes, packing interactions, aggregation, and amyloid formation are slowly becoming better understood. If amyloids are simply stores of protected protein, amyloidogenesis would have to be reversible and have a low energetic barrier to resolubilisation. Interestingly, the amyloid fibrils we have found (Figs. 7 and 8) instantly and completely revert to monomer upon altering the pH from 4 to 7. "Molecular recycling" has been shown to occur in amyloid fibrils (Carulla et al. 2005) and Karsai et al. have also shown that Aβ1–42 monomers can be mechanically removed from an amyloid fibril (Karsai et al. 2006). Most interestingly, Aβ immunotherapy has been shown to reduce extracellular Aβ plaques and intracellular Aβ accumulation in mice models, suggesting that the extracellular and intracellular stores are reversible (Oddo et al. 2004, 2006).

Tantalising structural insights to both amyloids and intermediates are being gained that might eventually inform the rational design of new therapeutics for preventing and treating amyloid-related diseases, perhaps by interfering with peptide/protein folding. Supramolecular devices incorporating amyloid-based templates also offer some promising approaches to synthetic monomolecular wires. Scaffolds for tissue growth based on amyloid-forming peptides offer the potential of mechanical support whilst incorporating biologically active motifs to direct cell growth. These and other applications are conceivable from studies that historically set out to better understand the pathology of human diseases.

Acknowledgements. We thank the Australian Research Council and the National Health & Medical Research Council for some financial support of the researchers who performed this work.

References

Agianian B, Leonard K, Bonte E, Van der Zandt H, Becker PB, Tucker PA (1999) The glutamine-rich domain of the Drosophila GAGA factor is necessary for amyloid fibre formation in vitro, but not for chromatin remodelling. J Mol Biol 285:527–544

Aguzzi A, Haass C (2003) Games played by rogue proteins in prion disorders and Alzheimer's disease. Science 302:814–818

Ahmad A, Uversky VN, Hong D, Fink AL (2005) Early events in the fibrillation of monomeric insulin. J Biol Chem 280:42669–42675

Aldave AJ, Gutmark JG, Yellore VS, Affeldt JA, Meallet MA, Udar N, Rao NA, Small KW, Klintworth GK (2004) Lattice corneal dystrophy associated with the Ala546Asp and Pro551Gln missense changes in the TGFBI gene. Am J Ophthalmol 138:772–781

Alexandrescu AT (2001) An NMR-based quenched hydrogen exchange investigation of model amyloid fibrils formed by cold shock protein A. Pac Symp Biocomput 67–78

Alexandrescu AT (2005) Amyloid accomplices and enforcers. Protein Sci 14:1–12

Alexandrescu AT, Rathgeb-Szabo K (1999) An NMR investigation of solution aggregation reactions preceding the misassembly of acid-denatured cold shock protein A into fibrils. J Mol Biol 291:1191–1206

Altland K, Winter P (1999) Potential treatment of transthyretin-type amyloidoses by sulfite. Neurogenetics 2:183–188

Altland K, Winter P, Saraiva MJ, Suhr O (2004) Sulfite and base for the treatment of familial amyloidotic polyneuropathy: two additive approaches to stabilize the conformation of human amyloidogenic transthyretin. Neurogenetics 5:61–67

Alzheimer A, Stelzmann RA, Schnitzlein HN, Murtagh FR (1995) An English translation of Alzheimer's 1907 paper, "Uber eine eigenartige Erkankung der Hirnrinde". Clin Anat 8:429–431

Ancsin JB (2003) Amyloidogenesis: historical and modern observations point to heparan sulfate proteoglycans as a major culprit. Amyloid 10:67–79

Ando Y, Nakamura M, Araki S (2005) Transthyretin-related familial amyloidotic polyneuropathy. Arch Neurol 62:1057–1062

Andreola A, Bellotti V, Giorgetti S, Mangione P, Obici L, Stoppini M, Torres J, Monzani E, Merlini G, Sunde M (2003) Conformational switching and fibrillogenesis in the amyloidogenic fragment of apolipoprotein A-I. J Biol Chem 278:2444–2451

Arimon M, Diez-Perez I, Kogan MJ, Durany N, Giralt E, Sanz F, Fernandez-Busquets X (2005) Fine structure study of Abeta 1–42 fibrillogenesis with atomic force microscopy. FASEB J 19:1344–1346

Atwood CS, Scarpa RC, Huang X, Moir RD, Jones WD, Fairlie DP, Tanzi RE, Bush AI (2000) Characterization of copper interactions with Alzheimer amyloid beta peptides: identification of an attomolar-affinity copper binding site on amyloid beta 1–42. J Neurochem 75:1219–1233

Atwood CS, Martins RN, Smith MA, Perry G (2002) Senile plaque composition and posttranslational modification of amyloid-beta peptide and associated proteins. Peptides 23:1343–1350

Azriel R, Gazit E (2001) Analysis of the minimal amyloid-forming fragment of the islet amyloid polypeptide. An experimental support for the key role of the phenylalanine residue in amyloid formation. J Biol Chem 276:34156–34161

Balbach JJ, Ishii Y, Antzutkin ON, Leapman RD, Rizzo NW, Dyda F, Reed J, Tycko R (2000) Amyloid fibril formation by A beta 16–22, a seven-residue fragment of the Alzheimer's beta-amyloid peptide, and structural characterization by solid state NMR. Biochemistry 39:13748–13759

Bamberger ME, Harris ME, McDonald DR, Husemann J, Landreth GE (2003) A cell surface receptor complex for fibrillar beta-amyloid mediates microglial activation. J Neurosci 23:2665–2674

Baskakov IV, Legname G, Baldwin MA, Prusiner SB, Cohen FE (2002) Pathway complexity of prion protein assembly into amyloid. J Biol Chem 277:21140–21148

Baxa U, Cheng N, Winkler DC, Chiu TK, Davies DR, Sharma D, Inouye H, Kirschner DA, Wickner RB, Steven AC (2005) Filaments of the Ure2p prion protein have a cross-beta core structure. J Struct Biol 150:170–179

Behl C, Davis JB, Lesley R, Schubert D (1994) Hydrogen peroxide mediates amyloid beta protein toxicity. Cell 77:817–827

Bellotti V, Mangione P, Merlini G (2000) Review: immunoglobulin light chain amyloidosis—the archetype of structural and pathogenic variability. J Struct Biol 130:280–289

Benson MD, Liepnieks J, Uemichi T, Wheeler G, Correa R (1993) Hereditary renal amyloidosis associated with a mutant fibrinogen alpha-chain. Nat Genet 3:252–255

Benson MD, Liepnieks JJ, Yazaki M, Yamashita T, Hamidi Asl K, Guenther B, Kluve-Beckerman B (2001) A new human hereditary amyloidosis: the result of a stop-codon mutation in the apolipoprotein AII gene. Genomics 72:272–277

Bergstrom J, Murphy C, Eulitz M, Weiss DT, Westermark GT, Solomon A, Westermark P (2001) Codeposition of apolipoprotein A-IV and transthyretin in senile systemic (ATTR) amyloidosis. Biochem Biophys Res Commun 285:903–908

Bergstrom J, Murphy CL, Weiss DT, Solomon A, Sletten K, Hellman U, Westermark P (2004) Two different types of amyloid deposits—apolipoprotein A-IV and transthyretin—in a patient with systemic amyloidosis. Lab Invest 84:981–988

Berson JF, Theos AC, Harper DC, Tenza D, Raposo G, Marks MS (2003) Proprotein convertase cleavage liberates a fibrillogenic fragment of a resident glycoprotein to initiate melanosome biogenesis. J Cell Biol 161:521–533

Bieri O, Wildegger G, Bachmann A, Wagner C, Kiefhaber T (1999) A salt-induced kinetic intermediate is on a new parallel pathway of lysozyme folding. Biochemistry 38:12460–12470

Bironaite D, Lindgren S, Janciauskiene S, Dichtl W, Moraga F, Ares MP, Crisby M, Nilsson J, Carlemalm E, Eriksson S (2001) Fibrillogenic C-terminal fragment of alpha-1-antitrypsin activates human monocytes via oxidative mechanisms. Cell Tissue Res 305:87–98

Bitan G, Lomakin A, Teplow DB (2001) Amyloid beta-protein oligomerization: prenucleation interactions revealed by photo-induced cross-linking of unmodified proteins. J Biol Chem 276:35176–35184

Bitan G, Kirkitadze MD, Lomakin A, Vollers SS, Benedek GB, Teplow DB (2003a) Amyloid beta-protein (Abeta) assembly: Abeta 40 and Abeta 42 oligomerize through distinct pathways. Proc Natl Acad Sci USA 100:330–335

Bitan G, Vollers SS, Teplow DB (2003b) Elucidation of primary structure elements controlling early amyloid beta-protein oligomerization. J Biol Chem 278:34882–34889
Blake C, Serpell L (1996) Synchrotron X-ray studies suggest that the core of the transthyretin amyloid fibril is a continuous beta-sheet helix. Structure 4:989–998
Bodles AM, Guthrie DJS, Greer B, Irvine GB (2001) Identification of the region of non-Ab component (NAC) of Alzheimer's disease amyloid responsible for its aggregation and toxicity. J Neurochem 78:384–395
Bohne S, Sletten K, Menard R, Buhling F, Vockler S, Wrenger E, Roessner A, Rocken C (2004) Cleavage of AL amyloid proteins and AL amyloid deposits by cathepsins B, K, and L. J Pathol 203:528–537
Bollen YJ, Sanchez IE, van Mierlo CP (2004) Formation of on- and off-pathway intermediates in the folding kinetics of Azotobacter vinelandii apoflavodoxin. Biochemistry 43:10475–10489
Bouchard M, Zurdo J, Nettleton E, Dobson C, Robinson C (2000) Formation of insulin amyloid fibrils followed by FTIR simultaneously with CD and electron microscopy. Protein Sci 9:1960–1967
Bouma B, Kroon-Batenburg LM, Wu YP, Brunjes B, Posthuma G, Kranenburg O, de Groot PG, Voest EE, Gebbink MF (2003) Glycation induces formation of amyloid cross-beta structure in albumin. J Biol Chem 278:41810–41819
Bousset L, Briki F, Doucet J, Melki R (2003) The native-like conformation of Ure2p in fibrils assembled under physiologically relevant conditions switches to an amyloid-like conformation upon heat-treatment of the fibrils. J Struct Biol 141:132–142
Brais B (2003) Oculopharyngeal muscular dystrophy: a late-onset polyalanine disease. Cytogenet Genome Res 100:252–260
Breslau NA (2000) Calcium homeostasis. In: Griffin JA, Ojeda SR (eds) Textbook of endocrine physiology, 4th edn. Oxford University Press, New York
Briknarova K, Akerman ME, Hoyt DW, Ruoslahti E, Ely KR (2003) Anastellin, an FN3 fragment with fibronectin polymerization activity, resembles amyloid fibril precursors. J Mol Biol 332:205–215
Broome BM, Hecht MH (2000) Nature disfavors sequences of alternating polar and non-polar amino acids: implications for amyloidogenesis. J Mol Biol 296:961–968
Brown JH, Jardetzky TS, Gorga JC, Stern LJ, Urban RG, Strominger JL, Wiley DC (1993) Three-dimensional structure of the human class II histocompatibility antigen HLA-DR1. Nature 364:33–39
Bucciantini M, Giannoni E, Chiti F, Baroni F, Formigli L, Zurdo J, Taddei N, Ramponi G, Dobson CM, Stefani M (2002) Inherent toxicity of aggregates implies a common mechanism for protein misfolding diseases. Nature 416:507–511
Bucciantini M, Calloni G, Chiti F, Formigli L, Nosi D, Dobson CM, Stefani M (2004) Pre-fibrillar amyloid protein aggregates share common features of cytotoxicity. J Biol Chem 279:31374–31382
Bunn CW, Garner EV (1947) The crystal structure of two polyamides ('nylons'). Proc R Soc Lond Ser A 189:39–68
Burke MJ, Rougvie MA (1972) Cross-protein structures. I. Insulin fibrils. Biochemistry 11:2435–2439
Burley SK, Petsko GA (1985) Aromatic-aromatic interaction: a mechanism of protein structure stabilization. Science 229:23–28
Bush AI (2003) The metallobiology of Alzheimer's disease. Trends Neurosci 26:207–214
Butterfield DA, Martin L, Carney JM, Hensley K (1996) A beta (25–35) peptide displays H2O2-like reactivity towards aqueous Fe2+, nitroxide spin probes, and synaptosomal membrane proteins. Life Sci 58:217–228
Buxbaum JN (2003) Diseases of protein conformation: what do in vitro experiments tell us about in vivo diseases? Trends Biochem Sci 28:585–592
Calado A, Tome FM, Brais B, Rouleau GA, Kuhn U, Wahle E, Carmo-Fonseca M (2000) Nuclear inclusions in oculopharyngeal muscular dystrophy consist of poly(A) binding protein 2 aggregates which sequester poly(A) RNA. Hum Mol Genet 9:2321–2328
Calamai M, Taddei N, Stefani M, Ramponi G, Chiti F (2003) Relative influence of hydrophobicity and net charge in the aggregation of two homologous proteins. Biochemistry 42:15078–15083
Calamai M, Canale C, Relini A, Stefani M, Chiti F, Dobson CM (2005) Reversal of protein aggregation provides evidence for multiple aggregated states. J Mol Biol 346:603–616
Cannon MJ, Williams AD, Wetzel R, Myszka DG (2004) Kinetic analysis of beta-amyloid fibril elongation. Anal Biochem 328:67–75
Carrotta R, Manno M, Bulone D, Martorana V, San Biagio PL (2005) Protofibril formation of amyloid beta-protein at low pH via a non-cooperative elongation mechanism. J Biol Chem 280:30001–30008
Carulla N, Caddy GL, Hall DR, Zurdo J, Gairi M, Feliz M, Giralt E, Robinson CV, Dobson CM (2005) Molecular recycling within amyloid fibrils. Nature 436:554–558
Chapman MR, Robinson LS, Pinkner JS, Roth R, Heuser J, Hammar M, Normark S, Hultgren SJ (2002) Role of Escherichia coli curli operons in directing amyloid fiber formation. Science 295:851–855

Chauhan A, Ray I, Chauhan VP (2000) Interaction of amyloid beta-protein with anionic phospholipids: possible involvement of Lys28 and C-terminus aliphatic amino acids. Neurochem Res 25:423–429
Chen CD, Huff ME, Matteson J, Page L, Phillips R, Kelly JW, Balch WE (2001a) Furin initiates gelsolin familial amyloidosis in the Golgi through a defect in Ca(2+) stabilization. EMBO J 20:6277–6287
Chen S, Berthelier V, Yang W, Wetzel R (2001b) Polyglutamine aggregation behavior in vitro supports a recruitment mechanism of cytotoxicity. J Mol Biol 311:173–182
Chen S, Berthelier V, Hamilton JB, O'Nuallain B, Wetzel R (2002) Amyloid-like features of polyglutamine aggregates and their assembly kinetics. Biochemistry 41:7391–7399
Chen YW, Dokholyan NV (2005) A single disulfide bond differentiates aggregation pathways of beta 2-microglobulin. J Mol Biol 354:473–482
Cherny RA, Legg JT, McLean CA, Fairlie DP, Huang X, Atwood CS, Beyreuther K, Tanzi RE, Masters CL, Bush AI (1999) Aqueous dissolution of Alzheimer's disease Abeta amyloid deposits by biometal depletion. J Biol Chem 274:23223–23228
Chiti F, Webster P, Taddei N, Clark A, Stefani M, Ramponi G, Dobson CM (1999) Designing conditions for in vitro formation of amyloid protofilaments and fibrils. Proc Natl Acad Sci USA 96:3590–3594
Chiti F, Taddei N, Bucciantini M, White P, Ramponi G, Dobson CM (2000) Mutational analysis of the propensity for amyloid formation by a globular protein. EMBO J 19:1441–1449
Chiti F, Bucciantini M, Capanni C, Taddei N, Dobson CM, Stefani M (2001) Solution conditions can promote formation of either amyloid protofilaments or mature fibrils from the HypF N-terminal domain. Protein Sci 10:2541–2547
Chiti F, Calamai M, Taddei N, Stefani M, Ramponi G, Dobson CM (2002a) Studies of the aggregation of mutant proteins in vitro provide insights into the genetics of amyloid diseases. Proc Natl Acad Sci USA 99(Suppl 4):16419–16426
Chiti F, Taddei N, Baroni F, Capanni C, Stefani M, Ramponi G, Dobson CM (2002b) Kinetic partitioning of protein folding and aggregation. Nat Struct Biol 9:137–143
Chiti F, Stefani M, Taddei N, Ramponi G, Dobson CM (2003) Rationalization of the effects of mutations on peptide and protein aggregation rates. Nature 424:805–808
Chow MK, Paulson HL, Bottomley SP (2004) Destabilization of a non-pathological variant of ataxin-3 results in fibrillogenesis via a partially folded intermediate: a model for misfolding in polyglutamine disease. J Mol Biol 335:333–341
Chromy BA, Nowak RJ, Lambert MP, Viola KL, Chang L, Velasco PT, Jones BW, Fernandez SJ, Lacor PN, Horowitz P, Finch CE, Krafft GA, Klein WL (2003) Self-assembly of Abeta(1–42) into globular neurotoxins. Biochemistry 42:12749–12760
Claessen D, Rink R, de Jong W, Siebring J, de Vreugd P, Boersma FG, Dijkhuizen L, Wosten HA (2003) A novel class of secreted hydrophobic proteins is involved in aerial hyphae formation in *Streptomyces coelicolor* by forming amyloid-like fibrils. Genes Dev 17:1714–1726
Clark PL (2004) Protein folding in the cell: reshaping the folding funnel. Trends Biochem Sci 29:527–534
Cohen AS, Calkins E (1959) Electron microscopic observations on a fibrous component in amyloid of diverse origins. Nature 183:1202–1203
Cohen FE, Prusiner SB (1998) Pathologic conformations of prion proteins. Annu Rev Biochem 67:793–819
Coles M, Bicknell W, Watson AA, Fairlie DP, Craik DJ (1998) Solution structure of amyloid beta-peptide(1–40) in a water-micelle environment. Is the membrane-spanning domain where we think it is? Biochemistry 37:11064–11077
Collins SR, Douglass A, Vale RD, Weissman JS (2004) Mechanism of prion propagation: amyloid growth occurs by monomer addition. PLoS Biol 2:e321
Collinson SK, Emody L, Muller KH, Trust TJ, Kay WW (1991) Purification and characterization of thin, aggregative fimbriae from Salmonella enteritidis. J Bacteriol 173:4773–4781
Cordes MH, Walsh NP, McKnight CJ, Sauer RT (2003) Solution structure of switch Arc, a mutant with 3(10) helices replacing a wild-type beta-ribbon. J Mol Biol 326:899–909
Cottingham MG, Hollinshead MS, Vaux DJ (2002) Amyloid fibril formation by a synthetic peptide from a region of human acetylcholinesterase that is homologous to the Alzheimer's amyloid-beta peptide. Biochemistry 41:13539–13547
Coustou-Linares V, Maddelein ML, Begueret J, Saupe SJ (2001) In vivo aggregation of the HET-s prion protein of the fungus Podospora anserina. Mol Microbiol 42:1325–1335
Cribbs DH, Azizeh BY, Cotman CW, LaFerla FM (2000) Fibril formation and neurotoxicity by a herpes simplex virus glycoprotein B fragment with homology to the Alzheimer's A beta peptide. Biochemistry 39:5988–5994
Damaschun G, Damaschun H, Gast K, Zirwer D (1999) Proteins can adopt totally different folded conformations. J Mol Biol 291:715–725

Damaschun G, Damaschun H, Fabian H, Gast K, Krober R, Wieske M, Zirwer D (2000) Conversion of yeast phosphoglycerate kinase into amyloid-like structure. Proteins 39:204–211
Darnell RB (2003) Memory, synaptic translation, and...prions? Cell 115:767–768
de Groot NS, Ventura S (2005) Amyloid fibril formation by bovine cytochrome c. Spectroscopy 19:199–205
Deane R, Du Yan S, Submamaryan RK, LaRue B, Jovanovic S, Hogg E, Welch D, Manness L, Lin C, Yu J, Zhu H, Ghiso J, Frangione B, Stern A, Schmidt AM, Armstrong DL, Arnold B, Liliensiek B, Nawroth P, Hofman F, Kindy M, Stern D, Zlokovic B (2003) RAGE mediates amyloid-beta peptide transport across the blood-brain barrier and accumulation in brain. Nat Med 9:907–913
Dehner A, Planker E, Gemmecker G, Broxterman QB, Bisson W, Formaggio F, Crisma M, Toniolo C, Kessler H (2001) Solution structure, dimerization, and dynamics of a lipophilic alpha/3(10)-helical, C alpha-methylated peptide. Implications for folding of membrane proteins. J Am Chem Soc 123:6678–6686
Delano WL (2005) MacPyMOL: a PyMOL-based molecular graphics application for MacOS X. DeLano Scientific, South San Francisco
deMello DE, Lin Z (2001) Pulmonary alveolar proteinosis: a review. Pediatr Pathol Mol Med 20:413–432
Derkatch IL, Uptain SM, Outeiro TF, Krishnan R, Lindquist SL, Liebman SW (2004) Effects of Q/N-rich, polyQ, and non-polyQ amyloids on the de novo formation of the [PSI+] prion in yeast and aggregation of Sup35 in vitro. Proc Natl Acad Sci USA 101:12934–12939
Diaz-Avalos R, Long C, Fontano E, Balbirnie M, Grothe R, Eisenberg D, Caspar DL (2003) Cross-beta order and diversity in nanocrystals of an amyloid-forming peptide. J Mol Biol 330:1165–1175
Dobson CM (1999) Protein misfolding, evolution and disease. Trends Biochem Sci 24:329–332
Dobson CM (2003) Protein folding and misfolding. Nature 426:884–890
Dobson CM (2004) Principles of protein folding, misfolding and aggregation. Semin Cell Dev Biol 15:3–16
Dodart JC, Bales KR, Gannon KS, Greene SJ, DeMattos RB, Mathis C, DeLong CA, Wu S, Wu X, Holtzman DM, Paul SM (2002) Immunization reverses memory deficits without reducing brain Abeta burden in Alzheimer's disease model. Nat Neurosci 5:452–457
Doig AJ, Williams DH (1992) Why water-soluble, compact, globular proteins have similar specific enthalpies of unfolding at 110 degrees C. Biochemistry 31:9371–9375
Dong A, Matsuura J, Manning MC, Carpenter JF (1998) Intermolecular beta-sheet results from trifluoroethanol-induced nonnative alpha-helical structure in beta-sheet predominant proteins: infrared and circular dichroism spectroscopic study. Arch Biochem Biophys 355:275–281
Dos Reis S, Coulary-Salin B, Forge V, Lascu I, Begueret J, Saupe SJ (2002) The HET-s prion protein of the filamentous fungus *Podospora anserina* aggregates in vitro into amyloid-like fibrils. J Biol Chem 277:5703–5706
Doyle DA, Lee A, Lewis J, Kim E, Sheng M, MacKinnon R (1996) Crystal structures of a complexed and peptide-free membrane protein-binding domain: molecular basis of peptide recognition by PDZ. Cell 85:1067–1076
Du HN, Tang L, Luo XY, Li HT, Hu J, Zhou JW, Hu HY (2003) A peptide motif consisting of glycine, alanine, and valine is required for the fibrillization and cytotoxicity of human alpha-synuclein. Biochemistry 42:8870–8878
Dzwolak W, Muraki T, Kato M, Taniguchi Y (2004) Chain-length dependence of alpha-helix to beta-sheet transition in polylysine: model of protein aggregation studied by temperature-tuned FTIR spectroscopy. Biopolymers 73:463–469
Eakin CM, Knight JD, Morgan CJ, Gelfand MA, Miranker AD (2002) Formation of a copper specific binding site in non-native states of beta-2-microglobulin. Biochemistry 41:10646–10656
Eakin CM, Berman AJ, Miranker AD (2006) A native to amyloidogenic transition regulated by a backbone trigger. Nat Struct Mol Biol 13:202–208
el-Agnaf OM, Irvine GB (2002) Aggregation and neurotoxicity of alpha-synuclein and related peptides. Biochem Soc Trans 30:559–565
Elam JS, Taylor AB, Strange R, Antonyuk S, Doucette PA, Rodriguez JA, Hasnain SS, Hayward LJ, Valentine JS, Yeates TO, Hart PJ (2003) Amyloid-like filaments and water-filled nanotubes formed by SOD1 mutant proteins linked to familial ALS. Nat Struct Biol 10:461–467
Elliot MA, Karoonuthaisiri N, Huang J, Bibb MJ, Cohen SN, Kao CM, Buttner MJ (2003) The chaplins: a family of hydrophobic cell-surface proteins involved in aerial mycelium formation in *Streptomyces coelicolor*. Genes Dev 17:1727–1740
Esler WP, Stimson ER, Jennings JM, Vinters HV, Ghilardi JR, Lee JP, Mantyh PW, Maggio JE (2000) Alzheimer's disease amyloid propagation by a template-dependent dock-lock mechanism. Biochemistry 39:6288–6295
Esteban JA (2004) Living with the enemy: a physiological role for the beta-amyloid peptide. Trends Neurosci 27:1–3

Eulitz M, Weiss DT, Solomon A (1990) Immunoglobulin heavy-chain-associated amyloidosis. Proc Natl Acad Sci USA 87:6542–6546
Fadika GO, Baumann M (2002) Peptides corresponding to gelsolin derived amyloid of the Finnish type (AGelFIN) adopt two distinct forms in solution of which only one can polymerize into amyloid fibrils and form complexes with apoE. Amyloid 9:75–82
Fändrich M, Dobson CM (2002) The behaviour of polyamino acids reveals an inverse side chain effect in amyloid structure formation. EMBO J 21:5682–5690
Fändrich M, Fletcher MA, Dobson CM (2001) Amyloid fibrils from muscle myoglobin. Nature 410:165–166
Fändrich M, Forge V, Buder K, Kittler M, Dobson CM, Diekmann S (2003) Myoglobin forms amyloid fibrils by association of unfolded polypeptide segments. Proc Natl Acad Sci USA 100:15463–15468
Fairlie DP, West ML, Wong AK (1998) Towards protein surface mimetics. Curr Med Chem 5:29–62
Fairlie DP, Tyndall JD, Reid RC, Wong AK, Abbenante G, Scanlon MJ, March DR, Bergman DA, Chai CL, Burkett BA (2000) Conformational selection of inhibitors and substrates by proteolytic enzymes: implications for drug design and polypeptide processing. J Med Chem 43:1271–1281
Fan X, Rouleau GA (2003) Progress in understanding the pathogenesis of oculopharyngeal muscular dystrophy. Can J Neurol Sci 30:8–14
Farrell HM Jr, Cooke PH, Wickham ED, Piotrowski EG, Hoagland PD (2003) Environmental influences on bovine kappa-casein: reduction and conversion to fibrillar (amyloid) structures. J Protein Chem 22:259–273
Fay N, Inoue Y, Bousset L, Taguchi H, Melki R (2003) Assembly of the yeast prion Ure2p into protein fibrils. Thermodynamic and kinetic characterization. J Biol Chem 278:30199–30205
Ferguson N, Berriman J, Petrovich M, Sharpe TD, Finch JT, Fersht AR (2003) Rapid amyloid fiber formation from the fast-folding WW domain FBP28. Proc Natl Acad Sci USA 100:9814–9819
Ferguson N, Becker J, Tidow H, Tremmel S, Sharpe TD, Krause G, Flinders J, Petrovich M, Berriman J, Oschkinat H, Fersht AR (2006) General structural motifs of amyloid protofilaments. Proc Natl Acad Sci USA 103:16248–16253
Fezoui Y, Teplow DB (2002) Kinetic studies of amyloid beta-protein fibril assembly. Differential effects of alpha-helix stabilization. J Biol Chem 277:36948–36954
Fezoui Y, Hartley DM, Walsh DM, Selkoe DJ, Osterhout JJ, Teplow DB (2000) A de novo designed helix-turn-helix peptide forms nontoxic amyloid fibrils. Nat Struct Biol 7:1095–1099
Figueroa KP, Pulst SM (2003) Identification and expression of the gene for human ataxin-2-related protein on chromosome 16. Exp Neurol 184:669–678
Florio T, Paludi D, Villa V, Principe DR, Corsaro A, Millo E, Damonte G, D'Arrigo C, Russo C, Schettini G, Aceto A (2003) Contribution of two conserved glycine residues to fibrillogenesis of the 106–126 prion protein fragment. Evidence that a soluble variant of the 106–126 peptide is neurotoxic. J Neurochem 85:62–72
Forloni G, Angeretti N, Chiesa R, Monzani E, Salmona M, Bugiani O, Tagliavini F (1993) Neurotoxicity of a prion protein fragment. Nature 362:543–546
Fowler DM, Koulov AV, Alory-Jost C, Marks MS, Balch WE, Kelly JW (2006) Functional amyloid formation within mammalian tissue. PLoS Biol 4:100–107
Fraser PE, Nguyen JT, Inouye H, Surewicz WK, Selkoe DJ, Podlisny MB, Kirschner DA (1992) Fibril formation by primate, rodent, and Dutch-hemorrhagic analogues of Alzheimer amyloid beta-protein. Biochemistry 31:10716–10723
Fujimoto N, Yajima M, Ohnishi Y, Tajima S, Ishibashi A, Hata Y, Enomoto U, Konohana I, Wachi H, Seyama Y (2002) Advanced glycation end product-modified beta 2-microglobulin is a component of amyloid fibrils of primary localized cutaneous nodular amyloidosis. J Invest Dermatol 118:479–484
Fukui T, Shiraki K, Hamada D, Hara K, Miyata T, Fujiwara S, Mayanagi K, Yanagihara K, Iida T, Fukusaki E, Imanaka T, Honda T, Yanagihara I (2005) Thermostable direct hemolysin of *Vibrio parahaemolyticus* is a bacterial reversible amyloid toxin. Biochemistry 44:9825–9832
Funayama T, Mashima Y, Kawashima M, Yamada M (2006) Lattice corneal dystrophy type III in patients with a homozygous L527R mutation in the TGFBI gene. Jpn J Ophthalmol 50:62–64
Fung SY, Keyes C, Duhamel J, Chen P (2003) Concentration effect on the aggregation of a self-assembling oligopeptide. Biophys J 85:537–548
Galea C, Bowman P, Kriwacki RW (2005) Disruption of an intermonomer salt bridge in the p53 tetramerization domain results in an increased propensity to form amyloid fibrils. Protein Sci 14:2993–3003
Ganesh S, Tayakumar R (2003) Structural transitions involved in a novel amyloid-like beta sheet assemblage of tripeptide derivatives. Biopolymers 70:336–345
Gasset M, Baldwin M, Lloyd D, Gabriel J, Holtzman D, Cohen F, Fletterick R, Prusiner S (1992) Predicted alpha-helical regions of the prion protein when synthesized as peptides form amyloid. Proc Natl Acad Sci USA 89:10940–10944

Gazit E (2002) A possible role for pi-stacking in the self-assembly of amyloid fibrils. FASEB J 16:77–83
Gebbink MF, Claessen D, Bouma B, Dijkhuizen L, Wosten HA (2005) Amyloids—a functional coat for microorganisms. Nat Rev Microbiol 3:333–341
Geddes AJ, Parker KD, Atkins ED, Beighton E (1968) Cross-beta' conformation in proteins. J Mol Biol 32:343–358
Gerhartz B, Ekiel I, Abrahamson M (1998) Two stable unfolding intermediates of the disease-causing L68Q variant of human cystatin C. Biochemistry 37:17309–17317
Ghiso J, Jensson O, Frangione B (1986) Amyloid fibrils in hereditary cerebral hemorrhage with amyloidosis of Icelandic type is a variant of gamma-trace basic protein (cystatin C). Proc Natl Acad Sci USA 83:2974–2978
Giacomelli CE, Norde W (2003) Influence of hydrophobic Teflon particles on the structure of amyloid beta-peptide. Biomacromolecules 4:1719–1726
Gibson G, El-Agnaf OM, Anwar Z, Sidera C, Isbister A, Austen BM (2005) Structure and neurotoxicity of novel amyloids derived from the BRI gene. Biochem Soc Trans 33:1111–1112
Gillespie P, Cicariello J, Olson GL (1997) Conformational analysis of dipeptide mimetics. Biopolymers 43:191–217
Giri K, Ghosh U, Bhattacharyya NP, Basak S (2003) Caspase 8 mediated apoptotic cell death induced by beta-sheet forming polyalanine peptides. FEBS Lett 555:380–384
Gobbi M, Colombo L, Morbin M, Mazzoleni G, Accardo E, Vanoni M, Del Favero E, Cantu L, Kirschner DA, Manzoni C, Beeg M, Ceci P, Ubezio P, Forloni G, Tagliavini F, Salmona M (2006) Gerstmann-Straussler-Scheinker disease amyloid protein polymerizes according to the "dock-and-lock" model. J Biol Chem 281:843–849
Gordon DJ, Balbach JJ, Tycko R, Meredith SC (2004) Increasing the amphiphilicity of an amyloidogenic peptide changes the beta-sheet structure in the fibrils from antiparallel to parallel. Biophys J 86:428–434
Goux WJ, Kopplin L, Nguyen AD, Leak K, Rutkofsky M, Shanmuganandam VD, Sharma D, Inouye H, Kirschner DA (2004) The formation of straight and twisted filaments from short Tau peptides. J Biol Chem 279:26868–26875
Graether SP, Slupsky CM, Sykes BD (2003) Freezing of a fish antifreeze protein results in amyloid fibril formation. Biophys J 84:552–557
Greenfield S, Vaux DJ (2002) Parkinson's disease, Alzheimer's disease and motor neurone disease: identifying a common mechanism. Neuroscience 113:485–492
Gregersen N, Bolund L, Bross P (2005) Protein misfolding, aggregation, and degradation in disease. Mol Biotechnol 31:141–150
Gross M, Wilkins DK, Pitkeathly MC, Chung EW, Higham C, Clark A, Dobson CM (1999) Formation of amyloid fibrils by peptides derived from the bacterial cold shock protein CspB. Protein Sci 8:1350–1357
Guijarro JI, Sunde M, Jones JA, Campbell ID, Dobson CM (1998) Amyloid fibril formation by an SH3 domain. Proc Natl Acad Sci USA 95:4224–4228
Gupta-Bansal R, Frederickson RC, Brunden KR (1995) Proteoglycan-mediated inhibition of A beta proteolysis. A potential cause of senile plaque accumulation. J Biol Chem 270:18666–18671
Gustavsson A, Engstrom U, Westermark P (1991) Normal transthyretin and synthetic transthyretin fragments form amyloid-like fibrils in vitro. Biochem Biophys Res Commun 175:1159–1164
Haggqvist B, Naslund J, Sletten K, Westermark GT, Mucchiano G, Tjernberg LO, Nordstedt C, Engstrom U, Westermark P (1999) Medin: an integral fragment of aortic smooth muscle cell-produced lactadherin forms the most common human amyloid. Proc Natl Acad Sci USA 96:8669–8674
Hall D, Minton AP (2003) Macromolecular crowding: qualitative and semiquantitative successes, quantitative challenges. Biochim Biophys Acta 1649:127–139
Halverson K, Fraser PE, Kirschner DA, Lansbury PT Jr (1990) Molecular determinants of amyloid deposition in Alzheimer's disease: conformational studies of synthetic beta-protein fragments. Biochemistry 29:2639–2644
Hamada D, Dobson CM (2002) A kinetic study of beta-lactoglobulin amyloid fibril formation promoted by urea. Protein Sci 11:2417–2426
Hamilton JA, Benson MD (2001) Transthyretin: a review from a structural perspective. Cell Mol Life Sci 58:1491–1521
Hammarström P, Jiang X, Hurshman AR, Powers ET, Kelly JW (2002) Sequence-dependent denaturation energetics: a major determinant in amyloid disease diversity. Proc Natl Acad Sci USA 99(Suppl 4):16427–16432
Hamodrakas SJ, Hoenger A, Iconomidou VA (2004) Amyloid fibrillogenesis of silkmoth chorion protein peptide-analogues via a liquid-crystalline intermediate phase. J Struct Biol 145:226–235

Harper JD, Lansbury PT Jr (1997) Models of amyloid seeding in Alzheimer's disease and scrapie: mechanistic truths and physiological consequences of the time-dependent solubility of amyloid proteins. Annu Rev Biochem 66:385–407

Harris JR (2002) In vitro fibrillogenesis of the amyloid beta 1–42 peptide: cholesterol potentiation and aspirin inhibition. Micron 33:609–626

Harris ME, Carney JM, Cole PS, Hensley K, Howard BJ, Martin L, Bummer P, Wang Y, Pedigo NW Jr, Butterfield DA (1995) beta-Amyloid peptide-derived, oxygen-dependent free radicals inhibit glutamate uptake in cultured astrocytes: implications for Alzheimer's disease. Neuroreport 6:1875–1879

Hasegawa K, Ohhashi Y, Yamaguchi I, Takahashi N, Tsutsumi S, Goto Y, Gejyo F, Naiki H (2003) Amyloidogenic synthetic peptides of beta 2-microglobulin—a role of the disulfide bond. Biochem Biophys Res Commun 304:101–106

Hatters DM, Minton AP, Howlett GJ (2002) Macromolecular crowding accelerates amyloid formation by human apolipoprotein C-II. J Biol Chem 277:7824–7830

He Y, Zhou H, Tang H, Luo Y (2006) Deficiency of disulfide bonds facilitating fibrillogenesis of endostatin. J Biol Chem 281:1048–1057

Hearing VJ (2000) The melanosome: the perfect model for cellular responses to the environment. Pigment Cell Res 13:23–34

Heise H, Hoyer W, Becker S, Andronesi OC, Riedel D, Baldus M (2005) Molecular-level secondary structure, polymorphism, and dynamics of full-length alpha-synuclein fibrils studied by solid-state NMR. Proc Natl Acad Sci USA 102:15871–15876

Hensley K, Carney JM, Mattson MP, Aksenova M, Harris M, Wu JF, Floyd RA, Butterfield DA (1994) A model for beta-amyloid aggregation and neurotoxicity based on free radical generation by the peptide: relevance to Alzheimer disease. Proc Natl Acad Sci USA 91:3270–3274

Hensley K, Aksenova M, Carney JM, Harris M, Butterfield DA (1995) Amyloid beta-peptide spin trapping. I. Peptide enzyme toxicity is related to free radical spin trap reactivity. Neuroreport 6:489–492

Hirano K, Hotta Y, Fujiki K, Kanai A (2000) Corneal amyloidosis caused by Leu518Pro mutation of betaigh3 gene. Br J Ophthalmol 84:583–585

Hirschfield GM (2004) Amyloidosis: a clinico-pathophysiological synopsis. Semin Cell Dev Biol 15:39–44

Holmes SE, O'Hearn E, Rosenblatt A, Callahan C, Hwang HS, Ingersoll-Ashworth RG, Fleisher A, Stevanin G, Brice A, Potter NT, Ross CA, Margolis RL (2001) A repeat expansion in the gene encoding junctophilin-3 is associated with Huntington disease-like 2. Nat Genet 29:377–378

Hong DP, Fink AL (2005) Independent heterologous fibrillation of insulin and its B-chain peptide. Biochemistry 44:16701–16709

Hosia W, Johansson J, Griffiths WJ (2002) Hydrogen/deuterium exchange and aggregation of a polyvaline and a polyleucine alpha-helix investigated by matrix-assisted laser desorption ionization mass spectrometry. Mol Cell Proteomics 1:592–597

Hoyer W, Antony T, Cherny D, Heim G, Jovin TM, Subramaniam V (2002) Dependence of alpha-synuclein aggregate morphology on solution conditions. J Mol Biol 322:383–393

Hua QX, Weiss MA (2004) Mechanism of insulin fibrillation: the structure of insulin under amyloidogenic conditions resembles a protein-folding intermediate. J Biol Chem 279:21449–21460

Huang CC, Faber PW, Persichetti F, Mittal V, Vonsattel JP, MacDonald ME, Gusella JF (1998) Amyloid formation by mutant huntingtin: threshold, progressivity and recruitment of normal polyglutamine proteins. Somat Cell Mol Genet 24:217–233

Huang X, Atwood CS, Moir RD, Hartshorn MA, Vonsattel JP, Tanzi RE, Bush AI (1997) Zinc-induced Alzheimer's Abeta 1–40 aggregation is mediated by conformational factors. J Biol Chem 272:26464–26470

Huang X, Cuajungco MP, Atwood CS, Hartshorn MA, Tyndall JD, Hanson GR, Stokes KC, Leopold M, Multhaup G, Goldstein LE, Scarpa RC, Saunders AJ, Lim J, Moir RD, Glabe C, Bowden EF, Masters CL, Fairlie DP, Tanzi RE, Bush AI (1999) Cu(II) potentiation of Alzheimer abeta neurotoxicity. Correlation with cell-free hydrogen peroxide production and metal reduction. J Biol Chem 274:37111–37116

Hurshman AR, White JT, Powers ET, Kelly JW (2004) Transthyretin aggregation under partially denaturing conditions is a downhill polymerization. Biochemistry 43:7365–7381

Iconomidou VA, Vriend G, Hamodrakas SJ (2000) Amyloids protect the silkmoth oocyte and embryo. FEBS Lett 479:141–145

Inouye H, Kirschner DA (2000) A beta fibrillogenesis: kinetic parameters for fibril formation from Congo red binding. J Struct Biol 130:123–129

Inouye H, Fraser PE, Kirschner DA (1993) Structure of beta-crystallite assemblies formed by Alzheimer beta-amyloid protein analogues: analysis by x-ray diffraction. Biophys J 64:502–519

Inouye H, Bond JE, Deverin SP, Lim A, Costello CE, Kirschner DA (2002) Molecular organization of amyloid protofilament-like assembly of betabellin 15D: helical array of beta-sandwiches. Biophys J 83:1716–1727

Isobe T, Osserman EF (1974) Patterns of amyloidosis and their association with plasma cell dyscrasias, monoclonal immunoglobulins and Bence Jones proteins. N Engl J Med 290:473–477

Ivanova MI, Gingery M, Whitson LJ, Eisenberg D (2003) Role of the C-terminal 28 residues of beta 2-microglobulin in amyloid fibril formation. Biochemistry 42:13536–13540

Iwata K, Fujiwara T, Matsuki Y, Akutsu H, Takahashi S, Naiki H, Goto Y (2006) 3D structure of amyloid protofilaments of beta 2-microglobulin fragment probed by solid-state NMR. Proc Natl Acad Sci USA 103:18119–18124

Jahn TR, Parker MJ, Homans SW, Radford SE (2006) Amyloid formation under physiological conditions proceeds via a native-like folding intermediate. Nat Struct Mol Biol 13:195–201

Janciauskiene S, Carlemalm E, Eriksson S (1995) In vitro fibril formation from alpha 1-antitrypsin-derived C-terminal peptides. Biol Chem Hoppe Seyler 376:415–423

Janowski R, Kozak M, Abrahamson M, Grubb A, Jaskolski M (2005) 3D domain-swapped human cystatin c with amyloid-like intermolecular beta-sheets. Proteins 61:570–578

Jansen R, Dzwolak W, Winter R (2005) Amyloidogenic self-assembly of insulin aggregates probed by high resolution atomic force microscopy. Biophys J 88:1344–1353

Jaroniec CP, MacPhee CE, Astrof NS, Dobson CM, Griffin RG (2002) Molecular conformation of a peptide fragment of transthyretin in an amyloid fibril. Proc Natl Acad Sci USA 99:16748–16753

Jarrett JT, Berger EP, Lansbury PT Jr (1993) The carboxy terminus of the beta amyloid protein is critical for the seeding of amyloid formation: implications for the pathogenesis of Alzheimer's disease. Biochemistry 32:4693–4697

Jenko S, Skarabot M, Kenig M, Guncar G, Musevic I, Turk D, Zerovnik E (2004) Different propensity to form amyloid fibrils by two homologous proteins-Human stefins A and B: searching for an explanation. Proteins 55:417–425

Johansson B, Wernstedt C, Westermark P (1987) Atrial natriuretic peptide deposited as atrial amyloid fibrils. Biochem Biophys Res Commun 148:1087–1092

John V, Latimer LH, Tung JS, Dappen MS (1997) Alzheimer's disease: recent advances on the amyloid hypothesis. Annu Rep Med Chem 32:11–20

Jones S, Manning J, Kad NM, Radford SE (2003) Amyloid-forming peptides from beta 2-microglobulin—insights into the mechanism of fibril formation in vitro. J Mol Biol 325:249–257

Kad NM, Myers SL, Smith DP, Smith DA, Radford SE, Thomson NH (2003) Hierarchical assembly of beta 2-microglobulin amyloid in vitro revealed by atomic force microscopy. J Mol Biol 330:785–797

Kagan BL, Hirakura Y, Azimov R, Azimova R (2001) The channel hypothesis of Huntington's disease. Brain Res Bull 56:281–284

Kallberg Y, Gustafsson M, Persson B, Thyberg J, Johansson J (2001) Prediction of amyloid fibril-forming proteins. J Biol Chem 276:12945–12950

Kallijärvi J, Haltia M, Baumann MH (2001) Amphoterin includes a sequence motif which is homologous to the Alzheimer's beta-amyloid peptide (Abeta), forms amyloid fibrils in vitro, and binds avidly to Abeta. Biochemistry 40:10032–10037

Kamenetz F, Tomita T, Hsieh H, Seabrook G, Borchelt D, Iwatsubo T, Sisodia S, Malinow R (2003) APP processing and synaptic function. Neuron 37:925–937

Kamihira M, Naito A, Tuzi S, Nosaka AY, Saito H (2000) Conformational transitions and fibrillation mechanism of human calcitonin as studied by high-resolution solid-state 13C NMR. Protein Sci 9:867–877

Kammerer RA, Kostrewa D, Zurdo J, Detken A, Garcia-Echeverria C, Green JD, Muller SA, Meier BH, Winkler FK, Dobson CM, Steinmetz MO (2004) Exploring amyloid formation by a de novo design. Proc Natl Acad Sci USA 101:4435–4440

Kanazawa I (1998) Dentatorubral-pallidoluysian atrophy or Naito-Oyanagi disease. Neurogenetics 2:1–17

Kaneko I, Morimoto K, Kubo T (2001) Drastic neuronal loss in vivo by beta-amyloid racemized at Ser(26) residue: conversion of non-toxic [D-Ser(26)]beta-amyloid 1–40 to toxic and proteinase-resistant fragments. Neuroscience 104:1003–1011

Karsai A, Martonfalvi Z, Nagy A, Grama L, Penke B, Kellermayer MS (2006) Mechanical manipulation of Alzheimer's amyloid beta 1–42 fibrils. J Struct Biol 155:316–326

Katsuno M, Adachi H, Tanaka F, Sobue G (2004) Spinal and bulbar muscular atrophy: ligand-dependent pathogenesis and therapeutic perspectives. J Mol Med 82:298–307

Kaul R, Balaram P (1999) Stereochemical control of peptide folding. Bioorg Med Chem 7:105–117

Kawasaki S, Nishida K, Quantock AJ, Dota A, Bennett K, Kinoshita S (1999) Amyloid and Pro501 Thr-mutated (beta)ig-h3 gene product colocalize in lattice corneal dystrophy type IIIA. Am J Ophthalmol 127:456–458

Kawooya JK, Emmons TL, Gonzalez-DeWhitt PA, Camp MC, D'Andrea SC (2003) Electrophoretic mobility of Alzheimer's amyloid-beta peptides in urea-sodium dodecyl sulfate-polyacrylamide gel electrophoresis. Anal Biochem 323:103–113

Kay CJ (1997) Mechanochemical mechanism for peptidyl free radical generation by amyloid fibrils. FEBS Lett 403:230–235

Kayed R, Head E, Thompson JL, McIntire TM, Milton SC, Cotman CW, Glabe CG (2003) Common structure of soluble amyloid oligomers implies common mechanism of pathogenesis. Science 300:486–489

Kelly JF, Furukawa K, Barger SW, Rengen MR, Mark RJ, Blanc EM, Roth GS, Mattson MP (1996) Amyloid beta-peptide disrupts carbachol-induced muscarinic cholinergic signal transduction in cortical neurons. Proc Natl Acad Sci USA 93:6753–6758

Kelly JW, Balch WE (2003) Amyloid as a natural product. J Cell Biol 161:461–462

Kenney JM, Knight D, Wise MJ, Vollrath F (2002) Amyloidogenic nature of spider silk. Eur J Biochem 269:4159–4163

Kiefhaber T (1995) Kinetic traps in lysozyme folding. Proc Natl Acad Sci USA 92:9029–9033

Kim JL, Nikolov DB, Burley SK (1993a) Co-crystal structure of TBP recognizing the minor groove of a TATA element. Nature 365:520–527

Kim Y, Geiger JH, Hahn S, Sigler PB (1993b) Crystal structure of a yeast TBP/TATA-box complex. Nature 365:512–520

Kim YS, Randolph TW, Stevens FJ, Carpenter JF (2002) Kinetics and energetics of assembly, nucleation, and growth of aggregates and fibrils for an amyloidogenic protein. Insights into transition states from pressure, temperature, and co-solute studies. J Biol Chem 277:27240–27246

Kirkitadze MD, Condron MM, Teplow DB (2001) Identification and characterization of key kinetic intermediates in amyloid beta-protein fibrillogenesis. J Mol Biol 312:1103–1119

Kishikawa M, Nakanishi T, Miyazaki A, Hatanaka M, Shimizu A, Tamoto S, Ohsawa N, Hayashi H, Kanai M (1998) A new nonamyloid transthyretin variant, G101S, detected by electrospray ionization/mass spectrometry. Mutations in brief No. 201. Online. Hum Mutat 12:363

Kishikawa M, Sass JO, Sakura N, Nakanishi T, Shimizu A, Yoshioka M (2002) The peak height ratio of S-sulfonated transthyretin and other oxidized isoforms as a marker for molybdenum cofactor deficiency, measured by electrospray ionization mass spectrometry. Biochim Biophys Acta 1588:135–138

Kishimoto A, Hasegawa K, Suzuki H, Taguchi H, Namba K, Yoshida M (2004) beta-Helix is a likely core structure of yeast prion Sup35 amyloid fibers. Biochem Biophys Res Commun 315:739–745

Kiuru S (1998) Gelsolin-related familial amyloidosis, Finnish type (FAF), and its variants found worldwide. Amyloid 5:55–66

Klein WL, Stine WB Jr, Teplow DB (2004) Small assemblies of unmodified amyloid beta-protein are the proximate neurotoxin in Alzheimer's disease. Neurobiol Aging 25:569–580

Klunk WE, Jacob RF, Mason RP (1999) Quantifying amyloid by Congo red spectral shift assay. Methods Enzymol 309:285–305

Knauer MF, Soreghan B, Burdick D, Kosmoski J, Glabe CG (1992) Intracellular accumulation and resistance to degradation of the Alzheimer amyloid A4/beta protein. Proc Natl Acad Sci USA 89:7437–7441

Knight JD, Hebda JA, Miranker AD (2006) Conserved and cooperative assembly of membrane-bound alpha-helical states of islet amyloid polypeptide. Biochemistry 45:9496–9508

Koga T, Taguchi K, Kobuke Y, Kinoshita T, Higuchi M (2003) Structural regulation of a peptide-conjugated graft copolymer: a simple model for amyloid formation. Chemistry 9:1146–1156

Konno T (2001) Multistep nucleus formation and a separate subunit contribution of the amyloidgenesis of heat-denatured monellin. Protein Sci 10:2093–2101

Koscielska-Kasprzak K, Otlewski J (2003) Amyloid-forming peptides selected proteolytically from phage display library. Protein Sci 12:1675–1685

Kotilinek LA, Bacskai B, Westerman M, Kawarabayashi T, Younkin L, Hyman BT, Younkin S, Ashe KH (2002) Reversible memory loss in a mouse transgenic model of Alzheimer's disease. J Neurosci 22:6331–6335

Kowalewski T, Holtzman DM (1999) In situ atomic force microscopy study of Alzheimer's beta-amyloid peptide on different substrates: new insights into mechanism of beta-sheet formation. Proc Natl Acad Sci USA 96:3688–3693

Kranenburg O, Kroon-Batenburg LM, Reijerkerk A, Wu YP, Voest EE, Gebbink MF (2003) Recombinant endostatin forms amyloid fibrils that bind and are cytotoxic to murine neuroblastoma cells in vitro. FEBS Lett 539:149–155

Krebs MR, Wilkins DK, Chung EW, Pitkeathly MC, Chamberlain AK, Zurdo J, Robinson CV, Dobson CM (2000) Formation and seeding of amyloid fibrils from wild-type hen lysozyme and a peptide fragment from the beta-domain. J Mol Biol 300:541–549

Kubo T, Nishimura S, Kumagae Y, Kaneko I (2002) In vivo conversion of racemized beta-amyloid ([D-Ser 26]A beta 1–40) to truncated and toxic fragments ([D-Ser 26]A beta 25–35/40) and fragment presence in the brains of Alzheimer's patients. J Neurosci Res 70:474–483

Kumita JR, Weston CJ, Choo-Smith LP, Woolley GA, Smart OS (2003) Prevention of peptide fibril formation in an aqueous environment by mutation of a single residue to Aib. Biochemistry 42:4492–4498

Kwiatkowski DJ, Stossel TP, Orkin SH, Mole JE, Colten HR, Yin HL (1986) Plasma and cytoplasmic gelsolins are encoded by a single gene and contain a duplicated actin-binding domain. Nature 323:455–458

La Spada AR, Taylor JP (2003) Polyglutamines placed into context. Neuron 38:681–684

Lachmann HJ, Hawkins PN (2006) Systemic amyloidosis. Curr Opin Pharmacol 6:214–220

Lansbury PT Jr, Costa PR, Griffiths JM, Simon EJ, Auger M, Halverson KJ, Kocisko DA, Hendsch ZS, Ashburn TT, Spencer RG, et al (1995) Structural model for the beta-amyloid fibril based on interstrand alignment of an antiparallel-sheet comprising a C-terminal peptide. Nat Struct Biol 2:990–998

Lashuel HA, LaBrenz SR, Woo L, Serpell LC, Kelly JW (2000) Protofilaments, filaments, ribbons, and fibrils from peptidomimetic self-assembly: implications for amyloid fibril formation and materials science. J Am Chem Soc 122:5262–5277

Lavrikova MA, Zamotin VV, Malisauskas M, Chertkova RV, Kostanyan IA, Dolgikh DA, Kirpichnikov MP, Morozova-Roche LA (2006) Amyloidogenic properties of the artificial protein albebetin and its biologically active derivatives. The role of electrostatic interactions in fibril formation. Biochemistry (Mosc) 71:306–314

Lebre AS, Brice A (2003) Spinocerebellar ataxia 7 (SCA7). Cytogenet Genome Res 100:154–163

Lee AS, Galea C, DiGiammarino EL, Jun B, Murti G, Ribeiro RC, Zambetti G, Schultz CP, Kriwacki RW (2003) Reversible amyloid formation by the p53 tetramerization domain and a cancer-associated mutant. J Mol Biol 327:699–709

LeVine H 3rd (1999) Quantification of beta-sheet amyloid fibril structures with thioflavin T. Methods Enzymol 309:274–284

Lieberman M, Sasaki TJ (1991) Iron(II) organizes a synthetic peptide into three-helix bundles. J Am Chem Soc 113:1470–1471

Lim A, Makhov AM, Bond J, Inouye H, Connors LH, Griffith JD, Erickson BW, Kirschner DA, Costello CE (2000) Betabellins 15D and 16D, de novo designed beta-sandwich proteins that have amyloidogenic properties. J Struct Biol 130:363–370

Lim A, Prokaeva T, McComb ME, Connors LH, Skinner M, Costello CE (2003a) Identification of S-sulfonation and S-thiolation of a novel transthyretin Phe33Cys variant from a patient diagnosed with familial transthyretin amyloidosis. Protein Sci 12:1775–1785

Lim A, Sengupta S, McComb ME, Theberge R, Wilson WG, Costello CE, Jacobsen DW (2003b) In vitro and in vivo interactions of homocysteine with human plasma transthyretin. J Biol Chem 278:49707–49713

Limprasert P, Nouri N, Nopparatana C, Deininger PL, Keats BJ (1997) Comparative studies of the CAG repeats in the spinocerebellar ataxia type 1 (SCA1) gene. Am J Med Genet 74:488–493

Linke RP, Joswig R, Murphy CL, Wang S, Zhou H, Gross U, Rocken C, Westermark P, Weiss DT, Solomon A (2005) Senile seminal vesicle amyloid is derived from semenogelin I. J Lab Clin Med 145:187–193

Litvinovich SV, Brew SA, Aota S, Akiyama SK, Haudenschild C, Ingham KC (1998) Formation of amyloid-like fibrils by self-association of a partially unfolded fibronectin type III module. J Mol Biol 280:245–258

Liu W, Crocker E, Zhang W, Elliott JI, Luy B, Li H, Aimoto S, Smith SO (2005) Structural role of glycine in amyloid fibrils formed from transmembrane alpha-helices. Biochemistry 44:3591–3597

Loferer H, Hammar M, Normark S (1997) Availability of the fibre subunit CsgA and the nucleator protein CsgB during assembly of fibronectin-binding curli is limited by the intracellular concentration of the novel lipoprotein CsgG. Mol Microbiol 26:11–23

Lomakin A, Chung DS, Benedek GB, Kirschner DA, Teplow DB (1996) On the nucleation and growth of amyloid beta-protein fibrils: detection of nuclei and quantitation of rate constants. Proc Natl Acad Sci USA 93:1125–1129

Lopez de la Paz ML, Serrano L (2004) Sequence determinants of amyloid fibril formation. Proc Natl Acad Sci USA 101:87–92

Lopez de la Paz M, Goldie K, Zurdo J, Lacroix E, Dobson CM, Hoenger A, Serrano L (2002) De novo designed peptide-based amyloid fibrils. Proc Natl Acad Sci USA 99:16052–16057

Lopez de la Paz M, de Mori GM, Serrano L, Colombo G (2005) Sequence dependence of amyloid fibril formation: insights from molecular dynamics simulations. J Mol Biol 349:583–596

Losic D, Martin LL, Mechler A, Aguilar MI, Small DH (2006) High resolution scanning tunnelling microscopy of the beta-amyloid protein (Abeta 1–40) of Alzheimer's disease suggests a novel mechanism of oligomer assembly. J Struct Biol 155:104–110

Loughlin WA, Tyndall JD, Glenn MP, Fairlie DP (2004) Beta-strand mimetics. Chem Rev 104:6085–6117

Luhrs T, Ritter C, Adrian M, Riek-Loher D, Bohrmann B, Dobeli H, Schubert D, Riek R (2005) 3D structure of Alzheimer's amyloid-beta(1–42) fibrils. Proc Natl Acad Sci USA 102:17342–17347
Ma B, Nussinov R (2002) Molecular dynamics simulations of alanine rich beta-sheet oligomers: insight into amyloid formation. Protein Sci 11:2335–2350
Mackay JP, Matthews JM, Winefield RD, Mackay LG, Haverkamp RG, Templeton MD (2001) The hydrophobin EAS is largely unstructured in solution and functions by forming amyloid-like structures. Structure 9:83–91
Makin OS, Serpell LC (2002) Examining the structure of the mature amyloid fibril. Biochem Soc Trans 30:521–525
Makin OS, Serpell LC (2005) Structures for amyloid fibrils. FEBS J 272:5950–5961
Malinchik SB, Inouye H, Szumowski KE, Kirschner DA (1998) Structural analysis of Alzheimer's beta(1–40) amyloid: protofilament assembly of tubular fibrils. Biophys J 74:537–545
Malisauskas M, Zamotin V, Jass J, Noppe W, Dobson CM, Morozova-Roche LA (2003) Amyloid protofilaments from the calcium-binding protein equine lysozyme: formation of ring and linear structures depends on pH and metal ion concentration. J Mol Biol 330:879–890
Mantuano E, Veneziano L, Jodice C, Frontali M (2003) Spinocerebellar ataxia type 6 and episodic ataxia type 2: differences and similarities between two allelic disorders. Cytogenet Genome Res 100:147–153
Markesbery WR (1997) Oxidative stress hypothesis in Alzheimer's disease. Free Radic Biol Med 23:134–147
Marks MS, Seabra MC (2001) The melanosome: membrane dynamics in black and white. Nat Rev Mol Cell Biol 2:738–748
Massi F, Straub JE (2001) Energy landscape theory for Alzheimer's amyloid beta-peptide fibril elongation. Proteins 42:217–229
Matsunaga N, Anan I, Forsgren S, Nagai R, Rosenberg P, Horiuchi S, Ando Y, Suhr OB (2002) Advanced glycation end products (AGE) and the receptor for AGE are present in gastrointestinal tract of familial amyloidotic polyneuropathy patients but do not induce NF-kappaB activation. Acta Neuropathol (Berl) 104:441–447
Mattson MP (2004) Pathways towards and away from Alzheimer's disease. Nature 430:631–639
Maury CP (1991) Gelsolin-related amyloidosis. Identification of the amyloid protein in Finnish hereditary amyloidosis as a fragment of variant gelsolin. J Clin Invest 87:1195–1199
Maury CP, Nurmiaho-Lassila EL, Rossi H (1994) Amyloid fibril formation in gelsolin-derived amyloidosis. Definition of the amyloidogenic region and evidence of accelerated amyloid formation of mutant Asn-187 and Tyr-187 gelsolin peptides. Lab Invest 70:558–564
Maury CP, Nurmiaho-Lassila EL, Liljestrom M (1997) Alzheimer's disease-associated presenilins 1 and 2: accelerated amyloid fibril formation of mutant 410 Cys->Tyr and 141 Asn->Ile peptides. Biochem Biophys Res Commun 235:249–252
Maury CP, Nurmiaho-Lassila EL, Boysen G, Liljestrom M (2003) Fibrillogenesis in gelsolin-related familial amyloidosis. Amyloid 10(Suppl 1):21–25
McDuff FO, Doucet A, Beauregard M (2004) Low concentration of guanidine hydrochloride induces the formation of an aggregation-prone state in alpha-urease. Biochem Cell Biol 82:305–313
Meehan S, Berry Y, Luisi B, Dobson CM, Carver JA, MacPhee CE (2004) Amyloid fibril formation by lens crystallin proteins and its implications for cataract formation. J Biol Chem 279:3413–3419
Merlini G, Westermark P (2004) The systemic amyloidoses: clearer understanding of the molecular mechanisms offers hope for more effective therapies. J Intern Med 255:159–178
Michelitsch MD, Weissman JS (2000) A census of glutamine/asparagine-rich regions: implications for their conserved function and the prediction of novel prions. Proc Natl Acad Sci USA 97:11910–11915
Michne WF, Schroeder JD (1996) Design and synthesis of a beta-strand inducer. Application to ICAM-1/LFA-1 mediated cellular adhesion. Int J Pept Protein Res 47:2–8
Mira H, Vilar M, Esteve V, Martinell M, Kogan MJ, Giralt E, Salom D, Mingarro I, Penarrubia L, Perez-Paya E (2004) Ionic self-complementarity induces amyloid-like fibril formation in an isolated domain of a plant copper metallochaperone protein. BMC Struct Biol 4:7
Miura T, Mitani S, Takanashi C, Mochizuki N (2004) Copper selectively triggers beta-sheet assembly of an N-terminally truncated amyloid beta-peptide beginning with Glu3. J Inorg Biochem 98:10–14
Modler AJ, Gast K, Lutsch G, Damaschun G (2003) Assembly of amyloid protofibrils via critical oligomers—a novel pathway of amyloid formation. J Mol Biol 325:135–148
Monti M, Garolla di Bard BL, Calloni G, Chiti F, Amoresano A, Ramponi G, Pucci P (2004) The regions of the sequence most exposed to the solvent within the amyloidogenic state of a protein initiate the aggregation process. J Mol Biol 336:253–262
Morel B, Casares S, Conejero-Lara F (2006) A single mutation induces amyloid aggregation in the alpha-spectrin SH3 domain: analysis of the early stages of fibril formation. J Mol Biol 356:453–468

Morgan CJ, Gelfand M, Atreya C, Miranker AD (2001) Kidney dialysis-associated amyloidosis: a molecular role for copper in fiber formation. J Mol Biol 309:339–345
Murphy RM (2002) Peptide aggregation in neurodegenerative disease. Annu Rev Biomed Eng 4:155–174
Mutter M, Vuilleumier S (1989) A chemical approach to protein design—template-assembled synthetic proteins (TASPs). Angew Chem Int Ed Engl 28:535–554
Myers JK, Pace CN, Scholtz JM (1998) Trifluoroethanol effects on helix propensity and electrostatic interactions in the helical peptide from ribonuclease T1. Protein Sci 7:383–388
Naito A, Kamihira M, Inoue R, Saito H (2004) Structural diversity of amyloid fibril formed in human calcitonin as revealed by site-directed 13C solid-state NMR spectroscopy. Magn Reson Chem 42:247–257
Nakagawa Asahina S, Fujiki K, Enomoto Y, Murakami A, Kanai A (2004) Case of late onset and isolated lattice corneal dystrophy with Asn544Ser (N544S) mutation of transforming growth factor beta-induced (TGFBI, BIGH3) gene. Nippon Ganka Gakkai Zasshi 108:618–620
Nakamura K, Jeong SY, Uchihara T, Anno M, Nagashima K, Nagashima T, Ikeda S, Tsuji S, Kanazawa I (2001) SCA17, a novel autosomal dominant cerebellar ataxia caused by an expanded polyglutamine in TATA-binding protein. Hum Mol Genet 10:1441–1448
Nelson R, Sawaya MR, Balbirnie M, Madsen AO, Riekel C, Grothe R, Eisenberg D (2005) Structure of the cross-beta spine of amyloid-like fibrils. Nature 435:773–778
Nettleton EJ, Tito P, Sunde M, Bouchard M, Dobson CM, Robinson CV (2000) Characterization of the oligomeric states of insulin in self-assembly and amyloid fibril formation by mass spectrometry. Biophys J 79:1053–1065
Nichols MR, Moss MA, Reed DK, Lin WL, Mukhopadhyay R, Hoh JH, Rosenberry TL (2002) Growth of beta-amyloid(1–40) protofibrils by monomer elongation and lateral association. Characterization of distinct products by light scattering and atomic force microscopy. Biochemistry 41:6115–6127
Niewold TA, Murphy CL, Hulskamp-Koch CA, Tooten PC, Gruys E (1999) Casein related amyloid, characterization of a new and unique amyloid protein isolated from bovine corpora amylacea. Amyloid 6:244–249
Nikolov DB, Chen H, Halay ED, Usheva AA, Hisatake K, Lee DK, Roeder RG, Burley SK (1995) Crystal structure of a TFIIB-TBP-TATA-element ternary complex. Nature 377:119–128
Nilsson G, Gustafsson M, Vandenbussche G, Veldhuizen E, Griffiths WJ, Sjovall J, Haagsman HP, Ruysschaert JM, Robertson B, Curstedt T, Johansson J (1998) Synthetic peptide-containing surfactants—evaluation of transmembrane versus amphipathic helices and surfactant protein C poly-valyl to poly-leucyl substitution. Eur J Biochem 255:116–124
Nilsson M, Wang X, Rodziewicz-Motowidlo S, Janowski R, Lindstrom V, Onnerfjord P, Westermark G, Grzonka Z, Jaskolski M, Grubb A (2004) Prevention of domain swapping inhibits dimerization and amyloid fibril formation of cystatin C—Use of engineered disulfide bridges, antibodies, and carboxymethylpapain to stabilize the monomeric form of cystatin C. J Biol Chem 279:24236–24245
Nilsson MR, Dobson CM (2003) In vitro characterization of lactoferrin aggregation and amyloid formation. Biochemistry 42:375–382
Nilsson MR, Raleigh DP (1999) Analysis of amylin cleavage products provides new insights into the amyloidogenic region of human amylin. J Mol Biol 294:1375–1385
Nilsson MR, Driscoll M, Raleigh DP (2002) Low levels of asparagine deamidation can have a dramatic effect on aggregation of amyloidogenic peptides: implications for the study of amyloid formation. Protein Sci 11:342–349
O'Neil KT, DeGrado WF (1990) A thermodynamic scale for the helix-forming tendencies of the commonly occurring amino acids. Science 250:646–651
O'Nuallain B, Williams AD, Westermark P, Wetzel R (2004) Seeding specificity in amyloid growth induced by heterologous fibrils. J Biol Chem 279:17490–17499
Oddo S, Caccamo A, Shepherd JD, Murphy MP, Golde TE, Kayed R, Metherate R, Mattson MP, Akbari Y, LaFerla FM (2003) Triple-transgenic model of Alzheimer's disease with plaques and tangles: intracellular Abeta and synaptic dysfunction. Neuron 39:409–421
Oddo S, Billings L, Kesslak JP, Cribbs DH, LaFerla FM (2004) Abeta immunotherapy leads to clearance of early, but not late, hyperphosphorylated tau aggregates via the proteasome. Neuron 43:321–332
Oddo S, Caccamo A, Smith IF, Green KN, LaFerla FM (2006) A dynamic relationship between intracellular and extracellular pools of Abeta. Am J Pathol 168:184–194
Ohashi K, Kisilevsky R, Yanagishita M (2002) Affinity binding of glycosaminoglycans with beta(2)-microglobulin. Nephron 90:158–168
Olsen A, Jonsson A, Normark S (1989) Fibronectin binding mediated by a novel class of surface organelles on Escherichia coli. Nature 338:652–655
Olsen A, Wick MJ, Morgelin M, Bjorck L (1998) Curli, fibrous surface proteins of Escherichia coli, interact with major histocompatibility complex class I molecules. Infect Immun 66:944–949

Otzen DE, Oliveberg M (1999) Salt-induced detour through compact regions of the protein folding landscape. Proc Natl Acad Sci USA 96:11746–11751

Otzen DE, Kristensen O, Oliveberg M (2000) Designed protein tetramer zipped together with a hydrophobic Alzheimer homology: a structural clue to amyloid assembly. Proc Natl Acad Sci USA 97:9907–9912

Oyanagi S (2000) Hereditary dentatorubral-pallidoluysian atrophy. Neuropathology 20(Suppl):S42–S46

Päiviö A, Nordling E, Kallberg Y, Thyberg J, Johansson J (2004) Stabilization of discordant helices in amyloid fibril-forming proteins. Protein Sci 13:1251–1259

Pallitto MM, Murphy RM (2001) A mathematical model of the kinetics of beta-amyloid fibril growth from the denatured state. Biophys J 81:1805–1822

Parrini C, Taddei N, Ramazzotti M, Degl'Innocenti D, Ramponi G, Dobson CM, Chiti F (2005) Glycine residues appear to be evolutionarily conserved for their ability to inhibit aggregation. Structure (Camb) 13:1143–1151

Pavlov NA, Cherny DI, Heim G, Jovin TM, Subramaniam V (2002) Amyloid fibrils from the mammalian protein prothymosin alpha. FEBS Lett 517:37–40

Pawar AP, Dubay KF, Zurdo J, Chiti F, Vendruscolo M, Dobson CM (2005) Prediction of "aggregation-prone" and "aggregation-susceptible" regions in proteins associated with neurodegenerative diseases. J Mol Biol 350:379–392

Pengo P, Pasquato L, Moro S, Brigo A, Fogolari F, Broxterman QB, Kaptein B, Scrimin P (2003) Quantitative correlation of solvent polarity with the alpha-/3(10)-helix equilibrium: a heptapeptide behaves as a solvent-driven molecular spring. Angew Chem Int Ed Engl 42:3388–3392

Pepys MB, Rademacher TW, Amatayakul-Chantler S, Williams P, Noble GE, Hutchinson WL, Hawkins PN, Nelson SR, Gallimore JR, Herbert J, et al (1994) Human serum amyloid P component is an invariant constituent of amyloid deposits and has a uniquely homogeneous glycostructure. Proc Natl Acad Sci USA 91:5602–5606

Pertinhez TA, Bouchard M, Tomlinson EJ, Wain R, Ferguson SJ, Dobson CM, Smith LJ (2001) Amyloid fibril formation by a helical cytochrome. FEBS Lett 495:184–186

Pertinhez TA, Bouchard M, Smith RA, Dobson CM, Smith LJ (2002) Stimulation and inhibition of fibril formation by a peptide in the presence of different concentrations of SDS. FEBS Lett 529:193–197

Perutz MF, Johnson T, Suzuki M, Finch JT (1994) Glutamine repeats as polar zippers—their possible role in inherited neurodegenerative diseases. Proc Natl Acad Sci USA 91:5355–5358

Perutz MF, Finch JT, Berriman J, Lesk A (2002a) Amyloid fibers are water-filled nanotubes. Proc Natl Acad Sci USA 99:5591–5595

Perutz MF, Pope BJ, Owen D, Wanker EE, Scherzinger E (2002b) Aggregation of proteins with expanded glutamine and alanine repeats of the glutamine-rich and asparagine-rich domains of Sup35 and of the amyloid beta-peptide of amyloid plaques. Proc Natl Acad Sci USA 99:5596–5600

Petchanikow C, Saborio GP, Anderes L, Frossard MJ, Olmedo MI, Soto C (2001) Biochemical and structural studies of the prion protein polymorphism. FEBS Lett 509:451–456

Petkova AT, Ishii Y, Balbach JJ, Antzutkin ON, Leapman RD, Delaglio F, Tycko R (2002) A structural model for Alzheimer's beta-amyloid fibrils based on experimental constraints from solid state NMR. Proc Natl Acad Sci USA 99:16742–16747

Petkova AT, Buntkowsky G, Dyda F, Leapman RD, Yau WM, Tycko R (2004) Solid state NMR reveals a pH-dependent antiparallel beta-sheet registry in fibrils formed by a beta-amyloid peptide. J Mol Biol 335:247–260

Pettersson TM, Carlstrom A, Ehrenberg A, Jornvall H (1989) Transthyretin microheterogeneity and thyroxine binding are influenced by non-amino acid components and glutathione constituents. Biochem Biophys Res Commun 158:341–347

Pike CJ, Walencewicz-Wasserman AJ, Kosmoski J, Cribbs DH, Glabe CG, Cotman CW (1995) Structure-activity analyses of beta-amyloid peptides: contributions of the beta 25–35 region to aggregation and neurotoxicity. J Neurochem 64:253–265

Plakoutsi G, Taddei N, Stefani M, Chiti F (2004) Aggregation of the Acylphosphatase from Sulfolobus solfataricus: the folded and partially unfolded states can both be precursors for amyloid formation. J Biol Chem 279:14111–14119

Podesta A, Tiana G, Milani P, Manno M (2006) Early events in insulin fibrillization studied by time-lapse atomic force microscopy. Biophys J 90:589–597

Polverino de Laureto P, Taddei N, Frare E, Capanni C, Costantini S, Zurdo J, Chiti F, Dobson CM, Fontana A (2003) Protein aggregation and amyloid fibril formation by an SH3 domain probed by limited proteolysis. J Mol Biol 334:129–141

Porat Y, Stepensky A, Ding FX, Naider F, Gazit E (2003) Completely different amyloidogenic potential of nearly identical peptide fragments. Biopolymers 69:161–164

Prusiner SB, DeArmond SJ (1994) Prion diseases and neurodegeneration. Annu Rev Neurosci 17:311–339

Qian Y, Blaskovich MA, Saleem M, Seong CM, Wathen SP, Hamilton AD, Sebti SM (1994) Design and structural requirements of potent peptidomimetic inhibitors of p21ras farnesyltransferase. J Biol Chem 269:12410–12413

Ramirez-Alvarado M, Merkel JS, Regan L (2000) A systematic exploration of the influence of the protein stability on amyloid fibril formation in vitro. Proc Natl Acad Sci USA 97:8979–8984

Rankin J, Wyttenbach A, Rubinsztein DC (2000) Intracellular green fluorescent protein-polyalanine aggregates are associated with cell death. Biochem J 348:15–19

Raposo G, Marks MS (2002) The dark side of lysosome-related organelles: specialization of the endocytic pathway for melanosome biogenesis. Traffic 3:237–248

Rasia RM, Bertoncini CW, Marsh D, Hoyer W, Cherny D, Zweckstetter M, Griesinger C, Jovin TM, Fernandez CO (2005) Structural characterization of copper(II) binding to alpha-synuclein: insights into the bioinorganic chemistry of Parkinson's disease. Proc Natl Acad Sci USA 102:4294–4299

Rauk A, Armstrong DA, Fairlie DP (2000) Is oxidative damage by beta-amyloid and prion peptides mediated by hydrogen atom transfer from glycine alpha-carbon to methionine sulfur within beta-sheets? J Am Chem Soc 122:9761–9767

Raumann BE, Rould MA, Pabo CO, Sauer RT (1994) DNA recognition by beta-sheets in the Arc repressor-operator crystal structure. Nature 367:754–757

Reches M, Gazit E (2003) Casting metal nanowires within discrete self-assembled peptide nanotubes. Science 300:625–627

Reches M, Porat Y, Gazit E (2002) Amyloid fibril formation by pentapeptide and tetrapeptide fragments of human calcitonin. J Biol Chem 277:35475–35480

Relini A, Torrassa S, Rolandi R, Gliozzi A, Rosano C, Canale C, Bolognesi M, Plakoutsi G, Bucciantini M, Chiti F, Stefani M (2004) Monitoring the process of HypF fibrillization and liposome permeabilization by protofibrils. J Mol Biol 338:943–957

Richardson JS, Richardson DC (2002) Natural β-sheet proteins use negative design to avoid edge-to-edge aggregation. Proc Natl Acad Sci USA 99:2754–2759

Rocken C, Becker K, Fandrich M, Schroeckh V, Stix B, Rath T, Kahne T, Dierkes J, Roessner A, Albert FW (2006) ALys amyloidosis caused by compound heterozygosity in exon 2 (Thr70Asn) and exon 4 (Trp112Arg) of the lysozyme gene. Hum Mutat 27:119–120

Rosen DR, Siddique T, Patterson D, Figlewicz DA, Sapp P, Hentati A, Donaldson D, Goto J, O'Regan JP, Deng HX, et al (1993) Mutations in Cu/Zn superoxide dismutase gene are associated with familial amyotrophic lateral sclerosis. Nature 362:59–62

Ross CA (2002) Polyglutamine pathogenesis: emergence of unifying mechanisms for Huntington's disease and related disorders. Neuron 35:819–822

Rowland LP, Shneider NA (2001) Amyotrophic lateral sclerosis. N Engl J Med 344:1688–1700

Sadqi M, Hernandez F, Pan U, Perez M, Schaeberle MD, Avila J, Munoz V (2002) Alpha-helix structure in Alzheimer's disease aggregates of tau-protein. Biochemistry 41:7150–7155

Sanchez de Groot N, Pallares I, Aviles FX, Vendrell J, Ventura S (2005) Prediction of "hot spots" of aggregation in disease-linked polypeptides. BMC Struct Biol 5:18

Sasaki T, Kaiser ET (1989) Helichrome: synthesis and enzymic activity of a designed hemeprotein. J Am Chem Soc 111:380–381

Schaffar G, Breuer P, Boteva R, Behrends C, Tzvetkov N, Strippel N, Sakahira H, Siegers K, Hayer-Hartl M, Hartl FU (2004) Cellular toxicity of polyglutamine expansion proteins; mechanism of transcription factor deactivation. Mol Cell 15:95–105

Scheibel T, Bloom J, Lindquist SL (2004) The elongation of yeast prion fibers involves separable steps of association and conversion. Proc Natl Acad Sci USA 101:2287–2292

Schmidt AM, Yan SD, Yan SF, Stern DM (2000) The biology of the receptor for advanced glycation end products and its ligands. Biochim Biophys Acta 1498:99–111

Schmitt-Bernard CF, Chavanieu A, Derancourt J, Arnaud B, Demaille JG, Calas B, Argiles A (2000) In vitro creation of amyloid fibrils from native and Arg124Cys mutated betaIGH3 (110–131) peptides, and its relevance for lattice corneal amyloid dystrophy type I. Biochem Biophys Res Commun 273:649–653

Schmittschmitt JP, Scholtz JM (2003) The role of protein stability, solubility, and net charge in amyloid fibril formation. Protein Sci 12:2374–2378

Scholtz JM, Baldwin RL (1992) The mechanism of alpha-helix formation by peptides. Annu Rev Biophys Biomol Struct 21:95–118

Schwartz R, Istrail S, King J (2001) Frequencies of amino acid strings in globular protein sequences indicate suppression of blocks of consecutive hydrophobic residues. Protein Sci 10:1023–1031

Schwarz-Linek U, Werner JM, Pickford AR, Gurusiddappa S, Kim JH, Pilka ES, Briggs JA, Gough TS, Hook M, Campbell ID, Potts JR (2003) Pathogenic bacteria attach to human fibronectin through a tandem beta-zipper. Nature 423:177–181

Selkoe DJ (2003) Folding proteins in fatal ways. Nature 426:900–904
Serpell LC (2000) Alzheimer's amyloid fibrils: structure and assembly. Biochim Biophys Acta 1502:16–30
Serpell LC, Fraser PE, Sunde M (1999) X-ray fiber diffraction of amyloid fibrils. Methods Enzymol 309:526–536
Serpell LC, Berriman J, Jakes R, Goedert M, Crowther RA (2000) Fiber diffraction of synthetic alpha-synuclein filaments shows amyloid-like cross-beta conformation. Proc Natl Acad Sci USA 97:4897–4902
Seymour JF, Presneill JJ (2002) Pulmonary alveolar proteinosis: progress in the first 44 years. Am J Respir Crit Care Med 166:215–235
Shehi E, Fusi P, Secundo F, Pozzuolo S, Bairati A, Tortora P (2003) Temperature-dependent, irreversible formation of amyloid fibrils by a soluble human ataxin-3 carrying a moderately expanded polyglutamine stretch (Q36). Biochemistry 42:14626–14632
Shibata A, Yamamoto M, Yamashita T, Chiou JS, Kamaya H, Ueda I (1992) Biphasic effects of alcohols on the phase transition of poly (L-Lysine) between alpha-helix and beta-sheet conformations. Biochemistry 31:5728–733
Shimizu A, Yamada Y, Mizuta T, Haseba T, Sugaia S (2004) The contribution of the dynamic behavior of a water molecule to the amyloid formation of yeast alcohol dehydrogenase. J Mol Liquids 109:45–52
Shortle D, Stites WE, Meeker AK (1990) Contributions of the large hydrophobic amino acids to the stability of staphylococcal nuclease. Biochemistry 29:8033–8041
Shtilerman MD, Ding TT, Lansbury PT Jr (2002) Molecular crowding accelerates fibrillization of alpha-synuclein: could an increase in the cytoplasmic protein concentration induce Parkinson's disease? Biochemistry 41:3855–3860
Si K, Lindquist S, Kandel ER (2003) A neuronal isoform of the aplysia CPEB has prion-like properties. Cell 115:879–891
Siemer AB, Ritter C, Ernst M, Riek R, Meier BH (2005) High-resolution solid-state NMR spectroscopy of the prion protein HET-s in its amyloid conformation. Angew Chem Int Ed Engl 44:2441–2444
Sikorski P, Atkins ED, Serpell LC (2003) Structure and texture of fibrous crystals formed by Alzheimer's Abeta(11–25) peptide fragment. Structure (Camb) 11:915–926
Singh R, Barden A, Mori T, Beilin L (2001) Advanced glycation end-products: a review. Diabetologia 44:129–146
Sinha N, Tsai CJ, Nussinov R (2001) A proposed structural model for amyloid fibril elongation: domain swapping forms an interdigitating beta-structure polymer. Protein Eng 14:93–103
Sirangelo I, Malmo C, Iannuzzi C, Mezzogiorno A, Bianco MR, Papa M, Irace G (2004) Fibrillogenesis and cytotoxic activity of the amyloid-forming apomyoglobin mutant W7FW14F. J Biol Chem 279:13183–13189
Solomon A, Frangione B, Franklin EC (1982) Bence Jones proteins and light chain of immunoglobulins. Preferential association of the gamma VI subgroup of human light chains with amyloidosis AL. J Clin Invest 70:453–460
Solomon A, Murphy CL, Weaver K, Weiss DT, Hrncic R, Eulitz M, Donnell RL, Sletten K, Westermark G, Westermark P (2003) Calcifying epithelial odontogenic (Pindborg) tumor-associated amyloid consists of a novel human protein. J Lab Clin Med 142:348–355
Somers WS, Phillips SE (1992) Crystal structure of the met repressor-operator complex at 2.8 Å resolution reveals DNA recognition by beta-strands. Nature 359:387–393
Soreghan B, Kosmoski J, Glabe C (1994) Surfactant properties of Alzheimer's A beta peptides and the mechanism of amyloid aggregation. J Biol Chem 269:28551–28554
Soto C, Castano EM, Kumar RA, Beavis RC, Frangione B (1995) Fibrillogenesis of synthetic amyloid-beta peptides is dependent on their initial secondary structure. Neurosci Lett 200:105–108
Souillac PO, Uversky VN, Fink AL (2003) Structural transformations of oligomeric intermediates in the fibrillation of the immunoglobulin light chain LEN. Biochemistry 42:8094–8104
Srisailam S, Wang HM, Kumar TK, Rajalingam D, Sivaraja V, Sheu HS, Chang YC, Yu C (2002) Amyloid-like fibril formation in an all beta-barrel protein involves the formation of partially structured intermediate(s). J Biol Chem 277:19027–19036
Srisailam S, Kumar TK, Rajalingam D, Kathir KM, Sheu HS, Jan FJ, Chao PC, Yu C (2003) Amyloid-like fibril formation in an all beta-barrel protein. Partially structured intermediate state(s) is a precursor for fibril formation. J Biol Chem 278:17701–17709
Stefani M, Dobson CM (2003) Protein aggregation and aggregate toxicity: new insights into protein folding, misfolding diseases and biological evolution. J Mol Med 81:678–699
Storkel S, Schneider HM, Muntefering H, Kashiwagi S (1983) Iatrogenic, insulin-dependent, local amyloidosis. Lab Invest 48:108–111

Suk JY, Zhang F, Balch WE, Linhardt RJ, Kelly JW (2006) Heparin accelerates gelsolin amyloidogenesis. Biochemistry 45:2234–2242
Tahmassebi DC, Sasaki T (1998) Synthesis of a three-helix bundle protein by reductive amination. J Org Chem 63:728–731
Takahashi Y, Ueno A, Mihara H (2002) Amyloid architecture: complementary assembly of heterogeneous combinations of three or four peptides into amyloid fibrils. Chembiochem 3:637–642
Tcherkasskaya O, Sanders W, Chynwat V, Davidson EA, Orser CS (2003) The role of hydrophobic interactions in amyloidogenesis: example of prion-related polypeptides. J Biomol Struct Dyn 21:353–365
Tenidis K, Waldner M, Bernhagen J, Fischle W, Bergmann M, Weber M, Merkle ML, Voelter W, Brunner H, Kapurniotu A (2000) Identification of a penta- and hexapeptide of islet amyloid polypeptide (IAPP) with amyloidogenic and cytotoxic properties. J Mol Biol 295:1055–1071
Terazaki H, Ando Y, Suhr O, Ohlsson PI, Obayashi K, Yamashita T, Yoshimatsu S, Suga M, Uchino M, Ando M (1998) Post-translational modification of transthyretin in plasma. Biochem Biophys Res Commun 249:26–30
Tian X, Fujiki K, Wang W, Murakami A, Xie P, Kanai A, Liu Z (2005) Novel mutation (V505D) of the TGFBI gene found in a Chinese family with lattice corneal dystrophy, type I. Jpn J Ophthalmol 49:84–88
Tjernberg L, Hosia W, Bark N, Thyberg J, Johansson J (2002) Charge attraction and beta propensity are necessary for amyloid fibril formation from tetrapeptides. J Biol Chem 277:43243–43246
Tjernberg LO, Naslund J, Lindqvist F, Johansson J, Karlstrom AR, Thyberg J, Terenius L, Nordstedt C (1996) Arrest of beta-amyloid fibril formation by a pentapeptide ligand. J Biol Chem 271:8545–8548
Tjernberg LO, Callaway DJ, Tjernberg A, Hahne S, Lilliehook C, Terenius L, Thyberg J, Nordstedt C (1999) A molecular model of Alzheimer amyloid beta-peptide fibril formation. J Biol Chem 274:12619–12625
Tomiyama T, Asano S, Furiya Y, Shirasawa T, Endo N, Mori H (1994) Racemization of Asp23 residue affects the aggregation properties of Alzheimer amyloid beta protein analogues. J Biol Chem 269:10205–10208
Toniolo C, Benedetti E (1991) The polypeptide 310-helix. Trends Biochem Sci 16:350–353
Toniolo C, Crisma M, Formaggio F, Valle G, Cavicchioni G, Precigoux G, Aubry A, Kamphuis J (1993) Structures of peptides from alpha-amino acids methylated at the alpha-carbon. Biopolymers 33:1061–1072
Tracz SM, Abedini A, Driscoll M, Raleigh DP (2004) Role of aromatic interactions in amyloid formation by peptides derived from human Amylin. Biochemistry 43:15901–15908
Trapnell BC, Whitsett JA, Nakata K (2003) Pulmonary alveolar proteinosis. N Engl J Med 349:2527–2539
Tsuji S (1999) Dentatorubral-pallidoluysian atrophy (DRPLA): clinical features and molecular genetics. Adv Neurol 79:399–409
Tsuji S (2004) Spinocerebellar ataxia type 17: latest member of polyglutamine disease group highlights unanswered questions. Arch Neurol 61:183–184
Tyndall JD, Fairlie DP (1999) Conformational homogeneity in molecular recognition by proteolytic enzymes. J Mol Recognit 12:363–370
Tyndall JD, Nall T, Fairlie DP (2005) Proteases universally recognize beta strands in their active sites. Chem Rev 105:973–999
Uegaki K, Nakamura T, Yamamoto H, Kobayashi A, Odahara T, Harata K, Hagihara Y, Ueyama N, Yamazaki T, Yumoto N (2005) Amyloid fibril formation by the CAD domain of caspase-activated DNase. Biopolymers 79:39–47
Uemichi T, Liepnieks JJ, Benson MD (1994) Hereditary renal amyloidosis with a novel variant fibrinogen. J Clin Invest 93:731–736
Uemichi T, Liepnieks JJ, Yamada T, Gertz MA, Bang N, Benson MD (1996) A frame shift mutation in the fibrinogen A alpha chain gene in a kindred with renal amyloidosis. Blood 87:4197–4203
Uptain SM, Lindquist S (2002) Prions as protein-based genetic elements. Annu Rev Microbiol 56:703–741
Uversky VN, Cooper EM, Bower KS, Li J, Fink AL (2002) Accelerated alpha-synuclein fibrillation in crowded milieu. FEBS Lett 515:99–103
Villanueva J, Villegas V, Querol E, Aviles FX, Serrano L (2003) Monitoring disappearance of monomers and generation of resistance to proteolysis during the formation of the activation domain of human procarboxypeptidase A2 (ADA2 h) amyloid fibrils by matrix-assisted laser-desorption ionization-time-of-flight-MS. Biochem J 374:489–495
Villegas V, Zurdo J, Filimonov VV, Aviles FX, Dobson CM, Serrano L (2000) Protein engineering as a strategy to avoid formation of amyloid fibrils. Protein Sci 9:1700–1708
Volles MJ, Lansbury PT Jr (2003) Zeroing in on the pathogenic form of alpha-synuclein and its mechanism of neurotoxicity in Parkinson's disease. Biochemistry 42:7871–7878
Walling HW, Baldassare JJ, Westfall TC (1998) Molecular aspects of Huntington's disease. J Neurosci Res 54:301–308

Walsh DM, Hartley DM, Kusumoto Y, Fezoui Y, Condron MM, Lomakin A, Benedek GB, Selkoe DJ, Teplow DB (1999) Amyloid beta-protein fibrillogenesis. Structure and biological activity of protofibrillar intermediates. J Biol Chem 274:25945–25952

Walsh DM, Klyubin I, Fadeeva JV, Rowan MJ, Selkoe DJ (2002) Amyloid-beta oligomers: their production, toxicity and therapeutic inhibition. Biochem Soc Trans 30:552–557

Wang J, Gulich S, Bradford C, Ramirez-Alvarado M, Regan L (2005) A twisted four-sheeted model for an amyloid fibril. Structure 13:1279–1288

Wang L, Colon W (2005) Urea-induced denaturation of apolipoprotein serum amyloid A reveals marginal stability of hexamer. Protein Sci 14:1811–1817

Wang W, Hecht MH (2002) Rationally designed mutations convert de novo amyloid-like fibrils into monomeric beta-sheet proteins. Proc Natl Acad Sci USA 99:2760–2765

Watson AA, Fairlie DP, Craik DJ (1998) Solution structure of methionine-oxidized amyloid beta.-peptide (1–40). Does oxidation affect conformational switching? Biochemistry 37:12700–12706

Waugh DF (1957) A mechanism for the formation of fibrils from protein molecules. J Cell Physiol 49:145–164

West MW, Wang W, Patterson J, Mancias JD, Beasley JR, Hecht MH (1999) De novo amyloid proteins from designed combinatorial libraries. Proc Natl Acad Sci USA 96:11211–11216

Westermark GT, Engstrom U, Westermark P (1992) The N-terminal segment of protein AA determines its fibrillogenic property. Biochem Biophys Res Commun 182:27–33

Westermark P (2005) Aspects on human amyloid forms and their fibril polypeptides. FEBS J 272:5942–5949

Westermark P, Eriksson L, Engstrom U, Enestrom S, Sletten K (1997) Prolactin-derived amyloid in the aging pituitary gland. Am J Pathol 150:67–73

Westermark P, Benson MD, Buxbaum JN, Cohen AS, Frangione B, Ikeda SI, Masters CL, Merlini G, Saraiva MJ, Sipe JD (2005) Amyloid: toward terminology clarification—report from the Nomenclature Committee of the International Society of Amyloidosis. Amyloid 12:1–4

Wetzel R (2002) Ideas of order for amyloid fibril structure. Structure (Camb) 10:1031–1036

Wigley WC, Corboy MJ, Cutler TD, Thibodeau PH, Oldan J, Lee MG, Rizo J, Hunt JF, Thomas PJ (2002) A protein sequence that can encode native structure by disfavoring alternate conformations. Nat Struct Biol 9:381–388

Wilkins DK, Dobson CM, Gross M (2000) Biophysical studies of the development of amyloid fibrils from a peptide fragment of cold shock protein B. Eur J Biochem 267:2609–2616

Williams AD, Shivaprasad S, Wetzel R (2006) Alanine scanning mutagenesis of Abeta(1–40) amyloid fibril stability. J Mol Biol 357:1283–1294

Wong AK, Jacobsen MP, Winzor DJ, Fairlie DP (1998) Template assembled synthetic proteins (TASPs). Are template size, shape, and directionality important in formation of four-helix bundles? J Am Chem Soc 120:3836–3841

Wright CF, Teichmann SA, Clarke J, Dobson CM (2005) The importance of sequence diversity in the aggregation and evolution of proteins. Nature 438:878–881

Xiong H, Buckwalter B, Shieh H, Hecht M (1995) Periodicity of polar and nonpolar amino acids is the major determinant of secondary structure in self-assembling oligomeric peptides. Proc Natl Acad Sci USA 92:6349–6353

Xu S, Bevis B, Arnsdorf MF (2001) The assembly of amyloidogenic yeast Sup35 as assessed by scanning (atomic) force microscopy: an analogy to linear colloidal aggregation? Biophys J 81:446–454

Yamaguchi I, Suda H, Tsuzuike N, Seto K, Seki M, Yamaguchi Y, Hasegawa K, Takahashi N, Yamamoto S, Gejyo F, Naiki H (2003) Glycosaminoglycan and proteoglycan inhibit the depolymerization of beta 2-microglobulin amyloid fibrils in vitro. Kidney Int 64:1080–1088

Yang SC, Levine H, Onuchic JN (2005) Protein oligomerization through domain swapping: role of intermolecular interactions and protein concentration. J Mol Biol 352:202–211

Yazaki M, Varga J, Dyck PJ, Benson MD (2002) A new transthyretin variant Leu55Gln in a patient with systemic amyloidosis. Amyloid 9:268–271

Yin HL (1987) Gelsolin: calcium- and polyphosphoinositide-regulated actin-modulating protein. Bioessays 7:176–179

Yoburn JC, Tian W, Brower JO, Nowick JS, Glabe CG, Van Vranken DL (2003) Dityrosine cross-linked Abeta peptides: fibrillar beta-structure in Abeta(1–40) is conducive to formation of dityrosine cross-links but a dityrosine cross-link in Abeta(8–14) does not induce beta-structure. Chem Res Toxicol 16:531–535

Yoder G, Polese A, Silva R, Formaggio F, Crisma M, Broxterman QB, Kamphuis J, Toniolo C, Keiderling TA (1997) Conformational characterization of terminally blocked L-(alpha Me)Val homopeptides using vibrational and electronic circular dichroism. 3(10)-helical stabilization by peptide-peptide interaction. J Am Chem Soc 119:10278–10285

Yong W, Lomakin A, Kirkitadze MD, Teplow DB, Chen SH, Benedek GB (2002) Structure determination of micelle-like intermediates in amyloid beta -protein fibril assembly by using small angle neutron scattering. Proc Natl Acad Sci USA 99:150–154

Yutani K, Takayama G, Goda S, Yamagata Y, Maki S, Namba K, Tsunasawa S, Ogasahara K (2000) The process of amyloid-like fibril formation by methionine aminopeptidase from a hyperthermophile, *Pyrococcus furiosus*. Biochemistry 39:2769–2777

Zerovnik E (2002) Amyloid-fibril formation. Proposed mechanisms and relevance to conformational disease. Eur J Biochem 269:3362–3371

Zerovnik E, Pompe-Novak M, Skarabot M, Ravnikar M, Musevic I, Turk V (2002) Human stefin B readily forms amyloid fibrils in vitro. Biochim Biophys Acta 1594:1–5

Zhang KZ, Kaufman RJ (2006) The unfolded protein response—a stress signaling pathway critical for health and disease. Neurology 66:S102–S109

Zhang Q, Kelly JW (2003) Cys10 mixed disulfides make transthyretin more amyloidogenic under mildly acidic conditions. Biochemistry 42:8756–8761

Zhao H, Jutila A, Nurminen T, Wickstrom SA, Keski-Oja J, Kinnunen PK (2005) Binding of endostatin to phosphatidylserine-containing membranes and formation of amyloid-like fibers. Biochemistry 44:2857–2863

Zhu M, Souillac PO, Ionescu-Zanetti C, Carter SA, Fink AL (2002) Surface-catalyzed amyloid fibril formation. J Biol Chem 277:50914–50922

Rev Physiol Biochem Pharmacol (2007) 159:79 –113
DOI 10.1007/112_2006_0702

M. Kampa · A.-P. Nifli · G. Notas · E. Castanas

Polyphenols and cancer cell growth

Published online: 6 June 2007

Abstract Polyphenols constitute an important group of phytochemicals that gained increased research attention since it was found that they could affect cancer cell growth. Initial evidence came from epidemiologic studies suggesting that a diet that includes regular consumption of fruits and vegetables (rich in polyphenols) significantly reduces the risk of many cancers. In the present work we briefly review the effects of polyphenols on cancer cell fate, leading towards growth, differentiation and apoptosis. Their action can be attributed not only to their ability to act as antioxidants but also to their ability to interact with basic cellular mechanisms. Such interactions include interference with membrane and intracellular receptors, modulation of signaling cascades, interaction with the basic enzymes involved in tumor promotion and metastasis, interaction with oncogenes and oncoproteins, and, finally, direct or indirect interactions with nucleic acids and nucleoproteins. These actions involve almost the whole spectrum of basic cellular machinery—from the cell membrane to signaling cytoplasmic molecules and to the major nuclear components—and provide insights into their beneficial health effects. In addition, the actions justify the scientific interest in this class of compounds, and provide clues about their possible pharmaceutical exploitation in the field of oncology.

Introduction

Cancer is a multistep disease, integrating a number of factors (environmental, chemical, physical, metabolic, and genetic), playing a direct and/or indirect role in the instauration and expression of the malignant phenotype, as well as in its evolution over time and space.

M. Kampa · A.-P. Nifli · E. Castanas (✉)
University of Crete, School of Medicine, Laboratory of Experimental Endocrinology,
P.O. Box 2208, 71003 Heraklion, Greece
e-mail: castanas@med.uoc.gr · Tel.: +30 2810 394580 · Fax: +30 2810 394581

G. Notas
University of Crete, School of Medicine, Laboratory of Gastroenterology,
71003 Heraklion, Greece

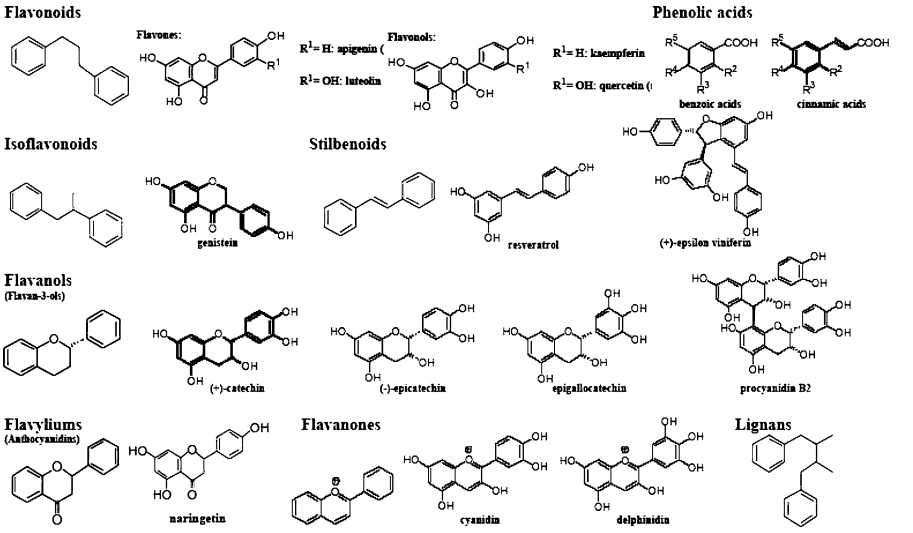

Fig. 1 Chemical structure of major classes of phenolic compounds

Strong and consistent epidemiologic evidence suggests a diet that includes regular consumption of fruits and vegetables significantly reduces the risk of many cancers. Different microchemicals present in the diet could be effective agents for the prevention of cancer incidence and mortality (Boone et al. 1990). Measuring the effects of such agents has now become a major area of experimental cancer research. One group of promising phytochemicals comprises the so-called phenol-containing dietary substances or polyphenols, which includes the flavonoids (e.g., catechins, quercetin, kaempferol, apigenin, baicalein, and naringin), isoflavonoids (genistein and daidzein), lignans (sesaminol and sesamin), trihydroxystilbenes (resveratrol and polydatin), curcumin, and phenolic acids (*p*-coumaric, caffeic, gentisic, ferulic, and vanillic acids). Polymeric aggregation of polyphenols such as resveratrol and catechin could lead to viniferins and procyanidins respectively (Fig. 1). Some of the polyphenols are also referred to as phytoestrogens since their structure is similar to the human estrogen 17β-estradiol and they have the ability to exert weak estrogen hormone activity. This review presents, in brief, the effects of polyphenols on different cancer cell systems and their proposed mode of action. It is mainly concentrated on the data available during the last decade. The generic term "polyphenols" is widely used for the sake of brevity, while the name of the specific phenolic compound tested is stated when appropriate.

Epidemiologic studies

The first hint about the role of polyphenols in cancer was obtained through analysis of epidemiologic data. Several studies showed that tea, soy, olive oil, and whole grains consumption significantly reduces the risk of certain types of cancer. A study by Sun et al. conducted in eight countries showed that tea consumption reduces the risk of breast cancer (Sun et al. 2005). In addition, a prospective study by Severson and coworkers (1989) demonstrated a positive relationship between soy consumption (as tofu) and a decreased risk of prostate cancer. A much broader epidemiologic study on men in 59 countries demonstrated that a diet

rich in soy products was protective against prostate cancer mortality. On the other hand, it should be mentioned that there are several studies reporting no considerable association, such as the Netherlands Cohort Study on Diet and Cancer, which reported no significant association between black tea consumption and cancer (Goldbohm et al. 1996). Nevertheless, the positive role of polyphenol-rich foods in reducing cancer risk or mortality (or both) cannot be doubted.

Animal models

Apart from epidemiologic data, a great body of evidence concerning the relationship between tumor development and multiple components in fruits, vegetables, herbs, and spices comes from experimental animal models. Green and black teas have shown cancer chemopreventive activity against ultraviolet light irradiation, as well as in chemically induced and genetic models of cancer, such as cancer of the skin, lung, prostate, bladder, liver, colon, oral cavity, esophagus, stomach, small intestine, and pancreas (Lambert and Yang 2003). For example, oral consumption of 0.1% green tea polyphenols decreased tumor incidence by 65% in a transgenic mouse prostate adenocarcinoma model (TRAMP model) (Gupta et al. 2001). Green tea (0.6%) as a drinking fluid reduced the number of tumors and tumor volume in the dimethylbenz[a]anthracene (DMBA)-induced hamster model of oral carcinogenesis (Li et al. 2002). In addition, green tea decreased mammary tumor volume, decreased the production of foci of aberrant crypts in the colon (Weisburger et al. 1997), and inhibited the spontaneous formation of lung rhabdomyosarcomas in AJ mice (Landau et al. 1998). A soy-rich diet has been associated with a growth delay of LNCaP cell graft in severe combined immunodeficiency (SCID) mice (Bylund et al. 2000). A tomato-enriched diet resulted in decreased prostate tumor growth, as observed in the *N*-methyl-*N*-nitrosourea androgen-induced tumor and the Dunning R-3327H prostate cancer models (Boileau et al. 2003).

Polyphenol effects in cancer

Polyphenols exhibit a wide range of biologic activities, including inhibition of lipid peroxidation, platelet aggregation, capillary permeability, and the activity of enzyme systems including lipoxygenase. They exert anticarcinogenic, antimutagenic, anti-inflammatory, and antiviral actions. In the following sections, we review in brief the cellular actions of these compounds and their antioxidant effects.

In vitro studies in cancer cell lines yield a valuable initial estimate of the effect of different agents on cell growth, proliferation, and apoptosis. In this model, extracts from different nutrients and beverages (e.g., tea, wine, and olive oil) have been studied in a number of malignant cell lines, representing different evolutionary stages of the disease. Our group has shown that wine extracts and isolated polyphenols (resveratrol, quercetin, catechin, and epicatechin) (Damianaki et al. 2000; Kampa et al. 2000), as well as phenolic acids found specifically in virgin olive oil (caffeic, sinapic, syringic, protocatechuic, ferulic and 3,4-dihydroxy-phenylacetic) (Kampa et al. 2004), decrease the proliferation of breast (T47D, MCF7, MDA-MB-231) and prostate (DU-145, PC3, LNCaP) cancer cells in a time- and dose-specific manner. Similar results with wine and tea extracts have been reported in several cell systems, although usually the effective concentrations depend on the system and the substance studied. More specifically, major green tea polyphenols (epicatechin, epigallocat-

echin, epicatechin-3-gallate, and epigallocatechin-3-gallate) were found to suppress growth of pancreatic cancer cells (Mia Pa Ca-2), lung tumor cells (H661 and H1299) colorectal carcinoma cells (HCT-116), head and neck carcinoma cells (H891), and endothelial and vascular smooth muscle cells (see Nichenametla et al. 2006 for a review). In addition, Chung et al. reported an inhibitory effect of green tea polyphenols and black tea theaflavins on Ras-transformed cells 30.7b Ras 12, suggesting that the presence of the galloyl structure on the B ring and the gallate moiety is important for the polyphenol and theaflavin action (Chung et al. 1999).

Stilbene resveratrol and the flavonol quercetin are two polyphenols that also exhibit a strong inhibitory effect on cancer cell proliferation. Hence, their effects have also been studied in a large number of cancer types such as breast, prostate, hepatoma, colon (Ramos et al. 2005), skin (Yanez et al. 2004), and leukemia (Gao et al. 2002). Furthermore, genistein (mainly found in soybeans) and procyanidins (flavonoid oligomers) have received attention because of their antiproliferative effect on different cancer cell lines (Gosse et al. 2005; Polkowski and Mazurek 2000). Finally, growth-inhibitory effects in different cancers [colon (Kuntz et al. 1999), prostate (Knowles et al. 2000), liver (Zhang et al. 2000), stomach, cervix, pancreas, breast (Kanno et al. 2005), and leukemias (Miyahara et al. 2000)] have also been exerted by a number of polyphenols that are not so extensively studied. These include several flavones such as apigenin, baicalein, luteolin and rutin, flavonols such as kaempferol, flavonones such as hesperidin and naringin, and sesame lignans such as sesaminol, sesamin, and episesamin.

Although cancer cell lines are a valuable tool for the study of new antitumor agents, in vivo experiments must also be performed in order to verify their efficacy. Polyphenols were found to inhibit in vivo breast, prostate, skin, nasopharyngeal, colon or gastric tumor xenografts in athymic and severe immunodeficient mice, the DMBA-induced breast or colon carcinogenesis, and the development and progression of prostate cancer in the TRAMP model.

The inhibitory effect of polyphenols in tumorigenesis and tumor growth can be explained by two main actions that are discussed below:

1. Modification of the redox status
2. Interference with basic cellular functions (apoptosis, cell cycle, angiogenesis, invasion and metastasis)

Modification of the redox status

When the cellular concentration of oxidant species is highly increased, the endogenous antioxidant defenses may be overcomed. In such cases, a series of events are triggered, leading to lipid, protein, and DNA damage. Reactive oxygen species, in particular hydrogen peroxide, are fine regulators of cell replication and exert important signal-transduction activities. Hence, oxidative damage is considered a main factor interfering in carcinogenesis and evolution of cancer. Polyphenols (due to their ability to act as chelators of divalent cations, to scavenge and reduce the production of free radicals) can exert a major chemopreventive activity (Middleton 1996). Indeed, it has been shown that tea polyphenols inhibit carcinogen-induced DNA damage and oxidative stress (Higdon and Frei 2003). In addition, they are able to prevent or reduce the harmful effects of UV light on skin. Some of them (e.g., ferulic acid) are strong UV absorbers (Saija et al. 2000), while others inhibit protooncogene expression. In UVB-treated normal human keratinocytes (NHEK), epigal-

locatechin gallate (EGCG) inhibited the production of H_2O_2 by 66–80%. H_2O_2 inhibition was also observed in SKH-1 hairless mice skin by resveratrol (Afaq et al. 2002) and tannins (Gali-Muhtasib et al. 2000). Similarly, quercetin diminished ROS generation in a human hepatocellular carcinoma-derived cell line (HepG2) (Alia et al. 2005). Resveratrol reduced oxidative damage induced by H_2O_2 in calf thymus DNA (Burkhardt et al. 2001) and also in several cancer cell lines such as breast cancer (Damianaki et al. 2000).

In addition to their antioxidant activity, polyphenols may exert their inhibitory effect by acting as pro-oxidants on cancer cells, at least in vitro. Indeed, several plant polyphenols such as tannins and *trans*-stilbenes possess oxidative DNA-cleavage properties (Ahmad et al. 2000; Khan and Hadi 1998; Rahman et al. 1989). Yang et al. have shown that the apoptosis of H661 lung cancer cells and Ras-transformed human bronchial cells induced by EGCG was blocked by inclusion of catalase in the medium (Yang et al. 2000). Moreover, Hong et al. reported that EGCG induced the production of H_2O_2 by HT-29 cells (Hong et al. 2002). However, it has been proposed that this oxidative property depends on the amount of dissolved oxygen in the test medium (Agullo et al. 1996), and it is questionable whether a similar mechanism can also occur in vivo. Recently, a mechanism was advanced, based on the redox potential of a number of polyphenols. A cascade of redox reactions occurs in the cell or in a given tissue, and a direct electron flux is transferred through polyphenols that can therefore act as anti- or pro-oxidants (Barbaste et al. 2002).

Interference with cancer cell functions

Cell cycle

Cellular proliferation is controlled by the cell cycle, which is governed by the cyclical activation of the cyclin-dependent kinase (cdk) complexes [cyclin-endogenous cdk inhibitors (CKIs)]. A dysregulated cell cycle due to overexpression of cyclins and cdks, and inactivation of the retinoblastoma (Rb) and the p53 tumor suppressor proteins, is a hallmark of cancer. Any agent downregulating cyclins or cdks will result in cell cycle arrest that can occur either at G_1/S or G_2/M phase, an irreversible process that will ultimately lead to cell apoptosis.

Polyphenols have been shown to induce cell cycle arrest in several different cancer lines including gastric, hepatoma, endometrial, nasopharyngeal, prostate, breast, pancreatic, and lymphoma. Arrest was observed in G_1/S phase, or in G_2/M phase when a mutated p53 gene was present and G_1 phase arrest could not occur. Polyphenols induce a cell cycle arrest by affecting a number of factors associated with cell cycle progression (Fig. 2), but it is still unclear whether they exert an indirect or direct effect. In HepG2 hepatocellular carcinoma (Ramos et al. 2005), and leukemic cells (Yoshida et al. 1992), quercetin induced a G_1 phase arrest that led to apoptosis. In contrast, breast cancer cells were arrested in the G_2/M phase (Choi et al. 2001) and colorectal tumor cells in the S phase (Richter et al. 1999) by the same agent. Several studies have shown a G_1-phase arrest of human breast and prostate cancer cells, induced by EGCG modulating the levels of cyclins D1 and E, cdks 2 and 4, Rbp phosphorylation (Liberto and Cobrinik 2000), as well as cdk inhibitors p21 and p27 (Gupta et al. 2003; Liang et al. 1999). It has also been shown that EGCG can directly inhibit cdks (Liang et al. 1999). Induced expression of p21 and p27 and decreased expression of cyclin D1 by EGCG was also observed in head and neck squamous carcinoma cells (Masuda et al. 2001). Downregulation of cyclin D1 and cdks 4 and 6, and a decreased phosphorylation of Rbp (leading to cell cycle arrest) were found in NBT-II bladder tumor cells treated with

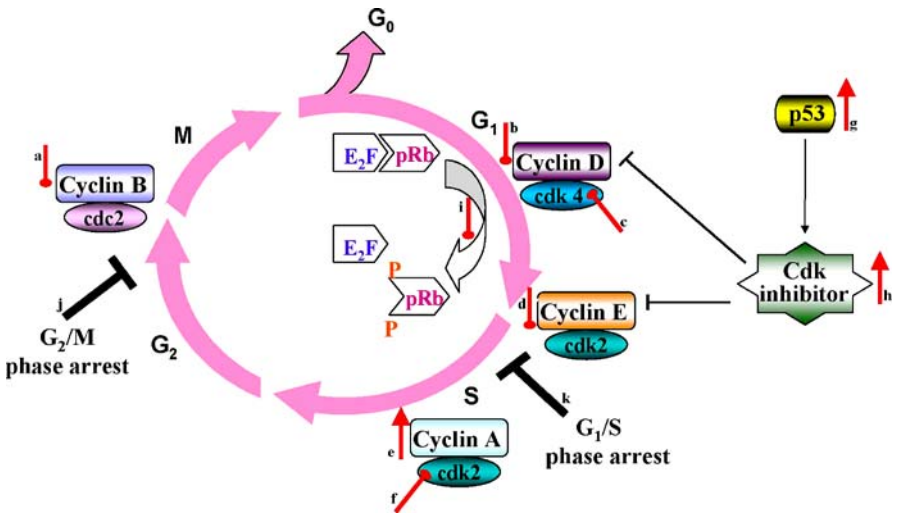

Fig. 2 Polyphenols and cell cycle: ↑ activation, ↓ inhibition. **a** Baicalein. **b** EGCG, resveratrol, baicalein. **c** Resveratrol, EGCG. **d** Resveratrol, EGCG. **e** Resveratrol, EGCG. **f** Resveratrol, EGCG. **g** EGCG. **h** EGCG. **i** EGCG. **j** Resveratrol, quercetin, kaempferol, apigenin, genistein, curcumin. **k** Quercetin, resveratrol, EGCG, baicalein

EGCG (Chen et al. 2004b). G_1-phase arrest was also demonstrated in A431 human epidermoid carcinoma cells after treatment with resveratrol, as well as in gastric adenocarcinoma cells (Atten et al. 2001). This occurred due to increased p21 and decreased expression of cyclins D1, D2, and E and cdks 2, 4, and 6 (Ahmad et al. 2001). Treatment of JCA-1 and LNCaP prostate cancer cells with baicalein also resulted in cell accumulation in G_1 phase (Chen et al. 2001). The same agent resulted in an inhibition of the S phase in HepG2 cells (Chen et al. 2000). On the other hand, treatment of the human lung squamous carcinoma cells CH27 with baicalein reduced the levels of cdk4 and cyclins B1 and D1 (Lee et al. 2005), and resulted in an S-phase arrest. Moreover, resveratrol has been found to arrest cells in S and G_2/M phase too, in different cell lines. S-phase arrest was observed in HL60 and MOLT-4 leukemic cells (Ragione et al. 1998), while G_2/M arrest was observed in HT-29 colon carcinoma (Liang et al. 2003) and lung cancer A549 cells (Lee et al. 2004a).

The ability of resveratrol to induce an S-phase arrest accounts for its protective effect on paclitaxel-induced apoptosis of SH-SY5Y neuroblastoma cells (Rigolio et al. 2005). In a related study, screening the effect of several polyphenols (resveratrol, EGCG, quercetin, baicalein, apigenin, genistein, and curcumin) on PC3 and LNCaP prostate cancer cells, resveratrol and EGCG induced an S-phase arrest, while the rest of them arrested cells at G_2/M phase (Shenouda et al. 2004). The same effect was exerted by genistein in malignant B cells (Mansour et al. 2004) as well as in AT6.3 prostate cancer cells. In contrast, Knowles et al. have reported that when PC3 cells were treated with quercetin or kaempferol, an S and a G_2/M phase arrest were observed respectively (Knowles et al. 2000).

Apoptosis

Malignant cells are characterized by excessive proliferation and reduced apoptosis. The latter is the specific form of cell death that is activated by the host immune system against cancer and by several chemotherapeutics. Apoptosis can be triggered by a number of different stimuli, including oxidative stress, DNA damage, ion fluctuations, and cytokines.

Any agent accounting for one of the above stimuli leads to apoptosis. Polyphenols have been found to affect cancer cell growth by inducing apoptosis in many cell lines (see Beltz et al. 2006 for a review) such as the pancreatic Mia Pa Ca-2; the hepatocellular carcinoma HepG2; the colon SW620, HT-29, and CaCo-2; the colorectal HCT-116; the prostate DU-145, LNCaP, and JCA1; the lungA549; the breast MCF7; the melanoma B16F10, SK-MEL-28 and SK-MEL-1; the CEM-C7H2 and Molt 4B leukemia cells; and the neuroblastoma cells (neuro-2a), both in vitro and in vivo. In many cases, apoptosis induced by polyphenols was caspase 3-dependent. This was demonstrated either by using caspase 3-deficient cells (Hsu et al. 2003) or by using a specific caspase inhibitor, like z-VAD (Qanungo et al. 2005). Quercetin, apigenin, kaempferol, and myricetin induced apoptosis in Jurkat T cells by activating caspase 3 and the cleavage of poly(ADP-ribose) polymerase (PARP), a mechanism also observed in HL-60 cells (Wang et al. 1999). This correlated with their ability to inhibit proteasome activity and accumulate Bax (Chen et al. 2005).

The induction of apoptosis by polyphenols can also be attributed to their ability to stimulate H_2O_2 generation by cancer cells. This was derived from the fact that polyphenol-induced apoptosis of the H661 lung cancer cells and the 21 BES H-ras-transformed bronchial epithelial cells was prevented by catalase (Yang et al. 1998b). Moreover, free radical-scavengers blocked the effect of polyphenols on apoptosis (Kong et al. 1998). On the other hand, apoptosis was induced by polyphenols (e.g., resveratrol) in different leukemia B-cell lines by inhibiting the NO system (Quiney et al. 2004) [NO exerts its antiapoptotic effect by partly inactivating caspases through *S*-nitrosylation of their active site (Li et al. 1997) and the Fas/FasL system (Su et al. 2005)]. The latter was also found to be an important mechanism of resveratrol-induced cell death in T47D breast carcinoma cells (Clement et al. 1998). Apoptosis can also result after cell cycle arrest, due to inhibition of nuclear factor (NF)-κB transcriptional activity and p53 activation (Brownson et al. 2002), as was found in EGCG-treated LNCaP cells. These two important transcription factors were stabilized and downregulated respectively, causing a change in the ratio of the pro-/antiapoptotic Bax/Bcl-2 ratio, in a manner favoring apoptosis (Hastak et al. 2003). A decrease in the mitochondrial Bcl-2 protein was observed in HepG2 (Chang et al. 2002) and in human squamous carcinoma CH27 cells (Lee et al. 2005) when treated with baicalein. An inhibited Bcl-2 and Bcl-X_L expression was also the result of treating A549 lung cancer cells with kaempferol. This, together with increased Bax levels, led to apoptosis, associated with the cleavage of caspase 7 and PARP, while inactivation of Akt and activation of MEK-MAPK (Nguyen et al. 2003) was also involved.

Finally, in contrast to the apoptotic effect exerted by polyphenols, an antiapoptotic effect, mainly attributed to their ability to scavenge free radicals, has also been observed. For example, resveratrol prevented apoptosis in human erythroleukemia K562 cells (MacCarrone et al. 1999) by inhibiting lipoxygenase and cyclooxygenase activity, either directly or indirectly. In addition, tea catechins exerted a neuroprotective effect by inhibiting the 6-hydroxydopamine-induced apoptosis in PC12 cells (Nie et al. 2002).

Invasion and metastasis

The ability of cancer cells to detach from the primary tumor mass, migrate through surrounding tissues toward blood vessels or lymphatic vessels, and create secondary lesions, involves the loss of homotypic cell–cell adhesion and cytoskeletal remodeling. Several secreted proteins and adhesion molecules and their downstream (lipid and tyrosine) kinases play an important role.

Besides having an inhibitory effect on cancer cell growth and proliferation, polyphenols were found to suppress malignant cell migration, invasion, and metastasis. These phenomena require continuous assembly and disassembly of cell-extracellular matrix (ECM) or cell–cell contacts, and constant remodeling of the associated actin cytoskeleton. In this respect, polyphenols have been shown to modulate the expression of a number of adhesion molecules. EGCG upregulates the expression of β1-integrin subunit in the medulloblastoma-derived DAOY cell line (Pilorget et al. 2003). In contrast, kaempferol, chrysin, apigenin, and luteolin inhibited ICAM-1 (intercellular adhesion molecule-1) expression in TNF-α-stimulated A549 alveolar epithelial cancer cells. The attenuation of the inflammatory response by flavonoids was mediated via the Jun N-terminal kinase (JNK) activity, c-jun messenger RNA (mRNA) expression, and the regulation of transcriptional activity of activator protein (AP)-1 and NF-κB (Chen et al. 2004a). Moreover, intravenous administration of pterostilbene and quercetin in a mouse melanoma animal model resulted in a 73% reduced metastasis of B16M-F10 cells in the liver, involving the inhibition of VCAM-1 (vascular adhesion molecule-1) by the hepatic sinusoidal endothelium (Ferrer et al. 2005). In addition, flavonoids could control cell metastasis by regulating the expression of integrin partners. Resveratrol treatment of the erythroleukemia K562 cell line increased expression of tensin, a cell-matrix adhesion protein capable of binding integrins and cytoskeletal actin filaments. This resulted in increased cell adhesion to fibronectin, cell spreading, and actin polymerization. It is interesting that resveratrol induced similar cytoskeletal changes in the tensin-deficient MCF7 human breast cancer cell line and abrogated estrogen-induced MCF7 cancer cell invasion (Rodrigue et al. 2005).

Recently, it has also been found that gap-junction proteins, such as connexins, mediate heterocellular interactions and functional cell coupling. Using in vitro migration assays, Czyz et al. showed that apigenin inhibited connexin signaling (Czyz et al. 2005). Apigenin treatment resulted in a significant inhibition of translocation of both HeLa-connexin 43 transfectants and their normal counterparts. Moreover, in the presence of apigenin, HeLa-connexin 43 cells, which displayed a highly invasive phenotype, failed to invade and engulf chick heart tissue fragments in a co-culture system. Furthermore, apigenin has been reported to inhibit the signaling of the oncogene *ras* and reverse malignant cell phenotype. Indeed, apigenin was able to subvert gelsolin downregulation in HCT116 cells (Klampfer et al. 2004). Gelsolin is an actin-binding protein whose expression is frequently reduced or absent in colorectal cancer cell lines (Apc^{-}) and primary tumors. Its turnover seems to be associated with the beneficial effect of apigenin in cancer cell transformation. Similar changes have been observed in human melanoma cells treated with a flavonoid of the anthocyanidin class, cyanidin-3-*O*-β-glucopyranoside (C-3-G). This flavonoid induced a strong increase in dendrite outgrowth, accompanied by a remodeling of the microtubular network, a dramatic increase of focal adhesions, and an increased expression of "brain specific" cytoskeletal components such as NF-160 and NF-200 neurofilament proteins. C-3-G treatment resulted in enhanced melanin synthesis, melanosome maturation, and upregulation of the melanoma differentiation antigen Melan-A/MART-1, revealing the reversal of melanoma cell phenotype from the proliferating tumorigenic to the differentiated state (Serafino et al. 2004).

The key role of tyrosine kinases and their substrate focal adhesion kinase (FAK) in flavonoids' antimetastatic activity has been studied in experimental animal models. Liu et al. found that green tea catechins suppress in vitro B16-F3m melanoma cell migration and spreading on a number of different ECM substrates, through long-term inhibition of FAK activity (Bruder et al. 2001). In vivo administration of (–)-epigallocatechin-3-gallate (EGCG) in mice bearing B16-F3m melanomas reduced primary tumor growth and lung metastasis, and increased the animal survival rate. Similar results have been obtained using a mouse

model of colorectal cancer: administration of (+)-catechin in C57BL/6J-Min/+ mice inhibited intestinal tumor formation by 70% and suppressed focal adhesion kinase activation. Morphologic studies linked this effect to (+)-catechin-induced changes in integrin-mediated intestinal cell survival signaling, including structural alteration of the actin cytoskeleton and decreased FAK tyrosine phosphorylation (Weyant et al. 2001).

Experimental data from our group (Nifli et al. 2005a) indicate that, on the breast cancer hormone-sensitive cell line T47D, flavonoids could trigger actin rearrangement within minutes and induce cell apoptosis. We reported that both the prototype red wine flavanols catechin and epicatechin, as well as their dimers B2 and B5, compete with testosterone for binding on membrane androgen receptors. They induce potent actin cytoskeleton reorganization regulated by a similar signaling cascade as described for testosterone-activated membrane receptors, leading ultimately to cell apoptosis. The application of catechin and epicatechin induced a moderate induction of filopodia. In contrast, application of B2 and especially B5 epicatechin dimers induced a peripheral redistribution and an increased intensity of actin cytoskeleton structures, with a massive induction of filopodia formation. Further analysis revealed that this effect is due to the transient activation of upstream modulators of actin polymerization, such as FAK and PI3 kinases. Similar morphologic changes have been observed in MDA-MB-231 human breast cancer cells, where the stilbene resveratrol has been found to attenuate epidermal growth factor (EGF)-directed response and inhibit cell migration. In this model, resveratrol induced a rapid global array of filopodia, and decreased focal adhesions and FAK activity (Azios and Dharmawardhane 2005). Furthermore, resveratrol treatment of bovine pulmonary artery endothelial cells resulted in reduced proliferation and increased assembly of both actin microfilaments and microtubules, which was dependent on intracellular calcium and tyrosine kinase activity (Bruder et al. 2001). In addition, the flavonol quercetin has been found to inhibit the proliferation of the human cholangiocarcinoma cell line HuCC-T1, under basal conditions. This effect was more prominent after the induction of hyperthermia. In this latter case, quercetin delayed the reorganization of F-actin (Kudo et al. 1999). Quercetin seemed to modulate the expression and the activity of heat shock proteins hsp27 and hsp90, resulting in increased disruption and aggregation of microfilaments (Loktionova and Kabakov 1998)

Finally, polyphenols have been reported to interact directly with proteins of the major cytoskeletal network. Tachibana et al. identified a 67-kDa membrane protein that serves as a laminin receptor and mediates green tea flavonoid (–)-epigallocatechin-3-gallate antimetastatic activity at nanomolar concentrations (Tachibana et al. 2004). Pull-down experiments revealed also that EGCG could bind directly to vimentin, a protein that is essential in maintaining the structure and mechanical integration of the cellular space. The interaction of EGCG inhibited vimentin phosphorylation and could further explain EGCG antiproliferative and antitumor promoting action (Ermakova et al. 2005). Those findings led to the synthesis of promising therapeutic drugs, such as the resveratrol derivative (Z)-3,5,4′-trimethoxystilbene (R3). R3 is 100-fold more effective than resveratrol in inducing growth arrest in human colon cancer Caco-2 cells. In addition, R3 partially inhibited colchicine binding to its binding site on tubulin and exerted cytotoxic effects by depleting the intracellular pool of polyamines and by altering microtubule polymerization (Schneider et al. 2003).

Angiogenesis

Another important phenomenon in tumor growth is angiogenesis, as malignant cells are in search of nutrient supply. This process implies either cellular chemotaxis toward a preexisting vascular network, or the infiltration of vascular endothelial cells in cancer structures,

leading to neovascularization. In this respect, secreted growth factors, such as vascular endothelial growth factor (VEGF)/VPF, basic fibroblast growth factor (bFGF), transforming growth factor (TGF)-β, platelet-derived growth factor (PDGF), and endothelin-1, as well as ECM proteolytic enzymes, are key regulators of angiogenesis, including modulation of metalloproteinases (MMPs) and their tissue inhibitor TIMPs, chemotaxis, and reorganization of vascular endothelial cells. Flavonoids have been reported to affect malignant cell invasion and control the expression of the implicated molecules. Silymarin, an isomer mixture of silibinin, isosilibinin, silicristin, and silidianin, in non-cytotoxic concentrations, reduced human vascular endothelial (HUVEC) tube formation on a reconstituted extracellular matrix, and MMP-2 secretion (Jiang et al. 2000). Its antiangiogenic effect was apparent in DU-145 prostate cancer cells and MCF-7 and MDA-MB-468 breast cancer cells, since it reduced VEGF secretion 1 h after its application. Similar results have been obtained in U-87 glioblastoma cells treated with EGCG, where pro-MMP-2 secretion was reduced through inactivation of MT1-MMP, suggesting that flavonoids not only affect the transcription of matrix metalloproteinases, but also regulate their posttranslational modification and transport (Annabi et al. 2002).

The inhibitory effect of flavonoids on vascularization has been also studied in vivo. Luteolin inhibited tumor growth and angiogenesis in a murine xenograft model, while decreased VEGF-induced angiogenesis in a rabbit corneal assay (Bagli et al. 2004). In a TRAMP animal model, green tea polyphenol infusion resulted in marked inhibition of effectors of angiogenesis and metastasis, notably VEGF, uPA, and MMP-2 and -9 (Adhami et al. 2004). Among them, the inhibition of pro-MMP-2 secretion was crucial for EGCG-induced tumor cell inactivation during angiogenesis (Sartor et al. 2004). Moreover, in SCID mice, where gastric cancer cells were peritoneally disseminated, the citrus flavonoid nobiletin significantly decreased both the number and the size of dissemination nodules, via inhibition of MMP-9 activity (Minagawa et al. 2001).

Flavonoids could also act as downstream regulators of growth factors signaling, affecting kinase activity and transcription factors activation during angiogenesis. Apigenin attenuated angiogenic processes by inhibiting VEGF early cascade, through PI3K/AKT/p70S6K1 and HDM2/p53 pathways (Fang et al. 2005). Nobiletin and quercetin markedly inhibited pro-MMP-7 protein and its mRNA expression in HT-29 colorectal cancer cells by reducing AP-1 DNA binding (Kawabata et al. 2005). Similarly, nobiletin treatment of HT-1080 fibrosarcoma cells resulted in increased TIMP-1 levels, with a concomitant decrease in MMP-1 and -9 expression, due to inactivation of AP-1 and reduction of redox-triggered PI-3 phosphorylation (Sato et al. 2002). Luteolin was able to revert VEGF-induced HUVEC cells migration by abolishing activation of Akt, a downstream target of PI3K, conveying both survival and mitotic downstream signals (Bagli et al. 2004).

Another potential mechanism of cancer cell invasion involves endothelins, a family of vasoconstricting peptides, and their membrane receptors. Two endothelin receptors, ET-A and ET-B, are found in normal tissue, while malignant cells are characterized by the loss of ET-B receptors and increased levels of endothelin-1 (ET-1). ET-1 is a mitogenic autocrine growth factor secreted by, among others, vascular endothelial cells. However, it could act as a co-mitogen, as its effects are potentiated in the presence of growth factors, including bFGF, IGF-1, and PDGF, or promote tumor angiogenesis in collaboration with VEGF. Recent research showed that crude grape seed extract, rich in oligomeric flavan-3-ols, could trigger cytoskeletal changes in endothelial cells, similar to those during laminar shear stress, and modification of protein tyrosine kinases activity. This effect was due to the inhibition of ET-1 synthesis, resulting in the restoration of endothelial function. It also suggests a possible mechanism through which procyanidins could regulate endothelial cell infiltration during

tumor anchoring and proliferation (Corder et al. 2004). Finally, in addition to the aforementioned mechanisms, flavonoids could control the overall angiogenetic process through regulation of Cox-2 and iNOS enzymes, or though p53 oncosuppressor gene activity (discussed in the following section).

As reviewed above, polyphenols may exert a number of actions in cellular systems, leading to a number of cell responses. In the following section we will briefly discuss our current knowledge on the potential mechanisms implicated in polyphenol–cell interactions, or elicited after polyphenol internalization.

Interaction with steroid and growth factor receptor-mediated effects

Steroids and steroid receptors play an important role in the proliferation, differentiation, maintenance, and function of hormone-responsive tissues. They are also involved in the development and progression of certain cancers, such as prostate and breast cancer. Some polyphenols, due to their structural similarity to estrogens, are able to interact with steroid receptors and/or modulate their expression and function. These polyphenols are also known as *phytoestrogens*. Several studies indicate that such a mechanism may be implied in the inhibitory effects of polyphenols (Fig. 3). Our group has reported that several wine polyphenols (resveratrol, quercetin, catechin, and epicatechin) were able to interact with estrogen and androgen receptors in breast cancer (MCF7 and T47D) and prostate cancer cells (LNCaP), respectively, at the nanomolar range. This result suggests that their anticancer action may be partly mediated by a decreased estrogen or androgen binding to their cognitive receptors (Damianaki et al. 2000; Kampa et al. 2000). Gehm et al. reported that resveratrol increased the expression of native estrogen-regulated genes, acting as an estrogen receptor agonist (Gehm et al. 1997). It has also been shown that resveratrol and quercetin at micromolar concentrations decreased the expression and function of the androgen receptor (AR) in LNCaP cells (Mitchell et al. 1999; Xing et al. 2001) by overexpressing c-Jun (Yuan et al. 2004), a main component of the AP-1 protein complex, which can directly activate or induce transcription of many genes. In addition, the two polyphenols repressed the expression of the AR-specific coactivator ARA70 and various AR-regulated genes (e.g., prostate-specific antigen, PSA). In a related study, the same authors have demonstrated that resveratrol, although suppressing PSA expression, did not alter AR expression (Hsieh and Wu 2000). Resveratrol was also reported to interact with both ERα and ERβ estrogen receptors. This interaction can result in an agonistic, antagonistic, or mixed effect (Bowers et al. 2000). In MCF7 breast carcinoma and in Ishikawa endometrial adenocarcinoma cells, resveratrol was found to exhibit ER-antagonist activity in the presence of estradiol (Bowers et al. 2000). Interestingly, Maggiolini et al. have demonstrated, in LNCaP and MCF7 cells, that quercetin and genistein have a biphasic, concentration-dependent effect, acting as AR agonists only at low concentrations (Maggiolini et al. 2002). However, catechins such as EGCG and ECG have been also shown to bind to ERα and ERβ, in MCF7 cells, eliciting an ER-mediated gene expression (Goodin et al. 2002). In addition, androgen receptor expression in LNCaP cells was inhibited by baicalein (Chen et al. 2001).

Nowadays when steroid actions are studied one should take into consideration the notion that, in addition to their action as nuclear transcription factors, steroids may also elicit nongenomic effects. These effects are rapid, triggered at the plasma membrane level, possibly through specific membrane receptor sites, and are mediated by several signaling pathways involving adenylate cyclase, phospholipase C, protein kinases A and C, intracellular ion (calcium, potassium) fluxes, mitogen-activated protein kinase cascades (MAPK), PI3K/Akt, c-Src, and/or FAK. Hence, phytoestrogens may also exert their effects via more

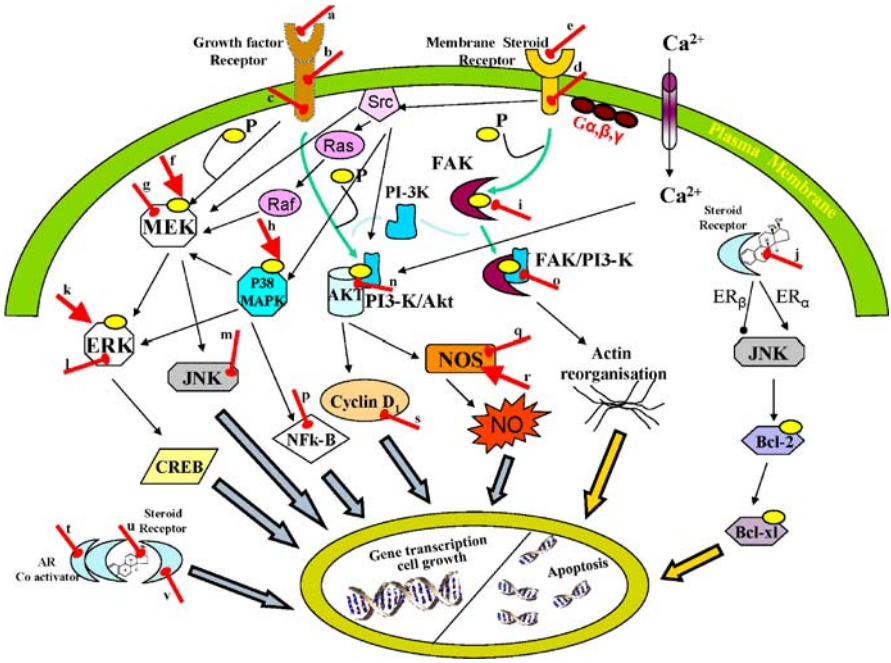

Fig. 3 Polyphenol interference with steroid and growth factor receptors, and signaling kinase activities: ↑ activation, ↓ inhibition. **a** EGCG, genistein, quercetin, kaempferol, resveratol. **b** EGCG. **c** Theaflavin (TF) 2, 2a 2b, 3 genistein. **d** Catechin, epicatechin, B2, B5, EGCG, black tea polyphenols. **e** Resveratrol, quercetin, epicatechin, catechin, baicalein. **f** EGCG. **g** Quercetin, vaticanol, Kaempferol. **h** Quercetin. **i** Green tea catechins. **j** Resveratrol, EGCG, ECG, epicatechin, catechin, quercetin. **k** Resveratrol, EGCG, quercetin, ellagic acid. **l** Green tea polyphenols, quercetin, genistein. **m** Green tea polyphenols, EGCG, theaflavins. **n** Green tea polyphenols, daidzein, genistein. Biochanin A quercetin, resveratrol, EGCG, rutin. **o** Catechins, resveratrol. **p** EGCG. **q** EGCG, resveratrol, apigenin, curcumin, genistein, silymarin. **r** Resveratrol, flavone acetic acid, oleuropein delphinidin, phenyl acetic acid. **s** EGCG, resveratrol, baicalein. **t** Resveratrol, quercetin. **u** Quercetin, resveratrol, catechin, genistein, epicatechin. **v** Quercetin, resveratrol. Vaticanol, kaempferol, resveratrol

rapid signaling cascades. Indeed, it has been shown that resveratrol exerts nongenomic effects, supplementary to genomic ones, on cell survival by decreasing Akt (a survival factor) and FAK phosphorylation (Brownson et al. 2002). In addition, our group has reported an interaction of catechin and epicatechin monomers and dimmers (B2 and B5) with membrane androgen receptors in T47D human breast cancer cells, initiating rapid phosphorylation of signaling molecules and actin cytoskeleton rearrangements, leading cells to apoptosis (Nifli et al. 2005a).

The enhanced proliferation of cancer cells is also characterized by overexpression of growth factors, such as EGF, PDGF, insulin-like growth factor I (IGF-I), and VEGF and their cognitive receptors (Spencer-Cisek 2002). Selective effects that interfere with growth factor actions, either by competition with ligand, or inhibition of growth factor-receptor expression, activity, homo- or hetero-dimerization and downstream signaling, have been shown to inhibit cell growth and induce apoptosis. A number of investigators, using diverse approaches, suggest that the IGF-I network may be an important stimulant of carcinogenesis. In vitro and in vivo studies have shown that IGF-I stimulates and/or inhibits apoptosis in a variety of normal and cancer cells (Peruzzi et al. 1999; Remacle-Bonnet et al. 2000) and that the ratio IGF-I receptor to insulin receptor substrate-1 (IRS-1) defines the cellular

response. Wang et al. have demonstrated that polyphenols block IGF-I regulated events in prostate cancer cells. Genistein, quercetin, kaempferol, and resveratrol antagonize IGF-I in AT6.3 rat prostate cells, by reducing the IRS-1 and modulating specific intracellular events such as phosphorylation of Akt and ERK1/2 (Wang et al. 2003). Decreased phosphorylation of Akt, due to reduced IGF-I receptor 1 auto-phosphorylation, was also observed in DU-145 cells after treatment with black tea polyphenols (Klein and Fischer 2002).

Increased levels of HER/neu family oncogenes, including EGF receptor (EGFR)—possessing transmembrane tyrosine kinase activity—were found in several cancers and were associated with poor overall survival, increased metastatic potential, and resistance to chemotherapeutic agents. The authors suggested that suppression of HER2/neu phosphorylation by black tea polyphenols and EGCG was the underlying mechanism for the antiproliferative effects in MCF-7 and NF639 breast cancer and SMF and Ba/F3 cells (Pianetti et al. 2002; Way et al. 2004b). Moreover, polyphenols have been shown to interfere with epidermal growth factor receptor (EGFR) function, as well as with its downstream targets (ERK, STAT3 and Akt), leading to cell growth inhibition and apoptosis. Teaflavin (TF)-1, TF-2, TF-2a, TF-2b, and TF-3 inhibited the effect of EGF on autophosphorylation of its receptor in A431 cells (Yang et al. 1998a). EGCG has been found to inhibit EGF mediated EGFR activation in cervical tumor cells by reducing EGFR dependent ERK1/2 and Akt activity or by directly inhibiting them (Sah et al. 2004). In addition, in A431 epidermoid carcinoma cells, Liang et al. have demonstrated that EGCG inhibited the kinase activity of EGFR and blocked EGF binding to EGFR (Liang et al. 1997). EGFR tyrosine kinase activity was also suppressed by genistein in A431 cells (Akiyama et al. 1987). Resveratrol was found to antagonize EGFR activation of ERK1/2 in prostate cancer cells (Stewart and O'Brian 2004), which is involved in the development of androgen-independent cancer. In addition, resveratrol and quercetin could suppress proliferation of Ishikawa cells by downregulation of EGF expression (Kaneuchi et al. 2003a; Kaneuchi et al. 2003b). Moreover, cocoa procyanidins have been reported to inhibit the expression of HER2/neu (Kenny et al. 2004). A number of authors suggest that membrane estrogen (Levin 2001) or androgen (Bonaccorsi et al. 2004) actions could be mediated through membrane-anchored ER or AR and their interaction with EGFR. In this respect, the effect of polyphenols on EGFR could be explained through binding to steroid receptors, and after heterodimerization, propagating their effects through interaction with EGFR.

Genistein, being a tyrosine kinase inhibitor, can also alter other growth-factor-induced effects, exerted via membrane receptor protein kinases, such as PDGF and VEGF receptors. Indeed, in rat hepatic stellate cells, genistein inhibited basal and PDGF-induced cell growth (Liu et al. 2002b). Similarly, EGCG potently inhibited PDGFR autophosphorylation and hence kinase activity in rat hepatic stellate, and in A431 epidermoid carcinoma cells (Liang et al. 1997). An inhibition of PDGF was also observed in A172 human glioblastomas (Sachinidis et al. 2000). It was suggested that EGCG binds to PDGF (preferably to the PDGF-BB isoform), reducing the ligand binding, and hence inhibiting the downstream signaling pathways (Weber et al. 2004). Finally, a polyphenol-inhibitory effect on VEGF expression (a major pro-angiogenic factor that correlates with microvessel density in tumors and stimulates the expression of several proteins) has been demonstrated by several investigators. For example, EGCG was able to inhibit VEGF expression in different carcinoma cells (e.g., breast, head and neck, and leukemia) (Jung et al. 2001; Lee et al. 2004c; Masuda et al. 2002; Sartippour et al. 2002).

Alteration of specific protein kinase activities

Intracellular signaling cascades that mediate the effects of several stimuli (such as growth factors, mitogens, stress, ROS, and inflammatory cytokines) that promote cancer cell growth, include the ubiquitously expressed mitogen-activated protein kinase (MAPK) cascades, the phosphoinositide-3-kinase (PI3K) and protein kinase B (PKB also known as Akt), and the kinases involved in the Janus kinase (JAK)-signal transducer and activator of transcription (STAT) pathway. These cascades lead to altered activity of target genes, including several transcription factors, and to a range of biologic responses (e.g., cell growth and apoptosis). In tumor cells, proteins that are key molecules in the above signaling pathways are overexpressed, leading to the constitutive activation of such pathways. Polyphenols such as curcumin, EGCG, resveratrol, quercetin, genistein, etc., can upregulate or downregulate signaling cascades, and subsequently induce stress response genes, growth arrest or apoptosis (Manson 2003; see Fig. 3).

Green tea polyphenols have been found to significantly inhibit prostate cancer in vitro and in animal models. It was demonstrated that they mediate their effect by modulating ERK1/2, PI3K and phosphorylated Akt levels in DU-145 and LNCaP prostate cancer cells (Siddiqui et al. 2004). An activation of extracellular signal-regulated kinase 1/2 (ERK1/2) was observed in HT-29 human colon cells (Siddiqui et al. 2004) when treated with EGCG, but this effect seemed to be due to an oxidative stress, induced by EGCG, since antioxidants were able to block it. EGCG has been suggested to inhibit phosphorylation of MAP/ERK kinase 1/2 (MEK1/2, ERK1/2) and Elk-1, as well as c-Jun, in 30.7b Ras 12 cells (Ras-transformed mouse epidermal cells). Possibly Elk1 phosphorylation was inhibited by ERK1/2 because EGCG competed for the binding site on it (Chung et al. 2001). Reduced phosphorylation of ERK1/2 and JNK as well as decreased protein levels of the MAPK p38 were also observed in UV irradiated skin of SKH-1 hairless mice, when green tea polyphenols were applied topically (Afaq et al. 2003). Inhibition of JNK phosphorylation, leading to a reduced activation of the transcription factor AP-1, was found when EGF or tissue plasminogen activator (TPA)-transformed JB6 mouse epidermal cells were treated with EGCG or theaflavins (Dong et al. 1997). Finally, green tea polyphenols were found to inhibit the levels of IGF and IGFBP-3 in a mouse transgenic prostate adenocarcinoma (TRAMP) model, through inhibition of protein expression of PI3-kinase and Akt-phosphorylated forms (Adhami et al. 2004).

Several studies have demonstrated that the apoptotic effect of quercetin also involves the MAPK and the PI3K/Akt pathways in different cancer cell systems. In A549 lung cancer cell line, quercetin inhibited the phosphorylation of Akt, but induced phosphorylation of MEK1/2, and subsequently ERK1/2, as well as JNK. c-Jun phosphorylation was also observed, as was an induced caspase 3 cleavage (Nguyen et al. 2004). Increased phosphorylation of MAPKs by quercetin was observed in the human leukemia cell line MOLT-4. Indeed, treatment of MOLT-4 cells with quercetin resulted in an increased p38 phosphorylation. Similarly, quercetin and ellagic acid, when applied in combination, had a synergistic effect that also resulted in JNK1/2 and ERK phosphorylation (Mertens-Talcott et al. 2005). In contrast, in PC3 prostate cancer cells, quercetin inhibited basal, EGF-induced, and TGFα-induced phosphorylation of Akt-1, Elk-1, c-Raf, and MAPK (Huynh et al. 2003). Decreased Akt phosphorylation, induced by quercetin, was also observed in MCF7 cells.

The MAPK and PI3K pathways seem to mainly mediate resveratrol's inhibitory effects on cancer cells. ERK1/2 appears to play a central role by inducing apoptosis when modulating their activity. Furthermore, it has been suggested that ERK1/2 in prostate cancer is important in the development of androgen independence. Evidence exists indicating

that the constitutive ERK1/2 activation is substantial in neoplastic epithelial cells of early stage prostate cancer specimens, sharply increased in the neoplastic epithelium of advanced prostate cancer, and undetectable in nonneoplastic epithelial cells (Gioeli et al. 1999). In PC3 cells, resveratrol suppressed TPA- or EGF-induced ERK1/2 activation by inhibiting protein kinase C (PKC)α (Stewart and O'Brian 2004). In DU-145 cells, however, resveratrol activated ERK1/2-induced nuclear translocation of p53 and p53-induced apoptosis. Indeed, an inhibitor of PKC enhanced resveratrol-induced phosphorylation of p53 (Stewart and O'Brian 2004). In LNCaP cells, p53 phosphorylation was also induced by resveratrol, although inhibition of PKC resulted in a reduction in p53 activation and apoptosis. These data suggest that resveratrol-induced apoptosis in these two cell lines occurred though different PKC- and MAPK-dependent pathways (Shih et al. 2004). Studies performed on human leukemia HL-60 cells showed that resveratrol can activate cdc42 (a Rho family GTPase member), which in turn activates the MAPKKK/ASK1 pathway, triggering in turn the expression of FasL and leading to apoptosis (Su et al. 2005). Moreover, vaticanol (a resveratrol tetramer) induced apoptosis in HL-60 cells by decreasing the levels of phosphorylated ERK and MEK, as well as Akt, leading to apoptosis. In MCF7 cells, resveratrol and genistein, in addition to a decreased Akt phosphorylation, increased PTEN and p27 protein levels. Furthermore, resveratrol inhibited PI3K activity by modulating ERα binding to the p85 subunit PI3K (Pozo-Guisado et al. 2004). It is noteworthy that different effects of polyphenols on Akt phosphorylation have been suggested as estrogen receptor-sensitive. Resveratrol decreased Akt phosphorylation in nonmetastatic ER-positive T47D cells, while increased Akt phosphorylation was observed in metastatic estrogen receptor-negative MDA-MB-231 cells (Brownson et al. 2002). Finally, kaempferol-induced apoptosis in A459 lung cancer cells was attributed to its ability to inactivate Akt-1 and activate MAPKs, since prolonged activation of MEK-MAPK activity inhibits DNA synthesis and triggers apoptosis (Nguyen et al. 2003). In AT6.3 prostate cancer cells, additionally, treatment with genistein, kaempferol, or quercetin inhibited IGF-I-stimulated Akt and ERK1/2 phosphorylation, and thus interfered with the IGF signal transduction cascade (Wang et al. 2003).

Therefore, polyphenols can interfere with intracellular signaling cascades that mediate the effects of mitogenic stimuli by modulating the activity of several kinases. ERK1/2, PI3K, and phosphorylated Akt levels are mainly affected, as well as phosphorylation of JNK and MAPK p38 protein levels. Subsequently this modulation leads to reduced activation of transcription factors and induction of growth arrest or apoptosis (Fig. 3).

Inhibition of enzymes involved in tumor promotion and metastasis

Proteasome Polyphenols can exert, in addition to their modulatory actions on the signaling machinery, a specific effect on a number of metabolic, redox, or ubiquitin-proteasome related enzymes. The 20S proteasome constitutes the catalytic key component of the ubiquitous proteolytic machinery, namely the 26S proteasome. There are three major proteasomal activities: chymotrypsin-like, trypsin-like, and peptidyl-glutamyl peptide hydrolyzing activity. The chymotrypsin-like but not trypsin-like activity of the proteasome is associated with tumor cell survival. Many cell cycle and cell death regulators have been identified as targets of the ubiquitin-proteasome-mediated degradation pathways, including p53, Rbp, p21, p27Kip1, IκB-α, and Bax. It has been shown that ester bond-containing tea polyphenols, such as EGCG and tannic acid, are potent and specific inhibitors of the chymotrypsin-like activity of the proteasome, leading to the accumulation of natural proteasome substrates such as p27 (Kip1) and IκB-α. The accumulation is followed by growth arrest in the G1 phase of the cell cycle and apoptosis in several cell lines including Jurkat leukemia cells, LNCaP and

PC-3 prostate cancer cells, MCF7 breast cancer cells, and SV40-transformed (VA-13) human fibroblasts (Nam et al. 2001). This structure–activity relationship of green tea polyphenols as proteasome inhibitors led to the production and study of several synthetic analogs (Kuhn et al. 2005). Green tea polyphenols catechin-3-gallate and epicatechin-3-gallate can also inhibit the proteasomal chymotrypsin-like activity (Wan et al. 2004). Curcumin-induced apoptosis was mediated through the impairment of the ubiquitin-proteasome pathway (Lin 2004), while genistein decreased proteasome activity in p815 and RBL-2H mast cell tumor cell lines (Park et al. 2002). Apigenin-induced degradation of mature HER2/neu was reported to involve polyubiquitination of HER2/neu and subsequent hydrolysis by the proteasome (Way et al. 2004a). Apigenin, as well as quercetin, inhibited the chymotrypsin-like activity of purified 20S and 26S proteasomes in intact leukemia Jurkat T cells, leading to the accumulation of Bax and IκB-α (Chen et al. 2005), and subsequently to apoptosis. Finally, resveratrol inhibited human ovarian cancer cells A2780/CP70 and OVCAR-3 by stimulating hypoxia-inducible factor 1α (HIF-1α) protein degradation, through the proteasome pathway (Cao et al. 2004).

Metalloproteinases MMPs are associated with tumor cell invasion of the basement membrane and stroma, blood vessel penetration, and metastasis, and they have more recently been implicated in primary and metastatic growth and angiogenesis. Several polyphenols have been reported to interact with these enzymes. Genistein inhibited MMP secretion by prostate cancer cells (Huang et al. 2005)**,** MMP-2 and MMP-9 by head and neck cancer cell lines (Alhasan et al. 2001); EGCG inhibited MMP-2 and MMP-9 while inducing the activity of their inhibitors TIMP-1 and TIMP-2 in different cancer cells such as neuroblastoma, fibrosarcoma (Garbisa et al. 2001)**,** glioblastoma (Annabi et al. 2002)**,** prostate (Vayalil and Katiyar 2004), endothelial (Fassina et al. 2004), and human gastric cancer cells (Kim et al. 2004). Moreover, EGCG directly inhibited MT1-MMP activity in HT-1080 human fibrosarcoma cells and HUVEC cells, leading to accumulation of nonactivated MMP-2 at the cell surface (Dell'Aica et al. 2002; Yamakawa et al. 2004). EGCG treatment of HT-29 colon cancer cells increased both intracellular and extracellular pro-MMP-7 protein levels (Kim et al. 2005). Epicatechin gallate, EGCG, and theaflavin strongly suppressed the invasion of HT-1080 fibrosarcoma cells into the monolayer of HUVECs/gelatin membrane, through suppression of gelatin degradation mediated by MMP-2 and MMP-9, whereas epicatechin, epigallocatechin, tea flavonols, tea flavones, and gallate derivatives had no effect (Maeda-Yamamoto et al. 1999). *trans*-Resveratrol decreased the secretion of MMP-2 by cultured human liver myofibroblasts (Godichaud et al. 2000) and delphinidin inhibited the activity of MMP-2 and MMP-9 in human fibrosarcoma HT-1080 cells, an effect that may be responsible for its ability to inhibit tumor cell invasiveness (Nagase et al. 1998). Luteolin and quercetin suppressed EGF-induced secretion of MMP-2 and MMP-9 in A431 (Huang et al. 1999) and MiaPaCa-2 cells (Lee et al. 2004b). Proanthocyanidins from grape seeds inhibit the expression of matrix metalloproteinases in human prostate carcinoma DU145 cells (Vayalil et al. 2004).

Telomerase Telomerase activity is one of the most important factors that have been linked to multiple developmental processes, including cell proliferation, differentiation, aging, and senescence. Dysregulation of telomerase has often been found in developmental abnormalities and cancer, where telomere dysfunction leads to an increase in initiation of tumor lesions, due to enhanced genomic instability. Recently, a number of studies have described polyphenol effects on telomerase inhibition. Naasani et al. reported that EGCG directly in-

hibited telomerase in cell extracts and in living U937 monoblastoid leukemia and HT-29 colon adenocarcinoma cells, suggesting that telomerase inhibition could be one of the major mechanisms underlying their anticancer effects (Naasani et al. 1998). Indeed, EGCG was found to inhibit telomerase activity in several cervical cancer cell lines (Yokoyama et al. 2004), leading to suppression of cell viability and induction of apoptosis. Furthermore, in a nude mice model bearing both telomerase-dependent and independent xenograft tumors, cloned from a single human cancer progeny, only the telomerase-dependent tumors responded to prolonged oral administration of EGCG (Naasani et al. 2003). As for the other polyphenols, only daidzein (one of the most common phytoestrogens) was reported to inhibit the growth of HeLa cells, arrest cells at G_0/G_1 or G_2/M phase and decrease the expression of human telomerase catalytic subunit (Guo et al. 2004).

Cyclooxygenases Cyclooxygenase (COX) catalyzes the formation of prostaglandins (PG) from arachidonic acid. COX has two isoforms: COX-1 and COX-2. The former is expressed in a variety of cells and tissues, whereas cytokines, growth factors, and tumor promoters induce the expression of the latter. Increased COX-2 expression is thought to be associated with colon, lung, breast, esophagus, and prostate carcinogenesis. A large body of evidence suggests that inhibiting COX-2, the inducible form of COX, will be an important strategy for preventing cancer. Three lipoxygenases (LOXs: 5-LOX, 12-LOX, and 15-LOX) have been reported to be present in human tissues. LOXs are nonheme iron dioxygenases that insert molecular oxygen into polyunsaturated fatty acids, resulting in the formation of hydroperoxyeicosatetraenoic acid molecules. Their oxidation products have also been reported to be important regulators of the proliferation and apoptosis of cancer cell lines (Tang et al. 1996). The above data suggest that the regulation of arachidonic acid metabolism is important in the prevention and evolution of different types of cancer, and especially those of the digestive tract. EGCG, EGC, and ECG have been reported to affect arachidonic acid metabolism in human colon mucosa and colon tumors by inhibiting LOX and COX activity (Hong et al. 2001). Silymarin, a flavonoid compound isolated from the milk thistle plant, reduced UVB radiation-induced non-melanoma skin cancer tumor incidence in mice and induced COX activity (Zhao et al. 1999). In another study utilizing an in vitro cell free model, however, silymarin and resveratrol each inhibited COX-1 (Liu et al. 2002a). Out of 12 flavonoids tested for possible effects on COX mRNA expression, 10 had an effect on its expression to some extent. Quercetin was the most potent suppressor of COX-2 transcription, while catechin and epicatechin showed a weak activity. An intermediate effect was reported for rhamnetin, genistein, eriodictyol, luteolin, kaempferol, fisetin, and phloretin (Mutoh et al. 2000). Quercetin was also a potent competitive inhibitor of LOX that was entrapped within LOX and underwent degradation into protocatechuic acid that blocks LOX activity (Borbulevych et al. 2004). Genistein suppressed PGE2 synthesis in human oral squamous carcinoma line SCC-25 cells by directly inhibiting COX-2 activity (Ye et al. 2004). Furthermore, quercetin, in addition to amentoflavone, downregulated COX-2 in A549 human lung adenocarcinoma cells (Banerjee et al. 2002) and protected lung adenocarcinoma CL-3 cells from cooking-oil fumes-induced DNA damage by almost completely inhibiting COX-2 mRNA expression (Lin et al. 2002). In addition, several flavanones inhibit prostaglandin E2 by inhibiting COX-2 mRNA expression in NIH3T3 cells (Ko et al. 2002). Flavones also blocked prostaglandin E2 production via inhibition of COX-2 and inhibited epidermal growth factor-induced proliferation of epidermoid carcinoma A431 cells (Shen et al. 2004). It has also been reported that curcumin modulated arachidonic acid metabolism by affecting cytosolic cyclooxygenases in the murine macrophage RAW264.7 cells and in HT-29 human colon cancer cells

(Hong et al. 2004). *trans*-Resveratrol had inhibitory effects on COX-1, while both *trans*- and *cis*-resveratrol exhibited significant inhibitory activity on COX-2 (Waffo-Teguo et al. 2001). EGCG treatment in an induced rat esophageal tumorigenesis model decreased the expression of COX-2 by tumor cells (Li et al. 2002). However, a structure–activity relationship for COX-2-inhibiting properties of polyphenols may occur (Rosenkranz and Thampatty 2003).

Nitric oxide synthase The dual role of nitric oxide (NO) and the enzymes that produce it (nitric oxide synthases, NOSs, iNOS inducible, eNOS endothelial, and nNOS neuronal) on tumor growth and metastasis has been investigated in several cancer models. Whether nitric oxide is beneficial or deleterious in human neoplasias seems to be organ- and cell-specific, and depends on many factors including redox status. The NO/NOS pathway represents an alternative mode of action for polyphenols since it has been shown that they can interact with this pathway in many different ways, summarized below.

The expression of iNOS and NO production in mammary glands treated with lipopolysaccharide (LPS) was significantly inhibited by curcumin. It was reported that curcumin also had a direct scavenging activity for NO (Onoda and Inano 2000). The administration of curcumin significantly reduced the development of mammary tumors in irradiated rats, and this finding was estimated to occur through suppression of iNOS activity in the mammary gland (Inano and Onoda 2002). However, in acute leukemia cells, intracellular NO levels increased significantly after exposure to curcumin (Kellner and Zunino 2004).

Genistein was reported to block induced iNOS mRNA expression in C6 glioma (Lin et al. 2001) and human SK-N-MC neuroblastoma cells (Chen et al. 2003). EGCG reduced NO production by reducing iNOS mRNA expression and inhibiting iNOS enzyme activity (Lin and Lin 1997). 1,2,3,4,6-penta-*O*-galloyl-β-D-glucose (PGG), EGCG, and gallacetophenone significantly inhibited LPS-induced NO production in LPS-activated macrophages (Lee et al. 2003). Resveratrol inhibited the formation of inducible nitric oxide synthase (iNOS) in mouse macrophages stimulated with lipopolysaccharide (Jang and Pezzuto 1999) and B cell chronic lymphocytic leukemia cells (Roman et al. 2002). However, treatment of gastric adenocarcinoma SNU-1 cells with resveratrol resulted in stimulation of NOS activity (Holian et al. 2002). Quercetin inhibited NO and iNOS protein expression without affecting iNOS mRNA expression in the A549 human lung adenocarcinoma cell line (Banerjee et al. 2002), but increased intracellular NO levels in acute leukemia cells (Kellner and Zunino 2004). In addition, decreased levels of iNOS, and thus inhibition of the production of nitric oxide, were observed when MCF-7 cells were treated with the phytoestrogen biochanin A (Hsu et al. 2000). On the other hand, delphinidin, an anthocyanin present in red wine, increased endothelial NOS protein expression in bovine aortic endothelial cells and inhibited apoptosis (Martin et al. 2003b). A similar increase in eNOS activity was induced by flavone acetic acid (FAA) in a mouse RJ2-14 tumor model (Harris and Thorgeirsson 1997).

We have previously described that 3,4-dihydroxy-phenylacetic acid (PAA) directly decreased NOS activity by 40%, while caffeic acid did not. Furthermore, PAA increased iNOS mRNA while it concurrently reduced eNOS mRNA expression (Kampa et al. 2004). We have also reported that catechin, epicatechin, quercetin, and resveratrol decrease NO secretion by prostate cancer cell lines (LNCaP, PC3, and DU145) and inhibit NO production by T47D breast cancer cells. Although a concurrent decrease in total NOS (eNOS and iNOS) activity was observed after treatment for 24 h or longer, these agents induced a transient early increase in NOS activity. This bimodal effect indicated a possible dual action of polyphe-

nols, interfering both with NOS activity and its transcription. Bimodal modification of eNOS and iNOS mRNA expression was also observed in other systems (Nifli et al. 2005b).

Cytochrome P450s Cytochromes P450 (CYPs) constitute a superfamily of heme-thiolate isoenzymes involved in the metabolism of several chemicals (such as drugs, dietary chemicals, or environmental pollutants). In this respect, they play an important role in the bioactivation of several procarcinogens and in the activation and inactivation of several anticancer drugs. Metabolic activation of chemical carcinogens is mediated by a limited number of human CYP species, namely CYP1A1, CYP1A2, CYP1B1, CYP2A6, CYP2B6, CYP2E1, and CYP3A4 (Code et al. 1997). These CYPs are mainly expressed in the liver, except CYP1A1 and CYP1B1, which are extrahepatic isoenzymes in humans. Polyphenols' beneficial effects have been also attributed to their competitive inhibition of enzymes such as CYPs. Indeed, black tea polyphenols have been reported to inhibit the benzo(a)pyrene-induced activity and levels of cytochrome P4501A1 and 1A2 in mouse liver and lungs (Krishnan et al. 2005). Moreover, resveratrol was found to inhibit aryl hydrocarbon-induced CYP1A1 enzyme activity and expression in HepG2 cells. In addition, *trans*-resveratrol inhibited CYP1B1 activity and expression in MCF7 cells (Chang et al. 2000) while resveratrol has been reported as inhibitor of CYP3A4 and CYP2E1 in liver cells (Piver et al. 2001). Finally, epsilon-viniferin, a dimer of resveratrol, displaced a strong inhibitory effect for CYP1A1, CYP1B1, and CYP2B6, and to a lesser extent for CYP1A2, CYP2A6, CYP2E1, CYP3A4, and CYP4A (Piver et al. 2003). Several flavonoids also alter CYPs through binding to the aryl hydrocarbon receptor (AhR), a ligand-activated transcription factor, acting as either AhR agonists or antagonists. Inhibition of CYP enzymes, including CYP1A1, CYP1A2, CYP2E1, and CYP3A4 by competitive or mechanism-based mechanisms also occurs (Moon et al. 2006). It is noteworthy that quercetin increased CYP1A1 activity and expression in MCF7 cells, while kaempferol, a structurally related flavonoid, acted as an antagonist of TCDD-induced CYP1A1 transcription (Ciolino and Yeh 1999).

Interaction with oncogenes/tumor suppressor genes

Oncogenes are genes whose activation can contribute to the development of cancer. In contrast, tumor suppressor genes are those genes whose loss of function results in the promotion of malignancy. Both categories of genes are usually associated with modulation of major signaling cascades in the cell. Recent work presented evidence that polyphenols might have numerous anticancer effects via interactions with several oncogenes and tumor suppressor genes. In this section we are dealing with those oncogenes and oncoproteins that have not been described previously.

Oncogenes (Ras, c-myc, c-fos, c-raf)

EGCG was reported to inhibit the growth of H-ras transformed but not of normal fibroblasts (Wang and Bachrach 2002). Inhibition of c-myc, c-raf, and c-H-ras oncogenes by EGCG was observed in a mouse model of nitrosamine-induced lung oncogene expression (Hu et al. 1995) and a transgenic mouse model that develops spontaneous skin tumors due to overexpression of ornithine decarboxylase (ODC) and a v-Ha-ras transgene (Paul et al. 2005). In Ha-ras gene-transformed human bronchial epithelial 21BES cells, however, induction of Ha-ras was observed by EGCG treatment (Vittal et al. 2004). Resveratrol treatment of Neuro-2a neuroblastoma cells led to an increase of apoptosis and downregulation of Ras (Chen et al. 2003). Delphinidin has also been reported to inhibit Ras (Martin et al. 2003a). Curcumin

derivatives appeared to inhibit farnesyl protein transferase in porcine kidney epithelial-like LLC-PK 1 cells, human lung adenocarcinoma A549 cells, and human pancreatic cancer MIA PaCa-2 cells. This enzyme catalyzes Ras protein isoprenylation at a conserved cysteine residue near the carboxyl terminus in order to extend Ras protein biologic activity (Chen et al. 1997). Curcumin also inhibited proliferation of rat aortic smooth muscle cell line A7r5 through a G_0/G_1 cell cycle arrest, apoptosis and a concomitant reduction of c-myc mRNA levels (Chen and Huang 1998). A similar inhibition of c-Myc expression was induced by resveratrol, piceatannol, and EGCG in Caco-2 colon cancer cells (Wolter et al. 2003). EGCG arrested UVB-induced steady-state message and transcriptional activation of the c-fos gene and accumulation of the c-fos protein in human keratinocyte cell line, HaCaT via p38 MAPN (Chen et al. 1999). It also inhibited the stimulatory effect of PDGF-receptor β on the c-fos mRNA expression in cultured vascular smooth muscle cells from rat aorta (Ahn et al. 1999). However, EGCG and other green tea polyphenols induced c-JUN/c-FOS in HT-29 and Caco-2 colon cancer cell lines (Kim et al. 2004) and epidermal cells (Balasubramanian et al. 2002). Curcumin also inhibited the expression of c-FOS (Lin 2004).

p53

p53 is probably the most studied tumor suppressor gene and, under normal conditions, acts as a regulating mechanism for cell division. A number of studies have focused on the effect of polyphenols on p53 in several cancer models. EGCG increased p53 expression or activation in cervical (Sah et al. 2004), HepG2 (Kuo and Lin 2003), vascular smooth muscle (Hofmann and Sonenshein 2003), PC3 and LNCaP prostate carcinoma (Hastak et al. 2005), and MDA-MB468 human breast cancer cells (Roy et al. 2005). Resveratrol induced the expression of p53 while inhibiting the proliferation of pulmonary artery endothelial (Hsieh et al. 1999b) and vascular smooth muscle cells (Mnjoyan and Fujise 2003). However, a minor effect of resveratrol on p53 expression was reported in MDA-MB435 and MCF-7 breast carcinoma cells (Hsieh et al. 1999a) while in both wild-type p53-expressing and non-expressing HCT116 colon cancer cells, resveratrol induced apoptosis (Mahyar-Roemer et al. 2001).

Direct effect on nucleic acids and nucleoproteins

The inhibitory effect of polyphenols on cancer cells implies (in addition to kinase signaling regulation and cyclin and oncogene expression) a direct interaction with replication, recombination, repair, and transcription mechanisms, including enzymes and DNA. The first report of a direct interaction of quercetin with purified calf thymus DNA was published by Alvi et al. (1986). The authors reported a quercetin-induced stabilization of DNA secondary structure. However, prolonged treatment of DNA with quercetin solutions led to an extensive disruption of the double helix. This direct effect of quercetin was shared by curcumin, interacting with both single- and double-stranded DNA and ultimately producing strand scission, through a redox mechanism where the Cu(II)–Cu(I) couple was involved (Annaraj et al. 2005). Besides Cu^{2+}, quercetin can bind to rare earth metals such as lanthanoids (Zhou et al. 2001). The latter complexes could also modify DNA stability and proved to be efficient antiproliferative agents on a number of cancer cell lines.

As ethidium bromide (EtBr) could displace quercetin from its complexes with DNA, it was assumed that the latter acts as a DNA intercalator (Ahmed et al. 1994). Indeed, a comparative study of the hydrophobic quercetin and its nonplanar hydrophilic analog dihydroquercetin revealed that quercetin–DNA interaction is most probably due to its hydrophobic

core, which allows the agent to penetrate the DNA helix and to arrange its planar structure more or less parallel to the adjacent planes of the nitrogenous bases (Solimani 1996). However, a recent study showed that quercetin binds to DNA mainly through electrostatic interactions (Kang et al. 2004). Linear dichroism spectra analysis and infrared attenuated total reflection spectroscopy of quercetin, morin, and rutin revealed that electrostatic forces are favored at high DNA concentrations (Solimani 1997). Nevertheless, whatever the nature of the developed chemical forces, it seems that "intercalating" flavonoid molecules cover the polyanionic nucleic acid surface and do not alter the flexibility and hydrodynamic behavior of DNA. This suggests a protective role of flavonoids on DNA nucleophilic groups. Detailed structural analysis showed that quercetin, kaempferol, and delphinidin bound weakly to adenine, guanine (major groove), and thymine (minor groove) bases, as well as to the backbone phosphate group. Delphinidin, possessing a positive charge, induced a greater stabilizing effect on DNA duplex than quercetin and kaempferol, while a partial B-DNA to A-DNA transition occurred (Kanakis et al. 2005). Similarly, curcumin binding was limited in the minor groove of the double helix, and was sensitive to pH and salt concentrations (Zsila et al. 2004). Baicalein intercalated within the double helix too, an effect followed by possible interstrand cross-linking (Rossi et al. 2001). Furthermore, resveratrol and genistein interacted with DNA and RNA through base pairs and phosphate backbone groups (Usha et al. 2005). Another study, dealing with flavonoid oligomers, showed that anthocyanins significantly increased DNA stability, whereas the presence of a catechol B-ring and the scarcity of sugar substitution enhanced this action (Mas et al. 2000). In addition, EGCG binds to both DNA and RNA. Its galloyl and catechol groups are essential for DNA binding and it seems that this binding protects double-stranded DNA (dsDNA) oligomers from melting to single stranded (Kuzuhara et al. 2006).

In culture systems, flavonoids were efficient inhibitors of mutagenesis, induced by liver microsomal substrates. Their beneficial effect was not due to the modification of cytochrome P450 activity, but rather to a possible direct interaction with DNA (Edenharder et al. 1997). Moreover, treatment of RKO cells (a human colorectal carcinoma expressing E6 and E7 HPV transforming proteins) with sublethal concentrations of Polyphenon-100, a dietary supplement consisting of green tea catechins mixture, resulted in increased microsatellite sequence stability, while the expression of mismatch repair genes hMLH-1 and hMSH-2 remained unaffected (Ye et al. 2002). In this respect, a variety of DNA interacting proteins such as topoisomerases, polymerases, and acetylases might be involved.

DNA topoisomerases I and II are essential for cell survival and play a critical role in DNA metabolism and structure. Inhibitors of topoisomerases constitute a novel family of antitumor agents, with confirmed clinical activity in human malignancies. However, their clinical application is limited due to severe toxic effects on nontumor or normal cells. The use of polyphenols could overcome this limitation, as polyphenols exert differential effects on cancer cells and their normal counterparts. In vitro screening of the action of flavonoids on topoisomerase enzymes revealed that the majority of tested compounds are potential topoisomerase I and/or II inhibitors. This is achieved through both inhibition of relaxation activity and stabilization of the cleavable complex (poisoning) (Constantinou et al. 1995). Flavones and flavonols were more effective, while subtle pH changes can significantly affect their concomitant biologic activity (Webb and Ebeler 2004). Indeed, luteolin could directly interact with topoisomerase I catalytic subunit and intercalate to DNA, without binding to helices' minor groove. The resulting inhibition of topoisomerase I activity by luteolin was due to the stabilization of the topoisomerase-I DNA-cleavable complexes (Chowdhury et al. 2002). EGCG was also shown to inhibit topoisomerase I but not topoisomerase II activity in several human colon carcinoma cell lines (Berger et al. 2001), whereas quercetin,

acacetin, apigenin, kaempferol, and morin, inhibited topoisomerase I-catalyzed DNA religation by stabilizing the covalent enzyme-DNA complex in human HL-60 leukemia cells (Boege et al. 1996). However, catalytic moiety inhibitors could prevent DNA damage, while DNA-intercalative agents, such as fisetin and quercetin, seemed to enhance strand breaks formation and are considered as clastogenic. Indeed, genistein treatment resulted in mutagenesis, as it induced micronuclei formation and DNA migration in L5178Y mouse lymphoma cells (Boos and Stopper 2000). Although this effect was apparent within 1 h in a number of colon cancer cells, it was not a prerequisite for the induction of apoptosis (Salti et al. 2000). In addition, in a comparative study, it was found that quercetin differential clastogenic activity on HL-60 myeloblastic leukemia cell line and its H_2O_2-resistant clone was due to the prooxidant effect of the agent. Quercetin was less effective than luteolin regarding the inhibition of topoisomerase activity, while it increased the formation of 8-oxodG, an indicator of oxidative DNA damage (Yamashita and Kawanishi 2000). As flavonoid treatment of V79 Chinese hamster lung fibroblasts showed that catalytic topoisomerase inhibitors (biochanin, galangin and daidzein) could decrease or abolish the clastogenic properties of topoisomerase polyphenols poisons, it was assumed that total plant extracts could present different activities than their constituent phenolics (Snyder and Gillies 2003).

Recently, in an approach to explain the diverse actions of polyphenols, Howitz et al. suggested that the antiproliferative and oncosuppressive properties of resveratrol might be due to a mechanism that mimics caloric restriction and lifespan extension, and involves the sirtuin (SIRT) family of nicotinamide adenine dinucleotide $(NAD)^+$-dependent acetylases (Howitz et al. 2003). More specifically, resveratrol was found to directly interact with SIRT1 deacetylase, resulting in decreased acetylation of p53, increased DNA stability, and finally cell survival. Redox formation was implicated in the inhibition of histone deacetylase (HDAC) activity, leading to a chronic inflammatory-like response (Rahman et al. 2004). In this respect, resveratrol is a promising agent in the reversal of oxidative stress and rescue of mutant phenotypes.

Moreover, resveratrol antiproliferative activity has been shown to correlate with its ability to inhibit DNA polymerases α and δ in vitro (Stivala et al. 2001). Kaempferol and quercetin glycosides were found to inhibit mammalian replicative DNA polymerases α, δ, and ϵ, but not their β, κ, and λisomers (Mizushina et al. 2003). Kaempferol glycoside was a stronger and more selective inhibitor of DNA polymerase α than quercetin glycoside. However, the glycosides did not influence the activities of other mammalian DNA metabolic enzymes, such as human immunodeficiency virus (HIV)-1 reverse transcriptase, human telomerase, human DNA topoisomerases I and II, T7 RNA polymerase, and bovine deoxyribonuclease I. Detailed analysis of flavonoid aglycones revealed a variable degree of inhibition on a number of targeted enzymes: baicalein was moderately inhibitory to DNA polymerase-γ; quercetin was strongly inhibitory to DNA polymerase-β; quercetagetin was a potent inhibitor for DNA polymerases α, β, γ, and RNA polymerase; and myricetin was a strong inhibitor of DNA polymerase α and RNA polymerase. In all cases, terminal deoxynucleotidyl transferase was virtually insensitive. The presumptive mechanism involves competition with the template/primer in the case of the DNA polymerases, or competition with the triphosphate substrate (GTP) in the case of RNA polymerase (Ono and Nakane 1990).

Finally, due to the above competitive mechanism, quercetin, quercetagetin, myricetin, and especially baicalein were potent inhibitors of murine leukemia virus (MLV) (Rauscher and Moloney strains) and HIV-1 reverse transcriptases (Ono et al. 1989). Comparative studies with other flavonoids (hydroxyflavones, dihydroxyflavones and polyhydroxyflavones, and flavanones) revealed that the presence of both the unsaturated double bond between po-

sitions 2 and 3 of the flavonoid pyrone ring, and the three hydroxyl groups introduced in positions 5, 6, and 7, (i.e., baicalein) were a prerequisite for the inhibition of reverse transcriptase activity (Ono et al. 1989). In this respect, polyphenols could be effective in hindering the progression of viral infections. Further experiments have shown that flavonoids could downregulate viral entry also through inhibition of RNA polymerase II (Chao and Price 2001). HIV-1 protease activity was also suppressed by a number of flavones, flavanones, flavonols, catechols, and chalcones, whereas flavonols (quercetin, butein, and luteolin) were the most active (Xu et al. 2000). However, most flavonoid–enzymes interactions have been observed in solution, and hence are of questionable biologic value. In a first attempt to investigate a possible biologic action of these substances, flavopiridol, a synthetic flavonoid, first described as an antitumor agent and currently subjected to clinical trials, has been recently shown to block human immunodeficiency virus Tat transactivation and viral replication, through inhibition of positive transcription elongation factor b (P-TEFb or Cdk9/cyclin T1). Flavopiridol biologic activity is related to the phosphorylation of both RNA polymerase sII and the large subunit of the 5,6-dichloro-1-β-D-ribofuranosylbenzimidazole (DRB)-sensitivity-inducing factor, rather than inhibition of RNA polymerase itself (Chao and Price 2001).

In summary, the inhibitory effect of polyphenols can also be attributed to their ability to act as DNA intercalators or to interact with enzymes involved in DNA replication, recombination, repair, and transcription. Indeed, they can bind to DNA, cover the polyanionic nucleic acid surface, and thus protect DNA nucleophilic groups. They can bind weakly to adenine, guanine, and thymine bases, as well as to the backbone phosphate group. Therefore, they increase DNA stability and inhibit mutagenesis. In addition to their direct interaction with DNA, they can also interfere with DNA interacting enzymes such as topoisomerases, polymerases, and acetylases. They can act as topoisomerase I and/or II inhibitors, affecting the relaxation activity and the stabilization of the cleavage complex. Moreover, they can interact with SIRT1 deacetylase, and inhibit DNA polymerases and MLV and HIV-1 reverse transcriptases.

Conclusions

From the above review it becomes obvious that polyphenols, major micronutrients of almost any plant food and beverage, have, in addition to their antioxidant action, major implications on a number of basic cell mechanisms. These actions involve almost the whole spectrum of cellular basic machinery—from the cell membrane to signaling cytoplasmic molecules and to the major nuclear components—and provide insights into their health-beneficial effects. In addition, their actions justify the scientific interest in this class of compounds, and provide clues about their possible pharmaceutical exploitation in the field of oncology.

Acknowledgements. Some data of our group presented here were supported partially from an EU grant (COOP-CT-2003-508649 Project PARADOX). A.P.N. holds a scholarship from the Public Benefit Foundation A.S. Onassis.

References

Adhami VM, Siddiqui IA, Ahmad N, Gupta S, Mukhtar H (2004) Oral consumption of green tea polyphenols inhibits insulin-like growth factor-I-induced signaling in an autochthonous mouse model of prostate cancer. Cancer Res 64:8715–8722

Afaq F, Adhami VM, Ahmad N, Mukhtar H (2002) Botanical antioxidants for chemoprevention of photocarcinogenesis. Front Biosci 7:d784–d792

Afaq F, Ahmad N, Mukhtar H (2003) Suppression of UVB-induced phosphorylation of mitogen-activated protein kinases and nuclear factor κB by green tea polyphenol in SKH-1 hairless mice. Oncogene 22:9254–9264

Agullo G, Gamet-Payrastre L, Fernandez Y, Anciaux N, Demigne C, Remesy C (1996) Comparative effects of flavonoids on the growth, viability and metabolism of a colonic adenocarcinoma cell line (HT29 cells). Cancer Lett 105:61–70

Ahmad A, Farhan Asad S, Singh S, Hadi SM (2000) DNA breakage by resveratrol and Cu(II): reaction mechanism and bacteriophage inactivation. Cancer Lett 154:29–37

Ahmad N, Adhami VM, Afaq F, Feyes DK, Mukhtar H (2001) Resveratrol causes WAF-1/p21-mediated G(1)-phase arrest of cell cycle and induction of apoptosis in human epidermoid carcinoma A431 cells. Clin Cancer Res 7:1466–1473

Ahmed MS, Ramesh V, Nagaraja V, Parish JH, Hadi SM (1994) Mode of binding of quercetin to DNA. Mutagenesis 9:193–197

Ahn HY, Hadizadeh KR, Seul C, Yun YP, Vetter H, Sachinidis A (1999) Epigallocatechin-3 gallate selectively inhibits the PDGF-BB-induced intracellular signaling transduction pathway in vascular smooth muscle cells and inhibits transformation of sis-transfected NIH 3T3 fibroblasts and human glioblastoma cells (A172). Mol Biol Cell 10:1093–1104

Akiyama T, Ishida J, Nakagawa S, Ogawara H, Watanabe S, Itoh N, Shibuya M, Fukami Y (1987) Genistein, a specific inhibitor of tyrosine-specific protein kinases. J Biol Chem 262:5592–5595

Alhasan SA, Aranha O, Sarkar FH (2001) Genistein elicits pleiotropic molecular effects on head and neck cancer cells. Clin Cancer Res 7:4174–4181

Alia M, Mateos R, Ramos S, Lecumberri E, Bravo L, Goya L (2005) Influence of quercetin and rutin on growth and antioxidant defense system of a human hepatoma cell line (HepG2). Eur J Nutr 5:19–28

Alvi NK, Rizvi RY, Hadi SM (1986) Interaction of quercetin with DNA. Biosci Rep 6:861–868

Annabi B, Lachambre MP, Bousquet-Gagnon N, Page M, Gingras D, Beliveau R (2002) Green tea polyphenol (–)-epigallocatechin 3-gallate inhibits MMP-2 secretion and MT1-MMP-driven migration in glioblastoma cells. Biochim Biophys Acta 1542:209–220

Annaraj J, Srinivasan S, Ponvel KM, Athappan P (2005) Mixed ligand copper(II) complexes of phenanthroline/bipyridyl and curcumin diketimines as DNA intercalators and their electrochemical behavior under Nafion and clay modified electrodes. J Inorg Biochem 99:669–676

Atten MJ, Attar BM, Milson T, Holian O (2001) Resveratrol-induced inactivation of human gastric adenocarcinoma cells through a protein kinase C-mediated mechanism. Biochem Pharmacol 62:1423–1432

Azios NG, Dharmawardhane SF (2005) Resveratrol and estradiol exert disparate effects on cell migration, cell surface actin structures, and focal adhesion assembly in MDA-MB-231 human breast cancer cells. Neoplasia 7:128–140

Bagli E, Stefaniotou M, Morbidelli L, Ziche M, Psillas K, Murphy C, Fotsis T (2004) Luteolin inhibits vascular endothelial growth factor-induced angiogenesis; inhibition of endothelial cell survival and proliferation by targeting phosphatidylinositol 3′-kinase activity. Cancer Res 64:7936–7946

Balasubramanian S, Efimova T, Eckert RL (2002) Green tea polyphenol stimulates a Ras, MEKK1, MEK3, and p38 cascade to increase activator protein 1 factor-dependent involucrin gene expression in normal human keratinocytes. J Biol Chem 277:1828–1836

Banerjee T, Van der Vliet A, Ziboh VA (2002) Downregulation of COX-2 and iNOS by amentoflavone and quercetin in A549 human lung adenocarcinoma cell line. Prostaglandins Leukot Essent Fatty Acids 66:485–492

Barbaste M, Berke B, Dumas M, Soulet S, Delaunay JC, Castagnino C, Arnaudinaud V, Cheze C, Vercauteren J (2002) Dietary antioxidants, peroxidation and cardiovascular risks. J Nutr Health Aging 6:209–223

Beltz LA, Bayer DK, Moss AL, Simet IM (2006) Mechanisms of cancer prevention by green and black tea polyphenols. Anticancer Agents Med Chem 6:389–406

Berger SJ, Gupta S, Belfi CA, Gosky DM, Mukhtar H (2001) Green tea constituent (–)-epigallocatechin-3-gallate inhibits topoisomerase I activity in human colon carcinoma cells. Biochem Biophys Res Commun 288:101–105

Boege F, Straub T, Kehr A, Boesenberg C, Christiansen K, Andersen A, Jakob F, Kohrle J (1996) Selected novel flavones inhibit the DNA binding or the DNA religation step of eukaryotic topoisomerase I. J Biol Chem 271:2262–2270

Boileau TW, Liao Z, Kim S, Lemeshow S, Erdman JW Jr, Clinton SK (2003) Prostate carcinogenesis in N-methyl-N-nitrosourea (NMU)-testosterone-treated rats fed tomato powder, lycopene, or energy-restricted diets. J Natl Cancer Inst 95:1578–1586

Bonaccorsi L, Muratori M, Carloni V, Marchiani S, Formigli L, Forti G, Baldi E (2004) The androgen receptor associates with the epidermal growth factor receptor in androgen-sensitive prostate cancer cells. Steroids 69:549–552

Boone CW, Kelloff GJ, Malone WE (1990) Identification of cancer chemopreventive agents and their evaluation in animal models and human clinical trials. Cancer Res 50:2–9

Boos G, Stopper H (2000) Genotoxicity of several clinically used topoisomerase II inhibitors. Toxicol Lett 116:7–16

Borbulevych OY, Jankun J, Selman SH, Skrzypczak-Jankun E (2004) Lipoxygenase interactions with natural flavonoid, quercetin, reveal a complex with protocatechuic acid in its X-ray structure at 2.1 A resolution. Proteins 54:13–19

Bowers JL, Tyulmenkov VV, Jernigan SC, Klinge CM (2000) Resveratrol acts as a mixed agonist/antagonist for estrogen receptors alpha and beta. Endocrinology 141:3657–3667

Brownson DM, Azios NG, Fuqua BK, Dharmawardhane SF, Mabry TJ (2002) Flavonoid effects relevant to cancer. J Nutr 132:3482S–3489S

Bruder JL, Hsieh Tc T, Lerea KM, Olson SC, Wu JM (2001) Induced cytoskeletal changes in bovine pulmonary artery endothelial cells by resveratrol and the accompanying modified responses to arterial shear stress. BMC Cell Biol 2:1

Burkhardt S, Reiter RJ, Tan DX, Hardeland R, Cabrera J, Karbownik M (2001) DNA oxidatively damaged by chromium(III) and H(2)O(2) is protected by the antioxidants melatonin, N(1)-acetyl-N(2)-formyl-5-methoxykynuramine, resveratrol and uric acid. Int J Biochem Cell Biol 33:775–783

Bylund A, Zhang JX, Bergh A, Damber JE, Widmark A, Johansson A, Adlercreutz H, Aman P, Shepherd MJ, Hallmans G (2000) Rye bran and soy protein delay growth and increase apoptosis of human LNCaP prostate adenocarcinoma in nude mice. Prostate 42:304–314

Cao Z, Fang J, Xia C, Shi X, Jiang BH (2004) *trans*-3,4,5′-Trihydroxystilbene inhibits hypoxia-inducible factor 1alpha and vascular endothelial growth factor expression in human ovarian cancer cells. Clin Cancer Res 10:5253–5263

Chang TK, Lee WB, Ko HH (2000) *trans*-Resveratrol modulates the catalytic activity and mRNA expression of the procarcinogen-activating human cytochrome P450 1B1. Can J Physiol Pharmacol 78:874–881

Chang WH, Chen CH, Gau RJ, Lin CC, Tsai CL, Tsai K, Lu FJ (2002) Effect of baicalein on apoptosis of the human Hep G2 cell line was induced by mitochondrial dysfunction. Planta Med 68:302–306

Chao SH, Price DH (2001) Flavopiridol inactivates P-TEFb and blocks most RNA polymerase II transcription in vivo. J Biol Chem 276:31793–31799

Chen CC, Chow MP, Huang WC, Lin YC, Chang YJ (2004a) Flavonoids inhibit tumor necrosis factor-alpha-induced up-regulation of intercellular adhesion molecule-1 (ICAM-1) in respiratory epithelial cells through activator protein-1 and nuclear factor-kappaB: structure-activity relationships. Mol Pharmacol 66:683–693

Chen CH, Huang LL, Huang CC, Lin CC, Lee Y, Lu FJ (2000) Baicalein, a novel apoptotic agent for hepatoma cell lines: a potential medicine for hepatoma. Nutr Cancer 38:287–295

Chen D, Daniel KG, Chen MS, Kuhn DJ, Landis-Piwowar KR, Dou QP (2005) Dietary flavonoids as proteasome inhibitors and apoptosis inducers in human leukemia cells. Biochem Pharmacol 69:1421–1432

Chen HW, Huang HC (1998) Effect of curcumin on cell cycle progression and apoptosis in vascular smooth muscle cells. Br J Pharmacol 124:1029–1040

Chen J, Wersinger C, Sidhu A (2003) Chronic stimulation of D1 dopamine receptors in human SK-N-MC neuroblastoma cells induces nitric-oxide synthase activation and cytotoxicity. J Biol Chem 278:28089–28100

Chen JJ, Ye ZQ, Koo MW (2004b) Growth inhibition and cell cycle arrest effects of epigallocatechin gallate in the NBT-II bladder tumour cell line. BJU Int 93:1082–1086

Chen S, Ruan Q, Bedner E, Deptala A, Wang X, Hsieh TC, Traganos F, Darzynkiewicz Z (2001) Effects of the flavonoid baicalin and its metabolite baicalein on androgen receptor expression, cell cycle progression and apoptosis of prostate cancer cell lines. Cell Prolif 34:293–304

Chen W, Dong Z, Valcic S, Timmermann BN, Bowden GT (1999) Inhibition of ultraviolet B-induced c-fos gene expression and p38 mitogen-activated protein kinase activation by (–)-epigallocatechin gallate in a human keratinocyte cell line. Mol Carcinog 24:79–84

Chen X, Hasuma T, Yano Y, Yoshimata T, Morishima Y, Wang Y, Otani S (1997) Inhibition of farnesyl protein transferase by monoterpene, curcumin derivatives and gallotannin. Anticancer Res 17:2555–2564

Choi JA, Kim JY, Lee JY, Kang CM, Kwon HJ, Yoo YD, Kim TW, Lee YS, Lee SJ (2001) Induction of cell cycle arrest and apoptosis in human breast cancer cells by quercetin. Int J Oncol 19:837–844

Chowdhury AR, Sharma S, Mandal S, Goswami A, Mukhopadhyay S, Majumder HK (2002) Luteolin, an emerging anti-cancer flavonoid, poisons eukaryotic DNA topoisomerase I. Biochem J 366:653–661

Chung JY, Huang C, Meng X, Dong Z, Yang CS (1999) Inhibition of activator protein 1 activity and cell growth by purified green tea and black tea polyphenols in H-ras-transformed cells: structure-activity relationship and mechanisms involved. Cancer Res 59:4610–4617

Chung JY, Park JO, Phyu H, Dong Z, Yang CS (2001) Mechanisms of inhibition of the Ras-MAP kinase signaling pathway in 30. 7b Ras 12 cells by tea polyphenols (–)-epigallocatechin-3-gallate and theaflavin-3,3′-digallate. FASEB J 15:2022–2024

Ciolino HP, Yeh GC (1999) Inhibition of aryl hydrocarbon-induced cytochrome P-450 1A1 enzyme activity and CYP1A1 expression by resveratrol. Mol Pharmacol 56:760–767

Clement MV, Hirpara JL, Chawdhury SH, Pervaiz S (1998) Chemopreventive agent resveratrol, a natural product derived from grapes, triggers CD95 signaling-dependent apoptosis in human tumor cells. Blood 92:996–1002

Code EL, Crespi CL, Penman BW, Gonzalez FJ, Chang TK, Waxman DJ (1997) Human cytochrome P4502B6: interindividual hepatic expression, substrate specificity, and role in procarcinogen activation. Drug Metab Dispos 25:985–993

Constantinou A, Mehta R, Runyan C, Rao K, Vaughan A, Moon R (1995) Flavonoids as DNA topoisomerase antagonists and poisons: structure-activity relationships. J Nat Prod 58:217–225

Corder R, Warburton RC, Khan NQ, Brown RE, Wood EG, Lees DM (2004) The procyanidin-induced pseudo laminar shear stress response: a new concept for the reversal of endothelial dysfunction. Clin Sci (Lond) 107:513–517

Czyz J, Madeja Z, Irmer U, Korohoda W, Hulser DF (2005) Flavonoid apigenin inhibits motility and invasiveness of carcinoma cells in vitro. Int J Cancer 114:12–18

Damianaki A, Bakogeorgou E, Kampa M, Notas G, Hatzoglou A, Panagiotou S, Gemetzi C, Kouroumalis E, Martin PM, Castanas E (2000) Potent inhibitory action of red wine polyphenols on human breast cancer cells. J Cell Biochem 78:429–441

Dell'Aica I, Dona M, Sartor L, Pezzato E, Garbisa S (2002) (–)Epigallocatechin-3-gallate directly inhibits MT1-MMP activity, leading to accumulation of nonactivated MMP-2 at the cell surface. Lab Invest 82:1685–1693

Dong Z, Ma W, Huang C, Yang CS (1997) Inhibition of tumor promoter-induced activator protein 1 activation and cell transformation by tea polyphenols, (–)-epigallocatechin gallate, and theaflavins. Cancer Res 57:4414–4419

Edenharder R, Rauscher R, Platt KL (1997) The inhibition by flavonoids of 2-amino-3-methylimidazo[4,5-f]quinoline metabolic activation to a mutagen: a structure-activity relationship study. Mutat Res 379:21–32

Ermakova S, Choi BY, Choi HS, Kang BS, Bode AM, Dong Z (2005) The intermediate filament protein vimentin is a new target for epigallocatechin gallate. J Biol Chem 280:16882–16890

Fang J, Xia C, Cao Z, Zheng JZ, Reed E, Jiang BH (2005) Apigenin inhibits VEGF and HIF-1 expression via PI3K/AKT/p70S6K1 and HDM2/p53 pathways. FASEB J 19:342–353

Fassina G, Vene R, Morini M, Minghelli S, Benelli R, Noonan DM, Albini A (2004) Mechanisms of inhibition of tumor angiogenesis and vascular tumor growth by epigallocatechin-3-gallate. Clin Cancer Res 10:4865–4873

Ferrer P, Asensi M, Segarra R, Ortega A, Benlloch M, Obrador E, Varea MT, Asensio G, Jorda L, Estrela JM (2005) Association between pterostilbene and quercetin inhibits metastatic activity of B16 melanoma. Neoplasia 7:37–47

Gali-Muhtasib HU, Yamout SZ, Sidani MM (2000) Tannins protect against skin tumor promotion induced by ultraviolet-B radiation in hairless mice. Nutr Cancer 37:73–77

Gao X, Xu YX, Divine G, Janakiraman N, Chapman RA, Gautam SC (2002) Disparate in vitro and in vivo antileukemic effects of resveratrol, a natural polyphenolic compound found in grapes. J Nutr 132:2076–2081

Garbisa S, Sartor L, Biggin S, Salvato B, Benelli R, Albini A (2001) Tumor gelatinases and invasion inhibited by the green tea flavanol epigallocatechin-3-gallate. Cancer 91:822–832

Gehm BD, McAndrews JM, Chien PY, Jameson JL (1997) Resveratrol, a polyphenolic compound found in grapes and wine, is an agonist for the estrogen receptor. Proc Natl Acad Sci USA 94:14138–14143

Gioeli D, Mandell JW, Petroni GR, Frierson HF Jr, Weber MJ (1999) Activation of mitogen-activated protein kinase associated with prostate cancer progression. Cancer Res 59:279–284

Godichaud S, Krisa S, Couronne B, Dubuisson L, Merillon JM, Desmouliere A, Rosenbaum J (2000) Deactivation of cultured human liver myofibroblasts by *trans*-resveratrol, a grapevine-derived polyphenol. Hepatology 31:922–931

Goldbohm RA, Hertog MG, Brants HA, van Poppel G, van den Brandt PA (1996) Consumption of black tea and cancer risk: a prospective cohort study. J Natl Cancer Inst 88:93–100

Goodin MG, Fertuck KC, Zacharewski TR, Rosengren RJ (2002) Estrogen receptor-mediated actions of polyphenolic catechins in vivo and in vitro. Toxicol Sci 69:354–361

Gosse F, Guyot S, Roussi S, Lobstein A, Fischer B, Seiler N, Raul F (2005) Chemopreventive properties of apple procyanidins on human colon cancer-derived metastatic SW620 cells and in a rat model of colon carcinogenesis. Carcinogenesis 26:1291–1295

Guo JM, Kang GZ, Xiao BX, Liu DH, Zhang S (2004) Effect of daidzein on cell growth, cell cycle, and telomerase activity of human cervical cancer in vitro. Int J Gynecol Cancer 14:882–888

Gupta S, Hastak K, Ahmad N, Lewin JS, Mukhtar H (2001) Inhibition of prostate carcinogenesis in TRAMP mice by oral infusion of green tea polyphenols. Proc Natl Acad Sci USA 98:10350–10355

Gupta S, Hussain T, Mukhtar H (2003) Molecular pathway for (–)-epigallocatechin-3-gallate-induced cell cycle arrest and apoptosis of human prostate carcinoma cells. Arch Biochem Biophys 410:177–185

Harris SR, Thorgeirsson UP (1997) Flavone acetic acid stimulates nitric oxide and peroxynitrite production in subcutaneous mouse tumors. Biochem Biophys Res Commun 235:509–514

Hastak K, Gupta S, Ahmad N, Agarwal MK, Agarwal ML, Mukhtar H (2003) Role of p53 and NF-kappaB in epigallocatechin-3-gallate-induced apoptosis of LNCaP cells. Oncogene 22:4851–4859

Hastak K, Agarwal MK, Mukhtar H, Agarwal ML (2005) Ablation of either p21 or Bax prevents p53-dependent apoptosis induced by green tea polyphenol epigallocatechin-3-gallate. FASEB J 19:789–791

Higdon JV, Frei B (2003) Tea catechins and polyphenols: health effects, metabolism, and antioxidant functions. Crit Rev Food Sci Nutr 43:89–143

Hofmann CS, Sonenshein GE (2003) Green tea polyphenol epigallocatechin-3 gallate induces apoptosis of proliferating vascular smooth muscle cells via activation of p53. FASEB J 17:702–704

Holian O, Wahid S, Atten MJ, Attar BM (2002) Inhibition of gastric cancer cell proliferation by resveratrol: role of nitric oxide. Am J Physiol Gastrointest Liver Physiol 282:G809–G816

Hong J, Smith TJ, Ho CT, August DA, Yang CS (2001) Effects of purified green and black tea polyphenols on cyclooxygenase- and lipoxygenase-dependent metabolism of arachidonic acid in human colon mucosa and colon tumor tissues. Biochem Pharmacol 62:1175–1183

Hong J, Lu H, Meng X, Ryu JH, Hara Y, Yang CS (2002) Stability, cellular uptake, biotransformation, and efflux of tea polyphenol (–)-epigallocatechin-3-gallate in HT-29 human colon adenocarcinoma cells. Cancer Res 62:7241–7246

Hong J, Bose M, Ju J, Ryu JH, Chen X, Sang S, Lee MJ, Yang CS (2004) Modulation of arachidonic acid metabolism by curcumin and related beta-diketone derivatives: effects on cytosolic phospholipase A(2), cyclooxygenases and 5-lipoxygenase. Carcinogenesis 25:1671–1679

Howitz KT, Bitterman KJ, Cohen HY, Lamming DW, Lavu S, Wood JG, Zipkin RE, Chung P, Kisielewski A, Zhang LL, Scherer B, Sinclair DA (2003) Small molecule activators of sirtuins extend Saccharomyces cerevisiae lifespan. Nature 425:191–196

Hsieh TC, Wu JM (2000) Grape-derived chemopreventive agent resveratrol decreases prostate-specific antigen (PSA) expression in LNCaP cells by an androgen receptor (AR)-independent mechanism. Anticancer Res 20:225–228

Hsieh TC, Burfeind P, Laud K, Backer JM, Traganos F, Darzynkiewicz Z, Wu JM (1999a) Cell cycle effects and control of gene expression by resveratrol in human breast carcinoma cell lines with different metastatic potentials. Int J Oncol 15:245–252

Hsieh TC, Juan G, Darzynkiewicz Z, Wu JM (1999b) Resveratrol increases nitric oxide synthase, induces accumulation of p53 and p21(WAF1/CIP1), and suppresses cultured bovine pulmonary artery endothelial cell proliferation by perturbing progression through S and G2. Cancer Res 59:2596–2601

Hsu JT, Ying C, Chen CJ (2000) Regulation of inducible nitric oxide synthase by dietary phytoestrogen in MCF-7 human mammary cancer cells. Reprod Nutr Dev 40:11–18

Hsu S, Lewis J, Singh B, Schoenlein P, Osaki T, Athar M, Porter AG, Schuster G (2003) Green tea polyphenol targets the mitochondria in tumor cells inducing caspase 3-dependent apoptosis. Anticancer Res 23:1533–1539

Hu G, Han C, Chen J (1995) Inhibition of oncogene expression by green tea and (–)-epigallocatechin gallate in mice. Nutr Cancer 24:203–209

Huang X, Chen S, Xu L, Liu Y, Deb DK, Platanias LC, Bergan RC (2005) Genistein inhibits p38 map kinase activation, matrix metalloproteinase type 2, and cell invasion in human prostate epithelial cells. Cancer Res 65:3470–3478

Huang YT, Hwang JJ, Lee PP, Ke FC, Huang JH, Huang CJ, Kandaswami C, Jr ME, Lee MT (1999) Effects of luteolin and quercetin, inhibitors of tyrosine kinase, on cell growth and metastasis-associated properties in A431 cells overexpressing epidermal growth factor receptor. Br J Pharmacol 128:999–1010

Huynh H, Nguyen TT, Chan E, Tran E (2003) Inhibition of ErbB-2 and ErbB-3 expression by quercetin prevents transforming growth factor alpha (TGF-alpha)- and epidermal growth factor (EGF)-induced human PC-3 prostate cancer cell proliferation. Int J Oncol 23:821–829

Inano H, Onoda M (2002) Prevention of radiation-induced mammary tumors. Int J Radiat Oncol Biol Phys 52:212–223

Jang M, Pezzuto JM (1999) Cancer chemopreventive activity of resveratrol. Drugs Exp Clin Res 25:65–77

Jiang C, Agarwal R, Lu J (2000) Anti-angiogenic potential of a cancer chemopreventive flavonoid antioxidant, silymarin: inhibition of key attributes of vascular endothelial cells and angiogenic cytokine secretion by cancer epithelial cells. Biochem Biophys Res Commun 276:371–378

Jung YD, Kim MS, Shin BA, Chay KO, Ahn BW, Liu W, Bucana CD, Gallick GE, Ellis LM (2001) EGCG, a major component of green tea, inhibits tumour growth by inhibiting VEGF induction in human colon carcinoma cells. Br J Cancer 84:844–850

Kampa M, Hatzoglou A, Notas G, Damianaki A, Bakogeorgou E, Gemetzi C, Kouroumalis E, Martin PM, Castanas E (2000) Wine antioxidant polyphenols inhibit the proliferation of human prostate cancer cell lines. Nutr Cancer 37:223–233

Kampa M, Alexaki VI, Notas G, Nifli AP, Nistikaki A, Hatzoglou A, Bakogeorgou E, Kouimtzoglou E, Blekas G, Boskou D, Gravanis A, Castanas E (2004) Antiproliferative and apoptotic effects of selective phenolic acids on T47D human breast cancer cells: potential mechanisms of action. Breast Cancer Res 6:R63–74

Kanakis CD, Tarantilis PA, Polissiou MG, Diamantoglou S, Tajmir-Riahi HA (2005) DNA interaction with naturally occurring antioxidant flavonoids quercetin, kaempferol, and delphinidin. J Biomol Struct Dyn 22:719–724

Kaneuchi M, Sasaki M, Tanaka Y, Sakuragi N, Fujimoto S, Dahiya R (2003a) Quercetin regulates growth of Ishikawa cells through the suppression of EGF and cyclin D1. Int J Oncol 22:159–164

Kaneuchi M, Sasaki M, Tanaka Y, Yamamoto R, Sakuragi N, Dahiya R (2003b) Resveratrol suppresses growth of Ishikawa cells through down-regulation of EGF. Int J Oncol 23:1167–1172

Kang J, Zhuo L, Lu X, Liu H, Zhang M, Wu H (2004) Electrochemical investigation on interaction between DNA with quercetin and Eu-Qu3 complex. J Inorg Biochem 98:79–86

Kanno S, Tomizawa A, Hiura T, Osanai Y, Shouji A, Ujibe M, Ohtake T, Kimura K, Ishikawa M (2005) Inhibitory effects of naringenin on tumor growth in human cancer cell lines and sarcoma S-180-implanted mice. Biol Pharm Bull 28:527–530

Kawabata K, Murakami A, Ohigashi H (2005) Nobiletin, a citrus flavonoid, down-regulates matrix metalloproteinase-7 (matrilysin) expression in HT-29 human colorectal cancer cells. Biosci Biotechnol Biochem 69:307–314

Kellner C, Zunino SJ (2004) Nitric oxide is synthesized in acute leukemia cells after exposure to phenolic antioxidants and initially protects against mitochondrial membrane depolarization. Cancer Lett 215:43–52

Kenny TP, Keen CL, Jones P, Kung HJ, Schmitz HH, Gershwin ME (2004) Pentameric procyanidins isolated from Theobroma cacao seeds selectively downregulate ErbB2 in human aortic endothelial cells. Exp Biol Med (Maywood) 229:255–263

Khan NS, Hadi SM (1998) Structural features of tannic acid important for DNA degradation in the presence of Cu(II). Mutagenesis 13:271–274

Kim HS, Kim MH, Jeong M, Hwang YS, Lim SH, Shin BA, Ahn BW, Jung YD (2004) EGCG blocks tumor promoter-induced MMP-9 expression via suppression of MAPK and AP-1 activation in human gastric AGS cells. Anticancer Res 24:747–753

Kim M, Murakami A, Kawabata K, Ohigashi H (2005) (–)-Epigallocatechin-3-gallate promotes pro-matrix metalloproteinase-7 production via activation of the JNK1/2 pathway in HT-29 human colorectal cancer cells. Carcinogenesis 26:1553–1562

Klampfer L, Huang J, Sasazuki T, Shirasawa S, Augenlicht L (2004) Oncogenic Ras promotes butyrate-induced apoptosis through inhibition of gelsolin expression. J Biol Chem 279:36680–36688

Klein RD, Fischer SM (2002) Black tea polyphenols inhibit IGF-I-induced signaling through Akt in normal prostate epithelial cells and Du145 prostate carcinoma cells. Carcinogenesis 23:217–221

Knowles LM, Zigrossi DA, Tauber RA, Hightower C, Milner JA (2000) Flavonoids suppress androgen-independent human prostate tumor proliferation. Nutr Cancer 38:116–122

Ko CH, Shen SC, Lin HY, Hou WC, Lee WR, Yang LL, Chen YC (2002) Flavanones structure-related inhibition on TPA-induced tumor promotion through suppression of extracellular signal-regulated protein kinases: involvement of prostaglandin E2 in anti-promotive process. J Cell Physiol 193:93–102

Kong AN, Yu R, Lei W, Mandlekar S, Tan TH, Ucker DS (1998) Differential activation of MAPK and ICE/Ced-3 protease in chemical-induced apoptosis. The role of oxidative stress in the regulation of mitogen-activated protein kinases (MAPKs) leading to gene expression and survival or activation of caspases leading to apoptosis. Restor Neurol Neurosci 12:63–70

Krishnan R, Raghunathan R, Maru GB (2005) Effect of polymeric black tea polyphenols on benzo(a)pyrene [B(a)P]-induced cytochrome P4501A1 and 1A2 in mice. Xenobiotica 35:671–682

Kudo M, Naito Z, Yokoyama M, Asano G (1999) Effects of quercetin and sunphenon on responses of cancer cells to heat shock damage. Exp Mol Pathol 66:66–75

Kuhn D, Lam WH, Kazi A, Daniel KG, Song S, Chow LM, Chan TH, Dou QP (2005) Synthetic peracetate tea polyphenols as potent proteasome inhibitors and apoptosis inducers in human cancer cells. Front Biosci 10:1010–1023

Kuntz S, Wenzel U, Daniel H (1999) Comparative analysis of the effects of flavonoids on proliferation, cytotoxicity, and apoptosis in human colon cancer cell lines. Eur J Nutr 38:133–142

Kuo PL, Lin CC (2003) Green tea constituent (–)-epigallocatechin-3-gallate inhibits Hep G2 cell proliferation and induces apoptosis through p53-dependent and Fas-mediated pathways. J Biomed Sci 10:219–227

Kuzuhara T, Sei Y, Yamaguchi K, Suganuma M, Fujiki H (2006) DNA and RNA as new binding targets of green tea catechins. J Biol Chem 281:17446–17456

Lambert JD, Yang CS (2003) Mechanisms of cancer prevention by tea constituents. J Nutr 133:3262S–3267S

Landau JM, Wang ZY, Yang GY, Ding W, Yang CS (1998) Inhibition of spontaneous formation of lung tumors and rhabdomyosarcomas in A/J mice by black and green tea. Carcinogenesis 19:501–507

Lee EJ, Min HY, Joo Park H, Chung HJ, Kim S, Nam Han Y, Lee SK (2004a) G2/M cell cycle arrest and induction of apoptosis by a stilbenoid, 3,4,5-trimethoxy-4′-bromo-cis-stilbene, in human lung cancer cells. Life Sci 75:2829–2839

Lee HZ, Leung HW, Lai MY, Wu CH (2005) Baicalein induced cell cycle arrest and apoptosis in human lung squamous carcinoma CH27 cells. Anticancer Res 25:959–964

Lee LT, Huang YT, Hwang JJ, Lee AY, Ke FC, Huang CJ, Kandaswami C, Lee PP, Lee MT (2004b) Transinactivation of the epidermal growth factor receptor tyrosine kinase and focal adhesion kinase phosphorylation by dietary flavonoids: effect on invasive potential of human carcinoma cells. Biochem Pharmacol 67:2103–2114

Lee SJ, Lee IS, Mar W (2003) Inhibition of inducible nitric oxide synthase and cyclooxygenase-2 activity by 1,2,3,4,6-penta-O-galloyl-beta-D-glucose in murine macrophage cells. Arch Pharm Res 26:832–839

Lee YK, Bone ND, Strege AK, Shanafelt TD, Jelinek DF, Kay NE (2004c) VEGF receptor phosphorylation status and apoptosis is modulated by a green tea component, epigallocatechin-3-gallate (EGCG), in B-cell chronic lymphocytic leukemia. Blood 104:788–794

Levin ER (2001) Cell localization, physiology, and nongenomic actions of estrogen receptors. J Appl Physiol 91:1860–1867

Li J, Billiar TR, Talanian RV, Kim YM (1997) Nitric oxide reversibly inhibits seven members of the caspase family via S-nitrosylation. Biochem Biophys Res Commun 240:419–424

Li N, Chen X, Liao J, Yang G, Wang S, Josephson Y, Han C, Chen J, Huang MT, Yang CS (2002) Inhibition of 7,12-dimethylbenz[a]anthracene (DMBA)-induced oral carcinogenesis in hamsters by tea and curcumin. Carcinogenesis 23:1307–1313

Liang YC, Lin-shiau SY, Chen CF, Lin JK (1997) Suppression of extracellular signals and cell proliferation through EGF receptor binding by (–)-epigallocatechin gallate in human A431 epidermoid carcinoma cells. J Cell Biochem 67:55–65

Liang YC, Lin-Shiau SY, Chen CF, Lin JK (1999) Inhibition of cyclin-dependent kinases 2 and 4 activities as well as induction of Cdk inhibitors p21 and p27 during growth arrest of human breast carcinoma cells by (–)-epigallocatechin-3-gallate. J Cell Biochem 75:1–12

Liang YC, Tsai SH, Chen L, Lin-Shiau SY, Lin JK (2003) Resveratrol-induced G2 arrest through the inhibition of CDK7 and p34CDC2 kinases in colon carcinoma HT29 cells. Biochem Pharmacol 65:1053–1060

Liberto M, Cobrinik D (2000) Growth factor-dependent induction of p21(CIP1) by the green tea polyphenol, epigallocatechin gallate. Cancer Lett 154:151–161

Lin CH, Lin YF, Chang MC, Wu CH, Ho YS, Lee HM (2001) Advanced glycosylation end products induce nitric oxide synthase expression in C6 glioma cells: involvement of a p38 MAP kinase-dependent mechanism. Life Sci 69:2503–2515

Lin JK (2004) Suppression of protein kinase C and nuclear oncogene expression as possible action mechanisms of cancer chemoprevention by curcumin. Arch Pharm Res 27:683–692

Lin SY, Tsai SJ, Wang LH, Wu MF, Lee H (2002) Protection by quercetin against cooking oil fumes-induced DNA damage in human lung adenocarcinoma CL-3 cells: role of COX-2. Nutr Cancer 44:95–101

Lin YL, Lin JK (1997) (–)-Epigallocatechin-3-gallate blocks the induction of nitric oxide synthase by down-regulating lipopolysaccharide-induced activity of transcription factor nuclear factor-kappaB. Mol Pharmacol 52:465–472

Liu XH, Kirschenbaum A, Lu M, Yao S, Dosoretz A, Holland JF, Levine AC (2002a) Prostaglandin E2 induces hypoxia-inducible factor-1alpha stabilization and nuclear localization in a human prostate cancer cell line. J Biol Chem 277:50081–50086

Liu XJ, Yang L, Mao YQ, Wang Q, Huang MH, Wang YP, Wu HB (2002b) Effects of the tyrosine protein kinase inhibitor genistein on the proliferation, activation of cultured rat hepatic stellate cells. World J Gastroenterol 8:739–745

Loktionova SA, Kabakov AE (1998) Protein phosphatase inhibitors and heat preconditioning prevent Hsp27 dephosphorylation, F-actin disruption and deterioration of morphology in ATP-depleted endothelial cells. FEBS Lett 433:294–300

MacCarrone M, Lorenzon T, Guerrieri P, Agro AF (1999) Resveratrol prevents apoptosis in K562 cells by inhibiting lipoxygenase and cyclooxygenase activity. Eur J Biochem 265:27–34

Maeda-Yamamoto M, Kawahara H, Tahara N, Tsuji K, Hara Y, Isemura M (1999) Effects of tea polyphenols on the invasion and matrix metalloproteinases activities of human fibrosarcoma HT1080 cells. J Agric Food Chem 47:2350–2354

Maggiolini M, Vivacqua A, Carpino A, Bonofiglio D, Fasanella G, Salerno M, Picard D, Ando S (2002) The mutant androgen receptor T877A mediates the proliferative but not the cytotoxic dose-dependent effects of genistein and quercetin on human LNCaP prostate cancer cells. Mol Pharmacol 62:1027–1035

Mahyar-Roemer M, Katsen A, Mestres P, Roemer K (2001) Resveratrol induces colon tumor cell apoptosis independently of p53 and precede by epithelial differentiation, mitochondrial proliferation and membrane potential collapse. Int J Cancer 94:615–622

Manson MM (2003) Cancer prevention—the potential for diet to modulate molecular signalling. Trends Mol Med 9:11–18

Mansour A, McCarthy B, Schwander SK, Chang V, Kotenko S, Donepudi S, Lee J, Raveche E (2004) Genistein induces G2 arrest in malignant B cells by decreasing IL-10 secretion. Cell Cycle 3:1597–1605

Martin S, Favot L, Matz R, Lugnier C, Andriantsitohaina R (2003a) Delphinidin inhibits endothelial cell proliferation and cell cycle progression through a transient activation of ERK-1/-2. Biochem Pharmacol 65:669–675

Martin S, Giannone G, Andriantsitohaina R, Martinez MC (2003b) Delphinidin, an active compound of red wine, inhibits endothelial cell apoptosis via nitric oxide pathway and regulation of calcium homeostasis. Br J Pharmacol 139:1095–1102

Mas T, Susperregui J, Berke B, Cheze C, Moreau S, Nuhrich A, Vercauteren J (2000) DNA triplex stabilization property of natural anthocyanins. Phytochemistry 53:679–687

Masuda M, Suzui M, Weinstein IB (2001) Effects of epigallocatechin-3-gallate on growth, epidermal growth factor receptor signaling pathways, gene expression, and chemosensitivity in human head and neck squamous cell carcinoma cell lines. Clin Cancer Res 7:4220–4229

Masuda M, Suzui M, Lim JT, Deguchi A, Soh JW, Weinstein IB (2002) Epigallocatechin-3-gallate decreases VEGF production in head and neck and breast carcinoma cells by inhibiting EGFR-related pathways of signal transduction. J Exp Ther Oncol 2:350–359

Mertens-Talcott SU, Bomser JA, Romero C, Talcott ST, Percival SS (2005) Ellagic acid potentiates the effect of quercetin on p21waf1/cip1, p53, and MAP-kinases without affecting intracellular generation of reactive oxygen species in vitro. J Nutr 135:609–614

Middleton E (1996) Biological properties of plant flavonoids: an overview. Int J Pharmacognosy 34:344–348

Minagawa A, Otani Y, Kubota T, Wada N, Furukawa T, Kumai K, Kameyama K, Okada Y, Fujii M, Yano M, Sato T, Ito A, Kitajima M (2001) The citrus flavonoid, nobiletin, inhibits peritoneal dissemination of human gastric carcinoma in SCID mice. Jpn J Cancer Res 92:1322–1328

Mitchell SH, Zhu W, Young CY (1999) Resveratrol inhibits the expression and function of the androgen receptor in LNCaP prostate cancer cells. Cancer Res 59:5892–5895

Miyahara Y, Komiya T, Katsuzaki H, Imai K, Nakagawa M, Ishi Y, Hibasami H (2000) Sesamin and episesamin induce apoptosis in human lymphoid leukemia Molt 4B cells. Int J Mol Med 6:43–46

Mizushina Y, Ishidoh T, Kamisuki S, Nakazawa S, Takemura M, Sugawara F, Yoshida H, Sakaguchi K (2003) Flavonoid glycoside: a new inhibitor of eukaryotic DNA polymerase alpha and a new carrier for inhibitor-affinity chromatography. Biochem Biophys Res Commun 301:480–487

Mnjoyan ZH, Fujise K (2003) Profound negative regulatory effects by resveratrol on vascular smooth muscle cells: a role of p53-p21(WAF1/CIP1) pathway. Biochem Biophys Res Commun 311:546–552

Moon YJ, Wang X, Morris ME (2006) Dietary flavonoids: effects on xenobiotic and carcinogen metabolism. Toxicol In Vitro 20:187–210

Mutoh M, Takahashi M, Fukuda K, Komatsu H, Enya T, Matsushima-Hibiya Y, Mutoh H, Sugimura T, Wakabayashi K (2000) Suppression by flavonoids of cyclooxygenase-2 promoter-dependent transcriptional activity in colon cancer cells: structure-activity relationship. Jpn J Cancer Res 91:686–691

Naasani I, Seimiya H, Tsuruo T (1998) Telomerase inhibition, telomere shortening, and senescence of cancer cells by tea catechins. Biochem Biophys Res Commun 249:391–396

Naasani I, Oh-Hashi F, Oh-Hara T, Feng WY, Johnston J, Chan K, Tsuruo T (2003) Blocking telomerase by dietary polyphenols is a major mechanism for limiting the growth of human cancer cells in vitro and in vivo. Cancer Res 63:824–830

Nagase H, Sasaki K, Kito H, Haga A, Sato T (1998) Inhibitory effect of delphinidin from Solanum melongena on human fibrosarcoma HT-1080 invasiveness in vitro. Planta Med 64:216–219

Nam S, Smith DM, Dou QP (2001) Tannic acid potently inhibits tumor cell proteasome activity, increases p27 and Bax expression, and induces G1 arrest and apoptosis. Cancer Epidemiol Biomarkers Prev 10:1083–1088

Nguyen TT, Tran E, Ong CK, Lee SK, Do PT, Huynh TT, Nguyen TH, Lee JJ, Tan Y, Ong CS, Huynh H (2003) Kaempferol-induced growth inhibition and apoptosis in A549 lung cancer cells is mediated by activation of MEK-MAPK. J Cell Physiol 197:110–121

Nguyen TT, Tran E, Nguyen TH, Do PT, Huynh TH, Huynh H (2004) The role of activated MEK-ERK pathway in quercetin-induced growth inhibition and apoptosis in A549 lung cancer cells. Carcinogenesis 25:647–659

Nichenametla SN, Taruscio TG, Barney DL, Exon JH (2006) A review of the effects and mechanisms of polyphenolics in cancer. Crit Rev Food Sci Nutr 46:161–183

Nie G, Jin C, Cao Y, Shen S, Zhao B (2002) Distinct effects of tea catechins on 6-hydroxydopamine-induced apoptosis in PC12 cells. Arch Biochem Biophys 397:84–90

Nifli A, Bosson-Kouame A, Papadopoulou N, Kogia C, Kampa M, Castagnino C, Stournaras C, Vercauteren J, Castanas E (2005a) Monomeric and oligomeric flavanols are agonists of membrane androgen receptors. Exp Cell Res 309:329–339

Nifli A, Kampa M, Alexaki V, Notas G, Castanas E (2005b) Polyphenol interaction with the T47D human breast cancer cell line. J Dairy Res 72:1–7

Ono K, Nakane H (1990) Mechanisms of inhibition of various cellular DNA and RNA polymerases by several flavonoids. J Biochem (Tokyo) 108:609–613

Ono K, Nakane H, Fukushima M, Chermann JC, Barre-Sinoussi F (1989) Inhibition of reverse transcriptase activity by a flavonoid compound, 5,6,7-trihydroxyflavone. Biochem Biophys Res Commun 160:982–987

Onoda M, Inano H (2000) Effect of curcumin on the production of nitric oxide by cultured rat mammary gland. Nitric Oxide 4:505–515

Park BS, Baek SJ, Song KH, Kim KH, Jeong SJ, Jeong MH, Seo SY, Lee SW, Yoo KS, Yoo YH (2002) Genistein-induced apoptosis of p815 mastocytoma cells is mediated by Bax and augmented by a proteasome inhibitor, lactacystin. Nutr Cancer 42:248–255

Paul B, Hayes CS, Kim A, Athar M, Gilmour SK (2005) Elevated polyamines lead to selective induction of apoptosis and inhibition of tumorigenesis by (–)-epigallocatechin-3-gallate (EGCG) in ODC/Ras transgenic mice. Carcinogenesis 26:119–124

Peruzzi F, Prisco M, Dews M, Salomoni P, Grassilli E, Romano G, Calabretta B, Baserga R (1999) Multiple signaling pathways of the insulin-like growth factor 1 receptor in protection from apoptosis. Mol Cell Biol 19:7203–7215

Pianetti S, Guo S, Kavanagh KT, Sonenshein GE (2002) Green tea polyphenol epigallocatechin-3 gallate inhibits Her-2/neu signaling, proliferation, and transformed phenotype of breast cancer cells. Cancer Res 62:652–655

Pilorget A, Berthet V, Luis J, Moghrabi A, Annabi B, Beliveau R (2003) Medulloblastoma cell invasion is inhibited by green tea (–)epigallocatechin-3-gallate. J Cell Biochem 90:745–755

Piver B, Berthou F, Dreano Y, Lucas D (2001) Inhibition of CYP3A, CYP1A and CYP2E1 activities by resveratrol and other non volatile red wine components. Toxicol Lett 125:83–91

Piver B, Berthou F, Dreano Y, Lucas D (2003) Differential inhibition of human cytochrome P450 enzymes by epsilon-viniferin, the dimer of resveratrol: comparison with resveratrol and polyphenols from alcoholized beverages. Life Sci 73:1199–1213

Polkowski K, Mazurek AP (2000) Biological properties of genistein. A review of in vitro and in vivo data. Acta Pol Pharm 57:135–155

Pozo-Guisado E, Lorenzo-Benayas MJ, Fernandez-Salguero PM (2004) Resveratrol modulates the phosphoinositide 3-kinase pathway through an estrogen receptor alpha-dependent mechanism: relevance in cell proliferation. Int J Cancer 109:167–173

Qanungo S, Das M, Haldar S, Basu A (2005) Epigallocatechin-3-gallate induces mitochondrial membrane depolarization and caspase-dependent apoptosis in pancreatic cancer cells. Carcinogenesis 26:958–967

Quiney C, Dauzonne D, Kern C, Fourneron JD, Izard JC, Mohammad RM, Kolb JP, Billard C (2004) Flavones and polyphenols inhibit the NO pathway during apoptosis of leukemia B-cells. Leuk Res 28:851–861

Ragione FD, Cucciolla V, Borriello A, Pietra VD, Racioppi L, Soldati G, Manna C, Galletti P, Zappia V (1998) Resveratrol arrests the cell division cycle at S/G2 phase transition. Biochem Biophys Res Commun 250:53–58

Rahman A, Shahabuddin, Hadi SM, Parish JH, Ainley K (1989) Strand scission in DNA induced by quercetin and Cu(II): role of Cu(I) and oxygen free radicals. Carcinogenesis 10:1833–1839

Rahman I, Marwick J, Kirkham P (2004) Redox modulation of chromatin remodeling: impact on histone acetylation and deacetylation, NF-kappaB and pro-inflammatory gene expression. Biochem Pharmacol 68:1255–1267

Ramos S, Alia M, Bravo L, Goya L (2005) Comparative effects of food-derived polyphenols on the viability and apoptosis of a human hepatoma cell line (HepG2). J Agric Food Chem 53:1271–1280

Remacle-Bonnet MM, Garrouste FL, Heller S, Andre F, Marvaldi JL, Pommier GJ (2000) Insulin-like growth factor-I protects colon cancer cells from death factor-induced apoptosis by potentiating tumor necrosis factor alpha-induced mitogen-activated protein kinase and nuclear factor kappaB signaling pathways. Cancer Res 60:2007–2017

Richter M, Ebermann R, Marian B (1999) Quercetin-induced apoptosis in colorectal tumor cells: possible role of EGF receptor signaling. Nutr Cancer 34:88–99

Rigolio R, Miloso M, Nicolini G, Villa D, Scuteri A, Simone M, Tredici G (2005) Resveratrol interference with the cell cycle protects human neuroblastoma SH-SY5Y cell from paclitaxel-induced apoptosis. Neurochem Int 46:205–211

Rodrigue CM, Porteu F, Navarro N, Bruyneel E, Bracke M, Romeo PH, Gespach C, Garel MC (2005) The cancer chemopreventive agent resveratrol induces tensin, a cell-matrix adhesion protein with signaling and antitumor activities. Oncogene 24:3274–3284

Roman V, Billard C, Kern C, Ferry-Dumazet H, Izard JC, Mohammad R, Mossalayi DM, Kolb JP (2002) Analysis of resveratrol-induced apoptosis in human B-cell chronic leukaemia. Br J Haematol 117:842–851

Rosenkranz HS, Thampatty BP (2003) SAR: flavonoids and COX-2 inhibition. Oncol Res 13:529–535

Rossi M, Meyer R, Constantinou P, Caruso F, Castelbuono D, O'Brien M, Narasimhan V (2001) Molecular structure and activity toward DNA of baicalein, a flavone constituent of the Asian herbal medicine "Sho-saiko-to". J Nat Prod 64:26–31

Roy AM, Baliga MS, Katiyar SK (2005) Epigallocatechin-3-gallate induces apoptosis in estrogen receptor-negative human breast carcinoma cells via modulation in protein expression of p53 and Bax and caspase-3 activation. Mol Cancer Ther 4:81–90

Sachinidis A, Seul C, Seewald S, Ahn H, Ko Y, Vetter H (2000) Green tea compounds inhibit tyrosine phosphorylation of PDGF beta-receptor and transformation of A172 human glioblastoma. FEBS Lett 471:51–55

Sah JF, Balasubramanian S, Eckert RL, Rorke EA (2004) Epigallocatechin-3-gallate inhibits epidermal growth factor receptor signaling pathway. Evidence for direct inhibition of ERK1/2 and AKT kinases. J Biol Chem 279:12755–12762

Saija A, Tomatino A, Trombetta D, De Pasquale A, Uccela N, Barbuzzi T, Paolino D, Bonina F (2000) In vitro and in vivo evaluation of caffeic and ferulic acids as topical photoprotective agents. Int J Pharm 199:39–47

Salti GI, Grewal S, Mehta RR, Das Gupta TK, Boddie AW Jr, Constantinou AI (2000) Genistein induces apoptosis and topoisomerase II-mediated DNA breakage in colon cancer cells. Eur J Cancer 36:796–802

Sartippour MR, Shao ZM, Heber D, Beatty P, Zhang L, Liu C, Ellis L, Liu W, Go VL, Brooks MN (2002) Green tea inhibits vascular endothelial growth factor (VEGF) induction in human breast cancer cells. J Nutr 132:2307–2311

Sartor L, Pezzato E, Dona M, Dell'Aica I, Calabrese F, Morini M, Albini A, Garbisa S (2004) Prostate carcinoma and green tea: (–)epigallocatechin-3-gallate inhibits inflammation-triggered MMP-2 activation and invasion in murine TRAMP model. Int J Cancer 112:823–829

Sato T, Koike L, Miyata Y, Hirata M, Mimaki Y, Sashida Y, Yano M, Ito A (2002) Inhibition of activator protein-1 binding activity and phosphatidylinositol 3-kinase pathway by nobiletin, a polymethoxy flavonoid, results in augmentation of tissue inhibitor of metalloproteinases-1 production and suppression of production of matrix metalloproteinases-1 and -9 in human fibrosarcoma HT-1080 cells. Cancer Res 62:1025–1029

Schneider Y, Chabert P, Stutzmann J, Coelho D, Fougerousse A, Gosse F, Launay JF, Brouillard R, Raul F (2003) Resveratrol analog (Z)-3,5,4′-trimethoxystilbene is a potent anti-mitotic drug inhibiting tubulin polymerization. Int J Cancer 107:189–196

Serafino A, Sinibaldi-Vallebona P, Lazzarino G, Tavazzi B, Rasi G, Pierimarchi P, Andreola F, Moroni G, Galvano G, Galvano F, Garaci E (2004) Differentiation of human melanoma cells induced by cyanidin-3-O-beta-glucopyranoside. FASEB J 18:1940–1942

Severson RK, Nomura AM, Grove JS, Stemmermann GN (1989) A prospective study of demographics, diet, and prostate cancer among men of Japanese ancestry in Hawaii. Cancer Res 49:1857–1860

Shen SC, Ko CH, Hsu KC, Chen YC (2004) 3-OH flavone inhibition of epidermal growth factor-induced proliferaton through blocking prostaglandin E2 production. Int J Cancer 108:502–510

Shenouda NS, Zhou C, Browning JD, Ansell PJ, Sakla MS, Lubahn DB, Macdonald RS (2004) Phytoestrogens in common herbs regulate prostate cancer cell growth in vitro. Nutr Cancer 49:200–208

Shih A, Zhang S, Cao HJ, Boswell S, Wu YH, Tang HY, Lennartz MR, Davis FB, Davis PJ, Lin HY (2004) Inhibitory effect of epidermal growth factor on resveratrol-induced apoptosis in prostate cancer cells is mediated by protein kinase C-alpha. Mol Cancer Ther 3:1355–1364

Siddiqui IA, Adhami VM, Afaq F, Ahmad N, Mukhtar H (2004) Modulation of phosphatidylinositol-3-kinase/protein kinase B- and mitogen-activated protein kinase-pathways by tea polyphenols in human prostate cancer cells. J Cell Biochem 91:232–242

Snyder RD, Gillies PJ (2003) Reduction of genistein clastogenicity in Chinese hamster V79 cells by daidzein and other flavonoids. Food Chem Toxicol 41:1291–1298

Solimani R (1996) Quercetin and DNA in solution: analysis of the dynamics of their interaction with a linear dichroism study. Int J Biol Macromol 18:287–295

Solimani R (1997) The flavonols quercetin, rutin and morin in DNA solution: UV-vis dichroic (and mid-infrared) analysis explain the possible association between the biopolymer and a nucleophilic vegetable-dye. Biochim Biophys Acta 1336:281–294

Spencer-Cisek PA (2002) The role of growth factors in malignancy: a focus on the epidermal growth factor receptor. Semin Oncol Nurs 18:13–19

Stewart JR, O'Brian CA (2004) Resveratrol antagonizes EGFR-dependent Erk1/2 activation in human androgen-independent prostate cancer cells with associated isozyme-selective PKC alpha inhibition. Invest New Drugs 22:107–117

Stivala LA, Savio M, Carafoli F, Perucca P, Bianchi L, Maga G, Forti L, Pagnoni UM, Albini A, Prosperi E, Vannini V (2001) Specific structural determinants are responsible for the antioxidant activity and the cell cycle effects of resveratrol. J Biol Chem 276:22586–22594

Su JL, Lin MT, Hong CC, Chang CC, Shiah SG, Wu CW, Chen ST, Chau YP, Kuo ML (2005) Resveratrol induces FasL-related apoptosis through Cdc42 activation of ASK1/JNK-dependent signaling pathway in human leukemia HL-60 cells. Carcinogenesis 26:1–10

Sun CL, Yuan JM, Koh WP, Yu MC (2005) Green tea, black tea and breast cancer risk: a meta-analysis of epidemiological studies. Carcinogenesis 27:1310–1315

Tachibana H, Koga K, Fujimura Y, Yamada K (2004) A receptor for green tea polyphenol EGCG. Nat Struct Mol Biol 11:380–381

Tang DG, Chen YQ, Honn KV (1996) Arachidonate lipoxygenases as essential regulators of cell survival and apoptosis. Proc Natl Acad Sci USA 93:5241–5246

Usha S, Johnson IM, Malathi R (2005) Interaction of resveratrol and genistein with nucleic acids. J Biochem Mol Biol 38:198–205

Vayalil PK, Katiyar SK (2004) Treatment of epigallocatechin-3-gallate inhibits matrix metalloproteinases-2 and -9 via inhibition of activation of mitogen-activated protein kinases, c-jun and NF-kappaB in human prostate carcinoma DU-145 cells. Prostate 59:33–42

Vayalil PK, Mittal A, Katiyar SK (2004) Proanthocyanidins from grape seeds inhibit expression of matrix metalloproteinases in human prostate carcinoma cells, which is associated with the inhibition of activation of MAPK and NF kappa B. Carcinogenesis 25:987–995

Vittal R, Selvanayagam ZE, Sun Y, Hong J, Liu F, Chin KV, Yang CS (2004) Gene expression changes induced by green tea polyphenol (–)-epigallocatechin-3-gallate in human bronchial epithelial 21BES cells analyzed by DNA microarray. Mol Cancer Ther 3:1091–1099

Waffo-Teguo P, Hawthorne ME, Cuendet M, Merillon JM, Kinghorn AD, Pezzuto JM, Mehta RG (2001) Potential cancer-chemopreventive activities of wine stilbenoids and flavans extracted from grape (Vitis vinifera) cell cultures. Nutr Cancer 40:173–179

Wan SB, Chen D, Dou QP, Chan TH (2004) Study of the green tea polyphenols catechin-3-gallate (CG) and epicatechin-3-gallate (ECG) as proteasome inhibitors. Bioorg Med Chem 12:3521–3527

Wang IK, Lin-Shiau SY, Lin JK (1999) Induction of apoptosis by apigenin and related flavonoids through cytochrome c release and activation of caspase-9 and caspase-3 in leukaemia HL-60 cells. Eur J Cancer 35:1517–1525

Wang S, DeGroff VL, Clinton SK (2003) Tomato and soy polyphenols reduce insulin-like growth factor-I-stimulated rat prostate cancer cell proliferation and apoptotic resistance in vitro via inhibition of intracellular signaling pathways involving tyrosine kinase. J Nutr 133:2367–2376

Wang YC, Bachrach U (2002) The specific anti-cancer activity of green tea (–)-epigallocatechin-3-gallate (EGCG). Amino Acids 22:131–143

Way TD, Kao MC, Lin JK (2004a) Apigenin induces apoptosis through proteasomal degradation of HER2/neu in HER2/neu-overexpressing breast cancer cells via the phosphatidylinositol 3-kinase/Akt-dependent pathway. J Biol Chem 279:4479–4489

Way TD, Lee HH, Kao MC, Lin JK (2004b) Black tea polyphenol theaflavins inhibit aromatase activity and attenuate tamoxifen resistance in HER2/neu-transfected human breast cancer cells through tyrosine kinase suppression. Eur J Cancer 40:2165–2174

Webb MR, Ebeler SE (2004) Comparative analysis of topoisomerase IB inhibition and DNA intercalation by flavonoids and similar compounds: structural determinates of activity. Biochem J 384:527–541

Weber AA, Neuhaus T, Skach RA, Hescheler J, Ahn HY, Schror K, Ko Y, Sachinidis A (2004) Mechanisms of the inhibitory effects of epigallocatechin-3 gallate on platelet-derived growth factor-BB-induced cell signaling and mitogenesis. FASEB J 18:128–130

Weisburger JH, Rivenson A, Garr K, Aliaga C (1997) Tea, or tea and milk, inhibit mammary gland and colon carcinogenesis in rats. Cancer Lett 114:323–327

Weyant MJ, Carothers AM, Dannenberg AJ, Bertagnolli MM (2001) (+)-Catechin inhibits intestinal tumor formation and suppresses focal adhesion kinase activation in the min/+ mouse. Cancer Res 61:118–125

Wolter F, Turchanowa L, Stein J (2003) Resveratrol-induced modification of polyamine metabolism is accompanied by induction of c-Fos. Carcinogenesis 24:469–474

Xing N, Chen Y, Mitchell SH, Young CY (2001) Quercetin inhibits the expression and function of the androgen receptor in LNCaP prostate cancer cells. Carcinogenesis 22:409–414

Xu HX, Wan M, Dong H, But PP, Foo LY (2000) Inhibitory activity of flavonoids and tannins against HIV-1 protease. Biol Pharm Bull 23:1072–1076

Yamakawa S, Asai T, Uchida T, Matsukawa M, Akizawa T, Oku N (2004) (–)-Epigallocatechin gallate inhibits membrane-type 1 matrix metalloproteinase, MT1-MMP, and tumor angiogenesis. Cancer Lett 210:47–55

Yamashita N, Kawanishi S (2000) Distinct mechanisms of DNA damage in apoptosis induced by quercetin and luteolin. Free Radic Res 33:623–633

Yanez J, Vicente V, Alcaraz M, Castillo J, Benavente-Garcia O, Canteras M, Teruel JA (2004) Cytotoxicity and antiproliferative activities of several phenolic compounds against three melanocytes cell lines: relationship between structure and activity. Nutr Cancer 49:191–199

Yang EB, Zhang K, Cheng LY, Mack P (1998a) Butein, a specific protein tyrosine kinase inhibitor. Biochem Biophys Res Commun 245:435–438

Yang GY, Liao J, Kim K, Yurkow EJ, Yang CS (1998b) Inhibition of growth and induction of apoptosis in human cancer cell lines by tea polyphenols. Carcinogenesis 19:611–616

Yang GY, Liao J, Li C, Chung J, Yurkow EJ, Ho CT, Yang CS (2000) Effect of black and green tea polyphenols on c-jun phosphorylation and H(2)O(2) production in transformed and non-transformed human bronchial cell lines: possible mechanisms of cell growth inhibition and apoptosis induction. Carcinogenesis 21:2035–2039

Ye F, Wu J, Dunn T, Yi J, Tong X, Zhang D (2004) Inhibition of cyclooxygenase-2 activity in head and neck cancer cells by genistein. Cancer Lett 211:39–46

Ye J, Lu H, Zhou J, Wu H, Wang C (2002) [Inhibitory effect of all-*trans*-retinoid and polyphenon-100 on microsatellite instability in a colon cancer line]. Zhonghua Yi Xue Yi Chuan Xue Za Zhi 19:190–193

Yokoyama M, Noguchi M, Nakao Y, Pater A, Iwasaka T (2004) The tea polyphenol, (–)-epigallocatechin gallate effects on growth, apoptosis, and telomerase activity in cervical cell lines. Gynecol Oncol 92:197–204

Yoshida M, Yamamoto M, Nikaido T (1992) Quercetin arrests human leukemic T-cells in late G1 phase of the cell cycle. Cancer Res 52:6676–6681

Yuan H, Pan Y, Young CY (2004) Overexpression of c-Jun induced by quercetin and resverol inhibits the expression and function of the androgen receptor in human prostate cancer cells. Cancer Lett 213:155–163

Zhang M, Zhang JP, Ji HT, Wang JS, Qian DH (2000) Effect of six flavonoids on proliferation of hepatic stellate cells in vitro. Acta Pharmacol Sin 21:253–256

Zhao J, Sharma Y, Agarwal R (1999) Significant inhibition by the flavonoid antioxidant silymarin against 12-O-tetradecanoylphorbol 13-acetate-caused modulation of antioxidant and inflammatory enzymes, and

cyclooxygenase 2 and interleukin-1alpha expression in SENCAR mouse epidermis: implications in the prevention of stage I tumor promotion. Mol Carcinog 26:321–333
Zhou J, Wang LF, Wang JY, Tang N (2001) Synthesis, characterization, antioxidative and antitumor activities of solid quercetin rare earth(III) complexes. J Inorg Biochem 83:41–48
Zsila F, Bikadi Z, Simonyi M (2004) Circular dichroism spectroscopic studies reveal pH dependent binding of curcumin in the minor groove of natural and synthetic nucleic acids. Org Biomol Chem 2:2902–2910

Rev Physiol Biochem Pharmacol (2007) 159:115 –129
DOI 10.1007/112_2007_0703

M. Janitz

Assigning functions to genes—the main challenge of the post-genomics era

Published online: 1 May 2007

Abstract Genome-sequencing projects yield enormous amounts of information that can lead to revolutions in our understanding of life and provide new platforms for the treatment of human diseases. However, DNA sequencing alone does not provide enough information to determine the molecular pathways of an organism in healthy and disease states. A huge number of gene products await functional characterization. Hence, there is a strong demand for technological solutions that help to assign the functions of proteins and genes. This review discusses high-throughput molecular biology methods, which promise to meet the challenges of the post-genomic era.

Introduction

The completion of a high-quality human genome sequence was a landmark event in the history of biomedical sciences (Lander et al. 2001; Venter et al. 2001). However, the elucidation of DNA sequence was only a starting point in genomics research. The goals of functional genomics include understanding genomes, the products that they encode, how gene products interact to produce complex living organisms, and the importance of sequence variants. The progress of the Human Genome Project (HGP) has stimulated the development of new technologies that can provide answers to some of these questions on a genomics scale.

Post-translational modifications as clues to protein function

Living cells rely on a complex interplay among thousands of different molecules that maintain cellular integrity and morphology and perform numerous biological functions. Although protein functions are encoded in genes, the actual regulation of protein structure and function

M. Janitz (✉)
Max Planck Institute for Molecular Genetics,
Fabeckstrasse 60–62, 14195 Berlin, Germany
e-mail: janitz@molgen.mpg.de · Tel.: +49-308-4131463 · Fax: +49-308-4131462

generally is executed by specific post-translational modifications (PTMs) such as phosphorylation, glycosylation, and acetylation. Currently, it is well accepted that most proteins in a variety of species exhibit site-specific covalent modifications (Krishna and Wold 1993; Mann and Jensen 2003).

PTM of proteins enables enormous heterogeneity and diversity of gene products. As a result of allelic variations, mRNA splicing, and PTMs, the human genome can generate hundreds of thousands of different gene products from an estimated 30,000 open reading frames. However, only a distinct subset of these gene products is present in a given cell type under normal physiological conditions. Cell and tissue types as well as environmental stimuli influence the way proteins are post-translationally modified. Thus, cell-specific patterns of PTM will determine protein structure, subcellular localization, and interactions with other proteins.

Genome-wide protein localization studies

The eukaryotic cell is divided into a number of compartments to which particular protein activities are assigned. Thus, the subcellular localization of proteins can be a valuable source of information about protein function. Furthermore, proper localization of a protein within particular compartments is a prerequisite for interaction with other proteins in regulatory networks. Thus, aberrant protein translocation might lead to pathological changes in cell physiology.

In most cases, protein localization studies have been performed on a single-gene basis. Following the completion of genome sequencing projects for various organisms (in particular human and mouse), great efforts have been made to conduct genome-wide protein localization studies. Initially, large-scale studies were performed in fission and budding yeast (Ding et al. 2000; Kumar et al. 2002). Simpson and colleagues applied a novel cloning technology for rapid generation of N- and C-terminal green fluorescent protein fusions with a small library of cDNAs to examine intracellular protein localizations in a mammalian cell line. Over 100 fusion proteins were expressed in living cells, and for over 80% of these proteins, an unambiguous intracellular localization to known structures or organelles was determined (Simpson et al. 2000). In another study, automated transfection and immunostaining of mammalian cells in a 96-well plate format was utilized (Liebel et al. 2003). Although robust, the microwell plate-based approach is characterized by high reagent consumption and a need for automated liquid dispensing. Moreover, the microtiter plate assay requires a high number of cells per well, which can limit feasibility when primary cells are considered. A recently developed transfected-cell array technique (described in detail later) represents a cost-effective alternative to the microwell plate format for high-throughput functional genomics. Using this method, Hu et al. screened over 80 genes mapping to human chromosome 21 (Chr21) for the subcellular localization of their products in HEK cells. Plasmids encoding particular Chr21 genes were spotted in an array format and reverse transfected for protein expression (Fig. 1). Using this approach, the localizations of 34 proteins were described for the first time. In addition, the influences of some of the proteins on cellular morphology and apoptosis induction were characterized (Hu et al. 2006).

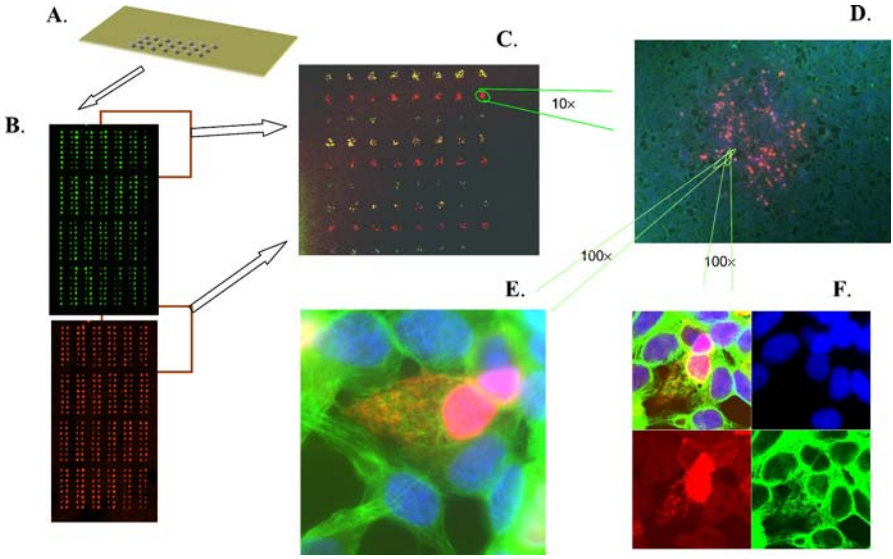

Fig. 1 High-throughput assay for protein sublocalization studies in mammalian cells using the cell array technique. cDNAs of the studied proteins are cloned in expression vector and spotted in an array format (**A**). Different proteins can be simultaneously detected through the anti-His6 tag staining using a CCD scanning system (**B**) or automated microscope (**C**). For detailed analysis of protein distribution, particular cell clusters (**D**) or single cells (**E**) with the help of organelles counter-staining (**F**) can be examined (from Hu et al. 2006)

The use of functional genomics to identify proteins involved in apoptosis

Apoptosis is the most common form of physiological cell death, serving to eliminate genetically altered cells. Apoptosis is defined by morphological criteria including chromatin condensation, nuclear fragmentation, plasma membrane blebbing, organelle disruption, loss of adhesion and rounding, and cell shrinkage. Apoptosis is required for normal development and maintenance of tissue homeostasis, and its dysregulation is associated with various pathological conditions.

Identification of pro- and anti-apoptotic genes

Proliferating tissues that fail to maintain normal cell turnover may tend to accumulate neoplastic cells, which leads to tumor formation. Moreover, defects in apoptotic signaling create a permissive environment for mutations and genetic instability (Igney and Krammer 2002).

Apoptosis resistance in cancer is mediated by diverse mechanisms that act at different points of the cell death pathway, leading to its disruption. Many of the responsible molecules have been identified and comprise potential targets for therapeutic intervention (Nicholson 2000). They can be divided into two major classes: (a) oncogenes with anti-apoptotic activities, which are frequently over-expressed due to transactivation or post-transcriptional regulation and (b) tumor suppressor genes with pro-apoptotic capabilities. In addition, death receptor signaling can be dampened by the expression of inactive decoy receptors on the cell surface (Ashkenazi 2002).

Recently, several large-scale screens for identifying pro-apoptotic genes have been performed. Mannherz and colleagues spotted 382 human gene sequences, mostly with unknown functions, on glass slides to investigate induction of apoptosis upon protein over-expression (Mannherz et al. 2006). They used the transfected-cell array technique combined with the TUNEL assay to identify ten genes with pro-apoptotic characteristics. In another study, a batch of 2,000 human open reading frames was investigated for pro-apoptotic activity, again using the protein over-expression approach in cell array format (Palmer et al. 2006). Over-expression of ten proteins resulted in the induction of apoptosis, which was evaluated further by genome-wide gene expression analysis. To date, a systematic, genome-wide screening of anti-apoptotic genes has not been performed. The commercial availability of apoptosis-specific sets of small interfering RNAs (siRNAs) will probably accelerate research in this direction. The combination of RNA interference and cell array technology has already proven to be very robust in several areas of functional genomics (Vanhecke and Janitz 2004).

Technologies for high-throughput functional genomics

Developments in the past decade resulted in a number of state-of-the art technologies that were adopted in many areas of functional genomics and proteomics. One of the most prominent technologies is the microarray technique. The microarray consists of hundreds to thousands of molecules spotted on a glass surface in a highly systematic manner so that the coordinates of each spot are defined. Chemical compounds, DNA, proteins, and even intact living cells can be printed in an array format in a high-throughput fashion. Accordingly, many microarray platforms have been developed including DNA microarrays, small-molecule microarrays, peptide microarrays, protein microarrays, and cell arrays. One distinct feature of these microarray-based platforms is that high-throughput screening of a variety of molecules can be performed in a single step. This allows for rapid data acquisition and parallel sample comparison.

DNA microarrays

DNA microarrays consist of a miniaturized, solid matrix on which thousands of known nucleic acid fragments [cDNAs, oligonucleotides, polymerase chain reaction (PCR) products] are deposited in a highly ordered fashion (Fan et al. 2006a). The highly specific hybridization of a single-stranded nucleic acid to a second complementary single strand, resulting in generation of a double-stranded DNA molecule, is fundamental to DNA microarrays. Potential target nucleic acids are labeled with radioactivity or fluorescent dyes and then hybridized to the array surface. After a washing step, the complementary target–probe complexes remain tightly bound, and the amount of the labeled target is quantified by measurement of its radioactivity or fluorescence. Signal detection is performed using charge-coupled devices (CCD) or laser-scanning digital imaging systems. Several DNA microarray platforms using various methods of nucleic acid molecules generation and immobilization are currently available.

Gene expression profiling

Expressed genes determine the phenotype of the cell and its response to environmental factors. Therefore, gene expression profiles can help to elucidate cellular functions, regulatory mechanisms, and biochemical pathways, both in normal and disease states. The knowledge derived from comparative studies between diseased cells or tissues and normal counterparts allows the identification of new molecular targets. As a result, more accurate diagnoses and individual predictions of clinical outcome can be made and new therapeutic targets can be characterized.

Currently, several technology platforms are in use for gene expression profiling. The most common are cDNA microarrays and oligonucleotide microarrays.

cDNA microarrays

A cDNA microarray comprises thousands of probes, usually corresponding to PCR products generated from cDNA libraries, expressed sequence tag clones, or long cloned genomic fragments using vector- or gene-specific primers (Cheung et al. 1999; Duggan 1999). The set of probes is printed at defined coordinates on a solid support using either contact or noncontact printing based on the ink jet principle. Spots are usually in the size range of 100–200 μm, with regular distribution throughout the array. One advantage of cDNA microarrays is that sequence information about spotted clones is not obligatory. Hence, the discovery of new genes is facilitated. This advantage is partially diminished by the current availability of the entire genome sequences from human and many other organisms. The large size of each probe (~500–2,000 bp) reduces cross-hybridization of unrelated genes under stringent hybridization conditions. However, closely related members of the same gene family are able to anneal to some extent, resulting in the failure to specifically detect individual genes. Furthermore, PCR amplification of clones for microarray generation is required. These factors substantially limit applicability of cDNA microarrays due to their relatively high cost and tedious production.

Oligonucleotide microarrays

Oligonucleotide microarrays using short (25–30 bp) or long (50–80 bp) oligonucleotides overcome some of the disadvantages of cDNA arrays. The oligonucleotide arrays are produced by immobilization of single-stranded DNA molecules on a glass surface. The probes are designed on the basis of sequence information available in databases. This eliminates the need to verify and maintain vast collections of cells, cDNA clones, and PCR products. Splice variants and closely related members of gene families can also be efficiently distinguished by designing specific probe sequences. In early nineties, Affymetrix established an oligonucleotide microarray (GeneChip) manufactured by photolithographic technology. Since then, high-density, short-oligonucleotide GeneChip arrays have become the standard in the field (Lipshutz et al. 1999). The latest GeneChip format contains more than one million different oligonucleotide sequences, 25 bases in length, on a GeneChip 11×11 mm in size, with sequences of up to 47,000 transcripts. For quantification of mRNA levels, each gene is represented by a probe set of 11–25 oligo pairs, which are in most cases complementary to the mRNA 3′ end. One probe of each pair perfectly matches the gene sequence (perfect match), whereas the other probe carries a one-base mismatch in the central po-

sition of the sequence. The mismatched probe serves as a negative control of hybridization.

Recently, long oligonucleotides have become a novel and interesting approach to microarray production. These long oligonucleotides can be synthesized separately on a large scale and spotted onto a glass surface. Alternatively, oligoprobes can be synthesized in situ on a glass array surface using ink jet printing technology (Agilent Technologies) (Wolber et al. 2006). The increased length of the oligoprobes results in greater specificity to the hybridized DNA. Hence, long-oligonucleotide microarrays are more similar to cDNA microarrays than to GeneChips. Likewise, the method of signal hybridization and detection is similar for long-oligonucleotide microarrays and cDNA microarrays. In both cases, two separate samples are labeled with different fluorescent nucleotides, such as Cy5 and Cy3. The former represents an experimental sample and the latter a reference sample. The two samples are co-hybridized to the same array, and competitive hybridization takes place. The Cy5/Cy3 ratio detected for each spot is proportional to the relative amounts of mRNA for that specific gene in the two samples. In contrast, a single sample is hybridized to the GeneChip, and signals from full-match and mismatch oligoprobes are compared.

Most gene expression data have been generated using cDNA arrays and long-oligonucleotide arrays, as well as Affymetrix GeneChips. Recently, a long-oligonucleotide, bead-based microarray from Illumina has become popular within the research community (Fan et al. 2006b). Whereas arrays produced by Affymetrix are fabricated by in situ synthesis of 25-mer oligonucleotides, the Illumina technology applies standard oligonucleotide synthesis. However, the oligonucleotides are attached to microbeads, which are then placed onto microarrays using a random self-assembly mechanism. The design and probe selection process also differs substantially between the Affymetrix and Illumina approaches. Affymetrix uses multiple probes for each gene, along with one-base mismatch probes used as controls against nonspecific hybridization. In contrast, the randomly generated Illumina arrays contain approximately 30 copies of each oligonucleotide, which provides an internal technical replication not present in Affymetrix chips. The location of each probe on the Illumina bead chip must be decoded using a molecular address attached to the probe. In contrast, the coordinates of Affymetrix oligoprobes are predefined so that no decoding step is necessary. It should be emphasized that both platforms are currently widely used not only for gene expression profiling studies but also for genome-wide genotyping (Kaller et al. 2007).

Protein microarrays

Protein microarrays contain a defined set of proteins immobilized in high density, regularly distributed on a solid support such as glass with various surface modifications (Angenendt et al. 2003).

The methodology developed for production of DNA microarrays was also successfully applied for fabrication of protein microarrays. Printing of the proteins is done with a regular microarray spotter. Typically, protein spots 200–250 μm in diameter are generated. In principle, proteins can be arrayed at high spatial density, similar to DNA, and a standard microscope slide can accommodate thousands of samples in parallel. The droplet can be delivered to the surface by direct contact between the spotter tip and the solid support. Proteins drops can be also delivered by noncontact printing using piezo-spotting (Auburn et al. 2005).

This type of spotting is characterized by greater precision and more controlled distribution of the volumes of dissolved proteins.

Protein microarray technology provides a platform for the in vitro study of protein function at a genome-wide level (Talapatra et al. 2002). Immobilized proteins can be assayed in parallel under many different conditions and with many different samples. However, whole-proteome microarrays are difficult to achieve for higher organisms. Until recently, they have been limited to studies of the yeast proteome because production of a large number of pure recombinant proteins in parallel is a tedious and expensive process. cDNAs must be cloned into expression vectors, and the translated proteins must be purified in large amounts. Furthermore, in the case of genome-wide approaches, the cDNA library must be normalized.

Recently, transfected-cell arrays have emerged as a cost-effective alternative to protein arrays (see following sections for details). In the former approach, proteins are synthesized in an array format by cells. Thus, the protein purification step can be avoided, and different cell types can be used at the same time for investigation of tissue-specific effects.

Protein–protein interaction screening systems

It is very difficult to predict interaction partners for particular proteins, even with knowledge of the properties of specific protein domains. An example is the SH3 domain, which preferentially binds to sequences containing the amino acid proline (Musacchio 2002). Therefore, experimental approaches are required to investigate protein–protein interactions (PPIs). In this review, only in vivo methodologies will be discussed because these are currently the most common approaches for PPI screens.

Yeast two-hybrid system

PPIs play a fundamental role in the regulation and execution of nearly all cellular processes. One of the most widely used techniques for detecting PPIs is the yeast two-hybrid (YTH) system. It takes advantage of the fact that many eukaryotic transcription factors can be divided into two functionally distinct domains that mediate DNA binding and transcriptional activation (Miller and Stagljar 2004). In the classical YTH approach, a bait protein is constructed by fusing a protein *X* to a DNA-binding domain of a transcription factor. Meanwhile, a prey protein is constructed by fusing a protein *Y* to the activation domain of a transcription factor. The bait and prey fusions are co-expressed in yeast, wherein the interaction of *X* and *Y* leads to the restoration of a functional transcription factor. Reconstitution of the transcription factor is measured by assaying the activity of reporter genes.

The ability to screen large cDNA libraries for proteins that interact with a protein of interest is the major advantage of the YTH system over biochemical methods for identifying PPIs (Armour and Lum 2005; Fields 2005). Two types of YTH screening procedures are used widely (Legrain and Selig 2000). In a typical library approach, bait proteins are screened against a random cDNA library that encodes highly redundant, unknown prey proteins. This redundancy results in repeated detection of some interactions while missing others. In matrix approaches, arrays of defined bait and prey proteins are screened against each other in a systematic manner. In this configuration, each interaction has the same probability of being identified. Moreover, the screens can be repeated in the same way. Although matrix screens are characterized by high degrees of reliability and efficiency, the proteins must be

screened against a matrix until no new interactions can be detected. Therefore, to reduce the number of experiments and increase accuracy, smart pooling (Thierry-Mieg 2006) and deconvolution strategies (Jin et al. 2006) have been proposed.

Mammalian two-hybrid systems

Because two-hybrid systems are in vivo assays, they offer advantages over in vitro biophysical or biochemical methods for the study of protein interactions. Indeed, some PPIs are too weak and/or transient to be detected in vitro, and some of these interactions require specific PTMs of the proteins or specific co-factors in the cellular microenvironment. Hence, it is advantageous to determine protein interaction networks in mammalian cells using mammalian two-hybrid assays as compared to the more commonly used YTH assays (Lee and Lee 2004). Until recently, high-throughput analyses of protein interactions were typically performed in yeast, and putative interactions were confirmed afterwards in mammalian two-hybrid assays on a gene-by-gene basis (Tavernier et al. 2002).

Currently, mammalian PPIs are primarily investigated using the YTH system. As noted previously, studying mammalian genes in yeast is problematic because, in many cases, post-translational procedures are essential for correct protein processing. These modifications can differ among organisms and even among different cell types (Colosimo et al. 2000). This results in a high rate of false negatives in organisms other than that from which the genes were derived. For example, the transforming growth factor β-mediated interaction between Smad3 and c-Jun proteins is detectable only in mammalian cells and not in the YTH system (Feng and Derynck 2001). Therefore, mammalian genes should be studied in mammalian cells, their natural environment. The principle of the mammalian two-hybrid assay is similar to the YTH system (Dang et al. 1991). Advantages of the mammalian two-hybrid system are that proteins maintain their native conformation, and additional factors necessary for the interactions of proteins are available. This is especially relevant for proteins that interact indirectly, e.g., through transcription factors, in multi-protein complexes. Thus, the mammalian two-hybrid system is often used to further evaluate protein interaction partners found in yeast (Leonhardt et al. 1998) or for small-scale studies (Dixon et al. 1997). The first attempts to conduct large-scale mammalian two-hybrid assays consisted of transfection in a 96-well or 384-well plate (Murakami et al. 2002; Zhao et al. 2004). Automated transfection and immunostaining of mammalian cells were recently established (Liebel et al. 2003). In either case, the use of a microwell plate format requires automation of liquid dispensing and is characterized by high consumption of reagents.

In my laboratory, a new and cost-effective method for the high-throughput detection of PPIs in mammalian cells was established that combines the advantages of mammalian two-hybrid systems with those of microarrays (Fig. 2). In this assay, mixtures of bait and prey expression plasmids, together with an auto-fluorescent reporter, are immobilized on glass slides in defined array formats. Adherent cells that grow on top of the microarray will become fluorescent only if the expressed proteins interact and subsequently transactivate the reporter. By using known interacting partners and screening a small prey library against the human androgen receptor ligand-binding domain, it was demonstrated that this assay allows the quantitative detection of protein interactions in several types of mammalian cells and under the influence of different compounds (Fiebitz et al., submitted).

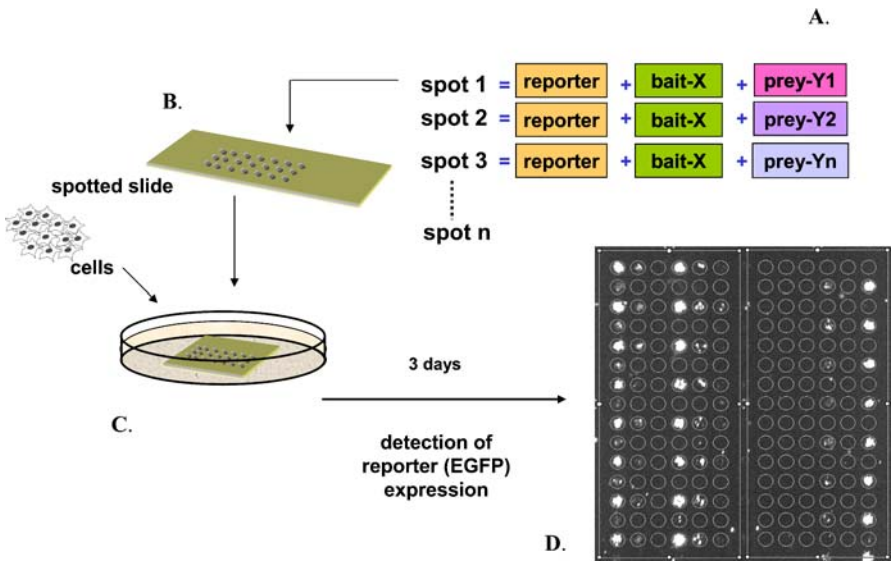

Fig. 2 Cell arrays can be applied for screening of protein–protein interactions in mammalian cells. Expression plasmids containing cDNAs for bait, reporter, and prey proteins (**A**) are spotted on the glass surface (**B**) and reverse transfected into adhesive cell line (**C**). After 3 days of incubation, proteins interactions are detected by the measurement of the reporter protein fluorescence (**D**). Since transfected cell clusters are separated by nontransfected cells, hundreds of different prey constructs can be investigated in a single experiment

RNA interference and its high-throughput applications

Among the most common ways to investigate gene function in the context of the entire organism are gain-of-function and loss-of-function studies using transgenic and knockout animal technology. Both approaches have drawbacks. One disadvantage is the enormous cost and time required to generate genetically modified animals. Moreover, the majority of genetically modified animals do not display a distinct change in phenotype that would allow unambiguous linkage to a mutated gene. Taking into account these aspects, there is a clear need for the identification of candidate genes before conducting in vivo studies.

RNA interference (RNAi) is an evolutionarily conserved biological phenomenon in plants and animals in which double-stranded RNA (dsRNA) induces the sequence-specific degradation of cognate RNA. During RNAi, dsRNA formed in cells by DNA- or RNA-dependent synthesis of complementary strands, or introduced into cells by viral infection or artificial expression, is processed to approximately 20-bp, double-stranded siRNAs containing 2-nt 3′ overhangs. The siRNAs are incorporated into an RNA-induced silencing complex that mediates the degradation of mRNAs with sequences fully complementary to the siRNA (Sontheimer 2005).

Although discovered as a natural process, RNAi quickly proved to be an excellent method for efficient gene silencing. Initially, silencing studies were performed in lower eukaryotes such as *Caenorhabditis elegans* (Carthew 2001) and *Drosophila melanogaster* (Kwon and Scholey 2004) using long dsRNA. Silencing of single genes was followed by high-throughput approaches, mostly in *C. elegans* (Lamitina 2006; Kuttenkeuler and Boutros 2004). Several recent studies in *C. elegans* clearly showed that the RNAi approach

can generate dozens of phenotypes, leading to the discovery of new genes and their functional characterization. For example, a genome-wide screen in *C. elegans* identified 21 genes stimulating apoptosis. Because apoptotic pathways are evolutionarily conserved, many of these genes have been implicated in the maintenance of mammalian genome stability, p53 activation, and the regulation of fertility (Lettre and Hengartner 2006). In another study, RNAi analysis of over 19,000 genes in *C. elegans* revealed over 1,500 phenotypes (Kamath et al. 2003).

RNAi in mammalian cells

Initially, the application of RNA interference in mammalian cells was hampered by the fact that dsRNA molecules longer than 30 bp trigger an interferon response, which ultimately leads to cell death. In contrast, 21-bp siRNAs do not stimulate the interferon response and can be delivered into cells, either as chemically synthesized molecules or via the transfection of plasmids that express siRNA. A wide range of mammalian genes involved in apoptosis, the cell cycle, and signal transduction have been knocked down successfully using this technique (Cullen and Arndt 2005). Chemically synthesized siRNAs are easy to transfect, and a high intracellular concentration of siRNA molecules can be achieved. However, high synthesis costs still hinder their broad application in high-throughput studies.

Gene silencing using direct transfection of siRNA is transient and limited by the rate of cell division. This is because mammalian cells, unlike *C. elegans*, are unable to amplify RNAi (Li et al. 2006). To overcome this obstacle and to increase the cost-effectiveness of RNAi studies, vector-based systems for siRNA delivery have been developed. Cells can be stably transfected with plasmids expressing short hairpin RNAs (shRNAs) so that the silencing effect can be constantly maintained (Bernards et al. 2006). Moreover, shRNA-encoding plasmids can carry drug-resistance markers, making the cells amenable to selection.

An alternative approach to plasmid transfection is to transduce cells with a virus that integrates a stable shRNA-expressing cassette into the genome of the target cell (Berns et al. 2004). Several groups have created large-scale shRNA libraries in retroviral-based (Sandy et al. 2005), adenoviral-based (Narvaiza et al. 2006), or lentiviral-based vectors (Moffat et al. 2006). These vectors can be used with packaging systems to generate viruses that will integrate shRNA-expressing sequences (along with a selectable marker) into various cell types, including primary and nondividing cells.

Although approximately 3,000 disease-modifying genes are thought to be present in the human genome, only around 500 have been subjected to pharmaceutical investigation. Therefore, the adaptation of genome-wide, loss-of-function screens using siRNAs for the interrogation of complex phenotypes promises the discovery of novel targets and, consequently, novel therapeutic strategies. However, some limitations of this technology should be discussed. It has been observed that gene silencing by siRNA is not entirely sequence-specific. False-positive results can arise due to sequence-independent, off-target effects of an interferon response induced by some siRNAs, but more prominently by shRNAs (Jackson et al. 2006). Since most off-target effects are likely to be concentration-dependent, considerable effort is being exerted to develop better methods of introducing siRNA into cells. These improved methods aim to reduce the amount of siRNA necessary for transfection and to reduce the cell toxicity of the transfection reagents (Amarzguioui et al. 2005).

False-negative results can be expected, depending upon the cell type and the gene of interest. False negatives may be due to redundancy of target genes, so that losing the func-

tion of one gene is compensated for by the products of functionally related genes. More frequently, however, inefficient knock-down of the RNA of interest and high stability of the analyzed protein will hamper the identification of important gene functions. Consequently, to obtain better gene silencing the prediction and validation of the optimal region within the gene must be further improved (Pei and Tuschl 2006).

Transfected-cell array as a functional genomics tool

A recently developed transfected-cell array (TCA) technique can be seen as a breakthrough for high-throughput functional genomics in cell biology. Full-length open reading frames of genes cloned in expression vectors or siRNAs are printed at a high density on a glass slide, along with a lipid transfection reagent. The microarray is subsequently covered with a layer of cells. Cells growing on top of the DNA/siRNA spots are transfected, resulting in the expression of specific proteins in spatially distinct groups of cells. The phenotypic effects of this 'reverse transfection' of hundreds or thousands of gene products can be detected using specific cell-based bioassays (Fig. 3) (Ziauddin and Sabatini 2001).

Because each cell cluster expresses a particular protein, and cell clusters are spatially separated, the TCA can be considered a particular type of protein microarray. The TCA utilizes eukaryotic cells, allowing for PTMs of expressed proteins. Utilization of different cell lines provides opportunities to screen for protein function in situations where cell-type-dependent PTMs and PPIs are important. Hence, the investigation of protein function within

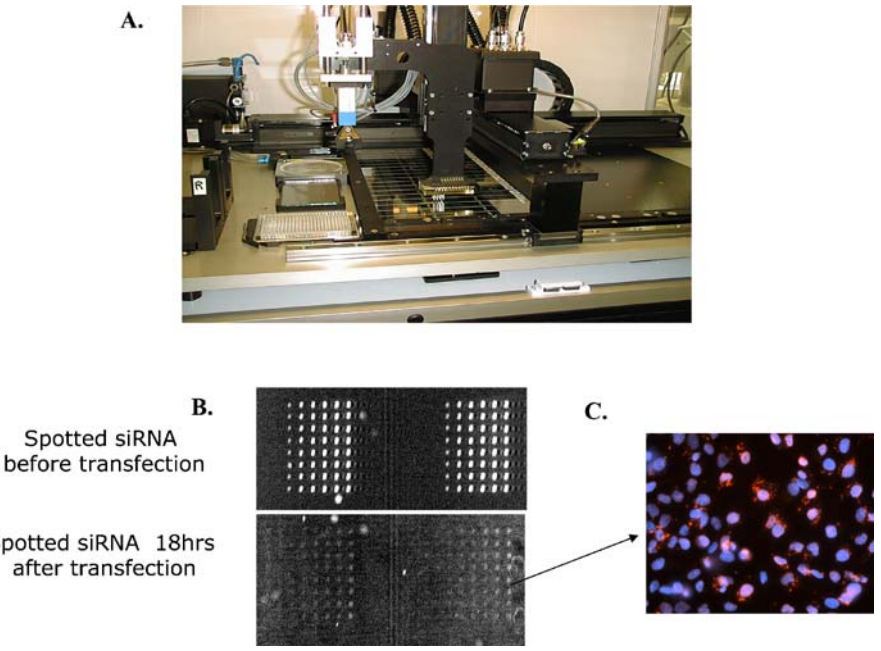

Fig. 3 RNA interference screens using cell arrays. siRNAs are spotted using a spotting robot at a high density on a microscopic slide (**A**). The quality of the generated microarray can be controlled by detection of the fluorescence from rhodamine-labeled siRNA (**B**). Efficiency of siRNA transfection can be monitored on a single-cell level using DAPI-counter-staining of nuclei (**D**). (Vanhecke et al., unpublished data)

the context of the living cell represents an attractive alternative in genome-wide functional studies, especially for RNA interference approaches.

Transfected-cell arrays have been applied to several aspects of protein functional analysis. Cell array-driven protein subcellular localization studies were mentioned previously in this review. In another example, the combination of transfected-cell technology with the mammalian two-hybrid system led to a powerful tool for screening whole cDNA libraries for proteins interacting with the gene product used as bait. An advantage of this PPI screening system is that the assay is performed in mammalian cells. Thus, interactions dependent on PTMs can be detected (Fiebitz et al., submitted).

Recently, an RNA interference-based cell array for loss-of-function studies in mammalian cells was developed by several groups including our own laboratory (Fig. 3). One study applied the combination of RNAi and reverse-transfection for validation of siRNA and shRNA probes in HeLa cells (Kumar et al. 2003). RNA probes targeting the MyoD gene were co-transfected together with the expression plasmid containing the MyoD gene as a reporter. In a similar experiment, Mousses et al. used arrayed rhodamine-labeled siRNA targeting GFP for knock-down of stable GFP expression in HeLa cells (Mousses et al. 2003).

Thus far, most studies have addressed RNAi silencing of co-transfected exogenous reporter genes or stably transfected genes. Recently, Erfle and co-workers have shown silencing of the endogenous βCOP gene in HeLa cells using the cell array method (Erfle et al. 2004). Moreover, primary and nonadherent cell lines, such as mesenchymal stem cells and human erythroleukemic cells, have also been used on RNAi cell microarrays (Yoshikawa et al. 2004; Kato et al. 2004). Thus, the applicability of the cell array platform to clinically important cells has been proved.

Conclusions

High-throughput techniques have had a profound impact on genome research. Compared with traditional biological experiments, high-throughput experiments require intensive data processing. Moreover, special care must be taken during analysis to obtain accurate and reproducible results. Nevertheless, microarray-based technologies have enabled substantial advancements in our understanding of cell biology. For example, these new tools have helped to elucidate, at least in part, the cell cycle regulatory pathways that lead to tumorigenesis. Furthermore, these tools have produced evidence that in type II diabetes, mitochondrial function may be a limiting factor in insulin resistance (Mootha et al. 2003). New commercial products such as diagnostic microarrays have emerged, thereby influencing actual clinical practice. Information obtained from these technologies can potentially influence clinical decisions such as the selection of appropriate drug therapy considering the unique genetic and metabolic profile of a given patient. Improved accuracy of gene expression profiling and genotyping at a genome-wide level will allow for therapy to be more precisely tailored to meet the molecular classification of the disease.

Acknowledgements. The author would like to acknowledge members of his laboratory: Dominique Vanhecke, Anna Guerasimova, Andrea Fiebitz, Yu-Hui Hu, Jian-Ping Liu, Xi Cheng, Irina Girnus, and Sabine Thamm. The author also thanks the following organizations for support: the European Commission (integrated project MolTools) and the German Federal Ministry of Education and Research (grant no. 0313068, 01GS0416, 01GR0414, 31P3674).

References

Amarzguioui M, Rossi JJ, Kim D (2005) Approaches for chemically synthesized siRNA and vector-mediated RNAi. FEBS Lett 579:5974–5981

Angenendt P, Glokler J, Sobek J, Lehrach H, Cahill DJ (2003) Next generation of protein microarray support materials: evaluation for protein and antibody microarray applications. J Chromatogr A 1009:97–104

Armour CD, Lum PY (2005) From drug to protein: using yeast genetics for high-throughput target discovery. Curr Opin Chem Biol 9:20–24

Arts GJ, Langemeijer E, Tissingh R, Ma L, Pavliska H, Dokic K, Dooijes R, Mesic E, Clasen R, Michiels F, van der Schueren J, Lambrecht M, Herman S, Brys R, Thys K, Hoffmann M, Tomme P, van Es H (2003) Adenoviral vectors expressing siRNAs for discovery and validation of gene function. Genome Res 13:2325–2332

Ashkenazi A (2002) Targeting death and decoy receptors of the tumor necrosis factor superfamily. Nat Rev Cancer 2:420–430

Auburn RP, Kreil DP, Meadows LA, Fischer B, Matilla SS, Russell S (2005) Robotic spotting of cDNA and oligonucleotide microarrays. Trends Biotechnol 23:374–379

Bernards R, Brummelkamp TR, Beijersbergen RL (2006) shRNA libraries and their use in cancer genetics. Nat Methods 3:701–706

Berns K, Hijmans EM, Mullenders J, Brummelkamp TR, Velds A, Heimerikx M, Kerkhoven RM, Madiredjo M, Nijkamp W, Weigelt B, Agami R, Ge W, Cavet G, Linsley PS, Beijersbergen RL, Bernards R (2004) A large-scale RNAi screen in human cells identifies new components of the p53 pathway. Nature 428:431–437

Brummelkamp TR, Bernards R, Agami R (2002) A system for stable expression of short interfering RNAs in mammalian cells. Science 296:550–553

Carthew RW (2001) Gene silencing by double-stranded RNA. Curr Opin Cell Biol 13:244–248

Cheung VG, Morley M, Aguilar F, Massimi A, Kucherlapati R, Childs G (1999) Making and reading microarrays. Nat Genet 21(Suppl):15–19

Colosimo A, Goncz KK, Holmes AR, Kunzelmann K, Novelli G, Malone RW, Bennett MJ, Gruenert DC (2000) Transfer and expression of foreign genes in mammalian cells. Biotechniques 29:314–324

Cullen LM, Arndt GM (2005) Genome-wide screening for gene function using RNAi in mammalian cells. Immunol Cell Biol 83:217–223

Dang CV, Barrett J, Villa-Garcia M, Resar LM, Kato GJ, Fearon ER (1991) Intracellular leucine zipper interactions suggest c-Myc hetero-oligomerization. Mol Cell Biol 11:954–962

Ding DQ, Tomita Y, Yamamoto A, Chikashige Y, Haraguchi T, Hiraoka Y (2000) Large-scale screening of intracellular protein localization in living fission yeast cells by the use of a GFP-fusion genomic DNA library. Genes Cells 5:169–190

Dixon EP, Johnstone EM, Liu X, Little SP (1997) An inverse mammalian two-hybrid system for beta secretase and other proteases. Anal Biochem 249:239–241

Duggan DJ (1999) Expression profiling using cDNA microarrays. Nat Genet 21:10–14

Erfle H, Simpson JC, Bastiaens PI, Pepperkok R (2004) siRNA cell arrays for high-content screening microscopy. Biotechniques 37:454–458, 460, 462

Fan JB, Chee MS, Gunderson KL (2006a) Highly parallel genomics assays. Nat Rev Genet 7:632–644

Fan JB, Gunderson KL, Bibikova M, Yeakley JM, Chen J, Wickham Garcia E, Lebruska LL, Laurent M, Shen R, Barker D (2006b) Illumina universal bead arrays. Methods Enzymol 410:57–73

Feng XH, Dernyck R (2001) Mammalian two-hybrid assays. Analyzing protein-protein interactions in transforming growth factor-beta signaling pathway. Mol Biol 177:221–239

Fields S (2005) High-throughput two-hybrid analysis. The promise and the peril. FEBS J 272:5391–5399

Goehler H, Lalowski M, Stelzl U, Waelter S, Stroedicke M, Worm U, Droege A, Lindenberg KS, Knoblich M, Haenig C, Herbst M, Suopanki J, Scherzinger E, Abraham C, Bauer B, Hasenbank R, Fritzsche A, Ludewig AH, Bussow K, Coleman SH, Gutekunst CA, Landwehrmeyer BG, Lehrach H, Wanker EE (2004) A protein interaction network links GIT1, an enhancer of huntingtin aggregation, to Huntington's disease. Mol Cell 15:853–865

Hu YH, Warnatz HJ, Vanhecke D, Wagner F, Fiebitz A, Thamm S, Kahlem P, Lehrach H, Yaspo ML, Janitz M (2006) Cell array-based intracellular localization screening reveals novel functional features of human chromosome 21 proteins. BMC Genomics 7:155

Igney FH, Krammer P (2002) Death and anti-death: tumor resistance to apoptosis. Nat Rev Cancer 2:277–288

Jackson AL, Burchard J, Leake D, Reynolds A, Schelter J, Guo J, Johnson JM, Lim L, Karpilow J, Nichols K, Marshall W, Khvorova A, Linsley PS (2006) Widespread siRNA "off-target" transcript silencing mediated by seed region sequence complementarity. RNA 12:1179–1187

Jackson AL, Linsley PS (2004) Noise amidst the silence: off-target effects of siRNA? Trends Genet 20:521–524

Jin F, Hazbun T, Michaud GA, Salcius M, Predki PF, Fields S, Huang J (2006) A pooling-deconvolution strategy for biological network elucidation. Nat Methods 3:183–189

Kaller M, Lundeberg J, Ahmadian A (2007) Arrayed identification of DNA signatures. Expert Rev Mol Diagn 7:65–76

Kamath RS, Fraser AG, Dong Y, Poulin G, Durbin R, Gotta M, Kanapin A, Le Bot N, Moreno S, Sohrmann M, Welchman DP, Zipperlen P, Ahringer J (2003) Systematic functional analysis of the Caenorhabditis elegans genome using RNAi. Nature 421:231–237

Kato K, Umezawa K, Miyake M, Miyake J, Nagamune T (2004) Transfection microarray of nonadherent cells on an oleyl poly(ethylene glycol) ether-modified glass slide. Biotechniques 37:444–452

Krishna RG, Wold F (1993) Post-translational modification of proteins. Adv Enzymol Relat Areas Mol Biol 67:265–298

Kumar R, Conklin DS, Mittal V (2003) High-throughput selection of effective RNAi probes for gene silencing. Genome Res 13:2333–2340

Kumar A, Agarwal S, Heyman JA, Matson S, Heidtman M, Piccirillo S, Umansky L, Drawid A, Jansen R, Liu Y Cheung KH, Miller P, Gerstein M, Roeder GS, Snyder M (2002) Subcellular localization of the yeast proteome. Genes Dev 16:707–719

Kuttenkeuler D, Boutros M (2004) Genome-wide RNAi as a route to gene function in Drosophila. Brief Funct Genomic Proteomic 3:168–176

Kwon M, Scholey JM (2004) Spindle mechanics and dynamics during mitosis in Drosophila. Trends Cell Biol 14:194–205

Lamitina T (2006) Functional genomic approaches in C. elegans. Methods Mol Biol 351:127–138

Lander ES, Linton LM, Birren B, et al. (2001) Initial sequencing and analysis of the human genome. Nature 409:860–921

Lee JW, Lee SK (2004) Mammalian two-hybrid assay for detecting protein-protein interactions in vivo. Methods Mol Biol 261:327–336

Legrain P, Selig L (2000) Genome-wide protein interaction maps using two-hybrid systems. FEBS Lett 480:32–36

Lehner B, Semple JI, Brown SE, Counsell D, Campbell RD, Sanderson CM (2004) Analysis of a high-throughput yeast two-hybrid system and its use to predict the function of intracellular proteins encoded within the human MHC class III region. Genomics 83:153–167

Leonhardt SA, Altmann M, Edwards DP (1998) Agonist and antagonists induce homodimerization and mixed ligand heterodimerization of human progesterone receptors in vivo by a mammalian two-hybrid assay. Mol Endocrinol 12:1914–1930

Lettre G, Hengartner MO (2006) Developmental apoptosis in C. elegans: a complex CEDnario. Nat Rev Mol Cell Biol 7:97–108

Li CX, Parker A, Menocal E, Xiang S, Borodyansky L, Fruehauf JH (2006) Delivery of RNA interference. Cell Cycle 5:2103–2109

Liebel U, Starkuviene V, Erfle H, Simpson JC, Poustka A, Wiemann S, Pepperkok R (2003) FEBS Lett 554:394–398

Lin X, Ruan X, Anderson MG, McDowell JA, Kroeger PE, Fesik SW, Shen Y (2005) siRNA mediated off-target gene silencing triggered by a 7 nt complementation. Nucleic Acids Res 33:4527–4535

Lipshutz RJ, Fodor SP, Gingeras TR, Lockhart DJ (1999) High density synthetic oligonucleotide arrays. Nat Genet 21(Suppl 1):20–24

Mann M, Jensen ON (2003) Proteomic analysis of post-translational modifications. Nat Biotechnol 21:255–261

Mannherz O, Mertens D, Hahn M, Lichet P (2006) Functional screening for proapoptotic genes by reverse transfection cell array technology. Genomics 87:665–672

Miller J, Stagljar I (2004) Using the yeast two-hybrid system to identify interacting proteins. Methods Mol Biol 261:247–262

Moffat J, Grueneberg DA, Yang X, Kim SY, Kloepfer AM, Hinkle G, Piqani B, Eisenhaure TM, Luo B, Grenier JK, Carpenter AE, Foo SY, Stewart SA, Stockwell BR, Hacohen N, Hahn WC, Lander ES, Sabatini DM, Root DE (2006) A lentiviral RNAi library for human and mouse genes applied to an arrayed viral high-content screen. Cell 124:1283–1298

Mootha VK, Lindgren CM, Eriksson KF, Subramanian A, Sihag S, Lehar J, Puigserver P, Carlsson E, Ridderstrale M, Laurila E, Houstis N, Daly MJ, Patterson N, Mesirov JP, Golub TR, Tamayo P, Spiegelman B, Lander ES, Hirschhorn JN, Altshuler D, Groop LC (2003) PGC-1alpha-responsive genes involved in oxidative phosphorylation are coordinately downregulated in human diabetes. Nat Genet 34:267–273

Mousses S, Caplen NJ, Cornelison R, Weaver D, Basik M, Hauteniemi S, Elkahloun AG, Lotfuo RA, Choudary A, Dougherty ER, Suh E, Kallioniemi O (2003) RNAi microarray analysis in cultured mammalian cells. Genome Res 13:2341–2347

Murakami Y, Fukazawa H, Kobatake T, Yamagoe S, Takebe Y, Tobiume M, Matsuda M, Uehara Y (2002) A mammalian two-hybrid screening system for inhibitors of interaction between HIV Nef and the cellular tyrosine kinase Hck. Antiviral Res 55:161–168

Musacchio A (2002) How SH3 domains recognize proline. Adv Protein Chem 61:211–268

Narvaiza I, Aparicio O, Vera M, Razquin N, Bortolanza S, Prieto J, Fortes P (2006) Effect of adenovirus-mediated RNA interference on endogenous microRNAs in a mouse model of multidrug resistance protein 2 gene silencing. J Virol 80:12236–12247

Nicholson DW (2000) From bench to clinic with apoptosis-based therapeutic agents. Nature 407:810–816

Paddison PJ, Silva JM, Conklin DS, Schlabach M, Li M, Aruleba S, Balija V, O'Shaughnessy A, Gnoj L, Scobie K, Chang K, Westbrook T, Cleary M, Sachidanandam R, McCombie WR, Elledge SJ, Hannon GJ (2004) A resource for large-scale RNA-interference-based screens in mammals. Nature 428:427–431

Palmer EL, Miller AD, Freeman TC (2006) Identification and characterisation of human apoptosis inducing proteins using cell-based transfection microarrays and expression analysis. BMC Genomics 7:145

Pei Y, Tuschl T (2006) On the art of identifying effective and specific siRNAs. Nat Methods 3:670–676

Sandy P, Ventura A, Jacks T (2005) Mammalian RNAi: a practical guide. Biotechniques 39:215–224

Simpson JC, Wellenreuther R, Poustka A, Pepperkok R, Wiemann S (2000) Systematic subcellular localization of novel proteins identified by large-scale cDNA sequencing. EMBO Rep 1:287–292

Sontheimer EJ (2005) Assembly and function of RNA silencing complexes. Nat Rev Mol Cell Biol 6:127–138

Talapatra A, Rouse R, Hardiman G (2002) Protein microarrays: challenges and promises. Pharmacogenomics 3:527–536

Tavernier J, Eyckerman S, Lemmens I, Van der Heyden J, Vandekerckhove J, Van Ostade X (2002) MAPPIT: a cytokine receptor-based two-hybrid method in mammalian cells. Clin Exp Allergy 32:1397–1404

Thierry-Mieg N (2006) A new pooling strategy for high-throughput screening: the Shifted Transversal Design. BMC Bioinformatics 7:28

Vanhecke D, Janitz M (2004) High-throughput gene silencing using cell arrays. Oncogene 23:8353–8358

Venter JC, Adams MD, Myers EW, et al. (2001) The sequence of the human genome. Science 291:1304–1351

Wolber PK, Collins PJ, Lucas AB, De Witte A, Shannon KW (2006) The Agilent in situ-synthesized microarray platform. Methods Enzymol 410:28–57

Yoshikawa T, Uchimura E, Kishi M, Funeriu DP, Miyake M, Miyake J (2004) Transfection microarray of human mesenchymal stem cells and on-chip siRNA gene knockdown. J Control Release 96:227–232

Zhang Y, Feng XH, Derynck R (1998) Smad3 and Smad4 cooperate with c-Jun/c-Fos to mediate TGF-beta-induced transcription. Nature 394:909–913

Zhao HF, Kiyota T, Chowdhury S, Purisima E, Banville D, Konishi Y, Shen SH (2004) A mammalian genetic system to screen for small molecules capable of disrupting protein-protein interactions. Anal Chem 76:2922–2927

Zhong J, Zhang H, Stanyon CA, Tromp G, and Finley RL Jr (2003) A strategy for constructing large protein interaction maps using the yeast two-hybrid system: regulated expression arrays and two-phase mating. Genome Res 13:2691–2699

Ziauddin J, Sabatini DM (2001) Microarrays of cells expressing defined cDNAs. Nature 411:107–110

Rev Physiol Biochem Pharmacol (2007) 159:131 –149
DOI 10.1007/112_2007_704

B. M. Jockusch · K. Murk · M. Rothkegel

The profile of profilins

Published online: 8 August 2007

Abstract Profilins are small proteins involved in actin dynamics. In accordance with this function, they are found in all eukaryotes and are structurally highly conserved. However, their precise role in regulating actin-related functions is just beginning to emerge. This article recapitulates the wealth of information on structure, expression and functions accumulated on profilins from many different organisms in the 30 years after their discovery as actin-binding proteins. Emphasis is given to their interaction with a plethora of many different ligands in the cytoplasm as well as in the nucleus, which is considered the basis for their various activities and the significance of the tissue-specific expression of profilin isoforms.

Introduction

About three decades ago, profilin was first described as a 15-kDa small protein that copurified with monomeric actin from calf spleen and inhibited actin polymerization (Carlsson et al. 1976, 1977). Its given name referred to this property, as it kept actin in the form of "pro-filamentous actin." Since then, we learned that profilins constitute a large family of proteins, generated mainly by separate genes, but in some cases also as splice products, in lower eukaryotes (Cooley et al. 1992; Haugwitz et al. 1991; Ozaki et al. 1983; Reichstein and Korn 1979; Tilney et al. 1983; Wilkes and Otto 2000; Wilkes and Otto 2003), plants (Staiger et al. 1993; Valenta et al. 1993), invertebrates (Cooley et al. 1992; Polet et al. 2006; Somboonwiwat et al. 2006) and vertebrates (Braun et al. 2002; Honoré et al. 1993; Witke et al. 1998, 2001). There is even a viral profilin (Blasco et al. 1991) whose gene organization is homologous to the mammalian profilins and may thus have been highjacked from a mammalian host cell. In tissue-forming organisms like animals or higher plants, profilins may be expressed in a tissue-specific manner, and it has been shown that deletion of profilins usually has severe consequences on viability of the afflicted organism. Hence, profilins

B. M. Jockusch (✉) · K. Murk · M. Rothkegel
Technical University of Braunschweig, Cell Biology, Zoological Institute,
38092 Braunschweig, Germany
e-mail: bmj@tu-bs.de · Tel.: +49-531-3913182 · Fax: +49-391-8203

have attracted the attention of many scientific groups, but the precise function of these small, ubiquitous proteins in cells and tissues still remains rather mysterious. Several reviews have been published in the last decade summarizing the knowledge on structure and function of profilins (e.g., Baatout 1996; Haarer and Brown 1990; Pollard and Quirk 1994; Schlüter et al. 1997; Witke 2004; Yarmola and Bubb 2006). The present review attempts to combine the wealth of information presented in these articles with the recent development in the field, trying to present the state of the art concerning this fascinating, multitasking protein.

Background

On the corporate identity of profilins

Genomic DNA sequences of putative profilins contain three exons that may be separated by introns of vastly different sizes (Huang et al. 1996), and can be dispersed throughout the genome. Consequently, identification of profilins has concentrated on sequencing the open reading frames and data comparison in search for homology. Numerous amino acid sequences of profilins have thus been deduced over the past three decades. While in the early days of this period the sequences of unicellular organisms (yeast, slime moulds, etc.) and of animals (insects, mammals) were primarily the focus of such investigations (reviewed in Schlüter et al. 1997), more recently plant profilins became very popular. Here, one finds numerous examples of proteins that were originally given different names but later on were identified as profilins. When comparing amino acid sequences of different origins, one learns that not only profilins of distantly related species may show less than 25% overall homology (Pollard and Quirk 1994), but even profilin sequences expressed within the same animal or plant species may vary considerably in sequence (Huang et al. 1996; Kandasamy et al. 2002; Obermann et al. 2005). Hence, in dealing with profilins, one wonders: how is a profilin defined?

One solid criterion to rely on is the structure. The secondary and tertiary structures of all profilins thus far elucidated are strikingly similar. Profilins of *Acanthamoeba*, mammalian or birch origin display a compact center comprising seven beta strands packed into a beta-sheet, surrounded by four alpha helices (Domke et al. 1997; Fedorov et al. 1997; Fedorov et al. 1994; Schutt et al. 1993). The N- and C-terminal regions, both being part of an alpha helix, are adjacent to each other (see Fig. 1A).

Another criterion commonly used to define a profilin is its capacity to interact with three classes of ligands. In general, profilins were found to have discrete and surface-exposed binding sites for actins (Schutt et al. 1993) including actin-related proteins (ARPs) (Machesky et al. 1994a), poly-L-proline (PLP) stretches (Mahoney et al. 1997), and phosphatidylinositol lipids (Lassing and Lindberg 1985), as shown in Fig. 1. These binding sites have been characterized in detail, and the motifs interacting with the different ligands have been identified for many profilins, including plant proteins (Thorn et al. 1997). Not surprisingly, the amino acid sequences comprising these motifs are relatively well conserved throughout different kingdoms (Huang et al. 1996). There are even a few residues consistently conserved throughout all organisms, for example, a tryptophan residue (W3) at the N-terminus, with only one exception, human profilin IV (Obermann et al. 2005). Yet, the affinity for the different ligands may differ by orders of magnitude between species and even isoforms (see Schlüter et al. 1997). Extreme examples are a minor mouse splice form that has been reported not to bind to G-actin (Di Nardo et al. 2000), and Vaccinia virus profilin which

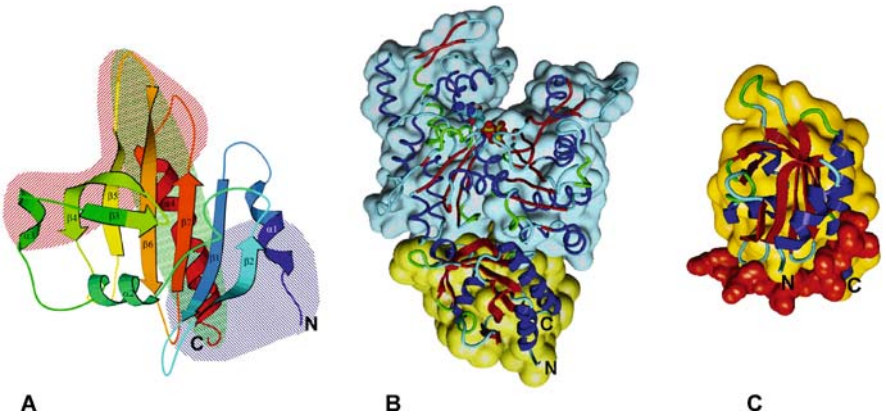

Fig. 1 The three major ligand-binding sites on profilin. **A** Schematic representation of the binding sites for actin (*red*), poly-L-proline (*PLP, blue*) and phosphatidylinositol-4,5-bisphosphate (*PIP2, green*) on the surface of a profilin molecule. (Modified after Cedergren-Zeppezauer et al. 1994). Note that the PIP2-binding area forms an extensive patch which overlaps with the binding areas for actin and PLP. **B** The complex of bovine profilin (*yellow*) with beta actin (*blue*). (Derived from Schutt et al. 1993). **C** The structure of human platelet profilin in complex with a 15mer of L-proline. (From Mahoney et al. 1997). Note that the orientations of the profilin molecules depicted in **B** and **C** are different. The figures were generated using the YASARA program, using PDB:1pne (**A**), PDB ID:1hlu (**B**) and pPDB ID:1cjf (**C**). (Berman et al. 2000)

does not bind to PLP (Machesky et al. 1994b). Low affinity for PLP may cause complications in biochemically characterizing a protein as a profilin, since this interaction is routinely employed to purify genuine as well as recombinant profilins by PLP affinity chromatography. More subtle differences in ligand binding may be the rationale for isoform-specific expression of profilins and their ligands in particular tissues (see section "The biological significance of isoforms").

In general, profilins within a given kingdom display a greater sequence homology than those between different kingdoms. This is particularly evident when one compares plant with animal profilins. Even the actin-binding surface of plant profilins is only partially conserved in animal profilins (Thorn et al. 1997). In some cases, however, profilin isoforms expressed in one species may show greater sequence homology to profilins of other species than to their fellow profilins within the same organism. Thus, profilin IV, the isoform identified in mammalian sperm cells during acrosome genesis, displays greater homology to *Drosophila* and yeast profilins than to other mammalian profilins (Obermann et al. 2005; Polet et al. 2007). Hence, this isoform has probably evolved prior to vertebrates, while profilins I, II and III are more closely related (Polet et al. 2007).

Profilin gene families and protein expression

The number of profilin genes per organism correlates roughly with its complexity. While lower eukaryotes contain one or two, occasionally three [i.e., *Dictyostelium discoideum* (Arasada et al. 2007) and *Caenorhabditis elegans*, (Polet et al. 2006)] genes, higher eukaryotes display higher numbers, with plants leading the list.

In mammals, four discrete profilin genes have been identified, *Pfn1-Pfn4*. While *Pfn1* gives rise to the ubiquitous isoform profilin I (Schlüter et al. 1997), *Pfn2* produces two splice variants, profilin II, primarily expressed in neuronal cells, and an mRNA for a minor form

(IIb), found mainly in the kidney (Di Nardo et al. 2000). *Pfn3* and *Pfn4* code for kidney- and testis-specific variants (Hu et al. 2001; Obermann et al. 2005). Expression of the sperm-specific profilins is developmentally regulated, and their existence may be correlated with actin-related proteins also specifically expressed in male germ cells (Kim et al. 1989; Tanaka et al. 2003).

In plants, both mono- and dicotyledones contain up to ten different profilin genes. While some of these genes may be pseudogenes, others give rise to isoform proteins that, according to their sequence similarity (Huang et al. 1996) or their biochemical properties (Kovar et al. 2000), can be assigned to two different classes. There are ubiquitous forms, found constitutively expressed in all tissues, others are restricted to reproductive tissues, and their expression is strictly regulated during development (Kandasamy et al. 2002). An excellent overview on plant profilins, with emphasis on the situation in *Arabidopsis thaliana*, was given by Huang et al. (1996), and since then, studies on the identification and biochemical characterization of profilins in many different plants have increased enormously. This is, at least in part, due to the fact that plant profilins are potent allergens (see section "Unphysiological activities"). Thus, in addition to raising the curiosity of cell and molecular plant biologists, they are of clinical relevance. It is tempting to speculate that the complexity of profilin expression in higher plants is correlated with the observation that the actin family is also more complex here than in other kingdoms (McDowell et al. 1996), and this is also true for an important class of PLP stretch ligands for profilins in *Arabidopsis thaliana*, the formins (Deeks et al. 2002).

Crosstalk with ligands

Interactions of the actin-binding site

As shown in Fig. 1A and B, the actin-binding site on profilin, as determined by X-ray analysis of the bovine beta-actin–profilin complex (Schutt et al. 1993), is roughly opposite to the C-and N-terminal region of the folded molecule. It comprises surface exposed motifs of the alpha helices 3 and 4, of beta strands 4, 5 and 6 and of extended loop regions in between. However, when comparing profilins from different species, the amino acids involved seem quite variable (Thorn et al. 1997). Stoichiometric complexes with G-actin are formed, and on the actin side, subdomains 1 and 3 are involved (Fig. 1B). The contact site thus covers a fairly large surface area [approximately 2,250 $Å^2$ (Schutt et al. 1993)]. Profilin binding to the actin monomer results in a slight deformation of the latter and the stabilization of an actin conformation with a wider nucleotide pocket, which facilitates the exchange of the bound ADP/ATP (Perelroizen et al. 1995; Selden et al. 1999; Minehardt et al. 2006). At growing F-actin filaments, the most distal actin subunit at the fast-growing end is oriented such that profilin can still be bound, at least transiently (Gutsche-Perelroizen et al. 1999).

In addition to binding to all bona fide isoforms of actin, profilin also interacts with some members of the actin-related proteins (ARPs), which together with the conventional actins comprise the actin superfamily. ARPs interact with a variety of polypeptides to form protein complexes employed in highly diverse processes, including chromatin modulation and cytoplasmic motility (reviewed in Muller et al. 2005). ARP2 and ARP3, two components of the ARP 2/3 complex, which is engaged in the organization and growth of the dynamic submembranous actin networks in cells (Pollard and Borisy 2003), have both been identified as profilin ligands (Kelleher et al. 1995; McCollum et al. 1996; Machesky et al. 1994a). In

Arabidopsis thaliana, orthologs of all seven subunits of the animal ARP 2/3 complex have been identified (Deeks and Hussey 2003).

Apart from actin-related proteins, the actin-binding site of profilins interacts with at least one additional protein, gephyrin. Gephyrins are dual function proteins existing in different splice forms. In plants and animals, they are involved in the synthesis of the molybdenum cofactor required by many different enzymes (Ramming et al. 2000). Furthermore, in the central mammalian nervous system, they contribute to the postsynaptic scaffold at the postsynaptic side of inhibitory neurons, thus supporting receptor clustering (Feng et al. 1998; Jockusch et al. 2004). Originally, gephyrin, which contains PLP stretches, was described as a ligand for the PLP-binding site on profilins (Mammoto et al. 1998), but was later on identified as a ligand for the actin-binding site, competing with actin for profilin binding (Giesemann et al. 2003).

Interactions of the poly-L-proline-binding site

The N- and C-terminal sequence regions of the compactly folded profilin both form the platform for binding to poly-L-proline stretches (PLPs, Fig. 1C). The number of proteins comprising suitable PLPs (at least eight to ten prolines, either in continuous sequence or interrupted by single glycines) is rather large, and as already mentioned above, the affinity of profilins for proteins comprising such stretches is variable (see Schlüter et al. 1997). Proteins that have been identified as ligands for profilin via their PLPs are compiled in Table 1. At a first glance, this list presents a large catalogue of proteins highly variable with respect to their cellular localization, structural organization and function. They reside in the cytoplasm as well as the nucleus, some are dual compartment proteins. The proposed or identified functions range from executing various types of cytoskeletal organization, signal perception and motility, to ribonucleo particle (RNP) maturation, storage and transport, and transcription. A closer inspection, however, reveals common features for a large group of cytoplasmic profilin ligands: Members of the Ena/VASP, formin and WASP/WAVE families are all large, multidomain proteins whose PLPs, the profilin-binding sites, comprise a motif in their central part, flanked by a G-actin- and frequently also by an adjacent F-actin-binding site (Michelot et al. 2005). This organization was first revealed in VASP (Walders-Harbeck et al. 2002; Hüttelmaier et al. 1999), which was also identified as the first biological ligand for the PLP-binding site of profilin (Reinhard et al. 1995). An analogous motif organization has been found in WAVE/WASP and formin proteins, in animals and plants (Stradal et al. 2004; Michelot et al. 2005). In members of all three protein families, binding sites for profilin, G- and F-actin are combined with binding sites for quite different proteins that are either members of cell adhesion complexes and/or of signaling pathways. These properties allow the Ena/VASP, formin and WAVE/WASP proteins to play vital roles in the transmission of external signals to the actin and/or microtubule cytoskeleton. Their affinity for their various ligands is frequently modulated by phosphorylation and oligomerization, which may regulate their cellular activity.

In contrast, other PLP proteins that have been identified as profilin ligands bear little resemblance to each other. However, since new PLP proteins are still being identified as profilin ligands, future research may fill in some gaps in this respect.

Interactions with phosphatidylinositol lipids

A phosphatidylinositol lipid-binding site was first reported for phosphatidylinositol-4,5-bisphosphate (PIP2) and bovine profilin (Lassing and Lindberg 1985), and was later confirmed for a variety of other profilins throughout different phyla. The motif was described as a hydrophobic patch within the actin-binding site (see Fig. 1A). More recently, a second binding site for PIP2 was described, overlapping with the poly-L-proline-binding site at the C-terminal region of the profilin molecule (Lambrechts et al. 2002; Skare and Karlsson 2002; Witke 2004). Both phospholipid binding sites are in fact part of a rather broad band of surface-exposed hydrophobic residues (Witke 2004). In analogy to the competition between PIP2 and actin binding on profilin, there is also competition between PIP2 and the PLP stretch ligands at the carboxyterminal site. This has been explicitly shown for mammalian profilin I, while there are conflicting data for profilin II, the neuronal profilin isoform (Gareus et al. 2006; Lambrechts et al. 1997). The affinity of different profilins for PIP2 is quite variable (see Fedorov et al. 1994; Schlüter et al. 1997; Lambrechts et al. 2002). Furthermore, other products of the phosphoinosite metabolism, like phosphatidylinositol-3,4-bisphosphate and phosphatidylinositol-3,4,5-trisphophate, bind to profilins with higher affinity than PIP2 (Lu et al. 1996). Thus, it may be the more finely tuned affinity of profilin for PIP2 which allows for competition with other PIP2 binding proteins, and this may be highly relevant for profilin's role in signal-dependent actin dynamics.

Regulation of profilin–ligand interaction

Apart from the observation of competition between PIP2 and actin, and PIP2 and PLP-stretch ligands, very little is known about what regulates the complex formation between profilins and their many different ligands. Serine phosphorylation by protein kinase C zeta has been reported to increase the affinity for G-actin and PLP, while the interaction with PIP2 remained unaltered (Sathish et al. 2004).

Cellular location

Profilins have been found mainly in three different locations in cells. The interaction of profilins with membrane-bound phospholipids and/or actin predicted that profilin should be enriched at dynamic plasma membranes in locomoting or spreading animal cells. This was confirmed with specific antibodies for cultured fibroblasts (Buss et al. 1992) and for epithelial cells (Mayboroda et al. 1997). In plants, the pollen-specific isoforms have been localized

Table 1 Protein ligands that interact with the poly-l-proline-binding site of profilin

Profilin ligands	Biochemical properties in addition to profilin binding	Proposed or established function
Ena/Mena/VASP/ family proteins (Reinhard et al. 1995) (Gertler et al. 1996)	Bind to cell adhesion proteins (Reinhard et al. 1992) (Reinhard et al. 1996) and to actin, nucleate actin filaments (Harbeck et al. 2000, Walders-Harbeck et al. 2002)	Control cellular dynamics (Gertler et al. 1996, Rottner et al. 1999) (Krause et al. 2003)

Table 1 (continued)

Profilin ligands	Biochemical properties in addition to profilin binding	Proposed or established function
Formin family proteins (Chang et al. 1997, Evangelista et al. 1997, Higgins 2005, Krebs et al. 2001, Manseau et al. 1996, Sato et al. 2006, Watanabe et al. 1997)	Bind to actin and nucleate filaments (Pruyne et al. 2002, Zigmond 2004), bind to tubulin and microtubules (Zhou et al. 2006) and to Rho small GTPases (Watanabe et al. 1997)	Control growth of linear actin filaments and thus cellular and tissue morphology (Faix and Grosse 2006, Sato et al. 2006, Schmitz et al. 2006, Wallar and Alberts 2003) (Michelot et al. 2005), stabilize and orient microtubules(Palazzo et al. 2001)
WASP and WAVE family proteins (Miki et al. 1998, Stradal et al. 2004, Suetsugu et al. 1998, Witke et al. 1998)	Bind to PIP2, Cdc42, ARP complexes and actin and nucleate filaments (Stradal et al. 2004)	Regulate site directed actin networks by connecting signaling to the actin cytoskeleton (Stradal et al. 2004, Witke et al. 1998)
Palladin (Boukhelifa et al. 2006)	Binds to Ena/VASP, alpha actinin and ezrin (Boukhelifa et al. 2006)	May concentrate adhesion-linked cytoskeletal proteins to the cell membrane (Boukhelifa et al. 2006)
Drebrin (Mammoto et al. 1998)	Binds to actin (Shirao 1995)	Participates in formation and motility of branched cell processes in neuronal (Shirao 1995) and nonneuronal (Peitsch et al. 2006) cells
Dynamin 1 GTPase (Gareus et al. 2006)	Binds to SH3-proteins (Solomaha et al. 2005)	Controls formation and motility of endocytotic vesicles and other defined plasma membrane regions (Kruchten and McNiven 2006)
Survival motoneuron protein (SMN) (Giesemann et al. 1999, Sharma et al. 2005)	Binds to ribonucleoproteins, (Mourelatos et al. 2001)	Participates in assembly, processing and trafficking of small nuclear RNPs (Zhang et al. 2006), supports motor neuron development (McWhorter et al. 2003)
P42POP (Lederer et al. 2005)	Displays several properties of a myb-like transcription factor (Lederer et al. 2005)	Modulates transcription repression (Lederer et al. 2005)
Prrp (Zhao et al. 2001)	Belongs to the hnRNP family, binds to mRNAs that localize to the vegetal cortex of *Xenopus* oocytes during oogenesis (Zhao et al. 2001)	May serve in targeted transport of localized mRNA and thus in regionalized translation (Zhao et al. 2001)
RIAM (Lafuente et al. 2004)	Binds to Ena/VASP and to the GTPase RAP1 (Lafuente et al. 2004)	Links RAP1 to integrin activation, regulates actin dynamics (Lafuente et al. 2004)
Piccolo/Aczonin (Wang et al. 1999)	Interacts with many different members of the presynaptic cytomatrix at active zones of nerve terminals (Garner et al. 2000)	Involved in structural and functional roles of vesicle exocytosis in excitatory and inhibitory synapses (Garner et al. 2000)

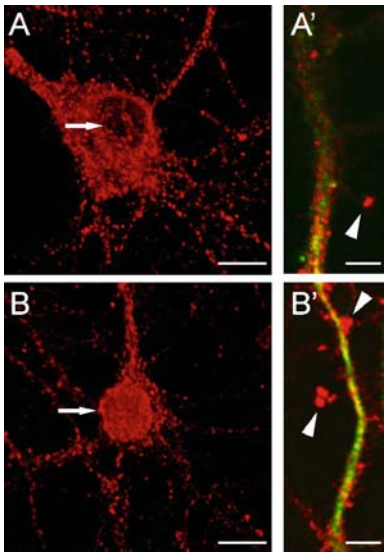

Fig. 2 Confocal laser scanning images of cultured murine hippocampal neurons. The cells were double-stained with isoform-specific monoclonal antibodies for profilin I (**A** and **A'**) or profilin II (**B** and **B'**) in *red*, for MAP 4 as an axonal marker in *green* (**A'** and **B'**). The pictures represent optical stacks. Note that both profilin isoforms are present in the cell body and in dendritic spine heads (*arrowheads* in **A'** and **B'**), but only profilin II is present in substantial amounts in the nucleus (*arrows*). *Bars*: **A**, **B**: 10 μm, **A', B'**: 2 μm

to the germinating pollen tube (see Hussey et al. 2006) for original references). Furthermore, profilin has also been observed in close association with internal membranes involved in vesicular transport, like Golgi-derived vesicles in fission yeast (Finger and Novick 1997) and mammalian cells (Dong et al. 2000). The neuronal isoform profilin II was identified as a constituent of the endocytotic machinery in mouse neurons (Gareus et al. 2006).

At present, there is some discrepancy about the location of profilins in neuronal structures. In one report, an increase in overall profilin content was seen in postsynaptic structures like dendritic spines in the lateral amygdala after fear conditioning of rats (Lamprecht et al. 2006). These data were obtained with antibody staining and support an earlier study performed with cultures of hippocampal neurons transfected with GFP-profilin II, showing that this isoform is translocated into dendritic spines after synaptic stimulation (Ackermann and Matus 2003). In contrast, another group, using specific antibodies for cellular localization and biochemical analysis of cell fractions, has reported that profilin II is primarily located in presynaptic matrices in the mouse brain (Boyl et al. 2007). These discrepancies are not easy to reconcile at the moment. In our own studies, using immunofluorescence with isoform-specific antibodies, we can clearly identify both profilin I and II in dendritic spines and spine heads of cultured mouse hippocampal cells (Fig. 2A', B').

Finally, profilins have been reported as residents of the nucleus. Immunofluorescence revealed nuclear profilin I in fibroblasts and epithelial cells (Mayboroda et al. 1997; Skare et al. 2003) and in bovine oocyte germinal vesicles and early embryos (Rawe et al. 2006). Nuclear profilin has also been described in several higher plants (see Hussey et al. 2006 for original references). Additionally, the existence of nuclear profilin–actin complexes can be deduced from studies on HeLa cells and *Xenopus* oocytes (Stüven et al. 2003). In a recent study with GFP-profilin transfected cells and polyclonal anti-serum, profilin II has been shown to accumulate in the nucleus of hippocampal neurons. This concentration was de-

scribed as being transient and dependent on activation with diverse stimuli (Birbach et al. 2006). However, in our own studies with monoclonal isoform-specific antibodies, profilin II is consistently seen as a prominent constituent of the nuclei of hippocampal cells. Notably, and in contrast to profilin II, profilin I is more highly concentrated in the cytoplasm than in the nucleus (Fig. 2A, B).

Physiological functions

Cytoplasmic activities

Based on a wealth of evidence, it is generally accepted that profilins regulate actin dynamics at plasma membranes, during the assembly, maintenance and disassembly of actin networks at the leading edge of locomoting animal cells, during cytokinesis, embryonic development and morphogenesis. The importance of this role is evident from the consequences on reducing the amount of profilin. *Dictyostelium* amoebae that lack profilin isoforms I and II are much larger, with a wide ring of filamentous actin beneath the plasma membrane, and a block in development (Haugwitz et al. 1994). Mice deficient in profilin I, normally expressed in all murine tissues and during all developmental stages, fail to develop beyond the blastocyst stage (Witke et al. 2001). Antibodies against profilin, when introduced into zygotes or early embryos, block bovine embryonic development (Rawe et al. 2006), and gene silencing of profilin leads to a reduction in actin filament formation, focal adhesions, cell migration and the morphogenesis of endothelial cords (Ding et al. 2006). A key event in these profilin-dependent processes is probably the direct interaction between profilin and actin in the cellular environment. In vitro, profilin forms a 1:1 complex with G-actin and catalyzes the exchange of the bound nucleotide. Under physiological conditions, this leads to a charging of G-actin with ATP. Results obtained from in vitro experiments with purified profilin and actin, and early observations made on lower eukaryotes like yeast and *Dictyostelium*, led to the assumption that profilin sequesters actin in cells, providing a pool of polymerization-competent ATP-G-actin. In a second period of "profilin research," however, profilin was considered to stabilize actin filaments and to stimulate actin polymerization, by the delivery of profilin:ATP-G-actin to the fast growing ends apposed to cell membranes (Pollard and Borisy 2003). This may be particularly important in animals, where the actin sequestering activity is provided by another actin ligand, thymosin β4 (for original references see Schlüter et al. 1997; Witke 2004; Yarmola and Bubb 2006). Today, several effects of profilin on actin in the cytoplasm are considered likely, ranging from actin filament growth stimulation to disassembly acceleration, but the precise mechanisms, in particular the time course of ATP hydrolysis at the fast growing end of nascent actin filaments, are still under debate (Kovar et al. 2006; Yarmola and Bubb 2006; Romero et al. 2007). In plants, the high profilin concentration found in some tissues like pollen is apparently sufficient to prevent actin polymerization (Hussey et al. 2006).

High local concentration and "molecular crowding" of the profilin-interacting proteins are certainly important factors in the regulation of actin-based cellular behavior. Many members of the PLP ligand families, Ena/VASP, WASP/WAVE and formins, are thought to bind not only profilin but profilin–actin complexes. While this still has to be demonstrated in vivo, cell-free experiments support this conclusion. For example, in animal cell extracts, the elongation of actin filaments by profilin-actin is markedly enhanced in the presence of formins (Romero et al. 2004), and in studies with *Arabidopsis thaliana* protein*s*, elonga-

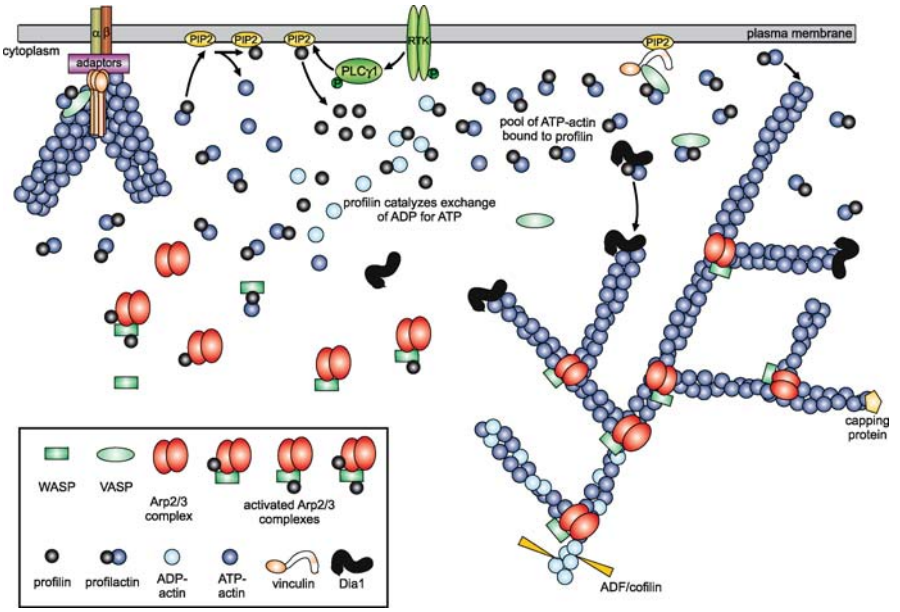

Fig. 3 Schematic representation of the multiple functional involvement of profilin at the plasma membrane. The ratio between membrane-bound and free profilin is regulated by the level of PIP2 and determines the complex formation of profilin with G-actin. Upon release from the membrane, profilin is involved in charging G-actin with ATP (*center*). Subsequently, the profilin-ATP-G-actin complex adds to nascent actin filaments and participates in the generation of actin filaments as needed for adhesion complexes (*left*) and lamellipodial actin networks (*right*). Details of this scenario show only selected examples of all possible constellations and are thus highly speculative, but consistent with the present knowledge

tion of actin filaments required the cooperation of profilin–actin with a formin (Michelot et al. 2005). The repetitive PLP stretches exposed in many of these multidomain proteins are capable of accommodating several profilin–actin complexes simultaneously, and may deliver the G-actin molecules to their adjacent binding sites. Furthermore, these membrane-apposed proteins are active in oligomeric form (Hüttelmaier et al. 1998; Li and Higgs 2003), and thus may provide dense clouds of profilin–actin and polymerization-competent G-actin precisely at the point of need. Subsequently, nascent filaments will be generated and then stabilized by the F-actin-binding sites and nucleating activity of these proteins. The fact that many of the PLP ligands are also members of several signal cascades, as mentioned above, and may transmit external stimuli upon activation, explains the signal dependence of localized actin filament growth. A particularly complicated case of such amplification cascades is represented by the WASP/WAVE proteins that have to be activated by PIP2 and the small GTPase Cdc42 before they can bind to profilin and actin (Stradal et al. 2004).

Multidomain proteins of the above quoted families and profilin participate not only in lamellipodial protrusion during locomotion but also in cell adhesion: VASP and profilin are both regular components of nascent adhesion complexes in spreading tissue culture cells (Hüttelmaier et al. 1998 and unpublished observations). In summary, the numerous profilin ligands and their different local concentrations may control actin polymerization, in conjunction with profilin–actin complexes, in a time- and space-controlled manner. Figure 3 presents a hypothetical model with selected examples of such processes at the cell membrane.

While profilin may regulate the available amount of polymerization-competent actin, conversely, the level of profilin is also subject to regulation. Two different mechanisms have been proposed that both start with profilin bound to cellular membranes via the PIP2-binding site. One model proposes that external signals activate tyrosine kinases to phosphorylate phospholipase C gamma 1 which subsequently splits PIP2, thus liberating membrane-bound profilin. This would then be available for complexing monomeric actin and charging it with ATP (Goldschmidt-Clermont et al. 1991). Profilin–actin complexes would then add to the fast growing end of actin filaments, thus actively participating in submembranous actin network formation (Fig. 3). An alternative hypothesis proposes that it is not PIP2 degradation but its signal-stimulated increase which might sequester profilin to the membrane, while the subsequently liberated actin molecules can add to the ends of actin filaments, without profilin (Witke 2004).

The importance of a finely regulated level of profilin and the ability of profilin molecules to interact with actin has also been revealed in studies demonstrating the role of profilin as a tumor suppressor. Human breast cancer cell lines contain consistently less profilin than normal breast epithelial cells, and raising the intracellular profilin level by transfection restores epithelial growth and abolishes tumor growth in nude mice (Janke et al. 2000). Notably, this requires a functional actin-binding site (Wittenmayer et al. 2004). The loss of profilin by gene disruption in profilin I-null mice (Witke et al. 2001), or by anti-profilin transfection in bovine oocytes (Rawe et al. 2006), leads to early embryonic death. This is probably due to defects in cytokinesis at time points when maternal profilin is diluted below a critical level. Reduction of the profilin I level in heterozygotes of the profilin I-null mutant results in loss of embryos, thus suggesting a dosage effect of this protein on cytokinesis (Witke et al. 2001). It is, however, conceivable that the absolute level of profilin and the profilin–actin ratio required for normal development and tumor suppression varies in different mammals, e.g., man and mouse (Witke 2004).

In addition to participating in actin-based processes like locomotion, adhesion, cytokinesis and morphogenesis, profilin is probably engaged in intracellular vesicle trafficking. In this case, the interaction with PLP stretch proteins seems especially important. In neurons, profilin II and dynamin 1 form complexes and profilin II competes with SH3 effector ligands of dynamin 1, and thus may down-regulate endocytosis of synaptic and clathrin-coated vesicles (Gareus et al. 2006), but also exocytosis of transmitter-containing vesicles at the presynapse of excitatory neurons in the mouse brain (Boyl et al. 2007). In general, a profilin–actin interaction can be envisioned as an important factor for vesicle mobility. However, in mature, isolated synaptic vesicles, profilin is conspicuously absent, while many of its bona fide ligands like dynamin 1, actin and the ARP 2/3 complex were identified as vesicle constituents (Takamori et al. 2006).

Nuclear activities

The functions of profilin and its ligands in the nucleus are much less well understood. Nuclear actin and nuclear ARPs are apparently engaged in a wide variety of different processes, ranging from participating in the transcriptional activity of all three types of RNA polymerases, chromatin remodeling to nuclear assembly and nuclear stability (Blessing et al. 2004; Grummt 2006), but the precise role of actins in these highly divergent processes is unknown. The finding that excessive actin has to be removed from somatic mammalian nuclei in the form of a profilin–actin complex (Stüven et al. 2003), i.e., in a specific, profilin-bound conformation, suggests that such a variety of nuclear functions might depend on discrete,

unconventional actin conformations, and at least one of these could be induced or stabilized by profilin (Jockusch et al. 2006). ARP2 and N-WASP, identified in the nucleus of chicken and human fibroblasts and HeLa cells, are believed to participate in RNA polymerase 2 activity by regulating actin polymerization (Wu et al. 2006), and monomeric actin, ARP3, VASP and the formin mDia 1 were found to colocalize with profilin in germinal vesicles and the zygotic pronuclei during bovine oocyte maturation and early development (Rawe et al. 2006). This implies that these proteins not only cooperate in cytoplasmic but also in nuclear functions with profilin. In addition, there are endogenous nuclear proteins that have also been identified as profilin partners. One of these is p42POP, a myb-related transcription factor that is regulated in its activity by profilin (Lederer et al. 2005). Furthermore, profilin was identified as a resident of nuclear and nucleolar bodies such as snRNP particles, spliceosomes, gems and Cajal bodies, and there is biochemical evidence suggesting that it interacts there with proteins like SMN (Giesemann et al. 1999; Sharma et al. 2005) and p80 coilin (Skare et al. 2003), proteins involved in pre-mRNA splicing and maturation. A functional significance of such interactions is suggested by the finding that anti-profilins can interfere with pre-mRNA splicing in vitro (Skare et al. 2003).

The biological significance of isoforms

In many studies, it was reported that the overall properties of profilins are so similar that one can cross-feed profilins from quite distant sources. For example, birch pollen profilin interacts faithfully with mammalian muscle actin in the test tube (Giehl et al. 1994) and with cytoplasmic actin in transfected mammalian cells (Rothkegel et al. 1996). Human profilin I controls actin polymerization induced by *Arabidopsis thaliana* formin in the same manner as plant profilins do (Michelot et al. 2005), and maize and bovine profilins rescue vital functions in *Dictyostelium* mutant amoebae lacking their endogenous profilins (Karakesisoglou et al. 1996; Schlüter et al. 1998). Yet, we observe a stunning number of isoforms, some of which are ubiquitous and constitutively expressed, others are developmentally or tissue-specifically regulated, as has been impressively demonstrated in plants (Kandasamy et al. 2002). We can only conclude that the differences in the affinity of the various isoforms for their ligands, as observed in biochemical assays, are important factors for preferential complex formation and competition between ligands in cells, thus determining different cellular and developmental processes. A general validity of this hypothesis awaits further examination, but evidence supporting this conclusion is emerging. In plants, different profilin isoforms can have discrete effects on actin dynamics and growth control in the same cell (Gibbon et al. 1998; McKenna et al. 2004). In mammals, the neuronal isoform profilin II associates preferentially with a subset of PLP ligands different from that bound to profilin I (Witke et al. 1998; Boyl et al. 2007), and of the two testis-specific isoforms profilin III and IV, the latter is involved in the regulation of testicular actin dynamics, in acrosome generation and spermatid nucleus morphogenesis, possibly in association with a specific actin isoform (Obermann et al. 2005).

The existence of profilin II, the isoform preferentially expressed in the mammalian neuronal system, has received much attention. Like other morphogenetic cellular processes, formation and maintenance of excitatory and inhibitory synapses depend on the actin cytoskeleton. Neurotransmitter release by vesicle exocytosis at the presynaptic side as well as receptor clustering and activation at the postsynaptic side both depend on microfilament networks (reviewed in Jockusch et al. 2004), and enforcement of specific synaptic connections, which are the basis for brain-specific tasks such as memory, require morphological shape

changes that are also executed by the cytoskeleton. Thus, it is not unexpected to find profilins present in synaptic structures, as described above, together with actin- and/or profilin-binding proteins like Mena, N-WASP, gephyrin, SMN, and proteins of the pre- or postsynaptic submembranous regions, such as piccolo/aczonin, delphilin (a formin protein) and drebrin (Jockusch et al. 2004; Witke 2004). Profilin I seems to carry out general functions in actin dynamics during neuritogenesis and synaptic plasticity (Lambrechts et al. 2006). It was identified in pre- as well as in postsynaptic structures in different regions of the mouse central nervous system, albeit in quite variable concentrations (Neuhoff et al. 2005), and in postsynaptic densities of inhibitory neurons of the spinal cord (Giesemann et al. 2003). Several reports have suggested that both profilin isoforms are involved in neuritogenesis (Da Silva et al. 2003; Lambrechts et al. 2006), but more recent data with mutant mice indicate that profilin II is not required for this complex morphogenetic process (Boyl et al. 2007). In early mouse embryos, this isoform is only weakly expressed and apparently cannot compensate for the loss of profilin I in development, but in adult mouse brain, profilin II accounts for two-thirds of the total profilin content (Witke et al. 2001). The above-mentioned increase in profilin II in spine heads of the lateral amygdala of rats after fear conditioning and in cultured hippocampal cells after chemical stimulation was paralleled by an enlargement of the membrane area of the spine heads and a stabilization of their morphology. Hence, these findings were interpreted as demonstrating a functional role of profilin II at the postsynaptic side, in the consolidation of memory formation by the actin-based stabilization of synaptic communication (Ackermann and Matus 2003; Lamprecht et al. 2006). However, a more recent study on mice lacking profilin II points to a different function. The mutant mice are viable and fertile, but display a distinct phenotype with hyperactivation and enhanced novelty-seeking behavior. These behavioral anomalies are correlated with increased synaptic excitability due to increased vesicle exocytosis. These findings, supported by biochemical, electrophysiological and immunohistochemical data, point to a selective or at least preferential function of profilin II at the presynaptic side. In this position, complex formation of profilin II with a specific set of WAVE proteins (Witke 2004) is proposed to regulate presynaptic actin polymerization and control neurotransmitter release (Boyl et al. 2007). Hence, at present, the data presented from different groups on profilin II in pre- or postsynaptic functions are at variance. Future research will have to clarify this situation.

Unphysiological activities

Profilins as allergens

Many people developing type I allergies against inhaled allergens, causing histamine release and a strong IgE response, are in fact reacting against plant and fungal profilins. This was first discovered in 1991, when a major birch pollen allergen (Bet v 2) was identified as profilin (Valenta et al. 1991). Since then, numerous studies have described that patients who developed allergies against grass or birch pollen profilin subsequently become allergic to vegetable food profilin, in particular to various fruits like nuts, melon, orange, and peach, or to vegetables like zucchini, celery, tomatoes and carrots, or to latex (cf. Breiteneder and Ebner 2001). Hence, profilins are cross-reactive allergens and are classified as panallergens (Valenta et al. 1992; van Ree et al. 1992). In later stages of the disease, the afflicted persons may react against their own profilin, and exhibit the classical symptoms of an autoimmune disease boostered by intake or inhalation of foreign profilins (Valenta et al. 1991). Notably,

the extent of crossreactivity of human IgE depends primarily on highly conserved conformational features, and less so on a high degree of amino acid sequence homology (Sankian et al. 2005), and detailed studies with natural and recombinant proteins have revealed partial or even lack of IgE cross-reactivity between some plant profilins (Radauer et al. 2006).

Conclusion

Despite the numerous published reports on profilins, their functions are still poorly understood, and in some cases, there are discrepancies that await resolution. A major task for future research will be the unraveling of the regulation of the interaction with different ligands. A detailed knowledge of the affinity of different profilin isoforms for their specific ligands, localization studies with highly specific antibodies and genetic studies involving conditional mutants will help to further understand the stunning variety of functions of these small, ubiquitous proteins.

Acknowledgements. This article relies on a wealth of data from many different laboratories. We have cited the appropriate original publications wherever possible, but want to apologize to all authors whose reports could not be cited because of space limitations. Our own research referred to here was supported by the "Deutsche Forschungsgemeinschaft," the "Deutsche Krebshilfe/Mildred Scheel Stiftung" and the "Fonds der Deutschen Chemischen Industrie." The neuronal cells used in Fig. 2 were provided by K. Michaelsen (Braunschweig).

References

Ackermann M, Matus A (2003) Activity-induced targeting of profilin and stabilization of dendritic spine morphology. Nat Neurosci 6:1194–1200

Arasada R, Gloss A, Tunggal B, Joseph JM, Rieger D, et al (2007) Profilin isoforms in Dictyostelium discoideum. Biochim Biophys Acta 1773:631–641

Baatout S (1996) Profilin: an update. Eur J Clin Chem Clin Biochem 34:575–577

Berman HM, Westbrook J, Feng Z, Gilliland G, Bhat TN, et al (2000) The Protein Data Bank. Nucleic Acids Res 28:235–242

Birbach A, Verkuyl JM, Matus A (2006) Reversible, activity-dependent targeting of profilin to neuronal nuclei. Exp Cell Res 312:2279–2287

Blasco R, Cole NB, Moss B (1991) Sequence analysis, expression, and deletion of a vaccinia virus gene encoding a homolog of profilin, a eukaryotic actin-binding protein. J Virol 65:4598–4608

Blessing CA, Ugrinova GT, Goodson HV (2004) Actin and ARPs: action in the nucleus. Trends Cell Biol 14:435–442

Boukhelifa M, Moza M, Johansson T, Rachlin A, Parast M, et al (2006) The proline-rich protein palladin is a binding partner for profilin. Febs J 273:26–33

Boyl PP, Di Nardo A, Mulle C, Sassoè-Pognetto M, Panzanelli P, Mele A, Kneussel M, Costantini V, Perlas E, Massimi M, Giustetto M, Rivera HV, Witke W (2007) Profilin2 contributes to synaptic vesicle exocytosis, neuronal excitability and novelty-seeking behavior. EMBO J 26:2991–3002

Braun A, Aszodi A, Hellebrand H, Berna A, Fassler R, Brandau O (2002) Genomic organization of profilin-III and evidence for a transcript expressed exclusively in testis. Gene 283:219–225

Breiteneder H, Ebner C (2001) Atopic allergens of plant foods. Curr Opin Allergy Clin Immunol 1:261–267

Buss F, Temm-Grove C, Henning S, Jockusch BM (1992) Distribution of profilin in fibroblasts correlates with the presence of highly dynamic actin filaments. Cell Motil Cytoskeleton 22:51–61

Carlsson L, Nystrom L, Sundkvist I, Markey F, Lindberg U (1976) Profilin, a low-molecular weight protein controlling actin polymerisability. In: Perry SV, Marzella A, Adelstein RS (eds) Contractile systems in non muscle tissues. North Holland Publishing, Amsterdam, pp 39–49

Carlsson L, Nyström NE, Sundkvist I, Markey F, Lindberg U (1977) Actin polymerizability is influenced by profilin, a low molecular weight protein in non-muscle cells. J Biochem Mol Biol 115:465–483

Cedergren-Zeppezauer ES, Goonesekere NC, Rozycki MD, Myslik JC, Dauter Z, et al (1994) Crystallization and structure determination of bovine profilin at 2.0 A resolution. J Mol Biol 240:459–475

Chang F, Drubin D, Nurse P (1997) cdc12p, a protein required for cytokinesis in fission yeast, is a component of the cell division ring and interacts with profilin. J Cell Biol 137:169–82
Cooley L, Verheyen E, Ayers K (1992) chickadee encodes a profilin required for intercellular cytoplasm transport during Drosophila oogenesis. Cell 69:173–184
Da Silva JS, Medina M, Zuliani C, Di Nardo A, Witke W, Dotti CG (2003) RhoA/ROCK regulation of neuritogenesis via profilin IIa-mediated control of actin stability. J Cell Biol 162:1267–1279
Deeks MJ, Hussey PJ (2003) Arp2/3 and 'the shape of things to come'. Curr Opin Plant Biol 6:561–567
Deeks MJ, Hussey PJ, Davies B (2002) Formins: intermediates in signal-transduction cascades that affect cytoskeletal reorganization. Trends Plant Sci 7:492–498
Di Nardo A, Gareus R, Kwiatkowski D, Witke W (2000) Alternative splicing of the mouse profilin II gene generates functionally different profilin isoforms. J Cell Sci 113:3795–3803
Ding Z, Lambrechts A, Parepally M, Roy P (2006) Silencing profilin-1 inhibits endothelial cell proliferation, migration and cord morphogenesis. J Cell Sci 119:4127–4137
Domke T, Federau T, Schluter K, Giehl K, Valenta R, et al (1997) Birch pollen profilin: structural organization and interaction with poly-(L-proline) peptides as revealed by NMR. FEBS Lett 411:291–295
Dong J, Radau B, Otto A, Muller E, Lindschau C, Westermann P (2000) Profilin I attached to the Golgi is required for the formation of constitutive transport vesicles at the trans-Golgi network. Biochim Biophys Acta 1497:253–260
Evangelista M, Blundell K, Longtine MS, Chow CJ, Adames N, et al (1997) Bni1p, a yeast formin linking Cdc42p and the actin cytoskeleton during polarized morphogenesis. Science 276:118–22
Faix J, Grosse R (2006) Staying in shape with formins. Dev Cell 10:693–706
Fedorov AA, Magnus KA, Graupe MH, Lattman EE, Pollard TD, Almo SC (1994) X-ray structures of isoforms of the actin-binding protein profilin that differ in their affinity for phosphatidylinositol phosphates. Proc Natl Acad Sci USA 91:8636–8640
Fedorov AA, Ball T, Mahoney NM, Valenta R, Almo SC (1997) The molecular basis for allergen cross-reactivity: crystal structure and IgE-epitope mapping of birch pollen profilin. Structure 5:33–45
Feng G, Tintrup H, Kirsch J, Nichol MC, Kuhse J, et al (1998) Dual requirement for gephyrin in glycine receptor clustering and molybdoenzyme activity. Science 282:1321–1324
Finger FP, Novick P (1997) Sec3p is involved in secretion and morphogenesis in Saccharomyces cerevisiae. Mol Biol Cell 8:647–662
Gareus R, Di Nardo A, Rybin V, Witke W (2006) Mouse profilin 2 regulates endocytosis and competes with SH3 ligand binding to dynamin 1. J Biol Chem 281:2803–2811
Garner CC, Kindler S, Gundelfinger ED (2000) Molecular determinants of presynaptic active zones. Curr Opin Neurobiol 10:321–327
Gertler FB, Niebuhr K, Reinhard M, Wehland J, Soriano P (1996) Mena, a relative of VASP and Drosophila enabled, is implicated in the control of microfilament dynamics. Cell 87:227–239
Gibbon BC, Zonia LE, Kovar DR, Hussey PJ, Staiger CJ (1998) Pollen profilin function depends on interaction with proline-rich motifs. Plant Cell 10:981–993
Giehl K, Valenta R, Rothkegel M, Ronsiek M, Mannherz HG, Jockusch BM (1994) Interaction of plant profilin with mammalian actin. Eur J Biochem 226:681–689
Giesemann T, Rathke-Hartlieb S, Rothkegel M, Bartsch JW, Buchmeier S, et al (1999) A role for polyproline motifs in the spinal muscular atrophy protein SMN: profilins bind to and colocalize with SMN in nuclear gems. J Biol Chem 274:37908–37914
Giesemann T, Schwarz G, Nawrotzki R, Berhörster K, Rothkegel M, et al (2003) Complex formation between the postsynaptic scaffolding protein gephyrin, profilin and Mena: a possible link to the microfilament system. J Neurosci 23:8330–8339
Goldschmidt-Clermont PJ, Kim JW, Machesky LM, Rhee SG, Pollard TD (1991) Regulation of phospholipase C-gamma 1 by profilin and tyrosine phosphorylation. Science 251:1231–1233
Grummt I (2006) Actin and myosin as transcription factors. Curr Opin Genet Dev 16:191–196
Gutsche-Perelroizen I, Lepault J, Ott A, Carlier MF (1999) Filament assembly from profilin-actin. J Biol Chem 274:6234–6243
Haarer BK, Brown SS (1990) Structure and function of profilin. Cell Motil Cytoskeleton 17:71–74
Harbeck B, Hüttelmaier S, Schlüter K, Jockusch BM, Illenberger S (2000) Phosphorylation of the vasodilator-stimulated phosphoprotein regulates its interaction with actin. J Biol Chem 275:30817–30825
Haugwitz M, Noegel AA, Rieger D, Lottspeich F, Schleicher M (1991) Dictyostelium discoideum contains two profilin isoforms that differ in structure and function. J Cell Sci 100:481–489
Haugwitz M, Noegel AA, Karakesisoglou J, Schleicher M (1994) Dictyostelium amoebae that lack G-actin-sequestering profilins show defects in F-actin content, cytokinesis, and development. Cell 79:303–314
Higgins HN (2005) Formin proteins: a domain-based approach. Trends Biochem Sci 30:342–353

Honoré B, Madsen P, Andersen AH, Leffers H (1993) Cloning and expression of a novel human profilin variant, profilin II. Febs Lett 330:151–155
Hu E, Chen Z, Fredrickson T, Zhu Y (2001) Molecular cloning and characterization of profilin-3: a novel cytoskeleton-associated gene expressed in rat kidney and testes. Exp Nephrol 9:265–274
Huang SR, McDowell JM, Weise MJ, Meagher RB (1996) The Arabidopsis profilin gene family—Evidence for an ancient split between constitutive and pollen-specific profilin genes. Plant Physiol 111:115–126
Hüttelmaier S, Mayboroda O, Harbeck B, Jarchau T, Jockusch BM, Rüdiger M (1998) The interaction of the cell-contact proteins VASP and vinculin is regulated by phosphatidylinositol-4,5-bisphosphate. Curr Biol 8:479–488
Hüttelmaier S, Harbeck B, Steffens O, Messerschmidt T, Illenberger S, Jockusch BM (1999) Characterization of the actin binding properties of the vasodilator-stimulated phosphoprotein VASP. FEBS Lett 451:68–74
Hussey PJ, Ketelaar T, Deeks MJ (2006) Control of the actin cytoskeleton in plant cell growth. Annu Rev Plant Biol 57:109–125
Janke J, Schluter K, Jandrig B, Theile M, Kolble K, et al (2000) Suppression of tumorigenicity in breast cancer cells by the microfilament protein profilin 1. J Exp Med 191:1675–1686
Jockusch BM, Rothkegel M, Schwarz G (2004) Linking the synapse to the cytoskeleton: a breath-taking role for microfilaments. Neuroreport 15:1535–1538
Jockusch BM, Schoenenberger CA, Stetefeld J, Aebi U (2006) Tracking down the different forms of nuclear actin. Trends Cell Biol 16:391–396
Kandasamy MK, McKinney EC, Meagher RB (2002) Plant profilin isovariants are distinctly regulated in vegetative and reproductive tissues. Cell Motil Cytoskeleton 52:22–32
Karakesisoglou I, Schleicher M, Gibbon BC, Staiger CJ (1996) Plant profilins rescue the aberrant phenotype of profilin-deficient Dictyostelium cells. Cell Motil Cytoskeleton 34:36–47
Kelleher JF, Atkinson SJ, Pollard TD (1995) Sequences, structural models, and cellular localization of the actin-related proteins Arp2 and Arp3 from Acanthamoeba. J Cell Biol 131:385–397
Kim E, Waters SH, Hake LE, Hecht NB (1989) Identification and developmental expression of a smooth-muscle gamma-actin in postmeiotic male germ cells of mice. Mol Cell Biol 9:1875–1881
Kovar DR, Drobak BK, Staiger CJ (2000) Maize profilin isoforms are functionally distinct. Plant Cell 12:583–598
Kovar DR, Harris ES, Mahaffy R, Higgs HN, Pollard TD (2006) Control of the assembly of ATP- and ADP-actin by formins and profilin. Cell 124:423–435
Krause M, Dent EW, Bear JE, Loureiro JJ, Gertler FB (2003) Ena/VASP proteins: regulators of the actin cytoskeleton and cell migration. Annu Rev Cell Dev Biol 19:541–564
Krebs A, Rothkegel M, Klar M, Jockusch BM (2001) Characterization of functional domains of mDia1, a link between the small GTPase Rho and the actin cytoskeleton. J Cell Sci 114:3663–3672
Kruchten AE, McNiven MA (2006) Dynamin as a mover and pincher during cell migration and invasion. J Cell Sci 119:1683–1690
Lafuente EM, van Puijenbroek AA, Krause M, Carman CV, Freeman GJ, et al (2004) RIAM, an Ena/VASP and Profilin ligand, interacts with Rap1-GTP and mediates Rap1-induced adhesion. Dev Cell 7:585–595
Lambrechts A, Verschelde JL, Jonckheere V, Goethals M, Vandekerckhove J, Ampe C (1997) The mammalian profilin isoforms display complementary affinities for PIP2 and proline-rich sequences. EMBO J 16:484–494
Lambrechts A, Jonckheere V, Dewitte D, Vandekerckhove J, Ampe C (2002) Mutational analysis of human profilin I reveals a second PIP2 binding site neighbouring the poly(L-proline)binding site. BMC Biochem 3:12
Lambrechts A, Jonckheere V, Peleman C, Polet D, De Vos W, et al (2006) Profilin-I-ligand interactions influence various aspects of neuronal differentiation. J Cell Sci 119:1570–1578
Lamprecht R, Farb CR, Rodrigues SM, LeDoux JE (2006) Fear conditioning drives profilin into amygdala dendritic spines. Nat Neurosci 9:481–483
Lassing I, Lindberg U (1985) Specific interaction between phosphatidylinositol 4,5-bisphosphate and profilactin. Nature 314:472–474
Lederer M, Jockusch BM, Rothkegel M (2005) Profilin regulates the activity of p42POP, a novel Myb-related transcription factor. J Cell Sci 118:331–341
Li F, Higgs HN (2003) The mouse Formin mDia1 is a potent actin nucleation factor regulated by autoinhibition. Curr Biol 13:1335–1340
Lu PJ, Shieh WR, Rhee SG, Yin HL, Chen CS (1996) Lipid products of phosphoinositide 3-kinase bind human profilin with high affinity. Biochemistry 35:14027–14034
Machesky LM, Atkinson SJ, Ampe C, Vandekerckhove J, Pollard TD (1994a) Purification of a cortical complex containing two unconventional actins from Acanthamoeba by affinity chromatography on profilin-agarose. J Cell Biol 127:107–115

Machesky LM, Cole NB, Moss B, Pollard TD (1994b) Vaccinia virus expresses a novel profilin with a higher affinity for polyphosphoinositides than actin. Biochemistry 33:10815–10824
Mahoney NM, Janmey PA, Almo SC (1997) Structure of the profilin-poly-L-proline complex involved in morphogenesis and cytoskeletal regulation. Nat Struct Biol 4:953–960
Mammoto A, Sasaki T, Asakura T, Hotta I, Imamura H, et al (1998) Interactions of drebrin and gephyrin with profilin. Biochem Biophys Res Commun 243:86–89
Manseau L, Calley J, Phan H (1996) Profilin is required for posterior patterning of the Drosophila oocyte. Development 122:2109–2116
Mayboroda O, Schlüter K, Jockusch BM (1997) Differential colocalization of profilin with microfilaments in PtK2 cells. Cell Motil. Cell Motil Cytoskeleton 37:166–177
McCollum D, Feoktistova A, Morphew M, Balasubramanian M, Gould KL (1996) The Schizosaccharomyces pombe actin-related protein, Arp3, is a component of the cortical actin cytoskeleton and interacts with profilin. EMBO J 15:6438–6446
McDowell JM, Huang S, McKinney EC, An YQ, Meagher RB (1996) Structure and evolution of the actin gene family in Arabidopsis thaliana. Genetics 142:587–602
McKenna ST, Vidali L, Hepler PK (2004) Profilin inhibits pollen tube growth through actin-binding, but not poly-L-proline-binding. Planta 218:906–915
McWhorter ML, Monani UR, Burghes AH, Beattie CE (2003) Knockdown of the survival motor neuron (Smn) protein in zebrafish causes defects in motor axon outgrowth and pathfinding. J Cell Biol 162:919–931
Michelot A, Guerin C, Huang S, Ingouff M, Richard S, et al (2005) The formin homology 1 domain modulates the actin nucleation and bundling activity of Arabidopsis FORMIN1. Plant Cell 17:2296–2313
Miki H, Suetsugu S, Takenawa T (1998) WAVE, a novel WASP-family protein involved in actin reorganization induced by rac. EMBO J 17:6932–6941
Minehardt TJ, Kollman PA, Cooke R, Pate E (2006) The open nucleotide pocket of the profilin/actin x-ray structure is unstable and closes in the absence of profilin. Biophys J 90:2445–2449
Mourelatos Z, Abel L, Yong J, Kataoka N, Dreyfuss G (2001) SMN interacts with a novel family of hnRNP and spliceosomal proteins. EMBO J 20:5443–5452
Muller J, Oma Y, Vallar L, Friederich E, Poch O, Winsor B (2005) Sequence and comparative genomic analysis of actin-related proteins. Mol Biol Cell 16:5736–5748
Neuhoff H, Sassoe-Pognetto M, Panzanelli P, Maas C, Witke W, Kneussel M (2005) The actin-binding protein profilin I is localized at synaptic sites in an activity-regulated manner. Eur J Neurosci 21:15–25
Obermann H, Raabe I, Balvers M, Brunswig B, Schulze W, Kirchhoff C (2005) Novel testis-expressed profilin IV associated with acrosome biogenesis and spermatid elongation. Mol Hum Reprod 11:53–64
Ozaki K, Sugino H, Hasegawa T, Takahashi S, Hatano S (1983) Isolation and characterization of Physarum profilin. J Biochem (Tokyo) 93:295–298
Palazzo AF, Cook TA, Alberts AS, Gundersen GG (2001) mDia mediates Rho-regulated formation and orientation of stable microtubules. Nat Cell Biol 3:723–729
Peitsch WK, Bulkescher J, Spring H, Hofmann I, Goerdt S, Franke WW (2006) Dynamics of the actin-binding protein drebrin in motile cells and definition of a juxtanuclear drebrin-enriched zone. Exp Cell Res 312:2605–2618
Perelroizen I, Carlier MF, Pantaloni D (1995) Binding of divalent cation and nucleotide to G-actin in the presence of profilin. J Biol Chem 270:1501–1508
Polet D, Lambrechts A, Ono K, Mah A, Peelman F, et al (2006) Caenorhabditis elegans expresses three functional profilins in a tissue-specific manner. Cell Motil Cytoskeleton 63:14–28
Polet D, Lambrechts A, Vandepoele K, Vandekerckhove J, Ampe C (2007) On the origin and evolution of vertebrate and viral profilins. FEBS Lett 581:211–217
Pollard TD, Borisy GG (2003) Cellular motility driven by assembly and disassembly of actin filaments. Cell 113:549
Pollard TD, Quirk S (1994) Profilins, ancient actin binding proteins with highly divergent primary structures. Soc Gen Physiol Ser 49:117–128
Pruyne D, Evangelista M, Yang C, Bi E, Zigmond S, et al (2002) Role of formins in actin assembly: nucleation and barbed-end association. Science 297:612–615
Radauer C, Willerroider M, Fuchs H, Hoffmann-Sommergruber K, Thalhamer J, et al (2006) Cross-reactive and species-specific immunoglobulin E epitopes of plant profilins: an experimental and structure-based analysis. Clin Exp Allergy 36:920–929
Ramming M, Kins S, Werner N, Hermann A, Betz H, Kirsch J (2000) Diversity and phylogeny of gephyrin: tissue-specific splice variants, gene structure, and sequence similarities to molybdenum cofactor-synthesizing and cytoskeleton-associated proteins. Proc Natl Acad Sci USA 97:10266–10271

Rawe VY, Payne C, Schatten G (2006) Profilin and actin-related proteins regulate microfilament dynamics during early mammalian embryogenesis. Hum Reprod 21:1143–1153
Reichstein E, Korn ED (1979) Acanthamoeba profilin. A protein of low molecular weight from Acanpthamoeba castellanii that inhibits actin nucleation. J Biol Chem 254:6174–6179
Reinhard M, Halbrugge M, Scheer U, Wiegand C, Jockusch BM, Walter U (1992) The 46/50 kDa phosphoprotein VASP purified from human platelets is a novel protein associated with actin filaments and focal contacts. EMBO J 11:2063–2070
Reinhard M, Giehl K, Abel K, Haffner C, Jarchau T, et al (1995) The proline-rich focal adhesion and microfilament protein VASP is a ligand for profilins. EMBO J 14:1583–1589
Reinhard M, Rudiger M, Jockusch BM, Walter U (1996) VASP interaction with vinculin: A recurring theme of interactions with proline-rich motifs. FEBS Lett 399:103–107
Romero S, Le Clainche C, Didry D, Egile C, Pantaloni D, Carlier MF (2004) Formin is a processive motor that requires profilin to accelerate actin assembly and associated ATP hydrolysis. Cell 119:419–429
Romero S, Didry D, Larquet E, Boisset N, Pantaloni D, Carlier MF (2007) How ATP hydrolysis controls filament assembly from profilin-actin: implication for formin processivity. J Biol Chem 282:8435–8445
Rothkegel M, Mayboroda O, Rohde M, Wucherpfennig C, Valenta R, Jockusch BM (1996) Plant and animal profilins are functionally equivalent and stabilize microfilaments in living animal cells. J Cell Sci 109:83–90
Rottner K, Behrendt B, Small JV, Wehland J (1999) VASP dynamics during lamellipodia protrusion. Nat Cell Biol 1:321–322
Sankian M, Varasteh A, Pazouki N, Mahmoudi M (2005) Sequence homology: a poor predictive value for profilins cross-reactivity. Clin Mol Allergy 3:13
Sathish K, Padma B, Munugalavadla V, Bhargavi V, Radhika KV, et al (2004) Phosphorylation of profilin regulates its interaction with actin and poly (L-proline). Cell Signal 16:589–596
Sato A, Khadka DK, Liu W, Bharti R, Runnels LW, et al (2006) Profilin is an effector for Daam1 in non-canonical Wnt signaling and is required for vertebrate gastrulation. Development 133:4219–4231
Schlüter K, Jockusch BM, Rothkegel M (1997) Profilins as regulators of actin dynamics. Biochim Biophys Acta 27:97–109
Schlüter K, Schleicher M, Jockusch BM (1998) Effects of single amino acid substitutions in the actin-binding site on the biological activity of bovine profilin I. J Cell Sci 111:3261–3273
Schmitz HP, Kaufmann A, Kohli M, Laissue PP, Philippsen P (2006) From function to shape: a novel role of a formin in morphogenesis of the fungus Ashbya gossypii. Mol Biol Cell 17:130–145
Schutt CE, Myslik JC, Rozycki MD, Goonesekere NC, Lindberg U (1993) The structure of crystalline profilin-beta-actin. Nature 365:810–816
Selden LA, Kinosian HJ, Estes JE, Gershman LC (1999) Impact of profilin on actin-bound nucleotide exchange and actin polymerization dynamics. Biochemistry 38:2769–2778
Sharma A, Lambrechts A, Hao le T, Le TT, Sewry CA, et al (2005) A role for complexes of survival of motor neurons (SMN) protein with gemins and profilin in neurite-like cytoplasmic extensions of cultured nerve cells. Exp Cell Res 309:185–197
Shirao T (1995) The roles of microfilament-associated proteins, drebrins, in brain morphogenesis: a review. J Biochem (Tokyo) 117:231–236
Skare P, Karlsson R (2002) Evidence for two interaction regions for phosphatidylinositol (4,5)-bisphosphate on mammalian profilin I. FEBS Lett 522:119–124
Skare P, Kreivi JP, Bergstrom A, Karlsson R (2003) Profilin I colocalizes with speckles and Cajal bodies: a possible role in pre-mRNA splicing. Exp Cell Res 286:12–21
Solomaha E, Szeto FL, Yousef MA, Palfrey HC (2005) Kinetics of Src homology 3 domain association with the proline-rich domain of dynamins: specificity, occlusion, and the effects of phosphorylation. J Biol Chem 280:23147–23156
Somboonwiwat K, Supungul P, Rimphanitchayakit V, Aoki T, Hirono I, Tassanakajon A (2006) Differentially expressed genes in hemocytes of Vibrio harveyi-challenged shrimp Penaeus monodon. J Biochem Mol Biol 39:26–36
Staiger CJ, Goodbody KC, Hussey PJ, Valenta R, Drobak BK, Lloyd CW (1993) The profilin multigene family of maize: differential expression of three isoforms. Plant J 4:631–641
Stradal TE, Rottner K, Disanza A, Confalonieri S, Innocenti M, Scita G (2004) Regulation of actin dynamics by WASP and WAVE family proteins. Trends Cell Biol 14:303–311
Stüven T, Hartmann E, Görlich D (2003) Exportin 6: a novel nuclear export receptor that is specific for profilin-actin complexes. EMBO J 22:5928–5940
Suetsugu S, Miki H, Takenawa T (1998) The essential role of profilin in the assembly of actin for microspike formation. EMBO J 17:6516–6926

Takamori S, Holt M, Stenius K, Lemke EA, Gronborg M, et al (2006) Molecular anatomy of a trafficking organelle. Cell 127:831–846
Tanaka H, Iguchi N, Egydio de Carvalho C, Tadokoro Y, Yomogida K, Nishimune Y (2003) Novel actin-like proteins T-ACTIN 1 and T-ACTIN 2 are differentially expressed in the cytoplasm and nucleus of mouse haploid germ cells. Biol Reprod 69:475–482
Thorn KS, Christensen HEM, Shigeta Jr R, Huddler Jr D, Shalaby L, et al (1997) The crystal structure of a major allergen from plants. Structure 5:19–32
Tilney LG, Bonder EM, Coluccio LM, Mooseker MS (1983) Actin from Thyone sperm assembles on only one end of an actin filament: a behavior regulated by profilin. J Cell Biol 97:112–124
Valenta R, Duchene M, Pettenburger K, Sillaber C, Valent P, et al (1991) Identification of profilin as a novel pollen allergen; IgE autoreactivity in sensitized individuals. Science 253:557–560
Valenta R, Duchene M, Ebner C, Valent P, Sillaber C, et al (1992) Profilins constitute a novel family of functional plant pan-allergens. J Exp Med 175:377–385
Valenta R, Ferreira F, Grote M, Swoboda I, Vrtala S, et al (1993) Identification of profilin as an actin-binding protein in higher plants. J Biol Chem 268:22777–22781
van Ree R, Voitenko V, van Leeuwen WA, Aalberse RC (1992) Profilin is a cross-reactive allergen in pollen and vegetable foods. Int Arch Allergy Immunol 98:97–104
Walders-Harbeck B, Khaitlina SY, Hinssen H, Jockusch BM, Illenberger S (2002) The vasodilator-stimulated phosphoprotein promotes actin polymerisation through direct binding to monomeric actin. FEBS Lett 26564:1–6
Wallar BJ, Alberts AS (2003) The formins: active scaffolds that remodel the cytoskeleton. Trends Cell Biol 13:435–446
Wang X, Kibschull M, Laue MM, Lichte B, Petrasch-Parwez E, Kilimann MW (1999) Aczonin, a 550-kD putative scaffolding protein of presynaptic active zones, shares homology regions with Rim and Bassoon and binds profilin. J Cell Biol 147:151–162
Watanabe N, Madaule P, Reid T, Ishizaki T, Watanabe G, et al (1997) p140mDia, a mammalian homologue of Drosophila diaphanous, is a target protein for rho small GTPases and is a ligand for profilin. EMBO J 16:3044–3056
Wilkes DE, Otto JJ (2000) Molecular cloning of profilin from Tetrahymena thermophila. Gene 246:295–301
Wilkes DE, Otto JJ (2003) Profilin functions in cytokinesis, nuclear positioning, and stomatogenesis in Tetrahymena thermophila. J Eukaryot Microbiol 50:252–262
Witke W (2004) The role of profilin complexes in cell motility and other cellular processes. Trends Cell Biol 14:461–469
Witke W, Podtelejnikov AV, Di Nardo A, Sutherland JD, Gurniak CB, et al (1998) In mouse brain profilin I and profilin II associate with regulators of the endocytic pathway and actin assembly. EMBO J 17:967–976
Witke W, Sutherland JD, Sharpe A, Arai M, Kwiatkowski DJ (2001) Profilin I is essential for cell survival and cell division in early mouse development. Proc Natl Acad Sci USA 98:3832–3836
Wittenmayer N, Jandrig B, Rothkegel M, Schluter K, Arnold W, et al (2004) Tumor suppressor activity of profilin requires a functional actin binding site. Mol Biol Cell 15:1600–1608
Wu X, Yoo Y, Okuhama NN, Tucker PW, Liu G, Guan JL (2006) Regulation of RNA-polymerase-II-dependent transcription by N-WASP and its nuclear-binding partners. Nat Cell Biol 8:756–763
Yarmola EG, Bubb MR (2006) Profilin: emerging concepts and lingering misconceptions. Trends Biochem Sci 31:197–205
Zhang H, Xing L, Rossoll W, Wichterle H, Singer RH, Bassell GJ (2006) Multiprotein complexes of the survival of motor neuron protein SMN with Gemins traffic to neuronal processes and growth cones of motor neurons. J Neurosci 26:8622–8632
Zhao W, Jiang C, Kroll TT, Huber PW (2001) A proline-rich protein binds to the localization element of Xenopus Vg1 mRNA and to ligands involved in actin polymerization. EMBO J 20:2315–2325
Zhou F, Leder P, Martin SS (2006) Formin-1 protein associates with microtubules through a peptide domain encoded by exon-2. Exp Cell Res 312:1119–1126
Zigmond SH (2004) Formin-induced nucleation of actin filaments. Curr Opin Cell Biol 16:99–105